Development of Self-consolidating High Performance Concrete Incorporating Rice Husk Ash

by

Md. Safiuddin

A thesis
presented to the University of Waterloo
in fulfillment of the
thesis requirement for the degree of
Doctor of Philosophy
in
Civil Engineering

Waterloo, Ontario, Canada, 2008

Author’s Declaration

I hereby declare that I am the sole author of this thesis. This is a true copy of the thesis, including any required final revisions, as accepted by my examiners.

I understand that the University of Waterloo may make my thesis electronically available to the public.

Abstract

The work presented in this thesis deals with the development of self-consolidating high performance concrete (SCHPC) incorporating rice husk ash (RHA) as a supplementary cementing material. Various SCHPCs were produced using the water-binder (W/B) ratios of 0.30, 0.35, 0.40 and 0.50, and RHA content in the range of 0 to 30% of cement by weight. In addition, a number of pastes and mortars formulated from the concretes were prepared and tested for the filling ability. The paste and mortar filling abilities were tested with respect to flow time and flow spread, respectively, at various dosages of high-range water reducer (HRWR). Also, the mortars were tested for the air content at various dosages of air-entraining admixture (AEA). It was observed that the flow time of the pastes increased with lower W/B ratio and higher RHA content, whereas the flow spread of the mortars decreased with higher W/B ratio and greater RHA content. Both paste and mortar filling abilities increased with higher HRWR dosages. In addition, the air content of the mortars decreased with lower W/B ratio and higher RHA content for given AEA dosages.

The fresh SCHPCs were tested for filling ability, passing ability, air-void stability, segregation resistance, unit weight and air content. The filling ability was determined with respect to slump and slump flow, inverted slump cone flow time and spread, and orimet flow time and spread. The passing ability was measured with regard to slump and slump flow with J-ring, inverted slump cone flow spread with J-ring, and orimet flow spread with J-ring. The air-void stability in several fresh SCHPC mixtures was investigated with respect to re-mixing of concrete and subsequent measurement of air content at different test stages.

The test results obtained for the fresh properties showed that the inverted slump cone and orimet flow times increased with lower W/B ratio and greater RHA content. In addition, the slump flow, inverted slump cone flow spread, and orimet flow spread with and without J-ring increased considerably with lower W/B ratio and greater RHA content. However, the increases in slump with and without J-ring at lower W/B ratio and higher RHA content were not significant. The unit weight of concrete slightly decreased with higher W/B ratio and greater RHA content, and with higher air content. Achieving the target air content required greater AEA dosages for lower W/B ratio and higher RHA content. However, the presence of RHA had no adverse effect on the air-void stability of concrete.

The segregation resistance of various SCHPCs was investigated by visual inspection of concrete in mixer pan, and during and after different flow tests. Slight bleeding and a thick layer of paste were noticed in mixer pan for several concretes. The dynamic segregation in the form of discontinuity or blockage of flow did not occur during the orimet and inverted slump cone flow tests for any concrete. No aggregate pile appeared in the slump flow, and orimet and inverted slump cone flow spreads of any concrete. But minor to severe mortar halos were noticed in the periphery of the flow spread of several concretes, particularly in the presence of high RHA content. The results of visual inspection suggest that both lower W/B ratio and greater RHA content improved the dynamic segregation resistance of concrete. In contrast, the higher RHA content resulted in a lower static segregation resistance, which was overcome in the presence of viscosity-enhancing admixture (VEA).

The static segregation resistance of several SCHPCs was quantitatively determined by sieve and column apparatus. The segregation index given by the sieve increased with lower W/B ratio and higher RHA content, thus indicating a reduced static segregation resistance. In contrast, the segregation factor given by the column apparatus decreased with lower W/B ratio suggesting an increased static segregation resistance. However, the segregation factor increased with higher RHA content, and thus revealed a reduction in static segregation resistance. In the presence of VEA, both segregation index and segregation factor decreased significantly, indicating an improvement in the static segregation resistance of concrete.

The hardened SCHPCs were tested for compressive strength, ultrasonic pulse velocity, water absorption, total porosity and electrical resistivity. Test results revealed that the compressive strength, ultrasonic pulse velocity and true electrical resistivity increased, whereas the water absorption and total porosity decreased with lower W/B ratio and higher RHA content. The entrained air-voids decreased the compressive strength, ultrasonic pulse velocity, water absorption and total porosity, but slightly increased the electrical resistivity of concrete. In general, the hardened properties indicated good durability of the concretes.

The empirical models for the filling ability (slump flow) and compressive strength of SCHPC were derived and verified with test data from this study and other data taken from the literature. The slump flow and compressive strength computed from the models were coherent with the measured values. Both filling ability and strength models were useful to develop a mixture design method for SCHPC with and without RHA.

Acknowledgements

The author expresses sincere gratitude to his supervisors Dr. Jeffrey S. West, Assistant Professor and Dr. Khaled A. Soudki, Professor, Department of Civil and Environmental Engineering for their precious guidance, advice, and encouragement throughout the research program.

The author is thankful to Mr. Cameron Monroe, Manager of Technical Services at the BASF Construction Chemicals Canada Ltd. for supplying chemical admixtures, and for his valuable technical support. The author is grateful to Lafarge North America Inc. for the supply of cement. The author is also grateful to Michael Rich, Renewable Energy Generation Inc. for his help in collecting rice husk ash required for the research program.

Sincere gratitude and indebtedness are conveyed to Dr. Giovanni Cascante, Associate Professor, Department of Civil and Environmental Engineering, Faculty of Engineering for his excellent cooperation in testing ultrasonic pulse velocity of the concretes. Deep thanks are due to all technical staff in the Faculty of Engineering Machine Shop, Civil and Environmental Engineering Laboratories, University of Waterloo, particularly John Boldt, Ken Bowman, Terry Ridgway, Richard Morrison, and Doug Hirst for their valuable input and assistance during the research program. Special thanks also go to all of my colleagues, particularly Han Tae Choi and Khanh Tran, and to all Undergraduate Research Assistants for their great help in experimental investigation.

Sincere and great appreciation goes to Natural Sciences and Engineering Research Council of Canada; Ontario Ministry of Training, Colleges and Universities; JNE Consulting Limited; and University of Waterloo for the financial support.

Dedication

This thesis is dedicated to the martyrs of Language Movement (Bhasa Andolon) who died in February 21 (declared as the International Mother Language Day by UNESCO), 1952 to establish Bengali as a state language of former Pakistan, and to all freedom fighters who sacrificed their lives for the independence of Bangladesh in 1971.

Table of Contents

List of Tables

List of Figures

List of Notation

Notation	Meaning
a	Ratio of top radius to the bottom radius of slump cone
AEA	Air-entraining admixture
$A(t)$	Kinetics function related to the compressive strength of reference concrete
A_a	Cross-sectional area of aggregate
A_c	Entrained air content of mortar
A_{ca}	Absorption of coarse aggregate
A_{fa}	Absorption of fine aggregate
A_{me}	Equivalent air content of mortar
A_p	Entrapped air content of concrete
A_t	Total design air content of concrete
B	Binder content of concrete or mortar
B/A	Binder-aggregate ratio
BD_{mad}	Maximum bulk density of air-dry aggregate blend
C	Cement
CA	Coarse aggregate
CA/FA	Coarse aggregate to fine aggregate mass ratio
CA/TS	Coarse aggregate to total solid volume ratio
CSH	Calcium silicate hydrate
C_B	Surface-dry mass of the coarse aggregate in bottom section of column apparatus
C_D	Drag coefficient
C_{fto}	Orimet flow time of concrete
C_{ftisc}	Inverted slump cone flow time of concrete
C_i	Surface-dry mass of the aggregate in ‘i’th section of column apparatus
C_T	Surface-dry mass of the coarse aggregates in top section of column apparatus

D	Diameter of concrete cylinder specimen, maximum size of aggregate
D_{ca}	Actual AEA dosage
D_{ce}	Estimated AEA dosage for the specified air content of concrete
D_h	Dosage of high-range water reducer
D_m	Mortar density
D_{me}	AEA dosage for the equivalent air content of mortar
FA	Fine aggregate
f'_{acr}	Equivalent average compressive strength of air-entrained SCHPC
F_b	Buoyant force
$f_c(t)$	Compressive strength at any time
f'_c	Specified design compressive strength of concrete
f'_{cr}	Specified design compressive strength of concrete
f'_{nacr}	Average compressive strength of non-air-entrained SCHPC
$f(t, t_s)$	Strength-time function
f_{cm}	Mean compressive strength at 28 days
f_{cs}	Specified compressive strength of concrete
f_{c28}	28-day compressive strength of concrete
F_d	Downward force
F_{dr}	Vertical drag force
F_f	Frictional force
F_g	Gravitational force
F_r	Restoring force
g	Gravitational acceleration
H	Height of concrete cylinder specimen, height of fresh concrete in slump cone
HRWR	High-range water reducer
HPC	High performance concrete
ISCF	Inverted slump cone flow
K	A coefficient that depends on the type of aggregate
K_c	A factor related to cement strength, strength contribution factor of rice husk ash

M_b	Buoyant mass of the saturated specimen in water
M_c	Mass of the mortar contained in concrete sample
M_{ca}	Moisture content of coarse aggregate
M_d	Oven-dry mass of the specimen in air
M_{fa}	Moisture content of fine aggregate
M_p	Mass of the mortar passing No. 4 sieve
M_s	Saturated surface-dry mass of the specimen in air
n	Experimental constant for slump flow model, number of column sections
R_{c28}	28-day compressive strength of cement
OF	Orimet flow
P_{ft}	Paste flow time
P_{rha}	Percent amount of rice husk ash in total binder
P_t	Total porosity
$\overline{P}$	Average of $\overline{P_t}$ and $\overline{P_b}$
$\overline{P_b}$	Average concrete property obtained from two bottom sections of column specimens
$\overline{P_t}$	Average concrete property obtained from two top sections of column specimens
RHA	Rice husk ash
r_a	Radius of aggregate
R_b	Bottom radius of concrete sample before deformation
R_d	Relative density of AEA
S	Slump
S/A	Sand-aggregate ratio
$(S/A)_{opt}$	Optimum sand-aggregate ratio
SCC	Self-consolidating concrete
SCM	Supplementary cementing material
SCHPC	Self-consolidating high performance concrete
SD	Saturation dosage

SF	Mass of silica fume, segregation factor of concrete
SI	Segregation index of concrete
S_f	Slump flow of concrete
S_h	Solid content of high-range water reducer
S_v	Volume fraction of solids, volume fraction of coarse and fine aggregates
t	Concrete age
T	Time period for the measurement of slump and slump flow
T_i	Inverted slump cone flow time
T_o	Orimet flow time
T_s	Slump time
V	Volume of concrete sample in slump cone
V_m	Mortar volume
VEA	Viscosity-enhancing admixture
V_a	Volume of aggregate
V_c	Air-free absolute volume of concrete
V_{ca}	Absolute volume of coarse aggregate
V_{fa}	Absolute volume of fine aggregate
V_{caad}	Voids in air-dry basis compacted aggregate blend
V_{cp}	Statistical coefficient of variation in concrete property
V_{dp}	Degree of variation in concrete property
V_{ep}	Excess paste
V_m	Air-free absolute volume of the mortar component of concrete
V_{mp}	Minimum paste volume
V_p	Paste volume of concrete
V_{ta}	Absolute volume of total aggregates
v_t	Terminal velocity
W	Water
W_a	Water absorption
W/B	Water-binder ratio
W/C	Water-cement ratio

W_b	Binder weight
W_c	Weight of cement
W_{ca}	Amount of saturated surface-dry coarse aggregate
W_{caad}	Adjusted air-dry weight of coarse aggregate
W_D	Water demand of RHA
W_{fa}	Amount of saturated surface-dry fine aggregate
W_{faad}	Adjusted air-dry weight of fine aggregate
W_{IO}	Increase in water content required for the binder paste without RHA
W_{IRHA}	Increase in water content needed for the binder paste with RHA
W_{HRWR}	Water content required for the saturation flow time in the presence of HRWR
W_O	Water content needed for the saturation flow time without any HRWR
W_R	Water reduction capacity of HRWR
W_{rha}	Weight of RHA
W_{ta}	Amount of total aggregate
W_w	Weight of water
W_{wad}	Adjusted weight of mixing water
y	A coefficient that accounts for the entrapped air volume
α	$2gV/\pi$, experimental constant for strength model
α_s	Shape factor
β	Experimental constant for slump flow and strength model
ϕ_{mc}	Volume fraction of the mortar component in concrete
η	Viscosity of matrix
μ	Plastic viscosity of concrete
v_e	Equilibrium velocity
ρ	Unit weight or density of fresh concrete
ρ_a	Density of aggregate
ρ_m	Density of matrix
ρ_r	Relative density of concrete
ρ_{rc}	Relative density of cement

ρ_{rca}	Saturated surface-dry basis relative density of coarse aggregate
ρ_{rcaad}	Air-dry basis relative density of coarse aggregate
ρ_{rfaad}	Air-dry basis relative density of fine aggregate
ρ_{rfa}	Saturated surface-dry basis relative density of fine aggregate
ρ_{rrha}	Relative density of RHA
ρ_{w}	Density of water
σ	Standard deviation
τ_{bm}	Maximum bottom shear stress
τ_{cmy}	Critical mortar yield stress needed to avoid segregation
τ_{y}	Yield stress

Chapter 1

Introduction

1.1 General

Advancements in concrete technology have resulted in the development of a new type of concrete, which is known as self-consolidating high performance concrete (SCHPC). The merits of SCHPC are based on the concept of self-consolidating and high performance concretes. Self-consolidating concrete (SCC) is a flowing concrete that spreads through congested reinforcement, fills every corner of the formwork, and is consolidated under its self-weight (Khayat 1999). SCC requires excellent filling ability, good passing ability, and adequate segregation resistance. But it does not include high strength and good durability as essential performance criteria. Conversely, high performance concrete (HPC) has been defined as a concrete that is properly designed, mixed, placed, consolidated, and cured to provide high strength and low transport properties or good durability (Russell 1999). HPC exhibits good segregation resistance. But HPC does not provide excellent filling ability and passing ability, and therefore needs external means such as rodding or vibration for proper consolidation. Hence, a concrete that fulfills the performance criteria of both SCC and HPC can be referred to as SCHPC. An SCHPC is that concrete, which offers excellent performance with respect to filling ability, passing ability, segregation resistance, strength, transport properties and durability.

SCHPC is produced by exploiting the benefits of high-range water reducer (HRWR) and supplementary cementing material (SCM). The use of HRWR is essential to produce SCHPC. A HRWR contributes to achieve excellent filling ability and passing ability. In addition, SCMs are incorporated in SCHPC mostly to enhance the strength and durability of concrete. It may also contribute to attain good segregation resistance. In Canada and other countries, several well-known SCMs such as silica fume, ground granulated blast-furnace slag, and fly ash have been used to produce SCHPC (Bouzoubaâ and Lachemi 2001, Khayat 2000, Okamura and Ozawa 1994, Persson 2001). In comparison, the use of rice husk ash (RHA) in SCHPC is very limited. RHA is obtained by controlled burning of rice husks,

which are agricultural wastes generated in the rice-milling industry. It has been found that RHA provides dramatic improvements in hardened properties and durability of concrete (Mehta and Folliard 1995, Maeda et al. 2001). Similar effects might be observed when RHA is used in SCHPC. SCMs are also essential for high strength and high durability of SCHPC. Moreover, the expense of some SCMs such as silica fume and high reactivity metakaolin increases the overall material cost of SCHPC. Therefore, the use of less-expensive RHA is more desirable to decrease the overall production cost of SCHPC. The usage of RHA also minimizes the environmental burden resolving vast waste disposal problems caused by rice milling industries. The recent yearly production of rice in the world is about 560 million metric tons (Vegas 2004). Rice husk constitutes approximately one fifth of the dried rice (Mehta 1992). Therefore, about 120 million metric tons of rice husks are available annually for disposal. This is causing a huge environmental load for rice-producing countries, which can be reduced if RHA is used in concrete production. Thus, the incorporation of RHA in SCHPC will be a novel solution to the environmental problem caused by rice husks. Also, the use of RHA lowers the demand for cement in construction industry, and thus reduces the cost of cement production and lessens the environmental pollution caused by cement factories. Hence, RHA not only improves concrete properties and durability, but also provides substantial economic and environmental benefits. Yet, no comprehensive research has been conducted to explore the potential of RHA by investigating its effect on fresh and hardened properties and durability of SCHPC.

The present study has attempted to develop SCHPCs utilizing RHA as a SCM. The key properties of SCHPCs and their binder paste and mortar components have been determined in this study. In particular, the effects of RHA on various properties of different binder pastes, mortars and SCHPCs have been examined. A simplified mixture proportioning process for SCHPC has been developed. New and modified test approaches have been applied to determine several properties of binder pastes, mortars and SCHPCs. The test apparatus have been developed to measure the filling ability, passing ability, and segregation resistance of SCHPCs. In addition, empirical models have been developed for the filling ability and compressive strength of SCHPC. The outcome of this study will extend the scope of SCHPC, and thus generate new opportunities for the construction industry. Although there

is not a large source of RHA in Canada, the findings of the present study will be useful for the rice-producing countries.

1.2 Scope of the Thesis

The contents of the thesis are given in ten chapters.

Chapter 1 introduces SCHPC with a short overview of the present research and briefly presents the scope of the thesis.

Chapter 2 presents a background of SCHPC, highlights the major issues of SCHPC, describes various constituent materials of SCHPC including their key aspects, identifies several research needs, and gives the research objectives.

Chapter 3 gives an overview of the research program and procedures for experimental investigation and development of test apparatus, modeling, and mixture design.

Chapter 4 discusses the selection and testing of constituent materials, describes the preparation and testing of aggregate blends, presents the characteristics of constituent materials and aggregate blends, and emphasizes their usefulness.

Chapter 5 presents the formulation, preparation and testing of various binder pastes, gives the test results for the filling ability of the pastes, discusses the significance of these results, highlights the effects of HRWR, RHA and water-binder (W/B) ratio on the filling ability of the pastes, reports the saturation dosage and water reduction capacity of HRWR, and depicts the water demand and suitability of RHA.

Chapter 6 presents the formulation, preparation and testing of various mortars, provides the test results for the filling ability and air content of the mortars, discusses the importance of these results, highlights the effects of HRWR, AEA, RHA and W/B ratio on the filling ability and air content of the mortars, focuses on the acceptability of saturation dosages of HRWR obtained from flow cone test of binder pastes, and depicts the suitability of RHA.

Chapter 7 presents the design and proportioning process of various concrete mixtures, and reports the primary and adjusted mixture proportions including the dosages of chemical admixtures.

Chapter 8 describes the development of flowing ability test apparatus, depicts the preparation and testing of various fresh concretes, presents the test results for the key fresh

properties of various SCHPCs including air-void stability, and discusses the significance of these results. In addition, this chapter discusses the effects of HRWR, AEA, RHA, W/B ratio and air content on the fresh properties of SCHPC, highlights the air-void stability in fresh SCHPC including the effects of re-mixing and filling ability, demonstrates inverted slump cone apparatus with test procedure and performance criteria for filling ability and passing ability, and develops correlations among several properties of fresh SCHPCs. This chapter also provides the correlations between flow properties of SCHPC and its paste and mortar components, gives the relationship between estimated and actual AEA dosages of various SCHPCs, establishes a model for filling ability and discusses it validity and application, and reports the optimum RHA content.

Chapter 9 presents the preparation of hardened test specimens, describes the test setup and testing of various hardened concretes, discusses the test results for hardened properties of various SCHPCs, highlights the importance of these results, discusses the effects of RHA, W/B ratio and air content, shows the relationships between different hardened properties, establishes a model for compressive strength and discusses its validity and application, and gives the optimum content of RHA.

Chapter 10 describes the development of a simplified column apparatus including the test procedure and performance criteria. This chapter also depicts the testing of several SCHPCs for segregation resistance, describes the segregation test results, compares the performance of sieve and column tests, discusses the effects of RHA, W/B ratio and VEA, and gives the optimum RHA content to produce segregation-resistant SCHPC.

Chapter 11 presents a mixture design procedure for SCHPC, highlights the principles and performance requirements of mixture design, and depicts materials selection and requirements for mixture composition. In addition, this chapter gives a design example and discusses the limitation of the mixture design procedure.

Chapter 12 provides a summary of the research findings, presents the contributions, and gives several recommendations for future study.

Chapter 2

Literature Review and Research Objectives

2.1 General

Self-consolidating high performance concrete (SCHPC) is relatively a new building material in the construction industry. This chapter presents a background and review of SCHPC. It primarily gives the definition and briefly describes the characteristics, advantages, applications, and economy of SCHPC. Then it provides a short background of SCHPC; depicts the basic principles, production approaches, flowing ability and microstructure of SCHPC; focuses on the performance criteria and material aspects of SCHPC; justifies the need for a different approach and presents the current methods for designing SCHPC; and discusses the mixing and stability of SCHPC. Also, this chapter highlights major fresh and hardened properties, and states the curing and testing issues of SCHPC. Finally, this chapter emphasizes certain modeling approaches, presents the research needs for SCHPC, and sets the research objectives.

2.2 Self-consolidating High Performance Concrete

The development of SCHPC has implied significant changes in the conceptual approach and construction methods for concrete structures, and opened new opportunities for design. The definition, characteristics, advantages, applications and economy of SCHPC are briefly discussed below.

2.2.1 Definition

Self-consolidating concrete (SCC) is a special type of concrete that spreads through the congested reinforcement, reaches every corner of the formwork, and is consolidated under its own weight. It provides excellent filling ability and passing ability, and exhibits good segregation resistance (Khayat 1999). When the performance criteria of high strength and durability for high performance concrete (HPC) are included in SCC with a low water-binder (W/B) ratio, it can be referred to as SCHPC. A SCHPC is that special concrete, which would

give the optimized performance with respect to flow characteristics, strength, transport properties and durability consistent with the requirements of service life under a given set of materials, loads and exposure conditions.

2.2.2 Characteristics

SCHPC differs from ordinary concrete with respect to its performance in fresh and hardened states that are mainly driven by exceptional material components and mixture proportions. It incorporates several special ingredients such as high-range water reducer (HRWR), supplementary cementing material (SCM), and viscosity-enhancing admixture (VEA) in addition to the basic materials used for ordinary concrete. The proportions of component materials in SCHPC are also significantly different from those of ordinary concrete (Okamura and Ozawa 1995; Okamura and Ouchi 2003). SCHPC includes a much higher quantity of binder, a lower water content, a greater fine aggregate content, and a lesser amount of coarse aggregate than ordinary concrete. The W/B ratio of SCHPC is also much lower than that of ordinary concrete. While ordinary concrete has the W/B ratio mostly above 0.50, SCHPC needs a W/B ratio that typically ranges from 0.20 to 0.40 (Persson 2001, Zhu and Bartos 2003).

2.2.3 Advantages

Self-consolidating high performance concrete offers many advantages. Some of these are as follows (Cameron 2003, EFNARC 2002, Okamura and Ouchi 2003):

a. Flows through and around reinforcing steel under self-weight and eliminates the need for vibration equipment or any other means of consolidation.
b. Reduces noise and improves the construction environment in the absence of concrete vibrating equipment.
c. Requires fewer laborers for transport and placement of concrete, and thus becomes more economical.
d. Eases concrete placement operations, and thus increases construction ability.
e. Reduces the volume of excavation and shoring involved in foundation trenches.
f. Allows the formwork to last longer due to the elimination of vibration equipment.

g. Favors the placement of a large amount of reinforcement in small sections such as those most often seen in high-rise buildings.
h. Saves a large quantity of concrete due to the reduced section of structural components.
i. Provides good finishing without any surface pores and improves the aesthetical appearance of concrete.
j. Results in greater strength due to enhanced compactness and reduced porosity.
k. Confers high early strength, allows a quicker reuse of formwork, and thus enhances the production rate.
l. Imparts improved water-tightness, and thus offers reduced transport properties and enhanced durability.
m. Simplifies the construction of the structures of complicated design due to the easement in casting and molding of the complex architectural forms.

2.2.4 Applications

Self-consolidating high performance concrete has been applied successfully in building, bridge, culvert, tunnel, diaphragm wall, tank, dam, and precast concrete products. It has also been used in repair and rehabilitation of existing structures. Several applications of SCHPC are mentioned in Table 2.1:

Table 2.1: Applications of self-consolidating high performance concrete

Structure	Location	Reference
Anchorages of Akashi-Kaikyo suspension bridge	Japan	Okamura and Ouchi 2003
Towers of a cable-stayed bridge	Japan	Okamura et al. 2000
Wall of a large LNG tank belonging to Osaka Gas Company	Japan	Okamura et al. 2000
Beam repair in the Webster parking structure in downtown Sherbrooke	Canada	Khayat 2000
Rehabilitation of slab and wall elements in a hydroelectric power plant	Canada	Khayat 2000
Continuous underground diaphragm walls	Japan	Seto et al. 1997
Precast cladding panels	UK	Watson 2003
Thin-wall prestressed concrete products	Japan	Nagai et al. 1999

2.2.5 Economy

The overall material cost of SCHPC is higher than that of ordinary concrete. The cost involved in quality control is also high in case of SCHPC due to instability problems. However, the increased cost for materials and quality control can be compensated through concrete quantity savings and productivity improvement. SCHPC is generally stronger than ordinary concrete. Therefore, the structural components will be made of thinner sections, and thus savings can be attained due to a less amount of concrete. The productivity improvement also reduces the cost involved in formwork. Moreover, SCHPC offers better mechanical and durability performance and greater service life than ordinary concrete, and hence can be acceptable over the increased initial cost. If the cost analysis is conducted based on the lifecycle costing, the cost-effectiveness of SCHPC in construction industry will be apparent.

The use of SCHPC in high-rise building, bridge, offshore platform and other special structures will be economical over the increased cost of materials and more rigorous quality control. In fact, the overall cost will be low due to drastic reduction in the geometry of the structural components, reduced number of laborers, decrease in reinforcement percentage, ease of conveyance and placement, and reduction in formwork and shoring. Indirect benefits can also be gained through the durability improvement leading to maintenance savings. The maintenance and repair costs are expected to be low in SCHPC. Thus, a lot of savings will be achieved particularly for the large projects if SCHPC is used (Ouchi et al. 2003).

2.3 Background of Self-consolidating High Performance Concrete

The construction of concrete structures needs thorough placement and good consolidation of fresh concrete to obtain good hardened properties and durability. However, the proper placement and consolidation were not always achievable with ordinary concretes, even though placed by skilled laborers. The lack of skilled laborers was also a great concern in construction industry. Then, the concept of SCHPC first came out in Japan to build durable concrete structures and to offset the growing shortage of skilled labors.

Okamura and Ozawa (1995) advocated the development of SCHPC in 1986 and developed the first prototype in 1988. However, the development of SCHPC did not occur rapidly. The literature shows that self-leveling and segregation-free concretes were produced using HRWR more than one decade before the development of SCHPC (Collepardi 1976).

These concretes were very similar to SCHPC in fluidity, cohesiveness, and low tendency to segregation. The stability of these concretes was maintained successfully despite the absence of VEA. However, the precursors of SCHPC were largely dependent of high paste volume. Therefore, the overall cost was very high and the application remained limited. Thereafter, the invention of more effective HRWR and VEA made the advent of modern SCHPC (Collepardi 1994, Khayat and Guizani 1997). The technology of SCHPC has been tailored and optimized in Japan during last decade. The Japanese concrete industry commercialized SCHPC under the trade names of "Non-vibrated Concrete," "Super-quality Concrete," and "Biocrete" (Bartos 2000). At the same time, SCHPC has become familiar in North America, Europe, and other parts of the world (Shah et al. 2002, Wallevik and Nielsson 2003).

2.4 Basic Principles of Self-consolidating High Performance Concrete

SCHPC can be produced by achieving self-consolidation capacity (self-compactability) through optimum flowing ability (filling ability and passing ability) and optimum segregation resistance, as illustrated in Figure 2.1. The optimum flowing ability can be obtained by using HRWR, limited coarse aggregate content, and an increased amount of cementing materials at low W/B ratio (Dehn et al. 2000, Okamura and Ouchi 2003). Conversely, the optimum segregation resistance can be attained either by limited coarse aggregate content and increased cementing materials at low W/B ratio, or by using a VEA (Okamura and Ozawa 1994, Okamura and Ozawa 1995). In addition, the aggregate size influences both flowing ability and segregation resistance of SCHPC (Bui et al. 2002, Saak et al. 2001). A reduced aggregate size is preferable to obtain optimum flowing ability (particularly passing ability) and optimum segregation resistance. The flowing ability and segregation resistance of SCHPC are also interrelated. Both poor and high segregation resistances may decrease the flowing ability, whereas a high flowing ability may cause segregation in SCHPC.

The main parameters that influence the flowing ability and segregation resistance of SCHPC are the volume concentrations of cementing materials and coarse aggregates. The limited coarse aggregate content and the increased amount of cementing materials at low W/B ratio result in higher relative distance between aggregate particles. Thus, the frequency of contact and collision between coarse aggregates decreases during the deformation of plastic concrete (Okamura et al. 2000). This greatly reduces the internal stress and thus

increases the flowing ability of concrete. However, the increased flowing ability tends to produce very high fluidity with low viscosity, which reduces the segregation resistance of SCHPC. Therefore, the flowing ability and segregation resistance of fresh SCHPC mixture must be balanced in such a way so that the self-consolidation capacity is achieved without any segregation. An adequately viscous paste is required to inhibit the segregation of coarse aggregates. The optimum segregation resistance with a sufficiently high viscosity hinders the separation of coarse aggregates from the paste, while maintaining a good flowing ability in concrete (Okamura and Ozawa 1994). It also prevents coarse aggregates from approaching each other and thereby eliminates the localized increase in internal stress. The optimum flowing ability and segregation resistance can be ensured by the proper use of coarse aggregates, cementing materials with a low W/B ratio, HRWR and VEA.

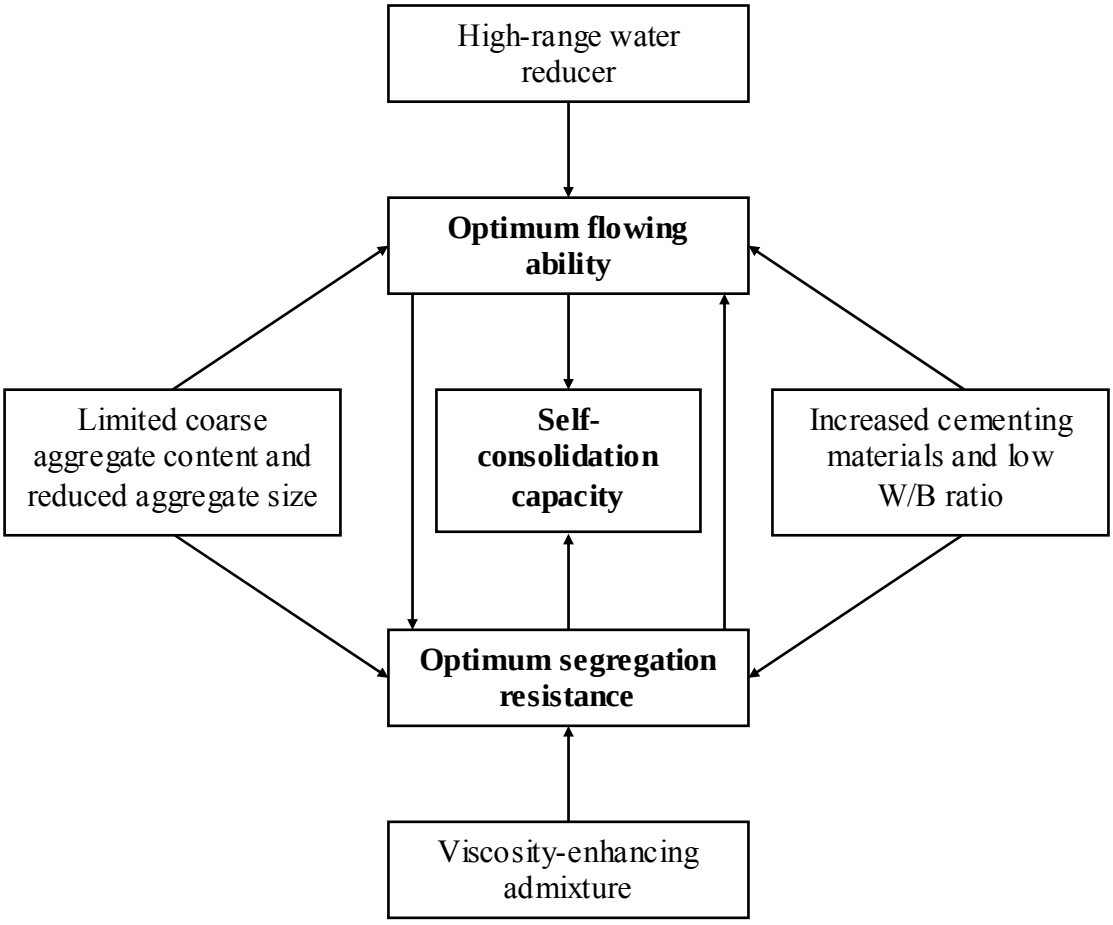

Figure 2.1: Basic principles of SCHPC (adapted from Okamura and Ozawa 1995)

2.5 Approaches to Obtain Self-consolidating High Performance Concrete

Three approaches have been identified to produce SCHPC:

a. Powder-type SCHPC using limited coarse aggregate content and increased amount of binder (Okamura and Ouchi 2003): This is achieved by using greater amount of fine aggregate and cementing material along with HRWR at low W/B ratio.
b. VEA-type SCHPC using VEA (Okamura and Ozawa 1995): A VEA is used with HRWR without increasing the content of binder or cementing material to produce SCHPC.
c. Combination-type SCHPC using both VEA and increased amount of binder (Shindoh and Matsuoka 2003): A VEA and an increased amount of cementing material are used with HRWR at low W/B ratio.

2.6 Flowing Ability of Self-consolidating High Performance Concrete

The flowing ability is a property of fresh SCHPC that allows it to flow into and fill the spaces within the formwork, or pass through tight openings between reinforcing bars under self-weight, and without any vibration or any other means of consolidation (EFNARC 2002). The flowing ability of SCHPC is controlled by its rheological parameters such as yield stress and plastic viscosity, which can be determined using a rheometer (Geiker et al. 2002) or by testing the slump, slump flow and slump time of concrete (Chidiac et al. 2000). Nevertheless, SCHPC exhibits exceptional flowing ability due to its low yield stress and moderate plastic viscosity (Nehdi et al. 2003a, Khayat 1999). In general, HRWR improves the flowing ability of SCHPC by reducing the yield stress and plastic viscosity. However, excessive dosage of HRWR results in very high fluidity that may cause an instability or segregation problem. The incorporation of a suitable SCM is an option to improve the segregation resistance, and thus to maintain stability as well as good flowing ability in fresh SCHPC. Most common SCMs such as silica fume, ground granulated blast-furnace slag, fly ash and limestone filler have been used to produce SCHPC with a good flowing ability (Lachemi et al. 2003, Okamura and Ozawa 1994). Similarly, rice husk ash (RHA) can be used in SCHPC. RHA may provide good benefits through increased plastic viscosity, which is required to prevent segregation in SCHPC. However, RHA possesses an extremely high specific surface area in comparison to other SCMs (Zhang and Malhotra 1996). Hence, RHA may cause a flowing ability problem in SCHPC that can be overcome using an efficient HRWR, such as polycarboxylate

copolymer. However, no comprehensive research has been conducted to explore the effects of RHA on the flowing ability of SCHPC.

The flowing ability of SCHPC is related to the flow behavior of its paste and mortar components. This is because SCHPC can be considered as a combination of coarse aggregates and mortar, or an aggregate skeleton and a matrix of paste. Many researchers investigated the flow properties of paste and mortar to design SCHPC with a good flowing ability (Domone 2006, Gettu et al. 2001, Kim et al. 1997, Okamura and Ozawa 1995). But none of these studies reported the correlation between flowing ability of SCHPC and its paste or mortar component. An earlier study reported that the flowing ability of SCHPC is well-correlated with the flowing ability of its mortar fraction (Jin and Domone 2002). Similar result can be found for SCHPC and its paste component. Unfortunately, limited studies have been conducted to establish the relationship between the flowing ability of SCHPC and its paste component incorporating RHA.

2.7 Microstructure of Self-consolidating High Performance Concrete

Concrete was considered, for a long time, as a purely two-phase material: paste and aggregate. Later a more rational and realistic approach took into account the existence of a particular zone of hydrated paste in the proximity of aggregates. This is called 'interfacial transition zone'. Indeed, from the microstructural standpoint, it is helpful to consider hardened concrete made up of three phases, namely aggregate, bulk cement paste and interfacial transition zone (Mehta and Aïtcin 1990). The interfacial transition zone mainly consists of a water film, a calcium hydroxide layer on the aggregate side, and a porous paste matrix layer between calcium hydroxide layer and bulk paste matrix (Hearn et al. 1997). This is shown in Figure 2.2.

Microstructural testing of fractured samples of ordinary concrete shows that the hydrated cement paste contains many large pores. During cement hydration, massive hexagonal lime crystal plates develop quickly within these large pores. Ettringite needles, monosulfonaluminate platelets and fibrous crystals of calcium silicate hydrates are also seen (Aïtcin 1997). In HPC, these hexagonal lime crystals, ettringite needles and fibrous CSH crystals cannot develop in a more homogeneous and compacted paste. Furthermore, the interfacial transition zone is more porous and crystallized in ordinary concrete due to the

presence of excessive water surrounding the aggregate. The water film usually surrounds the aggregates during mixing. This can also be supplemented by the entrapped bleed water. As a result, the water content of the paste in interfacial transition zone becomes higher than that of bulk paste matrix. In HPC, a very intimate contact between the aggregate and the hydrated cement paste develops. The hydrated cement paste in the transition zone has almost the same texture as that between the aggregates. This results in more homogeneous microstructure in concrete. In fact, there remain no preferential channels of penetration in the microstructure of HPC through which the aggressive agents can enter the concrete.

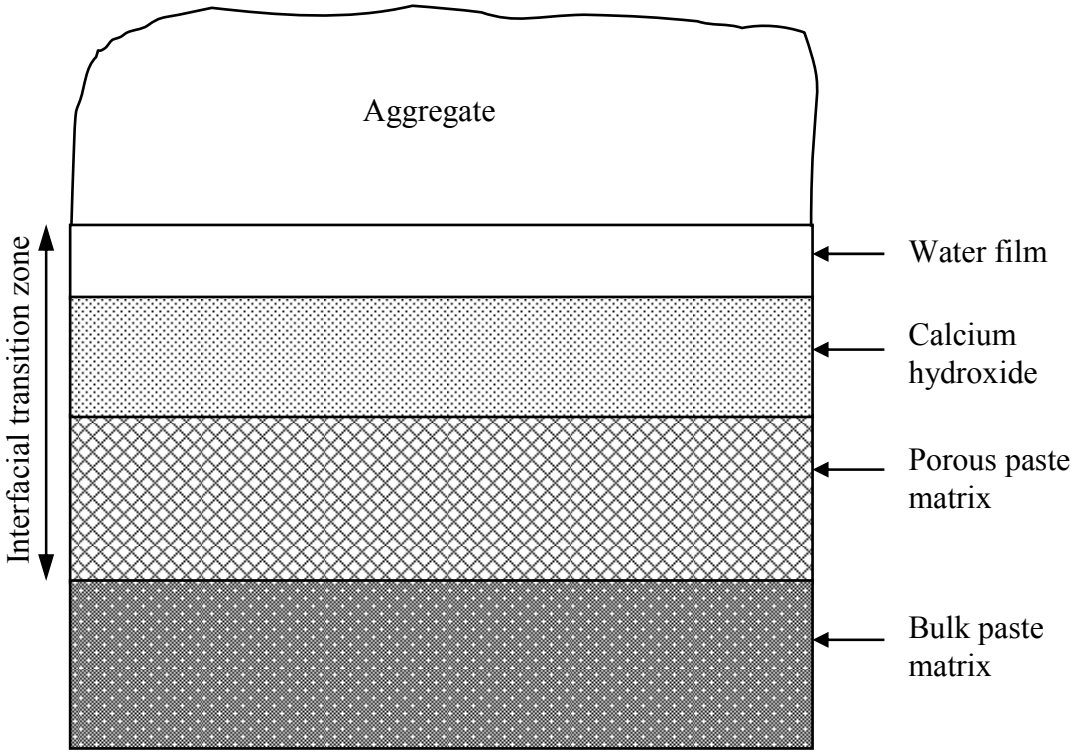

Figure 2.2: Schematic representation of aggregate-interfacial transition zone-bulk paste matrix microstructure (adapted from Hearn et al. 1997)

The rich microstructure of HPC is mainly due to the processes of filling in the capillary pores at reduced water content or low W/B ratio with HRWR. Also, the presence of SCM enhances capillary segmentation, pore refinement and porosity reduction due to micro-filling and pozzolanic effects. It is likely that a microstructural development similar to that of HPC (Moranville-Regourd 1994) also occurs in SCHPC, thus creates a rich microstructure. In the presence of HRWR and SCM, the microstructure of SCHPC can be enriched due to the

following features: formation of a continuous lattice of dense particles, formation of an amorphous and homogeneous matrix, pore refinement and porosity reduction, formation of a strong and dense transition zone, confinement of aggregates, presence of very little free water, and existence of very low free lime content. Figure 2.3 illustrates how SCM and HRWR can develop a rich microstructure in SCHPC.

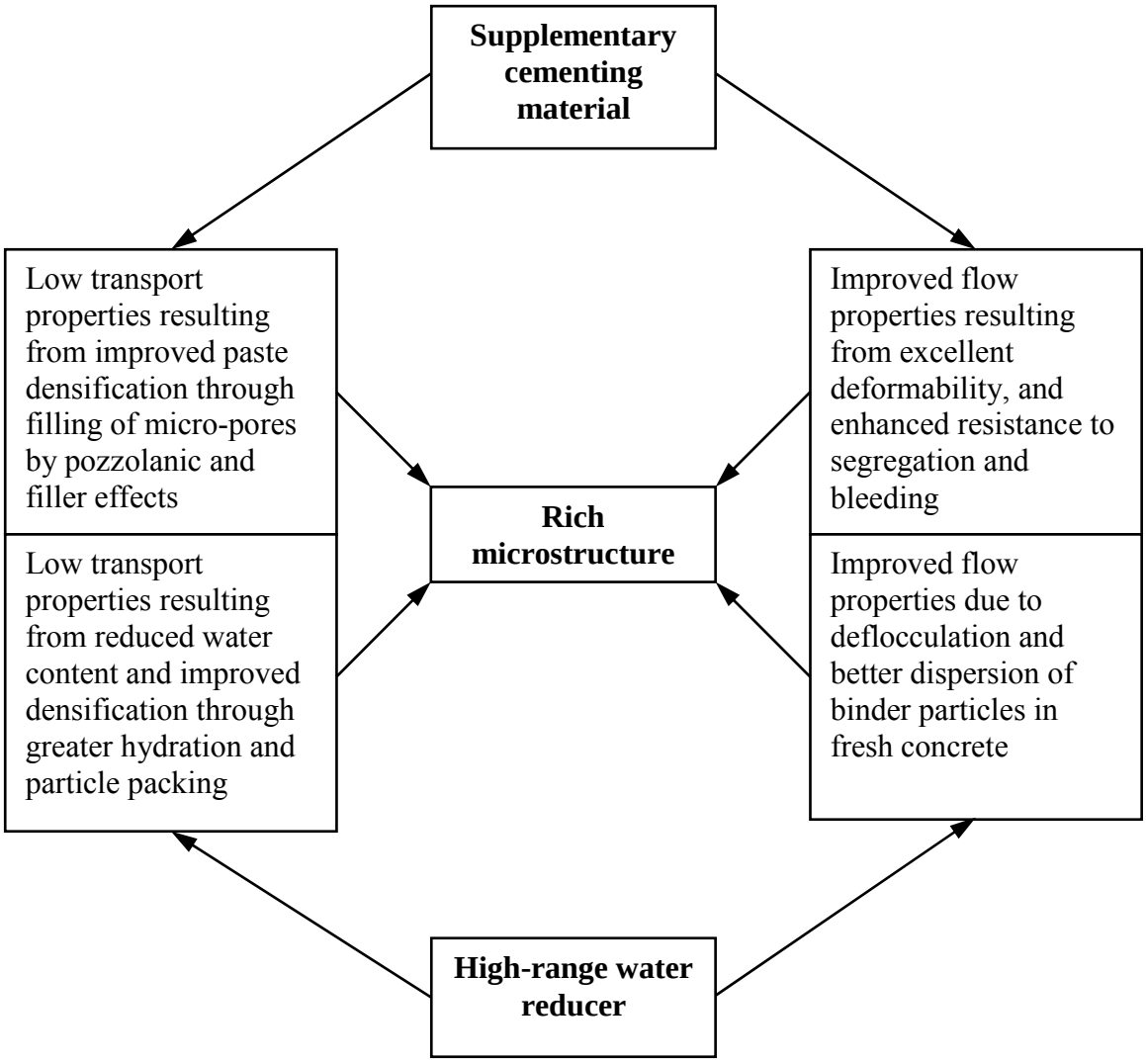

Figure 2.3: Development of rich microstructure in self-consolidating high performance concrete

2.8 Performance Criteria for Self-consolidating High Performance Concrete

SCHPC is a combination of SCC and HPC. In the fresh state, SCHPC must fulfill the performance criteria of SCC. SCHPC must also satisfy the performance criteria of hardened

HPC to achieve good hardened properties and high durability. Table 2.2 presents various performance criteria that may be specified for SCHPC (Brameshuber and Uebachs 2001, Bui et al. 2002, EFNARC 2002, Grünewald et al. 2004, Hearn 1996, Hearn et al. 1994, Khayat 2000, Kosmatka et al. 2002, Holland 1993, SCCEPG 2005, Perez et al. 2002, Shetty 2001, Vanwalleghem et al. 2003).

Table 2.2: Performance criteria for self-consolidating high performance concrete

Method	Property	Performance criteria
SCC properties		
Slump	Filling ability	250 - 280 mm
Slump flow	Filling ability, segregation resistance	550 - 850 mm
V-funnel flow	Filling ability, segregation resistance	5 - 14 s
Orimet flow with 80 mm orifice	Filling ability, segregation resistance	2.5 - 9 s
Filling percentage in fill-box	Filling ability, passing ability	90 - 100%
Blocking ratio in L-box	Filling ability, passing ability, segregation resistance	> 0.8
Filling height in U-box	Filling ability, passing ability	≤ 30 mm
Slump cone – J-ring flow	Reduction in slump flow as a measure of passing ability	≤ 50 mm
Penetration depth	Segregation resistance	≤ 8 mm
Sieve segregation	Segregation resistance	≤ 18 %
HPC properties		
Air content by pressure method	Fresh air content	4 to 8 %
Axial compression on cylinders	Early-age compressive strength	> 20 MPa
	28 and 91 days compressive strength	> 40 MPa
Ultrasonic pulse velocity by PUNDIT	Physical quality or condition (packing, uniformity, etc.)	≥ 4575 m/s
Porosity by fluid displacement method	Total porosity as an indicator of strength and transport properties	7 - 15 %
Absorption by water saturation technique	Water absorption as an indicator of durability	3 - 6 %
True electrical resistivity by Wenner probe	Electrical resistance to corrosion	> 5 - 10 kΩ-cm
Rapid chloride ion penetration	Electrical charged passed as an indicator of corrosion resistance	< 2000 C
Normal chloride ion penetration at 6 months	Penetrated chloride value as an indicator of corrosion resistance	< 0.07 %
Durability factor after 300 cycles of freeze-thaw	Resistance to freezing and thawing	> 0.80

2.9 Material Aspects for Self-consolidating High Performance Concrete

Self-consolidating high performance concrete consists of cement, aggregates, water, and chemical admixture and/or SCM. Most common chemical admixtures used for SCHPC are HRWR, VEA and AEA. Aggregates, cement, water, and HRWR are the principal materials where as SCM, VEA, AEA, and other chemicals can be used as the optional materials.

The production of SCHPC involves more stringent control on the selection of constituent materials than ordinary concrete to meet the requirements for fresh and hardened properties and durability. The reason is that the performance of SCHPC largely depends on the characteristics of its ingredients. The suitable properties of the constituent materials are the defining factors to achieve the expected benefits from SCHPC. Indeed, the constituent materials play important roles when they are combined in concrete. Therefore, suitable constituent materials should be selected and specifications must be given more enforcement to produce SCHPC. The following sections briefly illustrate the component materials of SCHPC emphasizing their properties.

2.9.1 Coarse aggregate

The aggregates retained on the 4.75-mm (No.4) sieve are defined as coarse aggregates (ASTM C125, 2004). They are granular materials, such as gravel or crushed stone, and are usually used with fine aggregate and cementing material or binder to produce concrete. As in any concrete, coarse aggregates are also a key component of SCHPC. Coarse aggregates significantly influence the performance of SCHPC by affecting the flowing ability, segregation resistance, and strength of concrete (Noguchi et al. 1999, Okamura and Ozawa 1995, Xie et al. 2002).

2.9.1.1 Physical properties

The physical characteristics such as the size, shape, surface texture, and porosity of coarse aggregates affect the properties and durability of concrete. The nominal maximum size for SCHPC can be 20 or 25 mm (Uomoto and Ozawa 1999). However, the smaller size is preferable to produce higher strength (ACI 211.4R-93, 2004; Kwan 2000) and to reduce segregation in fresh SCHPC (Bonen and Shah 2005). The shape and texture of coarse aggregates influence the packing of combined aggregates in SCHPC (Gettu et al. 2001). The

shape of the coarse aggregates also considerably affects the properties of SCHPC. Round aggregates are better than angular aggregates for flowing ability of SCHPC, since they induce less yield stress and plastic viscosity in concrete mixture due to less inter-particle friction (Geiker et al. 2002, Mindess et al. 2003). Conversely, rough and angular aggregates are conducive to high strength and strong interfacial bond due to rough surface texture and interlocking characteristic (Taylor et al. 1996). But the surface texture, aspect ratio, and angularity of angular aggregates are not conducive to the flowing ability of SCHPC because of greater water demand (Xie et al. 2002) and increased yield stress and plastic viscosity (Geiker et al. 2002). However, the required flowing ability can be maintained in the presence of HRWR.

The porosity and reactivity of coarse aggregate are also of great concerns for the durability of SCHPC. Porous aggregates produce less strength and less resistance to freezing and thawing. Some aggregates may cause alkali-aggregate reactions. Therefore, the selection of coarse aggregates should be conducted carefully. In general, good quality coarse aggregates should be used to enhance strength, aggregate-matrix bond, flow properties, and durability of SCHPC. The ASTM and CSA have specified some physical requirements for coarse aggregates (ASTM C33, 2004; CSA A23.1, 2004; CSA A23.2, 2004). These requirements are also applicable for the coarse aggregates to be used in SCHPC.

2.9.1.2 Gradation

The gradation of coarse aggregates affects the flow properties and segregation resistance of SCHPC. The well-graded coarse aggregates contribute to produce the optimum mixture with least particle interference (Shilstone, Sr. 1990), and thus enhance the flowing ability and reduce the tendency of segregation in fresh concrete (Neville 1996). They also improve the hardened properties and durability of concrete due to dense particle packing (Tasi et al. 2006). In addition, the gradation influences the volume content of the coarse aggregates to be used in SCHPC. The volume content of coarse aggregates can be increased when they are well-graded (Okamura and Ozawa 1995). It indicates that a lesser amount of mortar is required for well-graded coarse aggregates to achieve the target filling ability and passing ability in SCHPC.

The ASTM and CSA (ASTM C33, 2004; CSA A23.1, 2004) have the gradation requirement for the coarse aggregates to be used in concrete. This gradation requirement is also applicable for the coarse aggregates to be used in SCHPC. The reports based on the laboratory and field experience revealed that the coarse aggregates meeting ASTM C 33 (2004) grading specification can contribute to improve the placement, finishing and durability performance of concrete (Shilstone, Sr. 1990; Shilstone, Sr. and Shilstone, Jr. 1993).

2.9.2 Fine aggregate

Fine aggregates are the second ingredient of aggregate phase in SCHPC. Sand is the most commonly used fine aggregate for concrete. Fine aggregates pass the 4.75 mm (No. 4) sieve but are retained on the 75 μm (No. 200) sieve (ASTM C125, 2004). They occupy a greater volume in SCHPC, as compared to ordinary concrete (Bonen and Shah 2005). Similar to coarse aggregates, fine aggregates also influence the performance of SCHPC. They increase the flowing ability and segregation resistance when used at a suitable amount (Okamura and Ozawa 1995, Su et al. 2002). In addition, they modify the strength of concrete when used in varying proportion with cement and coarse aggregates (Xie et al. 2002).

2.9.2.1 Physical properties

The physical properties of fine aggregate influence the performance of concrete in fresh and hardened states. For instance, the particle shape, surface texture, surface area, and void content affect the mixing water requirement and compressive strength of concrete (ACI 211.4R-93, 2004). Also, the physical characteristics of fine aggregate considerably influence the mortar flow and thus it may affect the flowing ability of SCHPC (Hu and Wang 2005, Okamura and Ozawa 1995). The published guidelines show that fine aggregates may produce more significant effect than coarse aggregates on the fresh properties of SCHPC (SCCEPG 2005). Therefore, the physical properties of fine aggregate should be conducive to the performance of SCHPC.

The fine aggregates selected for SCHPC should be sharp, angular, chemically inert, sound, low absorbent, and free from deleterious substances to attain high strength and good durability. However, the sharp and angular fine aggregates are not beneficial to the flowing

ability of SCHPC, since they increase the viscosity of mortar phase (Westerholm 2006). This adverse effect can be minimized using increased HRWR dosage and reduced fine aggregate content. Nevertheless, the ASTM and CSA have specified the physical requirements for fine aggregates (ASTM C33, 2004; CSA A23.1, 2004; CSA A23.2, 2004). These requirements are also appropriate to select the fine aggregates for SCHPC.

2.9.2.2 Gradation

Gradation of fine aggregates represents the size distribution of particles in the range of 4.75 mm to 150 μm. The gradation of fine aggregates has an effect on the viscosity of mortar, and thereby on the flowing ability of fresh concrete (Murata and Kikukawa 1992). The poor sand grading affects the water and cement contents of concrete, and causes most mixing problems (Shilstone, Sr. and Shilstone, Jr. 2002). In general, the fine aggregates selected for SCHPC should be well-graded to reduce the paste content (SCCEPG 2005). The well-graded fine aggregates increase the flow of mortar (Hu and Wang 2005), and hence may improve the flowing ability of SCHPC. Furthermore, the well-graded fine aggregates contribute to improve the packing density, and thus the hardened properties and durability of concrete (Tasi et al. 2006).

The ASTM and CSA (ASTM C33, 2004; CSA A23.1, 2004) have specified the requirement of fine aggregate grading, which is valid for SCHPC. The laboratory and field experience showed that the gradation of fine aggregates meeting ASTM C 33 (2004) grading specification does not adversely affect the quality of concrete (Shilstone, Sr. and Shilstone, Jr. 1993). The gradation of fine aggregates is usually determined by sieve analysis. It introduces a parameter known as 'fineness modulus' for arriving at satisfactory gradation. The 'fineness modulus' is a ready index of the coarseness or fineness of fine aggregates. The larger the index, the coarser are the fine aggregates. A fineness modulus in the range of 2.5 to 3.2 is generally recommended for high-strength high performance concrete (ACI 211.4R-93, 2004; Nawy 1996), and can also be used for SCHPC.

2.9.3 Portland cement

Portland cement is most widely used to produce various types of concrete. It is a hydraulic cement, which is produced by pulverizing clinker consisting of calcium silicates, and usually

containing calcium sulfate as an interground addition (ASTM C150, 2004). Portland cement is also a key component of SCHPC. It is used alone or in combination with SCM to produce SCHPC. Portland cement improves the flowing ability of SCHPC when used with water to lubricate the aggregates (Okamura and Ozawa 1995). Portland cement can also affect the segregation resistance of SCHPC by affecting the density of cement paste matrix of concrete (Bonen and Shah 2005). After reacting with water, portland cement also reduces the porosity and results in a packed concrete mass leading to low transport properties and good durability (Neville 1996).

2.9.3.1 Physical properties

The physical properties of cement significantly influence the performance of concrete. This is also true for SCHPC. The cement used for SCHPC should have sound flow and setting properties. It should enhance the fluidity of concrete and should be free from false setting due to premature stiffening within a few minutes of mixing with water. Also, it should be compatible with the chemical admixtures such as HRWR, AEA and VEA.

Lump-free fresh cement should be used in SCHPC. The cement should possess carefully controlled fineness, and should produce low or moderate heat of hydration to control the volume changes in concrete (Struble and Hawkins 1994). The ASTM and CSA (ASTM C 150, 2004; CSA A23.1, 2004) have specified the physical property requirements for various portland cements, which are also useful to choose the proper cement for SCHPC.

2.9.3.2 Chemical composition

The chemical analysis of portland cement has revealed that it mostly consists of various oxide compounds. The major oxide compounds are lime, silica, alumina, and iron. In addition, two minor oxides namely sodium and potassium oxides are of some importance, particularly with regard to alkali-aggregate reactions in concrete. In addition, magnesia and sulfuric anhydrite can be present, although they are not beneficial constituents of cement. The typical chemical composition of portland cement is shown in Table 2.3. The ASTM and CSA (ASTM C 150, 2004; CAN/CSA A3001, 2003) have specified the chemical requirements for different types of portland cement. These requirements are also beneficial to select the appropriate cement for SCHPC.

Table 2.3: Typical chemical composition of portland cement (Brandt 1995)

Chemical		Mass content (%)
Name	Composition	
Calcium oxide (lime)	CaO	58 – 66
Silicon dioxide (silica)	SiO_2	18 – 26
Aluminum oxide (alumina)	Al_2O_3	4 – 12
Ferrous and ferric oxides (iron oxides)	Fe_2O_3 and FeO	1 – 6
Magnesium oxide (magnesia)	MgO	1 – 3
Sulfur trioxide (sulfuric anhydrite)	SO_3	0.5 – 2.5
Alkaline oxides (alkalis)	Na_2O and K_2O	≤ 1.0

2.9.4 Supplementary cementing materials

Supplementary cementing materials are finely divided materials, which contribute to the properties of the hardened concrete through hydraulic or pozzolanic activity, or both (CAN/CSA A3001, 2003). They are greatly beneficial for concrete properties and durability due to their effective physical and chemical effects on material packing and microstructure (Hassan et. al 2000, Khatri and Sirivivatnanon 1995, Mehta 1994). Indeed, the production of SCHPC cannot be achieved without using SCM, especially when high strength and good durability are the prime goal (Hooton 2000, Zhang and Malhotra 1996).

Supplementary cementing materials are classified as low reactive, cementitious or pozzolanic, or both cementitious and pozzolanic based on their role in hydration (Mindess et al. 2003). For example, limestone powder is low reactive, natural cement and hydraulic lime are cementitious, silica fume and Class F fly ash are pozzolanic, and ground granulated blast-furnace slag and Class C fly ash are both cementitious and pozzolanic SCMs. Based on the sources, SCMs are also categorized as natural and artificial. Limestone powder, volcanic tuffs, pumicite, calcined clay, opaline cherts, and shales are some of natural SCMs. The industrial by-products such as silica fume, fly ash, and ground granulated blast-furnace slag are frequently used as artificial SCMs. In addition, SCMs can be obtained from agricultural wastes such as RHA, and can be industrially manufactured such as high reactivity metakaolin. The artificial SCMs such as silica fume, ground granulated blast-furnace slag, and fly ash have most commonly been used in SCHPC (Bouzoubaâ and Lachemi 2001, Ghezal and Khayat 2002, Lachemi et al. 2003).

2.9.4.1 Physical requirements

The ASTM and CSA (ASTM C 618, 2004; ASTM C 989, 2004; ASTM C 1240, 2004; CAN/CSA A3001, 2003) have specified the physical requirements for natural, and most artificial SCMs such as silica fume, fly ash and ground granulated blast-furnace slag. These requirements mainly provide the limits for fineness, expansion or contraction, pozzolanic activity, uniformity, and reactivity. However, currently there are no ASTM or CSA physical requirements for RHA. Some of the physical requirements for silica fume given in ASTM C 1240 (2004) can be valid for RHA.

2.9.4.2 Chemical requirements

The ASTM and CSA (ASTM C 618, 2004; ASTM C 989, 2004; ASTM C 1240, 2004; CAN/CSA A3001, 2003) have specified the chemical requirements for silica fume, fly ash, ground granulated blast-furnace slag, and natural SCMs. These requirements mostly provide the limits for several chemical components and igneous loss. At present, there are no ASTM or CSA chemical requirements for RHA. However, the chemical requirements given for silica fume might be applicable to RHA due to their comparable chemical composition.

2.9.5 Rice husk ash

Rice husk ash is produced by incinerating the husks of rice paddy. Rice husk is a by-product of rice milling industry. Controlled incineration of rice husks between 500^0C and 800^0C produces non-crystalline amorphous RHA (Mehta and Monteiro 1993, Malhotra 1993). RHA is whitish or gray in color. The particles of RHA occur in cellular structure with a very high surface fineness. They have 90% to 95% amorphous silica (Mehta 1992). Due to high silica content, RHA possesses excellent pozzolanic activity.

2.9.5.1 Physical properties

The physical properties of RHA largely depend on burning conditions. Particularly, the period and temperature of burning affect the microstructure and characteristics of RHA (Nagataki 1994). The partial burning of rice husks produces black RHA whereas the complete burning results in either white or grey RHA (Ismail and Waliuddin 1996). In addition, the uncontrolled burning at high temperature produces crystalline RHA, which

possesses poor pozzolanic property. Conversely, the controlled burning at about 500^0C to 800^0C results in non-crystalline or amorphous silica, which shows very high pozzolanic activity (Mehta and Monteiro 1993, Nagataki 1994). The burning condition also affects the relative density of RHA. The relative density of grey RHA obtained from complete burning is generally 2.05 to 2.11 (Ismail and Waliuddin 1996, Nehdi et al. 2003b).

The RHA particles are mostly in the size range of 4 to 75 μm (Mehta 2002). The majority of the particles pass 45-μm (No. 325) sieve. The median particle diameter typically ranges from 6 to 38 μm (Mehta 2002), which is larger than that of silica fume. However, unlike silica fume, the RHA particles are porous and possess a honeycomb microstructure (Zhang and Malhotra 1996). Therefore, the specific surface area of RHA is extremely high. The specific surface area of silica fume is typically 20 m^2/g whereas that of non-crystalline RHA can be in the range of 50 to 100 m^2/g (Mehta 1992).

2.9.5.2 Chemical composition

Rice husk ash contains a high amount of amorphous silica, which originally comes from the surfaces of the husk (Jauberthie et al. 2000) after burning in moderately oxidizing environment at controlled temperature (500^0C to 800^0C) for a suitable time length generally ranging from 15 minutes to 1 hour (Nagataki 1994). The silica content (SiO_2) of RHA ranges between 90 to 95%, which is similar to that of silica fume (Mehta 1992, Zhang et al. 1996). The typical chemical composition of RHA is given in Table 2.4.

Table 2.4: Typical chemical composition of rice husk ash (Mehta 2002)

Component	Mass content (%)
Silicon dioxide (SiO_2)	94.37
Aluminum oxide (Al_2O_3)	0.06
Ferric oxide (Fe_2O_3)	0.04
Calcium oxide (CaO)	0.48
Magnesium oxide (MgO)	0.13
Sodium oxide (Na_2O)	0.08
Potassium oxide (K_2O)	1.97
Phosphorus oxide (P_2O_5)	1.19
Titanium oxide (TiO_2)	0.02
Sulfur trioxide (SO_3)	0.01
Igneous loss	1.18

2.9.5.3 Role in concretes

The role of RHA in SCHPC is the same as that in any other concretes. In concrete, the RHA mainly serves as a microfiller, pozzolan, and viscosity modifier. The RHA particles can fill the voids between the larger cement grains because of their smaller size, as shown in Figure 2.4. However, the microfilling ability of RHA is not as effective as silica fume. This is because the RHA particles are much larger than the silica fume particles. The typical median particle size of RHA is about 7 μm, while that of the cement and silica fume is 13 μm and 0.1 μm, respectively (Mehta 1994, Zhang and Malhotra 1996). Although RHA is not very fine in particle size, it behaves as a very reactive pozzolanic material because of its extreme surface fineness and high silica content (Mehta 1992, Mehta 1994). In the presence of water, the RHA actively reacts with $Ca(OH)_2$ liberated during cement hydration (pozzolanic reaction) and produces additional calcium silicate hydrate (CSH), as shown in Equation 2.1 and Equation 2.2.

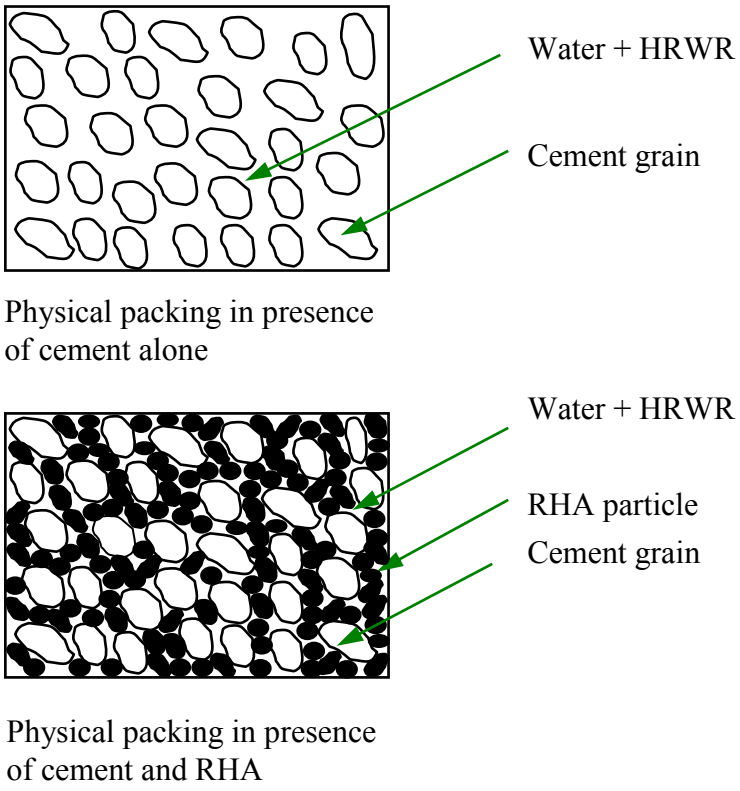

Figure 2.4: Microfilling effect of RHA

Hydration reaction: C_2S or $C_3S + H_2O \rightarrow$ primary CSH + $Ca(OH)_2$ (Equation 2.1)

Pozzolanic reaction: $Ca(OH)_2$ + RHA (SiO_2) + $H_2O \rightarrow$ secondary CSH (Equation 2.2)

The pozzolanic reaction product fills the pores existing between cement grains and results in dense calcium silicate hydrate, as shown in Figure 2.5. Both microfilling and pozzolanic effects of RHA play an important role to refine the pore structure in bulk paste matrix and interfacial transition zone of concrete. The pore refinement occurring due to the secondary reaction between RHA and $Ca(OH)_2$ makes the microstructure of concrete denser and improves the interfacial bond between aggregates and binder paste. As a result, the strength, transport properties and durability of concrete are improved.

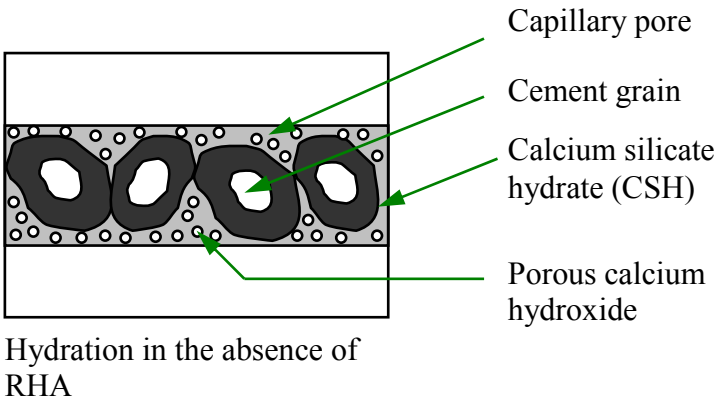

Figure 2.5: Pozzolanic effect of RHA

Similar to silica fume, the RHA can also act as a viscosity modifier (Rixom and Mailvaganam 1999). Due to extreme surface fineness, it increases the water-retaining capacity, and thus enhances the viscosity of concrete mixture.

2.9.5.4 Use in self-consolidating high performance concretes

The use of RHA in concrete was accelerated after Mehta's findings in 1973 (Mehta 1992). During the last two decades, RHA has been used to produce high strength and high performance concretes in many countries including Canada (Mahmud et al. 2004, Mehta 1992, Zhang and Malhotra 1996). In USA and Canada, RHA has been competently used to protect concrete structures from chloride attack (Mehta 1992, Zhang et al. 1996). Also, it has been used recently in Canada, as a part of composite cement to produce normal-strength SCC (Nehdi et al. 2004). However, the use of RHA to produce SCHPC has not been reported.

2.9.6 Water

Water is the readily available most important component of SCHPC. The hydration of cement can take place only in the presence of water. Adequate water is required for the hydration of cement, leading to the formation of paste to bind the aggregates. In addition, water is required in conjunction with HRWR to achieve the self-consolidation capacity of SCHPC (Okamura and Ozawa 1995). It contributes to attain good flowing ability of SCHPC by lubricating the fine and coarse aggregates.

2.9.6.1 Physical quality

Water intended for use in concrete should be clean, fresh and free of deleterious substances. Water containing harmful substances such as silts, suspended particles, organic matter, oil, or sugar can unfavorably affect the strength and setting properties of cement and disrupt the affinity between aggregate and cement paste (Nawy 1996). Therefore, the suitability of water should be examined before use. As a rule, any water with a silt content below 2000 mg/L is suitable for use in concrete (Shetty 2001). In general, the potable or drinkable water is safe for use in concrete. However, the criterion of potability is not absolute. Water not fit for drinking may also be used satisfactorily in making concrete.

2.9.6.2 Chemical quality

The mixing water for SCHPC should be chemically safe. The pH of mixing water should be in the range of 6.0 to 8.0 (Shetty 2001). It should not contain high amount of dissolved solids, chlorides, alkalis, carbonates, bicarbonates, sulfates, and other salts, which can interfere with the performance of concrete. Water containing chloride ion, SO_3 ion, and dissolved solids below 500, 1000, and 2000 mg/L, respectively, is generally satisfactory for making concrete (Neville and Brooks 1999, Owens 1992). Though dissolved solids exceeding 2000 mg/L are not always harmful, they can affect the strength and setting properties of cement adversely. Water including organic acids may also adversely affect the hydration of cement. Therefore, when the suitability of water is questionable, it must be tested prior to use in concrete. The ASTM and CSA (ASTM C 94/C 94M, 2004; CSA A23.1, 2004) have specified some physical and chemical limits to judge the acceptability of questionable mixing water.

2.9.7 High-range water reducer

High-range water reducer, also known as superplasticizer, has made a breakthrough in concrete industry. It is an essential material component that must be used to produce SCHPC. The HRWRs improve the flowing ability of SCHPC by their liquefying and dispersing actions. They reduce the yield stress and plastic viscosity of concrete by their liquefying action (Hu and De Larrard 1996, Yen et al. 1999), and thus provide a good flowing ability in SCHPC. In addition, the HRWRs deflocculate the cement particles and free the trapped water by their dispersing action (Aïtcin et al. 1994), and hence enhance the flowing ability of SCHPC. In dispersing action, the inter-particle friction and thus the flow resistance are also decreased, and therefore the flowing ability of concrete is improved.

High-range water reducers can either increase the strength by lowering the quantity of mixing water for a given flowing ability, or reduce both cement and water contents to achieve a given strength and flowing ability (Hover 1998). They contribute to achieve denser packing and lower porosity in concrete by increasing the flowing ability and improving the hydration through greater dispersion of the cement particles, and thus assist in producing high strength and good durability (Collepardi 1994).

There are mainly four categories of HRWR (Neville 1996, Mindess et al. 2003). They are sulfonated melamine-formaldehyde condensates, sulfonated naphthalene-formaldehyde condensates, modified lignosulfonates, and carboxylated acrylic ester copolymers or polycarboxylates.

2.9.7.1 Physical properties

High-range water reducers are generally formulated to produce high plasticity, normal-setting characteristics, and accelerated strengths in concrete. HRWRs are usually available in clear to dark brown liquid form but also obtainable in solid state as a brownish powder. They usually possess a viscosity in the range of 60 to 80 centipoises, and a solid content varying from 22 to 42% by weight (Aïtcin 1998). Also, the relative density of HRWR is near to that of water and hence it can be easily dispersed with water.

A particular type of HRWR can be used as a singular admixture or as a component in an admixture system, but it must fulfill some physical requirements and should be compatible with cementing materials for good performance in concrete. The ASTM has specified some physical requirements for HRWR (ASTM C 494/C 494M, 2004).

2.9.7.2 Chemical structure

Polycarboxylate HRWRs are generally used to produce SCHPC. They are produced from the relevant monomers by a free radical mechanism. The molecular structure of polycarboxylate HRWRs consists of a main chain and a graft chain. The main chain contains carboxylate groups (COO^-) while the graft chain comprises ethylene oxide (EO). The chemical structure of polycarboxylate HRWRs is shown in Figure 2.6.

2.9.7.3 Mechanisms of water reduction

High-range water reducers prevent the formation of cement-water agglomeration in concrete mixture and disperse the cement particles in aqueous phase, as can be seen from Figures 2.7 and 2.8. Thus, the water demand of concrete mixture is significantly reduced. HRWRs can exert the water-reducing action by two mechanisms, known as electrical and steric repulsions.

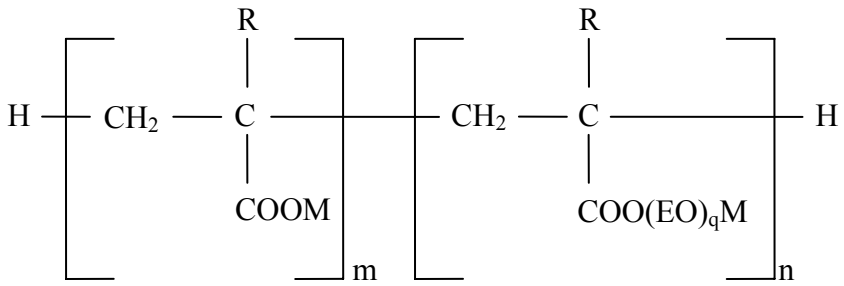

R = H, CH_3
M = Metal
EO = Ethylene oxide

Figure 2.6: Chemical structure of polycarboxylate HRWR (Palacios and Puertas 2005).

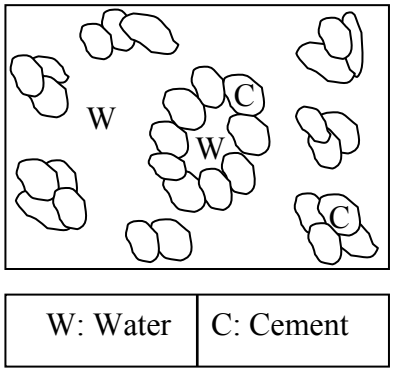

Figure 2.7: Cement-water agglomeration in absence of HRWR

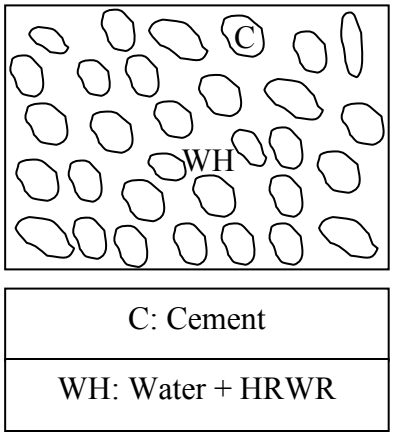

Figure 2.8: Dispersion of cement particles in presence of HRWR

The conventional or first-generation HRWR exerts the water reducing action by decreasing the surface tension of water and by equidirectional charging of the cement grains. When a HRWR is added to concrete, the cement particles are dispersed in the aqueous phase of fresh concrete and therefore the cement-water agglomerates cannot form (Dodson 1990). The dispersion mechanism is driven by the adsorption of the HRWR molecules on the cement grains. The adsorbed molecules bring about the repulsion forces between cement particles (electrical repulsion) due to their negative electrical charges. Consequently, flocculation is prevented and the cement particles are dispersed homogeneously in the fresh concrete (Erdogdu 2000). This results in an appreciable reduction in the quantity of mixing water, since the water molecules, which were previously entrapped in cement grain flakes now become free.

The second-generation HRWRs such as polycarboxylate HRWR work by steric hindrance effects (steric repulsion mechanism) to prevent cement-water agglomeration (Bigley and Greenwood 2003). It has unique graft chains (side chains) of polyethelene oxide that extend onto the surface of cement particles (Chandra and Björnström 2002). These graft chains move in water and steer the cement grains to disperse evenly in the mixture. Also, the main chains of polycarboxylate HRWR spread around the cement grains and prevent them from being in contact with each other. Hence, the cement grains cannot be associated to form cement-water agglomeration, and the water needed for a given flowing ability is greatly reduced.

2.9.8 Air-entraining admixture

Air-entraining admixture is used in portland cement paste, mortar or concrete for the purpose of entraining air in the respective masses (Dodson 1990). The main application of AEA in SCHPC is to protect the hardened concrete from frost attack and repeated freezing and thawing (Khayat 2000). An AEA incorporates millions of non-coalescing microscopic air bubbles in fresh concrete and forms a network of air-voids in hardened concrete. The air-voids act like pressure releasing valves, and thus reduce the stresses caused by the expanding frost. In addition, the air bubbles act like ball-bearings and thus enhance the flowing ability of concrete (Mindess et al. 2003). They can also decrease bleeding in concrete by reducing

the differential movement of water (Shetty 2001). However, they may reduce the segregation resistance of SCHPC by affecting the plastic viscosity of concrete (Khayat 2000).

2.9.8.1 Physical properties

Air-entraining admixture is generally formulated in liquid form. The relative density of AEA is closer to that of water. It is also soluble in water. Hence, the dispersion of AEA in concrete is enhanced when used with the mixing water. Also, most AEAs are not totally evaporable. They contain some solids. The solid content depends on the type of AEA. It usually varies in the range of 5% to 20% by weight (Rixom and Mailvaganam 1999).

The AEA intended for use in concrete must be compatible with other admixtures such as HRWR and VEA. The ASTM has specified several physical requirements for AEA to ensure its good performance in concretes (ASTM C 260, 2004).

2.9.8.2 Chemical properties

The chemical properties of AEAs depend on the raw materials from which they are made up. The AEA are usually formulated from neutralized wood resins, fatty-acid salts, alkyl-aryl sulfonates, alkyl sulfates and phenol ethoxylates (Rixom and Mailvaganam 1999). They can be anionic, cationic and non-ionic. However, most of the modern AEAs are anionic in character. They impart much better stability to the entrained air-voids.

The commercially available AEAs generally contain no chloride and possess a higher pH, thus do not promote corrosion of reinforcing steel in concrete. Also, they usually do not have any volatile organic compounds. However, currently there is no standard specification for the chemical requirements of AEA.

2.9.8.3 Mechanism of air entrainment

The mechanism of air entrainment can be explained by the thermodynamics of air bubble coalescence in aqueous phase of fresh concrete. The stability of air bubbles in fresh non-air entrained concrete largely depends on air pressure within the bubble and the solubility of air in surrounding aqueous phase (Dodson 1990). The extent of pressure inside the air bubbles is defined by the surface tension of cement solution and the diameter of the bubbles. The pressure within the air bubbles and their diameter are inversely related. The pressure inside

the bubbles is higher when the diameter is smaller. Again, the higher the pressure, the greater is the solubility of the air bubbles in the surrounding aqueous phase. Consequently, the process of air dissolution occurs in the proximity of the smaller bubbles. Hence, the smaller air bubbles tend to become even smaller and eventually disappear. The dissolution of air from the smaller bubbles causes an equivalent amount of air to enter the larger bubbles undergoing less pressure. As a result, the larger bubbles become larger at the expense of the smaller ones and get out of the concrete mixture.

The normal thermodynamics of air bubble coalescence is impeded in the presence of AEA. When an AEA is added to the concrete, it forms a coating at the interface of air bubble and aqueous phase. The stability of air-voids largely depends on the solubility of this coating. If the coating is insoluble and sufficiently elastic, it resists internal and external pressures in its environment, and inhibits the transmission of air from air bubble to aqueous phase (Dodson 1990). Most AEAs are predominantly anionic surfactants, which form an insoluble coating across air-void/aqueous phase interface (Rixom and Mailvaganam 1999). Thus, the air bubbles do not deteriorate with time. This means the air entrainment becomes stable in concrete mixture.

2.9.9 Viscosity-enhancing admixture

Viscosity-enhancing admixture is relatively a new addition to the family of admixtures for cement paste, mortar and concrete. The common application of VEA is to produce non-dispersible underwater concrete and SCHPC. VEA improves the viscosity and cohesion of fresh concrete, and thus reduces the bleeding, surface settlement and aggregate sedimentation resulting in a more stable and uniform fresh concrete (Khayat and Guizani 1997). In addition, VEA makes the fresh concrete more robust and less sensitive to the small variations in the conditions and proportions of other constituent materials (SCCEPG 2005).

Rixom and Mailvaganam (1999) have categorized the VEAs into five classes based on their physical actions in concrete. The classification is as follows:

Class A: Water-soluble synthetic and natural organic polymers, which increase the viscosity of concrete by increasing the viscosity of mixing water.

Class B: Organic water-soluble flocculants, which increase the viscosity of concrete by enhancing interparticle attraction between cement particles.

Class C: Emulsions of various organic materials, which improve the viscosity of concrete by increasing interparticle attraction and supplying additional superfine particles in the cement paste.

Class D: Water-swellable inorganic materials of high surface area that improve the viscosity of concrete by increasing the water-retaining capacity of the concrete.

Class E: Inorganic materials of high surface area that improve the viscosity of concrete by increasing the content of fine particles in concrete, and thereby resulting in greater thixotropy.

Most widely used VEAs for concrete are of Class A (Khayat 1998, Rixom and Mailvaganam 1999). The VEAs under this class can be further subdivided into natural, semi-synthetic and synthetic polymers.

2.9.9.1 Physical properties

The most common VEAs are water soluble. They are available in liquid form. They are generally lighter than other chemical admixtures such as HRWR and AEA with a relative density very close to that of water. They also contain a very small amount of solids, as compared to HRWR and AEA. Currently, there is no ASTM or CSA standard specification providing any physical requirements for VEA. Nevertheless, the VEAs should be compatible with other chemical admixtures, particularly HRWR, to produce cohesive yet highly flowable concrete mixtures (Mailvaganam 1994).

2.9.9.2 Chemical properties

The chemical properties of VEA vary depending on the type of admixture. The water-soluble synthetic and natural organic polymers (Class A VEA) are mostly used in concrete. The primary structure of Class A VEAs is built with a carbon backbone with side chains. The backbone is composed of six-carbon chains. Such chemical structure results in a high molecular weight and contributes to increase the viscosity of solution when used in concrete (Rixom and Mailvaganam 1999).

Most commercially available VEAs can be categorized under Class A. The Class A VEAs are more tolerant of salts and cations. They are also stable to the changes in pH and temperature. In addition, they contained no chloride and volatile organic compounds. Thus,

they are expected to cause no adverse effects on the properties and durability of concrete. However, presently there is no standard specification for the chemical requirements of VEA.

2.9.9.3 Mechanisms of viscosity enhancement

The mechanism of viscosity enhancement depends on the type of VEA. The VEAs under Class A work through the mechanisms of adsorption, association and intertwining (Khayat 1998). In adsorption, the long-chain polymer molecules adsorb and fix a part of the mixing water (Okamura and Ozawa 1995), and thus expand by adhering to the periphery of water molecules. As a result, the free movement of water molecules is obstructed, and the viscosity of the mixing water and that of the concrete mixture are increased. In association, the molecules of adjacent polymer chains develop attractive forces that further obstruct water movement and form a gel, resulting in an increase in the viscosity of concrete. In addition, the polymer chains can intertwine and entangle, resulting in an increase in the viscosity of the concrete mixture. However, such intertwining and entanglement depends on the concentration of VEA and deformation or shear rate of concrete.

2.10 Mixture Design for Self-consolidating High Performance Concrete

The mixture design of SCHPC is different from that of ordinary concrete. In general, compressive strength is the primary criterion for designing ordinary concrete. Conversely, the flowing ability and durability must be given equal importance with the compressive strength in designing SCHPC. Thus, a different design approach is needed for SCHPC.

2.10.1 Justification for a different method of mixture design

The process of mixture design for ordinary concrete is not applicable to SCHPC for the following reasons:

a. Established relationships between average and specified compressive strengths of ordinary concrete could be unacceptable for SCHPC possessing high strength.
b. Traditional curves for the relationship between W/B ratio and compressive strength could be misleading for SCHPC that needs a lower W/B ratio.
c. None of the traditional curves for W/B ratio and strength relationship accounts for the effect of SCM, HRWR, and VEA, which are usually used to produce SCHPC.

d. The coarse aggregate content of ordinary concrete is relatively high and unsuitable for SCHPC.
e. The fine aggregate content obtained from traditional method is generally much lower than that recommended for SCHPC.
f. The approximate water content of concrete mixture does not include the effects of SCM and HRWR, which are usually incorporated in SCHPC.
g. Slump alone is no longer a performance criterion for the flowing ability of SCHPC.

The aggregate content, the incorporation of SCM, and the presence of various chemical admixtures may have a significant influence on the flow characteristics, strength, transport properties and durability of SCHPC. Therefore, a different design approach should be followed, instead of traditional method, to design the mixture composition of SCHPC.

2.10.2 Current methods of mixture design

The mixture design method proposed by Okamura and Ozawa (1995) has mostly been used in Japan. The Japanese Ready-mixed Concrete Association (JRMCA) has simplified this method to standardize the mixture proportioning process of SCHPC in Japan (Su et al. 2001). Okamura and Ozawa's method has also been using in many countries of Europe with some modifications (EFNARC 2002, SCCEPG 2005). In this method, the coarse and fine aggregate contents are fixed and the self-consolidation capacity is achieved just by modifying the W/B ratio and HRWR dosage. The disadvantage of this method is that the W/B ratio cannot be fixed based on the strength requirement since it has to be decided through achieving the self-consolidation capacity. Therefore, the W/B ratio fixed on the basis of self-consolidation capacity may not provide the expected strength. In addition, it may take many trial mixtures to fix the proper W/B ratio and HRWR dosage, as these two must be balanced to provide optimum flowing ability and segregation resistance unless a VEA is used.

In North America, there is no ACI or CSA standard mixture design method for SCHPC. The ACI is currently working to develop a mixture design procedure for SCC (ACI Committee 211H, 2006). Recently, the International Centre for Aggregates Research (ICAR) in the University of Texas at Austin has developed a mixture design for SCC (Koehler and Fowler 2006). This method emphasizes to satisfy the criteria of filling ability, passing ability and segregation resistance, but does not give equal importance on strength and durability. For

example, it allows a W/B ≥ 0.45, which is not suitable to achieve high strength and good durability. Therefore, this method may not be valid for SCHPC. Saak et al. (2001) have also introduced a design methodology for SCC, assuming that the rheology and density of paste matrix dictate the flowing ability and segregation resistance of concrete. This methodology highlights how the segregation can be controlled in SCC, but it does not clearly explain how the aggregate characteristics and content influence the filling ability and passing ability of concrete. In addition, it does not give any clear guidelines for obtaining high strength and improved transport properties or durability. Nevertheless, the concrete industry is exploiting Shilstone's method to produce SCHPC (Monroe 2004). This mixture design method is based on aggregate particle distribution and several parameters for workability, coarseness and mortar fraction (Shilstone, Sr. 1990). The self-consolidation capacity can be obtained by adjusting the workability and coarseness parameters, and by fixing the water content and HRWR dosage based on trial mixtures. The mortar factor is useful to judge the water content and the quantity of cement. In addition, the aggregate particle distribution facilitates to provide the optimum graded mixture. Above all, this method concentrates on the gradation of aggregates and aggregate blend but does not discuss the effect of coarse aggregate content, and the role of cementing materials and chemical admixtures.

In China, Kwan (2000) developed a mixture design method for SCHPC incorporating silica fume. This method shows the process of getting SCHPC with a mean 28-day cube strength greater than 80 MPa and a slump above 200 mm. It uses a W/B ratio and strength relationship, which is different from that of ordinary concrete. But it fixes the dosage of HRWR at 3% by weight of binder, which may not be practical for any other SCHPC. Another mixture design method for SCHPC has been developed in China (Xie et al. 2002). It is specific to SCHPC incorporating ultra-pulverized fly ash. This method employs the fineness of ultra-pulverized fly ash and the optimum HRWR dosage to assess the flowing ability SCHPC. It includes a very high content of cementing material, which is not cost-effective. This method also uses relatively a high coarse aggregate content, which is not favorable for good passing ability.

In Taiwan, a mixture design method has been developed based on the concept of aggregate packing factor (Su et al. 2001). This method can predetermine the amount of SCM and the dosage of HRWR although they may need to be adjusted by trial mixtures. In this

method, the fine aggregate content is high, which enhances the filling ability and passing ability but reduces the compressive strength. Also, this method assumes that the relationship between compressive strength and W/B ratio is similar to that of ordinary concrete.

Several statistical mixture design methods such as factorial design approach (Ghezal and Khayat 2002), and three-factor central composite design method (Ozyildirim and Lane 2003) have been used in North America to produce SCHPC mainly for laboratory-based work. These approaches provide an optimum mixture composition from various mixture combinations. Nevertheless, they are not always practical due to the variability of constituent materials and the involvement of a greater number of variables in mixture design.

2.11 Mixing of Self-consolidating High Performance Concrete

Mixing is a mechanical operation to obtain a uniform mixture of concrete. A sound mixing is necessary for SCHPC to disperse the constituent materials uniformly. Conventional mixers can be used in producing SCHPC. However, the horizontal twin shaft type mixer is more suitable to increase the mixing efficiency (Chang and Peng 2001). Also, the mixing time for SCHPC is greater than that of ordinary concrete due to its higher plastic viscosity at low W/B ratio (Chopin et al. 2004).

The mixing sequence of SCHPC can be different from that of ordinary concrete due to the presence of chemical admixtures such as HRWR and VEA. In general, the aggregates are mixed first with a portion of mixing water followed by the addition of cementing materials. HRWR should be added once the aggregates and the cementing materials are wetted out. This will increase the effectiveness of HRWR (Chang and Peng 2001) and avoid the loss of HRWR through absorption by aggregates (Price 1994). When an AEA is selected for use, it is generally added at the initial stage of mixing, as it needs greater mixing time to achieve optimal performance (Kosmatka et al. 2002). In addition, when the VEA needs to be used in SCHPC to improve the stability of concrete mixture, it can be added either at the earlier or later stage of mixing (MBT 2002).

2.12 Stability of Self-consolidating High Performance Concrete

The stability of SCHPC refers to its ability to resist phase separation such as bleeding and segregation of the paste from the aggregates or the settlement of coarse aggregates during

and after placement. Generally, two forms of stability are a concern for the fresh SCHPC; static and dynamic stabilities. Both static and dynamic stabilities must be ensured in SCHPC to obtain uniform distribution of the constituent materials, particularly coarse aggregates, throughout the concrete component (Bui et al. 2002, Daczko 2002). Air-void stability is another issue that needs to be maintained in SCHPC exposed to freezing and thawing environment. All forms of the stability of SCHPC are affected by various factors such as constituent materials, mixture proportions and placement techniques.

2.12.1 Static stability

The stability of concrete after placement is known as the static stability. It refers to the resistance of the cast-in-place fresh concrete to segregation until the onset of hardening. The lack of static stability induces surface defects, affects the interfacial transition zone leading to impaired impermeability and mechanical properties, and weakens the bond to embedded reinforcement (Assaad et al. 2004).

SCHPC exhibits good static stability when the coarse aggregates remain suspended in the mixture. This criterion is controlled by the rheological properties of concrete. The yield stress and plastic viscosity play the key role. The difference between the relative densities of aggregate and matrix is also a critical factor. The yield stress opposes the sedimentation of coarse aggregates. The yield stress in SCHPC is relatively very low and therefore coarse aggregates tend to settle under static condition. For an aggregate of given size, the sedimentation of aggregate also depends on the viscosity and density of the matrix.

In cast-in-place fresh SCHPC, the aggregates are subjected to buoyancy, gravity and restoring or frictional force (Saak et al. 2001), as shown in Figure 2.9. The gravity or gravitational force is given as

$$F_g = g\rho_a V_a \qquad \text{(Equation 2.3)}$$

where:

g is the gravitational acceleration, ρ_a is the density of the aggregate, and V_a is the volume of aggregate. The buoyancy or buoyant force is given as

$$F_b = g\rho_m V_a \quad \text{(Equation 2.4)}$$

where:

ρ_m is the density of the matrix. The gravitational force acting on the aggregate becomes greater than the buoyant force, since the density of the aggregate is usually greater than that of the matrix. Therefore, the total downward force acting on the aggregate,

$$F_d = F_g - F_b = g\rho_a V_a - g\rho_m V_a = gV_a(\rho_a - \rho_m) \quad \text{(Equation 2.5)}$$

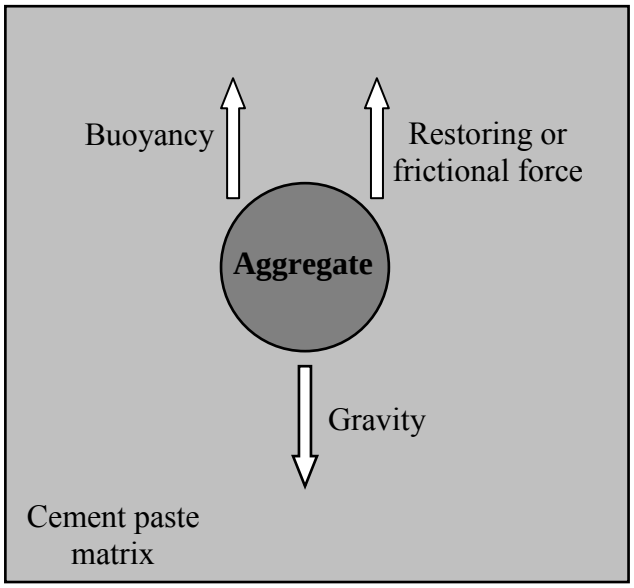

Figure 2.9: Schematic of aggregate suspended in paste matrix (adapted from Bonen and Shah 2005)

Under static condition, the restoring force is proportional to the yield stress of the matrix (Saak et al. 2001) and can be expressed as

$$F_r = \tau_y A_a \quad \text{(Equation 2.6)}$$

where:

τ_y is the yield stress of the matrix and A_a is the cross-sectional area of the aggregate immersed in the matrix. In order to keep the aggregate stationary,

$$F_r \geq F_d, \text{ i.e., } \tau_y A_a \geq g V_a (\rho_a - \rho_m) \quad \text{(Equation 2.7)}$$

For spherical aggregates, $A_a = \pi r_a^2$ and $V_a = 4\pi r_a^3/3$, where r_a = radius of aggregate. Therefore,

$$\tau_y \geq \frac{4}{3} g (\rho_a - \rho_m) r_a, \text{ i.e., } \frac{\tau_y}{(\rho_a - \rho_m)} \geq \frac{4}{3} g r_a \quad \text{(Equation 2.8)}$$

When $F_r < F_d$, aggregate settlement or sedimentation will occur. The aggregate will settle down through the matrix and the velocity of the aggregate will increase until the equilibrium of all forces is achieved (Bonen and Shah 2005). In this case, the restoring force, F_r is replaced by a frictional force F_f given by

$$F_f = 6\pi\eta r_a v_e \quad \text{(Equation 2.9)}$$

where:

η is the viscosity of the matrix, and v_e is the equilibrium velocity of the aggregate. Under equilibrium condition, the net forces acting on the aggregate are zero, and therefore the frictional force,

$$F_f = F_g - F_b = g V_a (\rho_a - \rho_m), \text{ i.e., } 6\pi\eta r_a v_e = g V_a (\rho_a - \rho_m) \quad \text{(Equation 2.10)}$$

By substituting V_a,

$$v_e = \frac{2 g r_a^2 (\rho_a - \rho_m)}{9\eta} \quad \text{(Equation 2.11)}$$

It is evident from Equation 2.8 that both yield stress and matrix density are crucial to control static stability. Also, Equation 2.11 indicates that the extent of static segregation depends on the aggregate size used in concrete, and the viscosity and density of the matrix.

2.12.2 Dynamic stability

The stability of fresh concrete during transport and placement is referred to as dynamic stability. It describes the resistance to dynamic segregation that generally occurs in the presence of obstruction and exhibits blockage of concrete. The lack of dynamic stability causes the differential accumulation of coarse aggregate and separation of the matrix. Such phenomena result in the heterogeneity due to the variations across the concrete, and degrade the properties of the concrete (Bonen and Shah 2005). SCHPC possesses good dynamic stability if the coarse aggregates move uniformly with the matrix as a cohesive fluid during flow. This criterion is achieved through improved viscosity of the matrix (Saak et al. 2001).

Dynamic segregation may occur in SCHPC during placement along horizontal and perpendicular directions. In horizontal flow, the aggregate is subjected to several forces such as lateral mixture drag, gravity, buoyancy, vertical drag, and viscous force or plastic viscosity, as presented in Figure 2.10. In contrast, the aggregate is subjected to gravity, buoyancy and vertical drag force during perpendicular flow, as shown in Figure 2.11. In horizontal flow, the lateral mixture drag and vertical drag help to keep the aggregates suspended in concrete mixture (Bonen and Shah 2005). Both lateral mixture drag and vertical drag depend on the velocity of the concrete mixture during placement. In this case, the plastic viscosity of the matrix also resists the separation of coarse aggregates, acting oppositely to the direction of lateral mixture drag. In perpendicular flow, the vertical drag resists the falling of the aggregate (Saak et al. 2001). The vertical drag force can be given by

$$F_{dr} = \frac{1}{2} C_D A_a \rho_m v_t^{\,2} \qquad \text{(Equation 2.12)}$$

where:

C_D is the drag coefficient and v_t is the constant terminal velocity of the aggregate. A_a and ρ_m are explained in Section 2.12.1.

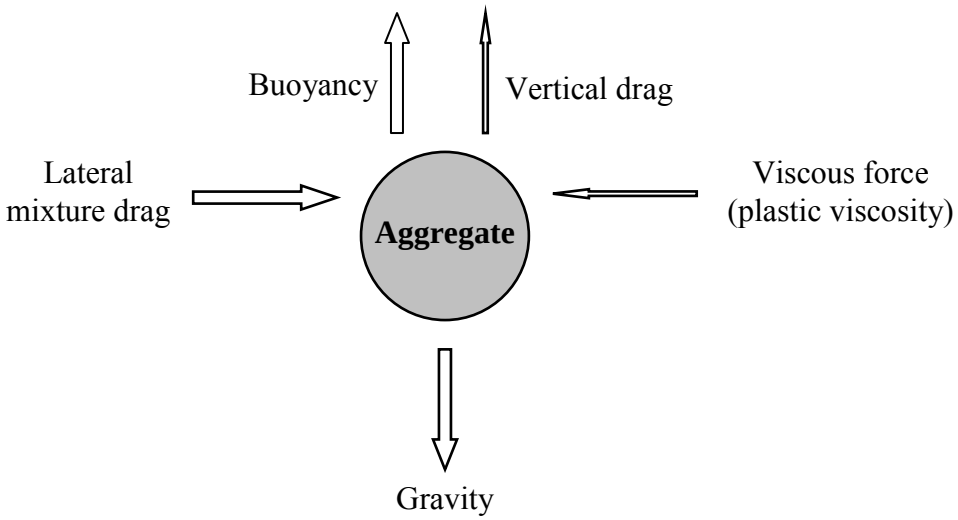

Figure 2.10: Forces acting on aggregate during horizontal flow (adapted from Bonen and Shah 2005)

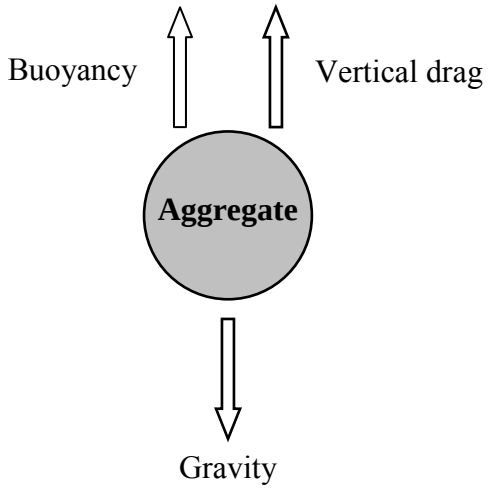

Figure 2.11: Forces acting on aggregate during perpendicular flow (adapted from Bonen and Shah 2005)

The total downward force will be equal to the vertical drag force when the aggregate reaches the constant terminal velocity. Thus, based on Equations 2.5 and 2.12,

$$\frac{1}{2} C_D A_a \rho_m v_t^{\,2} = g V_a (\rho_a - \rho_m) \qquad \text{(Equation 2.13)}$$

Simplifying Equation 2.13, the terminal velocity of the aggregate can be expressed as

$$v_t = \sqrt{\frac{8g(\rho_a - \rho_m) r_a}{3 C_D \rho_m}} \qquad \text{(Equation 2.14)}$$

The terminal velocity of the aggregate should be minimized to avoid dynamic segregation. It is obvious from Equation 2.14 that the terminal velocity depends on the matrix density of concrete for the given size and type of aggregate. Also, the terminal velocity is inversely related to the drag coefficient, as can be seen from Equation 2.14. The drag coefficient, C_D, greatly depends on the viscosity of matrix (Saak et al. 2001). When the viscosity of matrix is high, the drag coefficient becomes high. At high drag coefficient, the terminal velocity of the falling aggregate will be low. Hence, the aggregate falling will be slowed down and the segregation will be reduced.

2.12.3 Air-void stability

The entrained air-voids must be stable in concrete to ensure a good resistance to freezing and thawing. This is particularly more important for SCHPC, as the presence of HRWR tends to destabilize the entrained air-voids during transport and placement of concrete (Saucier et al. 1990, Khayat and Assaad 2002). Many research reports indicate that the HRWRs can cause some loss of air content during intermittent agitation (Jana et al. 2005, Johnston 1994). This is perhaps attributed to the production of a greater number of large-size bubbles, which could easily disappear with time. In addition, re-mixing, presence of SCM, re-dosing of HRWR, cement-admixture compatibility, and type of AEA affect the air-void stability in concrete (Baalbaki and Aïtcin 1994, Pigeon et al. 1989, Saucier et al. 1990, Baekmark et al. 1994). Excessive fluidity and segregation could be another factor that may cause air-void instability

problem in SCHPC. The air-void stability can be ensured in SCHPC by a proper mixture composition including a suitable combination of chemical admixtures. An increase in the amount of cementing material at a low W/B ratio or the use of VEA can maintain the appropriate air-void system during transport, placement and setting of SCHPC (Khayat 2000, Khayat and Assaad 2002).

2.12.4 Role of rice husk ash

The stability of SCHPC is mainly controlled by its mixture variables. The properties and proportions of cementing materials have significant effect on both static and dynamic stability (Saak et al. 2001) as well as on air-void stability of SCHPC (Khayat and Assaad 2002). If SCHPC suffers from instability problem, it can be eliminated by increasing the amount of SCM (Nagataki and Fujiwara 1995). However, it depends on some physical properties such as particle shape and size, specific surface area, and relative density of SCM. These properties influence the yield stress, viscosity and density of the cement paste matrix that affect the stability of SCHPC (Saak et al. 2001, Bonen and Shah 2005). Since the yield stress, plastic viscosity and density of the paste matrix are changed in the presence of RHA, both static and dynamic stability of SCHPC including RHA can be influenced. Also, the change in the viscosity of paste influences the formation of stable air-voids. Consequently, the air-void stability of SCHPC can also be affected in the presence of RHA. Nevertheless, limited studies investigated the effect of RHA on the stability of SCHPC.

2.13 Key Fresh Properties of Self-consolidating High Performance Concrete

The key fresh properties of SCHPC are the filling ability, passing ability and segregation resistance. These three properties must be satisfied regardless of the sophistication of the mixture design and other considerations such as cost. Among other fresh properties, plastic shrinkage, unit weight and air content are noteworthy.

2.13.1 Filling ability

Filling ability is defined as the ability of fresh SCHPC to flow into and fill the spaces within the formwork under self-weight at unconfined condition (Bartos 2000, EFNARC 2002). It is associated with the formability, self-leveling capacity, and finishing ability of SCHPC. The

filling ability is an essential property of SCHPC to achieve self-consolidation capacity. This property is crucial for concrete placement with proper casting technique (ACI 237R-07, 2007). The filling ability primarily depends on the aggregate content, W/B ratio, binder content and HRWR dosage of concrete (Okamura and Ozawa 1995). A good filling ability can be achieved by limiting the coarse aggregate content and increasing the amount of cementing materials, while adding a proper dosage of HRWR.

2.13.2 Passing ability

Passing ability is defined as the ability of fresh SCHPC to flow through tight openings or spaces confined by steel reinforcing bars (Bartos 2000, EFNARC 2002). Where structures are heavily reinforced, a good passing ability of SCHPC enables it to be placed and consolidated through dense reinforcing bars without any aggregate blockage (ACI 237R-07, 2007). The factors affecting the filling ability also influence the passing ability of concrete. In addition, the passing ability depends on the number and spacing of the reinforcing bars. A good passing ability can be achieved by increasing the filling ability of fresh concrete and by limiting the segregation of coarse aggregates.

2.13.3 Segregation resistance

The segregation resistance of SCHPC refers to its ability to remain uniform during and after placement without any loss of stability due to bleeding, mortar separation and coarse aggregate settlement (EFNARC 2002). In particular, the distribution of aggregates becomes non-uniform if SCHPC does not possess sufficient segregation resistance. This might affect the properties and durability of concrete. A recent study has reported that the water absorption and chloride penetration of SCHPC can be affected under poor segregation resistance (Daczko 2002). A good segregation resistance can be attained in SCHPC by a proper mixture composition. An increased amount of cementing materials, a small nominal maximum size of aggregate, a limited content of well-graded coarse aggregates, and a low W/B ratio should be used to achieve good segregation resistance (Bonen and Shah 2005). In addition, the segregation resistance of SCHPC can be improved by using VEA (Okamura and Ozawa 1994).

2.13.4 Unit weight

The unit weight of SCHPC refers to its mass per unit volume of fresh concrete. It depends on the mixture composition of concrete. The unit weight of concrete becomes slightly lower when a SCM such as RHA, fly ash and silica fume is incorporated (Zain et al. 1999). This is because most SCMs are lighter than cement. However, it also depends on the degree of materials packing in concrete.

2.13.5 Air content

Adequate air content must be maintained in SCHPC in order to protect it from freezing and thawing damage (Brameshuber and Uebachs 2003, Hayakawa et al. 1994). The network of entrained air bubbles offsets the hydraulic pressure posed by freezing water, and thus improves the performance of concrete in freezing and thawing environment (Hayakawa et al. 1994). However, obtaining the correct air content in SCHPC is not very straightforward. There are many factors such as mixture proportions, aggregate grading, cement composition, type of HRWR, type and composition of SCM, mixing or placing method, and temperature etc., that affect air-entrainment, and therefore achieving the target air content becomes much more difficult (ACI 201.2R-01, 2004; Du and Folliard 2005, Pigeon 1994).

2.13.6 Role of rice husk ash

The presence of RHA results in a high water demand due to high specific surface area (Mahmud et al. 2004, Zhang and Malhotra 1996). Thus, the filling ability and passing ability can be affected if the increased water demand is not reduced with the adequate dosage of HRWR. Moreover, the incorporation of RHA reduces the unit weight of concrete (Ismail and Waliuddin 1996). The air content of concrete is also affected in the presence of RHA. The concrete requires more AEA for a given air content when RHA is used with cement (Zhang and Malhotra 1996). It was also reported that RHA reduces bleeding and segregation in non-self-consolidating concrete (Mehta 1992, Zhang and Malhotra 1996) due to enhanced viscosity. However, a decrease in bleeding increases the susceptibility of plastic shrinkage cracking. In addition, the incorporation of RHA lowers the density of paste matrix and thus may adversely affect the segregation resistance of SCHPC, particularly in static condition.

However, very few studies have been conducted to investigate the effects of RHA on the fresh properties of SCHPC.

2.14 Curing of Self-consolidating High Performance Concrete

Curing is ideally a process that keeps the concrete element completely saturated or as much saturated as possible until the water-filled spaces are substantially reduced by hydration products (Gowripalan et al. 1992, Mather 1987). Concrete properties and durability are significantly influenced by curing since it greatly affects the hydration of cement. The hydration of cement virtually ceases when the relative humidity within the capillaries drops below 80% (Neville 1996). The lack of moisture in cement paste can also result in autogenous shrinkage due to self-desiccation. This is particularly a concern for the concretes with higher binder content and lower W/B ratio (Neville 1996). Moreover, the drying of concrete surfaces results in shrinkage cracks that may aggravate the durability problems. Therefore, an efficient curing method is inevitable to prevent the concrete from drying and self-desiccation, and to maintain the relative humidity above 80%.

A proper curing of SCHPC is crucial to produce greater hydration products, and to reduce the porosity and drying shrinkage cracking of concrete, and thus to achieve higher strength and greater resistance to physical or chemical attacks in aggressive environments. If SCHPC is not well cured, particularly at the early age, it will not gain the properties and durability at the desired level due to a lower degree of hydration, and would suffer from irreparable loss. Therefore, a suitable curing method such as water ponding, spraying of water, covering with wet burlap and plastic sheet, storing in a moist room, wrapping with polyfilm, or storing in an oven with controlled temperature is essential to produce strong and durable SCHPC. Water ponding, spraying of water, storing in a moist room and covering with wet burlap are different forms of water curing, which is most effective to improve the hardened properties of concrete (Aïtcin et al. 1994). In addition, wrapped curing, such as wrapping with polyfilm, provides concrete properties closer to those given by water curing (Zain et al. 2000). Hence, water curing should be the first choice to cure SCHPC. In case of water shortage, wrapped curing can be adopted to cure SCHPC. The curing period should be at least 7 days to improve the properties and durability of concrete (ACI 308R-01, 2001).

This is more crucial for SCHPC to reduce its autogenous and drying shrinkages caused by high binder content and low W/B ratio.

2.15 Testing of Self-consolidating High Performance Concrete

Testing of SCHPC includes the testing of both fresh and hardened concretes. The testing of fresh concretes usually includes the tests for rheological parameters (yield stress and plastic viscosity), flowing ability (filling ability and passing ability), segregation resistance, air content, unit weight, etc. The testing of hardened concretes includes both destructive and non-destructive tests. Among various destructive tests, the compression test is of great importance. The other important destructive tests are flexural (bending), and direct and indirect (splitting) tension tests. The non-destructive testing includes tests for ultrasonic pulse velocity, modulus of elasticity, porosity, absorption, permeability, electrical resistivity, etc.

Most of the test methods available for determining the fresh properties of ordinary concrete are not suitable for SCHPC due to different workability characteristics. However, very few standard test methods were established for fresh SCHPC. The most common slump test has been used widely with some modifications to examine the filling ability of SCHPC (Shindoh and Matsuoka 2003). Recently, the ASTM has standardized the slump flow test for determining the filling ability of SCC (ASTM C 1611/C 1611M, 2007), which is also applicable for SCHPC. In addition, the V-funnel and Orimet have been using to determine the filling ability of SCHPC (Bartos 2000, EFNARC 2002). Similar to filling ability, there were few standard test methods to measure the passing ability of SCHPC. Lately, the ASTM has standardized the J-ring to measure the passing ability of SCC (ASTM C 1621/C 1621M, 2007). This test method is also applicable to SCHPC. Moreover, the U-box, L-box and Fill-box have been used for determining the passing ability of SCHPC (EFNARC 2002, Okamura and Ouchi 2003). The segregation resistance is mostly being measured by standard No. 4 sieve (EFNARC 2002, Nagataki and Fujiwara 1995) and column apparatus (Assaad et al. 2004, Sonebi 2004a). The ASTM has also standardized a column apparatus for testing the segregation resistance of SCC (ASTM C 1610/C 1610M, 2006), which is also valid for freshly mixed SCHPC. For other fresh properties of SCHPC such as unit weight and air content, the existing test methods for ordinary concrete can be used with some modifications, particularly for the procedures of filling and consolidation.

In case of hardened SCHPC, the test methods used for ordinary concrete can be employed to determine the concrete properties. However, the testing ages should be extended to 56 or 91 days for most hardened properties. This is because SCHPC most often contains SCMs; some of these hydrate at a slower rate than portland cement (Lessard and Aïtcin 1994). In addition, a higher specified loading rate can be applied to SCHPC as compared to ordinary concrete, while conducting the destructive strength test. This is because the strength of SCHPC is much higher than that of ordinary concrete. Also, the capping conditions for the compression test of SCHPC may not be the same as for ordinary concrete. Nevertheless, these changes do not enforce to employ completely new test methods for hardened SCHPC.

2.16 Key Hardened Properties of Self-consolidating High Performance Concrete

Compressive strength, porosity, ultrasonic pulse velocity, absorption, permeability, and electrical resistivity are some of the key hardened properties of SCHPC. They are briefly discussed below.

2.16.1 Compressive strength

Compressive strength is the most important mechanical property of concrete. In general, for a given set of cement and aggregates, and under the same mixing, curing and testing conditions, the compressive strength of a concrete primarily depends on W/B ratio, binder/aggregate (B/A) ratio, mixture composition, and degree of consolidation. However, it is the W/B ratio that chiefly controls the development of compressive strength in concrete. The limits of W/B ratio to achieve a targeted compressive strength in high-strength HPC are as follows (Lessard et al. 1995):

50 MPa – 75 MPa, for $0.30 \leq W/B \leq 0.40$

75 MPa – 100 MPa, for $0.25 \leq W/B \leq 0.35$

100 MPa – 125 MPa, for $0.20 \leq W/B \leq 0.30$

125 MPa and above, for $W/B \leq 0.20$

Ordinary concrete generally produces a compressive strength in the range of 20 to 40 MPa. The compressive strength of SCHPC is much higher than that of ordinary concrete. For a compressive strength varying from 50 to 125 MPa, the aforementioned range of W/B ratios is also valid for SCHPC (Persson 2001). Another observation is that the kinetics of strength

increase is notably faster in SCHPC (Persson 2001) as compared to ordinary concrete due to increased gel/space ratio at lower W/B ratio.

2.16.2 Porosity

Porosity refers to a fraction of the total concrete volume that is occupied by the pores in bulk cement paste, interfacial transition zone and aggregates. It is one of the major factors that control the strength of concrete (Neville 1996). Porosity also affects the electrical resistivity, and thus the corrosion resistance of concrete (Claisse et al. 2001). The porosity of concrete can be characterized into two forms – total and capillary or suction porosity (Nokken and Hooton 2002). The total porosity is mainly comprised of capillary and air porosity. In contrast, the network of open pores mainly constitutes the capillary porosity of concrete. The capillary porosity has considerable effects on the transport properties and hence on the durability of concrete (Hearn et al. 1994).

The total and capillary porosity are expected to be low in SCHPC (7 to 15%) as compared to ordinary concrete due to compacted pore structure. The pore system in SCHPC is more refined than that in ordinary concrete (Attiogbe et al. 2002). This is mainly because of a low W/B ratio. The higher degree of packing due to good consolidation, the greater degree of hydration due to deflocculation and dispersion of cement particles in the presence of HRWR, and the pozzolanic and micro-filling effects of SCM also contribute to form a refined pore structure in SCHPC.

2.16.3 Ultrasonic pulse velocity

The ultrasonic pulse velocity is defined as the traversed distance of the pulse or sonic wave per unit transit time. This is obtained from the path length (length of the interposed concrete specimen) and transit time. The ultrasonic pulse velocity of concrete is mainly influenced by the mixture composition of concrete, moisture and maturity of concrete, curing conditions, and temperature. Generally, a high ultrasonic pulse velocity through concrete indicates that the concrete is of good quality. An ultrasonic pulse velocity above 4575 m/sec states the ‘excellent’ quality of concrete whereas an ultrasonic pulse velocity below 2135 m/sec reveals the ‘very poor’ condition of concrete (Leslie and Cheeseman 1949, Shetty 2001).

Ultrasonic pulse velocity can be used to evaluate the physical quality of SCHPC. It is also useful to detect the cracks and flaws, and to study the freeze-thaw durability of SCHPC. The ultrasonic pulse velocity of SCHPC is expected to be much higher than that of ordinary concrete. This is due to the refined pore structure and dense microstructure of SCHPC. However, no considerable studies have been conducted on the non-destructive evaluation of SCHPC using ultrasonic pulse velocity method.

2.16.4 Absorption

Absorption is a process by which a liquid gets into and tends to fill the open pores in a porous solid body such as a component of concrete (ASTM C 125, 2004). The absorption is generally more significant in surface layer than the core of concrete due to strong capillary action. The rate at which a dry concrete surface absorbs a liquid can be taken as a predictor of the durability of concrete. Water is the most common liquid with which the concrete comes in contact. Hence, water absorption is widely used to indicate the absorptivity of concrete. It can be determined based on the increase in mass of a concrete specimen due to the penetration of water into its open pores.

Water absorption is directly related to concrete's resistance to water penetration, which plays an important role in various deterioration mechanisms and carries many deleterious agents from the surroundings. Like other engineering properties, the water absorption of concrete is directly influenced by the porosity (Hearn et al. 1994). The porosity controls the microstructure and thus the absorption of concrete, depending on the relative quantities of the pores of various types and sizes (Hearn et al. 1997). When the porosity decreases, the water absorption is also reduced. It was reported that SCHPC provides a water absorption in the range of 3 to 6% (Schutter et al. 2003, Vanwalleghem et al. 2003).

2.16.5 Permeability

Permeability of concrete is defined as the movement of liquid and/or gas through a mass of concrete under a constant pressure gradient. It is an intrinsic property of concrete that chiefly depends upon the geometric arrangement and characteristics of the constituent materials. The permeability of concrete is mainly controlled by the compactness and porosity of the hydrated paste present in bulk paste matrix and interfacial transition zone. In the hydrated

paste, the capillary and gel pores can be distinguished. The gel pores are very small. Although they constitute a network of open pores, the permeability of this network is very low. Conversely, the capillary pores are relatively large spaces existing between the cement grains. It is the capillary porosity that greatly affects the permeability of concrete (Perraton et al. 1994).

The permeability of SCHPC is typically lower than that of ordinary concrete. The previous research showed that SCHPC results in very low water and gas permeability (Zhu and Bartos 2003, Schutter et al. 2003). This is mostly attributed to the superior flow properties, dense microstructure and refined pore structure that develop in the presence of SCM and HRWR at low W/B ratio. Good flow properties result in excellent packing condition due to improved consolidation, and thus contribute to reduce the permeability of concrete.

2.16.6 Electrical resistivity

The corrosion-resisting performance of concrete is influenced by its electrical resistivity, which refers to the resistance that the electrical charges experience while passing through the concrete. The electrical resistivity must be sufficiently high to inhibit the corrosion process in concrete. The increased electrical resistivity of concrete hinders the movement of electrons from the anodic to the cathode regions, and thereby retards the propagation of corrosion process. It has been reported that the corrosion rate becomes very low when the true electrical resistivity (apparent resistivity/cell correction factor) of concrete is greater than 10 kΩ-cm (Hearn 1996). HPC has been known to provide higher electrical resistivity (Hansen et al. 1993, Tasi et al. 2006).

Limited studies have been carried out to investigate the electrical resistivity of SCHPC. Hwang and Hung (2002) determined the electrical resistivity of SCHPC as a measure of the durability at different W/B ratios. They found that SCHPC provides an electrical resistivity much higher than 10 kΩ-cm at later ages (≥ 28 days). This is mainly attributed to the reduced porosity of SCHPC. The reduction in porosity lessens the amount of electrolyte and impedes the movement of electrical charges, and thus increases the electrical resistivity of concrete.

2.16.7 Role of rice husk ash

The published literature shows that the hardened properties of concrete are improved in the presence of RHA. For example, RHA provided significant improvements in compressive and tensile strengths, ultrasonic pulse velocity, and transport properties of high strength and high performance concretes (Ismail and Waliuddin 1996, Zhang and Malhotra 1996, Mahmud et al. 2004). Similar performance of RHA is expected in case of SCHPC. However, limited studies have been conducted to investigate the effect of RHA on the hardened properties of SCHPC.

2.17 Modeling of Self-consolidating High Performance Concrete

The modeling of fresh and hardened concrete properties is useful for mixture design and performance prediction. In published literature, there are several models available for fresh and hardened concretes. Most of these models are related to the filling ability and compressive strength of concrete, and can be applicable for SCHPC.

2.17.1 Models for filling ability

The slump and slump flow are two fresh properties that express the filling ability of concrete. Hu et al. (1996) proposed a semi-empirical model relating the slump to the yield stress of fresh concrete as follows:

$$\tau_y = \frac{\rho}{270}(300 - S) \qquad \text{(Equation 2.15)}$$

where:

S is the slump (mm), τ_y is the yield stress (Pa), and ρ is the unit weight or density of fresh concrete (kg/m^3).

For the above model, the correlation between yield stress and slump is poor when the plastic viscosity of concrete exceeds 300 Pa.s. Ferraris and de Larrard (1998) improved the accuracy of Hu's model by changing the value of the slope term and adding a constant term

as shown in Equation 2.16. They implied that the modified version of Hu's model is valid for very fluid concrete such as SCHPC.

$$\tau_y = \frac{\rho}{347}(300 - S) + 212 \qquad \text{(Equation 2.16)}$$

Ferraris and de Larrard (1998) also provided a relationship among the plastic viscosity, slump and slump time of concrete as follows:

$$\mu = \frac{1.08}{1000}\rho T_s (S - 175) \qquad \text{(Equation 2.17)}$$

where:

μ is the plastic viscosity (Pa.s) and T_s is slump time (s), S is the slump (mm), and ρ is the density of fresh concrete (kg/m^3). This relationship is given for a slump value in the range of 200 to 260 mm. Therefore, it is also valid for SCHPC.

Murata (1984) produced a relationship to calculate the maximum bottom shear stress, and developed a model for the slump flow and yield stress as follows:

$$\tau_{bm} = \frac{1}{2}\left(\frac{\rho g V}{\pi R_b^2}\right) \qquad \text{(Equation 2.18)}$$

$$\frac{S_f}{2} = \sqrt{\frac{\tau_{bm}}{2\tau_y}} R_b \qquad \text{(Equation 2.19)}$$

where:

τ_{bm} is the maximum bottom shear stress (Pa), S_f is the slump flow of concrete (m), τ_y is the yield stress of concrete (Pa), R_b is the bottom radius of concrete sample before deformation (m), ρ is the density of fresh concrete (kg/m^3), g is gravitational acceleration (9.806 m/s^2), and V is the volume of concrete sample (m^3). The frictional resistance between concrete

sample and rubber sheet was considered in this model. This model is valid for the concretes possessing a yield stress in the range of 0 to 1000 Pa, and thus can be applied to SCHPC.

Murata and Kukawa (1992) also proposed an empirical model relating the slump and yield stress of concrete in the following form:

$$\tau_y = 714 - 473\left(\log\frac{S}{10}\right) \qquad \text{(Equation 2.20)}$$

where:

τ_y is the yield stress (Pa) and S is the slump (mm) of concrete. This relationship is valid for the slump ranging from 125 to 260 mm. Therefore, it is also applicable for SCHPC.

Tanigawa et al. (1992) proposed semi-empirical models for the yield stress and plastic viscosity of fresh concrete relating slump, slump flow, and slump time as follows:

$$\tau_y = \frac{\alpha_s \rho g (H - S)}{\sqrt{3}} \qquad \text{(Equation 2.21)}$$

$$S = H - \frac{1}{\left(\frac{\alpha_s \rho g}{600\mu} T_s + \frac{1}{H}\right)} \qquad \text{(Equation 2.22)}$$

$$\alpha_s = \frac{1 + a + a^2}{3} = \frac{4V}{\pi S_f^2 (H - S)} \qquad \text{(Equation 2.23)}$$

where:

τ_y is the yield stress (Pa), S is the slump of concrete (m), α_s is a shape factor, a is the ratio of top radius to the bottom radius of the slump cone, ρ is the density of fresh concrete (kg/m^3), g is the gravitational acceleration (9.806 m/s^2), H is the initial height of concrete sample (m), V is the volume of concrete sample (m^3), μ is the plastic viscosity (Pa.s), S_f is the slump flow of

concrete (m), and T_s is the slump time (s). The models are generally valid for any fresh concrete including SCHPC. However, the accuracy of these models depends on the variation of shape factor.

Chidiac et al. (2000) revised Equations 2.21 and 2.22 to avoid the effect of shape factor (α_s) and provided the relationships for the yield stress and plastic viscosity of concrete as follows:

$$\tau_y = \frac{4\rho g V}{\sqrt{3}\pi S_f^2} \qquad \text{(Equation 2.24)}$$

$$\mu = \frac{\rho g V H T_s}{150\pi S S_f^2} \qquad \text{(Equation 2.25)}$$

where:

τ_y is the yield stress (Pa); μ is the plastic viscosity (Pa.s), S_f is the slump flow of concrete (m), H is the initial height of concrete sample (m), S is the slump of concrete (m), T_s is the slump time (s), ρ is the density of fresh concrete (kg/m^3), g is the gravitational acceleration (9.806 m/s^2), and V is the volume of concrete sample (m^3). These equations can be used to estimate the yield stress and plastic viscosity of SCHPC.

2.17.2 Models for compressive strength

Duval and Kadri (1998) proposed a model for the compressive strength of silica fume HPC in the following form:

$$f_c(t) = KR_{c28}\frac{C}{(y+1)W}[A(t) + 1.36 - \{2.1(SF/C)^2 - 0.6\}^2] \qquad \text{(Equation 2.26)}$$

where:

$f_c(t)$ is the compressive strength at any time t; K is a coefficient that depends on the type of aggregates and is computed from the 28-day compressive strength of reference concrete

without silica fume; R_{c28} is the 28-day compressive strength of cement or standardized mortar; y is a coefficient that accounts for the entrapped air volume and depends on the consistency of concrete, and for a very plastic or fluid concrete the value is taken as 0.07; *C, W and SF* are the masses of cement, water and silica fume, respectively; *A(t)* is a kinetics function that is obtained from the compressive strength of reference concrete at a time t, assuming *A(t)* equals zero at 28 days. The model was produced based on the compressive strength of various concretes including normal and sulfate-resistant cements. This model is valid for the concrete age up to 28 days.

De Larrard (1994) also suggested a model for the compressive strength of silica fume HPC as follows:

$$f_{c28} = \frac{KR_{c28}}{\left[1 + \frac{3.1W/C}{1.4 - 0.4\exp(-11SF/C)}\right]^2} \qquad \text{(Equation 2.27)}$$

where:

f_{c28} is the compressive strength at 28 days, and the other terms convey the same meanings as in Duval and Kadri's model. The model was developed based on the compressive strength of concretes including normal portland cement. This model is only suitable for the computation of the 28 days compressive strength of concrete.

Gutiérrez and Cánovas (1996) proposed a model for the compressive strength of HPC in the following form:

$$f_{cm} = 140\, e^{-K_c\left(\frac{1}{1+4.75\,SF}\right)\frac{W}{C}} \qquad \text{(Equation 2.28)}$$

where:

f_{cm} is the mean compressive strength at 28 days, K_c is a parameter related to cement strength, and the other terms express the same meanings, as in Duval and Kadri's and De Larrard's

models. The model was developed based on the compressive strength of concretes prepared with high early-strength cements. This model also provides only the 28 days compressive strength of concrete.

Combining a function for the strength development and a second function correlating the strength with water-cement (W/C) ratio, silica fume content, and maximum size of coarse aggregate, Videla and Gaedicke (2004) also suggested a model for the compressive strength of portland blast-furnace slag cement HPC as follows:

$$f_c(t) = \frac{t^{0.75}}{(2.051 + t^{0.75})}\left[207.99\, e^{\left(-1.956\frac{W}{C} + 0.00394\, SF\right)} - 0.756\, D\right] \qquad \text{(Equation 2.29)}$$

Where:

$f_c(t)$, C, W and t convey the same meanings as mentioned before; SF is the amount of silica fume (mass percent) and D is the maximum size of coarse aggregates (mm). The model was derived based on the compressive strength of concretes including slag cement and silica fume. This model is applicable to estimate the compressive strength at any concrete age.

The above models are specific to HPC including silica fume, and for W/C ratio below 0.40. These models can be applied to SCHPC including RHA if silica fume and RHA produce similar effect on the compressive strength of concrete. Nevertheless, a similar model can be developed for SCHPC containing RHA based on the experimental results.

2.17.3 Other models

Bui et al. (2002) proposed a rheological model for SCHPC. This model is based on the concept of paste rheology, aggregate spacing and average aggregate diameter. The zones of low deformability or inadequate flowing ability, stability (satisfactory zone) and segregation (segregation zone) are discussed in this model. In addition, Ghezal and Khayat (2002), and Sonebi (2004b) derived the statistical models for normal-strength and medium-strength SCCs. These models predict the key fresh properties such as the filling ability and passing ability as well as the compressive strength of SCC. The development of these models

involved the testing of a number of concrete mixtures. Also, the mixture parameters such as cement content, SCM and HRWR, etc. are generally selected on trial basis. They are material-specific and therefore may not be directly applicable to other sets of materials. However, the derived models would be helpful to simulate different sets of materials in future SCC and SCHPC concrete mixtures, leading to time and cost savings from a reduced number of trail batches.

2.18 Research Needs

Self-consolidating high performance concrete has rapidly gained broad acceptance in North America. It could be used successfully in many structural as well as non-structural applications. However, comprehensive research is necessary to fill the existing knowledge gaps and to link different issues for the prospect of SCHPC in different sectors of construction. Based on the literature review, the following research needs have been identified in the field of SCHPC:

a. Potential for the use of waste materials such as RHA to improve concrete properties and durability.
b. Development of a simplified mixture design method.
c. Investigation of the relationship between the filling ability of concrete and the filling ability of its paste or mortar component.
d. Investigation of the air-void stability in fresh and hardened concretes.
e. Investigation of the effect of RHA on the fresh and hardened properties, and durability of concrete.
f. Investigation of the effect of RHA on the static and dynamic stabilities or segregation resistances of concrete.
g. Development of simple test apparatus to examine the filling ability, passing ability and segregation resistance of concrete.
h. Assessment of the physical quality of concrete by different non-destructive test methods.
i. Modeling of major fresh and hardened properties of concrete with respect to key mixture design parameters.

2.19 Research Objectives

The main objective of the study was to develop SCHPCs incorporating RHA, and to investigate their performance at fresh and hardened states. The sub-objectives of the study were as follows:

a. Investigation of the filling ability of various SCHPCs, and their paste and mortar components.
b. Development of a simple design approach for the mixture proportioning of SCHPC.
c. Development of simplified and single-operator test apparatus for assessing the filling ability, passing ability, and segregation resistance of SCHPC.
d. Evaluation of the air-void stability in various fresh SCHPCs with and without RHA.
e. Investigation of the effect of RHA on various properties of fresh and hardened SCHPCs.
f. Examination of the effect of RHA on the static and dynamic segregation resistances of various SCHPCs.
a. Development of empirical models for the filling ability (slump flow) and compressive strength of SCHPC.

Chapter 3

Research Program and Procedures

3.1 General

The research program was comprised of experimental investigation and modeling. The aim of the experimental investigation was to examine the suitability of component materials and to observe the performance of different binder pastes and mortars, and various fresh and hardened self-consolidating high performance concretes (SCHPCs). The pastes, mortars and concretes used contained rice husk ash (RHA) as a supplementary cementing material (SCM). This chapter discusses the research procedure and provides a flowchart for the overall research program.

3.2 Experimental Investigation

The experimental investigation for various SCHPCs was comprised of selection and testing of materials, testing of aggregate blends, testing of binder pastes, testing of mortars, design of concrete mixtures, preparation and testing of fresh concretes, and preparation and testing of hardened concretes. In addition, the development of several test apparatus for measuring the key fresh properties of SCHPC was included. The overall experimental investigation is shown in the flowchart given in Figure 3.1.

The following systematic procedure was followed to carry out the research on SCHPCs incorporating RHA:

Step 1: The constituent materials for SCHPCs were selected, collected, and tested for the key properties.

Step 2: Various aggregate blends were prepared by mixing concrete stone and concrete sand at different proportions. The aggregate blends were tested to determine the optimum sand-aggregate (S/A) ratio leading to maximum bulk density.

Step 3: The primary mixture proportions of SCHPCs were determined based on the results obtained from the testing of materials and aggregate blends, and by selecting the water-binder (W/B) ratio and estimating the mixing water requirement of concrete.

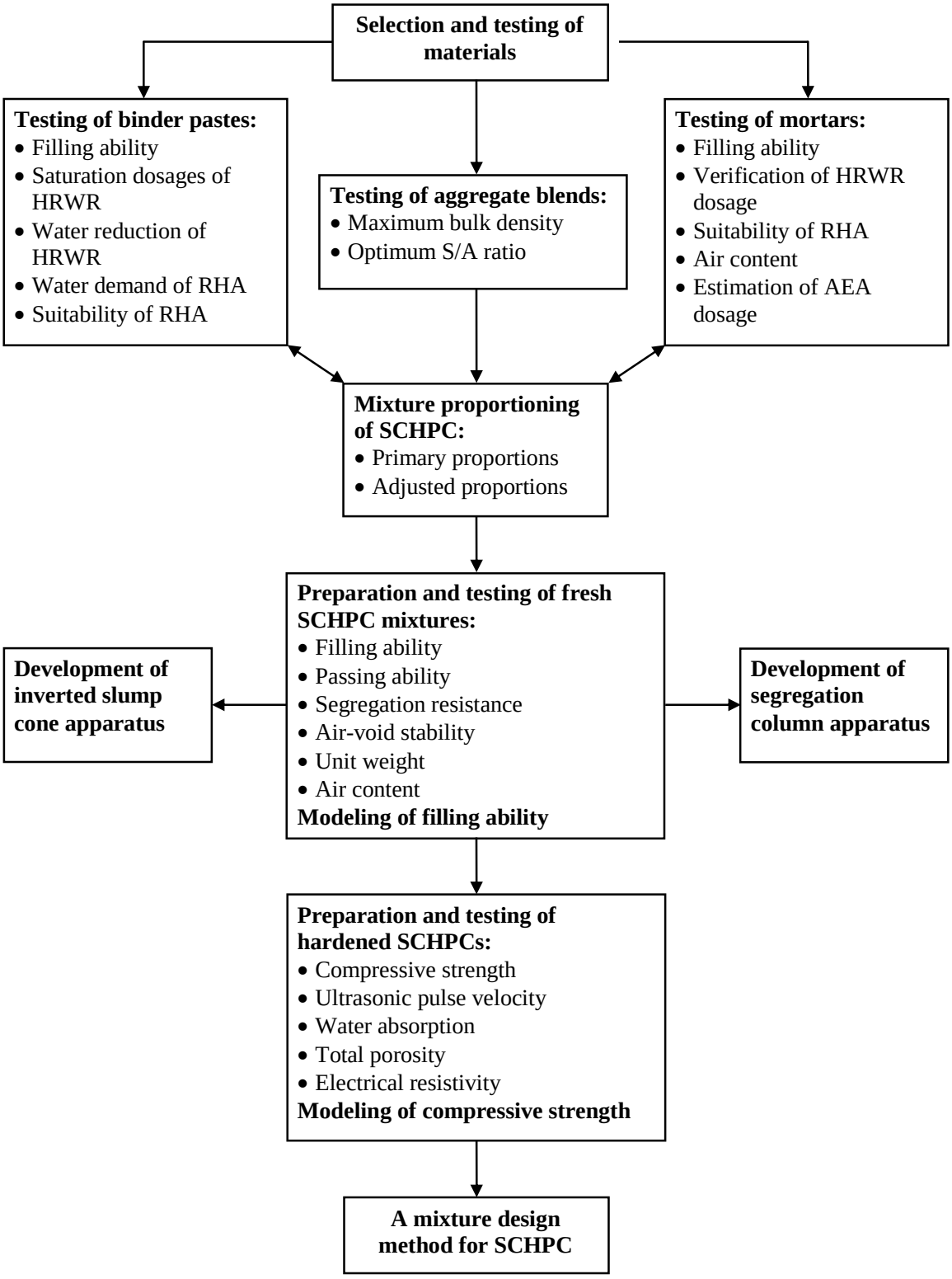

Figure 3.1: Overall research program

Step 4: Various binder pastes were formulated from the primary mixture proportions of the concretes. The binder pastes were tested using a standard grout flow cone to determine their filling ability with respect to flow time, to obtain the saturation dosages of high-range water reducer (HRWR), to find the water reduction caused by HRWR, to observe the suitability of RHA for use in SCHPC, and to assess the water demand of RHA.

Step 5: Various mortars were formulated based on the primary mixture proportions of the concretes. The mortars were tested using a standard flow mould to determine their filling ability with respect to flow spread, to verify the saturation dosages of HRWR obtained from flow cone test, and to observe the suitability of RHA for use in SCHPC. In addition, the mortars were tested using a Chace air indicator to obtain the air content, and thus to estimate the AEA dosages for the concretes.

Step 6: The mixture proportions of different SCHPCs were adjusted after fixing the dosages of HRWR, AEA and viscosity-enhancing admixture (VEA), and correcting the proportions of aggregates and water.

Step 7: The component materials were batched based on the adjusted mixture proportions, and mixed in a revolving type pan mixer to prepare the fresh SCHPC mixtures.

Step 8: New, modified and existing test apparatus were used to investigate the fresh properties of different SCHPCs. An inverted slump cone apparatus including the test procedure and performance criteria was developed for use without and with a J-ring to determine the filling ability and passing ability of SCHPC, respectively. In addition, a simplified column apparatus including the test method and performance criteria was developed to measure the static segregation resistance of SCHPC.

Step 9: The fresh SCHPC mixtures were tested for filling ability, passing ability, unit weight, and air content. In addition, several SCHPC mixtures were tested for air-void stability. The filling ability was determined with respect to slump and slump flow, orimet flow time and spread, and inverted slump cone flow time and spread. The passing ability was measured with regard to slump and slump flow, orimet flow spread, and inverted slump cone flow spread in the presence of a J-ring. The air-void stability was investigated with respect to the air content of concrete after re-mixing at different test stages.

Step 10: The segregation resistance of fresh SCHPCs was visually inspected by observing the quality of concrete resting in mixer pan and during slump flow, orimet flow

and inverted slump cone flow tests. In addition, the segregation resistance of several concretes was quantitatively determined by sieve and column segregation tests.

Step 11: The test specimens were cast after examining the fresh properties of the concretes. The specimens were cured and modified when necessary for determining the key hardened properties of SCHPC mixtures.

Step 12: Existing and modified test methods were used to investigate the hardened properties of different SCHPCs. The laboratory tests were carried out to determine the compressive strength, ultrasonic pulse velocity, water absorption, total porosity, and electrical resistivity of the concretes.

3.3 Modeling and Mixture Design

The models of two key properties such as filling ability and compressive strength and a mixture design method for SCHPC were developed. The filling ability model was developed based on the results of slump flow. The validity of the model was further examined based on the related data available in the literature. The strength model was developed based on the results of compression test for various SCHPC concrete mixtures. The validity of the strength model was also checked using a set of related data gathered from the literature. Finally, a mixture design method for SCHPC was produced based on the test results and developed models.

Chapter 4

Characteristics of Constituent Materials and Aggregate Blends

4.1 General

This chapter deals with the selection and testing of constituent materials for the concretes used in the present study. The physical characteristics of the constituent materials of concretes, the results of sieve analyses for concrete stone and sand (coarse and fine aggregates), and the chemical and particle size analyses of cement and rice husk ash (RHA) are presented and discussed in this chapter. The preparation and testing of the aggregate blends and their test results are also shown and discussed in this chapter. In addition, this chapter discusses the usefulness of the properties of constituent materials and aggregate blends.

4.2 Selection and Testing of Constituent Materials

Concrete stone, concrete sand, normal portland cement, amorphous RHA, normal tap water, polycarboxylate-based high-range water reducer (HRWR), synthetic air-entraining admixture (AEA), and modified polysaccharide-based viscosity-enhancing admixture (VEA) were selected to produce various self-consolidating high performance concretes (SCHPCs). The component materials were tested to examine their suitability and to obtain several physical properties required for the mixture proportioning process of concrete. The following sections describe the constituent materials along with the experiments conducted.

4.2.1 Concrete stone

Locally available concrete stone in the form of a blend of crushed and round aggregates was used as the coarse aggregate (CA). The weight percentage of round aggregate was 50% of the total aggregates. The concrete stone was tested for mass passing 75-μm sieve, oven-dry basis bulk density, void content, saturated surface-dry relative density, absorption, total evaporable moisture content, mass loss due to unconfined freeze-thaw, and accelerated mortar bar

expansion. In addition, the sieve analysis was performed for the concrete stone according to ASTM C 136 (2004).

4.2.2 Concrete sand

Locally available concrete sand in the form of natural pit sand by source was used as the fine aggregate (FA). The sand was found as deposits in soil, and obtained by forming pits into the soil. The concrete sand was tested for mass passing 75-µm sieve, oven-dry basis bulk density, void content, saturated surface-dry basis relative density, absorption, total evaporable moisture content, and accelerated mortar bar expansion. Moreover, the sieve analysis was performed for the concrete sand in accordance with ASTM C 136 (2004).

4.2.3 Normal portland cement

Lafarge normal portland cement (C) was used as the main cementing material. It complied with the requirements of ASTM Type I (CSA Type 10 or Type GU) cement (ASTM C 150, 2004; CAN/CSA A3001, 2003). The cement was tested for sieve fineness by 75-µm, 150-µm and 325-µm sieves, relative density, Blaine specific surface area, setting time, compressive strength, autoclave expansion and air content. It was also tested for the particle size distribution and chemical composition. A Malvern Mastersizer was used for the particle size analysis by laser diffraction method (ISO 13320-1, 1999). The chemical analysis was determined based on ASTM C 114 (2004) to obtain the oxide and compound compositions, free lime, insoluble residue and loss on ignition.

4.2.4 Amorphous rice husk ash

Amorphous (non-crystalline) RHA was used as a supplementary cementing material (SCM). It was available in very fine powder form with a grey color. RHA was tested for relative density, Blaine specific surface area, accelerated pozzolanic activity, particle size distribution, and chemical composition. The accelerated pozzolanic activity was determined according to the procedure used for silica fume, as given in ASTM C 1240 (2004). The hydrometer method, as mentioned in ASTM D 422 (2004) was applied for the particle size analysis of RHA. The borate fusion whole rock analysis by XRF spectrometry was used to determine the oxide composition and loss on ignition of RHA (Taggart, Jr. and Siems 2002).

In addition, the RHA was tested for the sulfur, carbon and chloride contents. The LECO C/S Analyzer was used to determine the total sulfur (Brown and Curry 2002a) and carbon (Brown and Curry 2002b) contents of RHA by combustion. The chloride content was obtained by the pressed powder XRF analysis (Bruker 2004).

4.2.5 Tap water

The normal tap water was used as the mixing water for preparing the concretes. The quality of water was verified with respect to pH, total solids, chlorides, sulfates, and alkalis, which were obtained from the tap water analysis conducted by the Regional Municipality of Waterloo (2003). The tap water was also tested for the density at the ambient temperature (24 ± 2^0C).

4.2.6 Polycarboxylate-based high-range water reducer

A polycarboxylate-based HRWR, commercially known as Glenium 3400 NV, was used to produce the required flowing ability of concrete. It was available in dark brown liquid form. The HRWR was tested to verify whether it complies with the ASTM physical requirements with respect to water content, setting time, compressive strength, flexural strength, length change and relative durability factor (ASTM C494/C 494M, 2004). It was also tested for relative density and solid content.

4.2.7 Synthetic air-entraining admixture

A synthetic AEA, commercially known as Micro Air, was used to produce the required air content in concretes. It was available as brown aqueous solution. The AEA chosen was tested to verify whether it conforms to the ASTM physical requirements with respect to bleeding, setting time, compressive strength, flexural strength, length change, and relative durability factor (ASTM C 260, 2004). It was also tested for relative density and solid content.

4.2.8 Modified polysaccharide-based viscosity-enhancing admixture

A water-soluble modified polysaccharide-based VEA, commercially known as Rheomac VMA 362, was used to improve the segregation resistance of several concretes. It was a

Class A VEA according to the classification given by Rixom and Mailvaganam (1999). The VEA was available as light brown liquid.

The ASTM or CSA currently has no standard specification for VEA. Nevertheless, the "harmlessness" tests were conducted on the VEA selected with regard to setting time, compressive strength, flexural strength, length change and relative durability factor in order to identify any adverse effect of Rheomac VMA 362. The VEA was also tested for relative density and solid content.

4.3 Characteristics of Concrete Stone

The concrete stone was characterized by a number of physical properties and gradation obtained from sieve analysis before using in concrete.

4.3.1 Physical properties

The test results for the physical properties of concrete stone are given in Table 4.1. These properties indicated that the concrete stone was suitable for use as coarse aggregate in producing concretes. The mass finer than 75-μm sieve, mass loss due to unconfined freeze-thaw, and mortar bar expansion were within the maximum permissible limits set by the ASTM or CSA (ASTM C 33, 2004; CSA A23.1, 2004; CSA A23.2, 2004).

Table 4.1: Physical properties of concrete stone

Property	Value	Maximum permissible limit
Mass passing 75-μm sieve*	0.8%	1% (ASTM C33)
Oven-dry basis bulk density	1670 kg/m^3	---
Void content	37%	---
Saturated surface-dry basis relative density	2.71	---
Absorption	1.5%	---
Total evaporable moisture content	0.1%	---
Mass loss due to unconfined freeze-thaw*	3.0%	6% (CSA A23.1)
Accelerated mortar bar expansion*	0.08%	0.15% (CSA A23.2)

* Test results obtained from Peto MacCallum Ltd., Toronto, Ontario, Canada.

The saturated surface-dry basis relative density of concrete stone was 2.71. Most natural aggregates possess relative densities between 2.4 to 2.9 (Kosmatka et al. 2002). The absorption of concrete stone was 1.5%. The absorption of coarse aggregates usually varies

from 0.5 to 4.5% (Neville 1996). Thus, the absorption of concrete stone was in the lower range, which is good for concretes. A higher absorption value is indicative of greater pores in aggregates that might affect the strength and durability of concretes.

The oven-dry basis bulk density of concrete stone determined under compacted condition was 1670 kg/m^3. The bulk density of concrete aggregates generally varies from 1200 to 1750 kg/m^3 (Kosmatka et al. 2002). It includes the pores and voids existing in aggregates. The void content of concrete stone computed based on the oven-dry basis bulk density was 37%. Thus, the void content obtained represents the percentage of voids between compacted aggregates. The void content of coarse aggregates usually ranges from 30 to 45% (Kosmatka et al. 2002).

The concrete stone used was air-dried. There was no free or surface moisture on the surface of aggregates. Therefore, the concrete stone contained a negligible amount of total evaporable moisture (0.1%). The moisture content of coarse aggregates is generally not considered in the primary mixture proportions of concrete. But the moisture content increases the quantity of mixing water that produces a higher W/B ratio and thus produces an impact on the properties of concrete. Hence, the moisture content of the aggregates should be given due allowance to adjust the mixture proportions of concrete.

4.3.2 Gradation

The gradation of concrete stone obtained from the sieve analysis is presented in Figure 4.1. The coefficient of gradation for the gradation curve of concrete stone was 1.12. It indicates that the concrete stone used was well-graded. A well-graded material usually provides a coefficient of gradation in the range of 1 to 3 (Das 1999). Moreover, the grading of the different sizes of concrete stone was between the upper and lower limits specified in ASTM C 33 (2004). The predominant portion of the concrete stone was between the coarser sieve sizes of 19 and 9.5 mm. Therefore, the fineness modulus of concrete stone was also higher. The fineness modulus obtained was 6.78. The fineness modulus of coarse aggregate can vary from 6.30 to 6.90 for the acceptable grading range specified by the ASTM (ASTM C 33, 2004).

The gradation of concrete stone or coarse aggregates affects the workability or flowing ability (filling ability and passing ability) of concrete. This is because it affects the

required water and cement contents of concrete. The grading of coarse aggregates also influences the segregation resistance of concrete, since the packing conditions of the aggregates are affected by the gradation (Neville 1996; Tasi et al. 2006). Thus, poorly graded coarse aggregates might have negative effects on the flowing ability and segregation resistance of SCHPC.

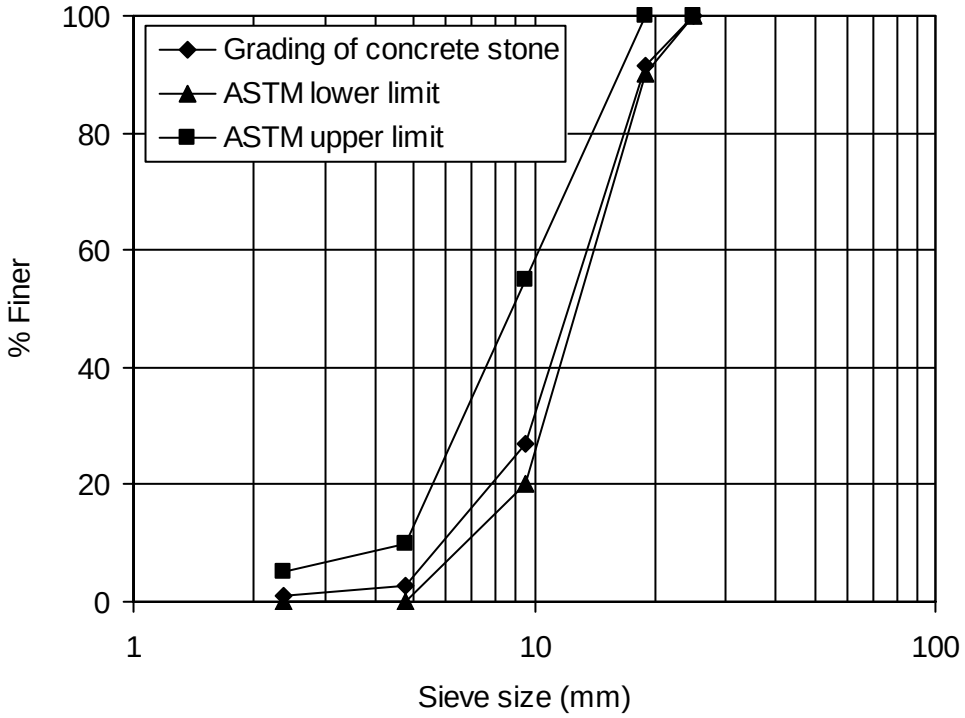

Figure 4.1: Gradation of concrete stone

The gradation also exhibits the maximum size of the coarse aggregates used. The nominal maximum size of the concrete stone was 19 mm, as observed during sieve analysis. The maximum size of the coarse aggregate influences the water content needed for a given flowing ability. An increase in maximum size decreases the required water content. An increased maximum size of coarse aggregate also reduces the cement content (Kosmatka et al. 2002). Thus, the maximum size of coarse aggregate plays a significant role in mixture design of concrete.

4.4 Characteristics of Concrete Sand

The concrete sand was characterized by means of various physical properties. In addition, the gradation of concrete sand was observed by conducting the sieve analysis.

4.4.1 Physical properties

The test results for the physical properties of concrete sand are presented in Table 4.2. The physical properties of concrete sand indicated that it was suitable for use to produce the concretes. The mass passing 75-μm sieve and accelerated mortar bar expansion of concrete sand were below the maximum permissible limits specified by the ASTM or CSA (ASTM C 33, 2004; CSA A23.2, 2004).

Table 4.2: Physical properties of concrete sand

Property	Value	Maximum permissible limit
Mass passing 75-μm sieve*	1.8%	3 to 5% (ASTM C 33)
Oven-dry basis bulk density	1860 kg/m^3	---
Void content	28%	---
Saturated surface-dry basis relative density	2.62	---
Absorption	1.0%	---
Total evaporable moisture content	0.1%	---
Accelerated mortar bar expansion*	0.138%	0.15% (CSA A23.1)

* Test results obtained from Peto MacCallum Ltd., Toronto, Ontario, Canada.

The absorption of concrete sand obtained was 1.0%. The absorption of fine aggregate generally varies in the range of 0.2 to 3.0% (Neville 1996). Hence, the absorption of concrete sand was in the lower range, which is beneficial for concrete properties and durability. Furthermore, the absorption of concrete sand was less than that of concrete stone. It indicates that concrete sand had less pores than concrete stone. Also, the total evaporable moisture content of concrete sand was 0.1%, which is the same as that of concrete stone. The reason may be the identical drying condition.

The oven-dry basis bulk density of concrete sand was 1860 kg/m^3, which is greater than that of concrete stone. The bulk density of sand is generally higher than that of coarse aggregate due to reduced void content. The void content of concrete sand was 28%, which is lower than that of concrete stone. The saturated surface-dry basis relative density of concrete sand was 2.62, which is less than that of concrete stone. Thus, the concrete sand was slightly lighter than the concrete stone. However, the difference between the relative densities of pit sand and concrete stone was insignificant (< 4%). A large difference between the relative densities of fine and coarse aggregates leads to increased segregation in concrete.

4.4.2 Gradation

The gradation of concrete sand obtained from the sieve analysis is shown in Figure 4.2. The coefficient of gradation was 1.03, which is greater than 1. Thus, the concrete sand was considered well-graded. Furthermore, the grading of different sizes of concrete sand was within the limits specified by the ASTM (ASTM C 33, 2004).

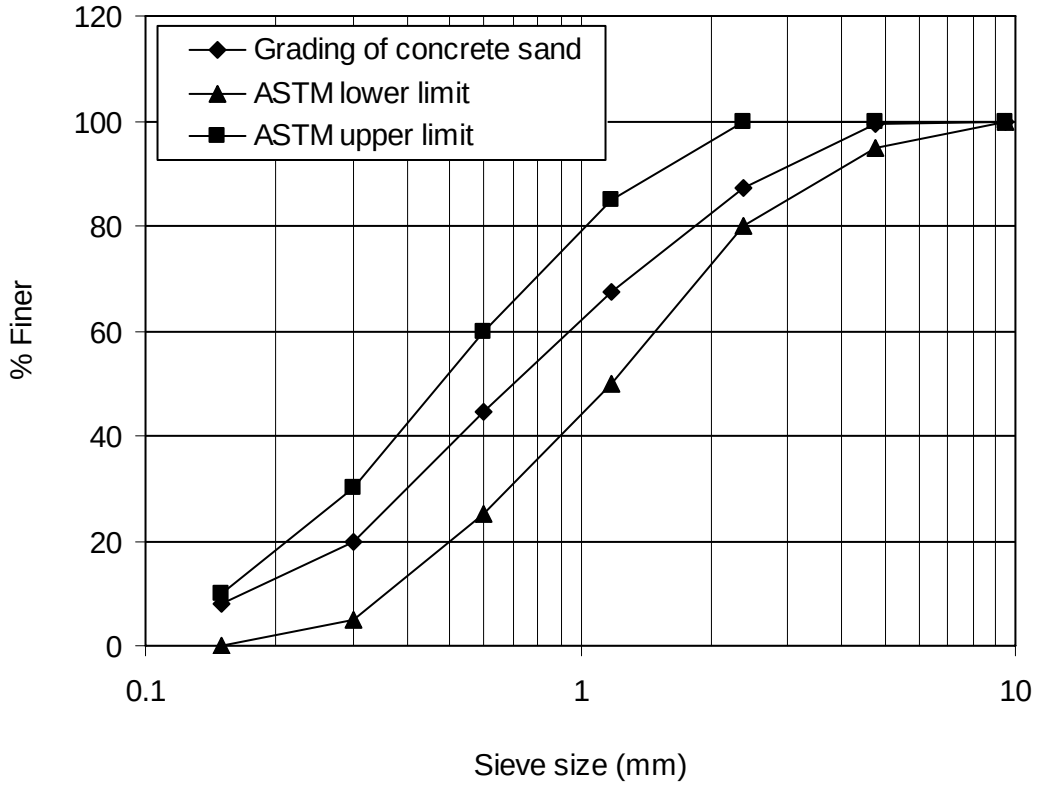

Figure 4.2: Gradation of concrete sand

The nominal maximum size and fineness modulus of concrete sand were obtained from the sieve analysis. The nominal maximum size and fineness modulus of concrete sand were 4.75 and 2.74, respectively. The fineness modulus indicated that the concrete sand was appropriate for producing concrete mixtures. The fineness modulus of sand for use in concrete generally varies in the range of 2.4 to 3.2 (ACI 211.4R-93, 2004; Nawy 1996, Kosmatka et al. 2002).

The gradation of sand influences the total surface area of the aggregates that determines the water demand as well as affects the compressive strength of concrete mixture (Neville 1996). Thus, it influences the mixture design of concrete. Moreover, the sand

gradation affects the flow properties of mortar (Hu and Wang 2005), and influences the physical packing of constituent materials in concrete (Tasi et al. 2006). Consequently, the sand gradation may affect the properties of SCHPC.

4.5 Characteristics of Normal Portland Cement

The normal portland cement was characterized by determining various physical properties, chemical composition and particle size distribution.

4.5.1 Physical properties

The test results for the physical properties of cement used are shown in Table 4.3. The sieve fineness by 45-μm sieve, Blaine specific surface area and compressive strength were above the minimum permissible limits where as the time of setting, autoclave expansion and air content were below the maximum permissible limits set by the ASTM and CSA (ASTM C150, 2004; CSA A23.1, 2004). In addition, the relative density of cement was 3.16. The density of portland cement usually varies from 3.10 to 3.25 (Kosmatka et al. 2002). Thus, the normal portland cement was physically suitable to produce the concretes for this study.

Table 4.3: Physical properties of normal portland cement

Property	Value	Permissible limit
Relative density	3.16	---
Fineness	Blaine specific surface area: 412 m^2/kg	≥ 280 (ASTM C 150)
	% passing 45-μm wet sieve*: 91.5	≥ 72% (CSA A23.1)
	% passing 75-μm dry sieve: 99.1	---
	% passing 150-μm dry sieve: 99.9	---
Time of setting (Vicat)*	Initial: 132 min	45 – 375 min (ASTM C 150)
Compressive strength*	3 days: 26.9 MPa	≥ 14.5 MPa (CSA A23.1)
	7 days: 32.2 MPa	≥ 20 MPa (CSA A23.1)
	28 days: 38.8 MPa	≥ 26.5 MPa (CSA A23.1)
Autoclave expansion*	0.11%	≤ 0.80% (ASTM C 150)
Air content*	7.2%	≤ 12% (ASTM C 150)

*Test results obtained from Lafarge North America, Woodstock, Ontario, Canada.

The Blaine specific surface area and both the dry and wet sieve finenesses assist to check the ground condition of cement. However, the Blaine specific surface area is widely

used to represent the surface fineness of cement. This is better than sieve fineness because it provides an idea of uniformity of the fineness. Also, the specific surface area acts as a measure for the frequency of the particles of average size.

The setting time is an indicator of the unsoundness of cement due to storage. The compressive strength of cement is used to indicate its contribution to the strength of concrete. The autoclave expansion indicates the soundness of cement. The air content indicates the suitability of cement for use in air-entrained concretes. The relative density of cement does not reflect the quality of cement, but it is used for the design and control of concrete mixtures.

4.5.2 Particle size distribution

The particle size distribution of normal portland cement is shown in Figure 4.3. The cement particles were well-graded. The coefficient of gradation was 1.084, which is greater than 1, hence indicating a good grading of the cement.

Most of the cement particles were in the smaller range. Approximately 90% of the cement particles were smaller than 45 μm, as can be seen from Figure 4.3. The median size of the cement was 15 μm. The particle size distribution is also related to the fineness of cement. The greater the amount of smaller cement particles, the higher is the cement fineness. A greater amount of smaller particle sizes increases the rate of cement hydration, and thus accelerates the strength development in concrete.

4.5.3 Chemical composition

The chemical composition of cement is shown in Table 4.4. The cement used fulfilled the chemical requirements specified by the ASTM and CSA (ASTM C 150, 2004; CAN/CSA A3001, 2003). It was mainly composed of the oxides of several metallic elements. The cement had magnesium oxide and sulfur trioxide below the maximum permissible limits. But the equivalent alkali content was higher than the maximum specified limit. The excessive amounts of magnesium oxide and sulfur trioxide make the cement unsound. In addition, the cement may cause alkali-aggregate reaction, efflorescence and staining in concrete if the alkali content is excessive. However, the limit for alkali content is given for the cement intended to be used with potentially reactive aggregates (ASTM C 150, 2004). Since, the

aggregates used in the present study were non-reactive, the alkali content of the cement can be considered acceptable.

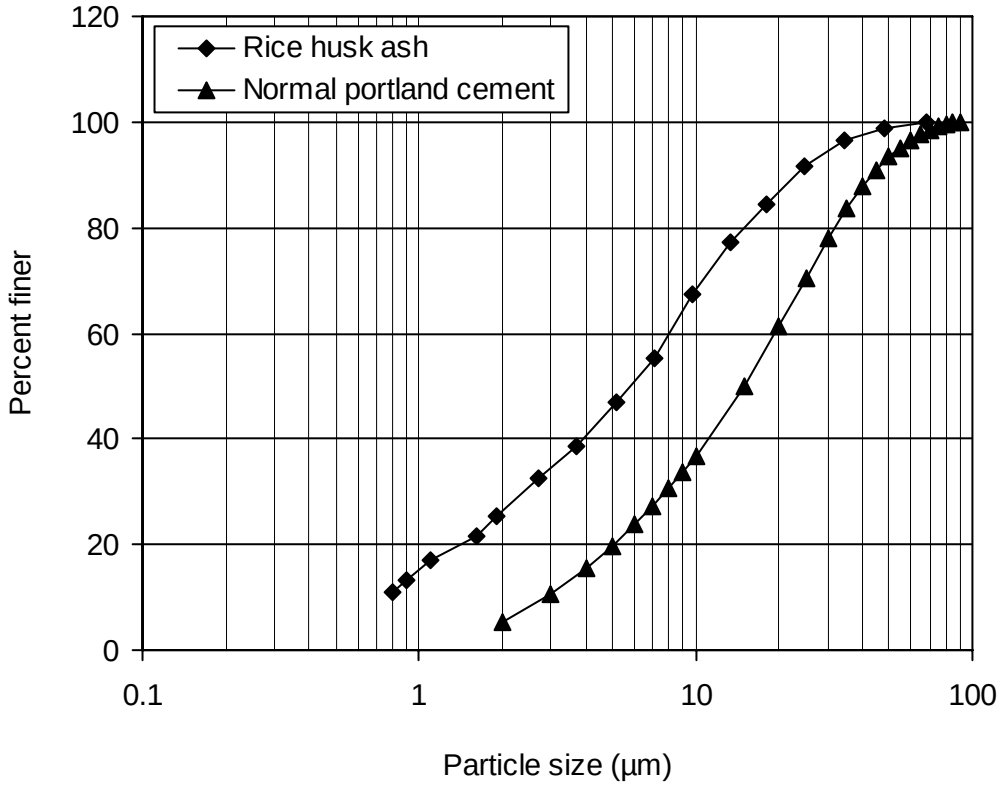

Figure 4.3: Particle size distribution of normal portland cement and rice husk ash

The major compounds of the cement are also shown in Table 4.4. The quantities of the compounds present in cement were consistent with the typical range (Brandt 1995). The cement used also contained a negligible amount of insoluble residue. It largely arises from the impurities of gypsum. The loss on ignition of the cement was below the maximum permissible limit set by the ASTM (ASTM C 150, 2004). A higher loss on ignition indicates pre-hydration and/or carbonation due to the exposure of cement to the atmosphere during improper or prolonged storage.

4.6 Characteristics of Amorphous Rice Husk Ash

The RHA was characterized by means of several physical properties, chemical composition and particle size distribution.

Table 4.4: Chemical composition of normal portland cement*

Chemical component	Mass content (%)	Permissible limit
Oxide composition		
Silicon dioxide or silica (SiO_2)	19.7	---
Aluminum oxide or alumina (Al_2O_3)	5.1	---
Iron oxide (Fe_2O_3)	2.5	---
Calcium oxide or lime (CaO)	62.3	---
Magnesium oxide or magnesia (MgO)	3.3	≤ 6% (ASTM C 150)
Sulfur trioxide or sulfuric anhydrite (SO_3)	2.9	3 – 3.5% (ASTM C 150)
Free lime (FCaO)	1.1	---
Equivalent alkalis or alkaline oxides ($Na_2O + 0.658K_2O$)	0.72	≤ 0.6% (ASTM C 150)
Compound composition		
Tricalcium silicate (C_3S)	58	---
Dicalcium silicate (C_2S)	13	---
Tricalcium aluminate (C_3A)	9	---
Tetracalcium aluminoferrite (C_4AF)	8	---
Others		
Insoluble residue	0.46	≤ 1.5% (CSA A23.1)
Loss on ignition	2.7	≤ 3% (ASTM C 150)

* Test results obtained from Lafarge North America, Woodstock, Ontario, Canada.

4.6.1 Physical properties

The results for the tested physical properties are shown in Table 4.5. The relative density of RHA was 2.07. It generally varies in the range of 2.05 to 2.10 for most sources of RHA (Mehta 2002, Nehdi et al. 2003b). The Blaine specific surface area of RHA was 2326 m^2/kg. The Blaine air permeability method is not convenient to measure the high specific surface area of RHA. However, it was used to obtain the Blaine specific surface area of RHA for comparison with normal portland cement. The Blaine specific surface area of RHA was about 5.65 times that of normal portland cement. The specific surface area of cementing material or binder influences the strength of concrete. The greater the fineness of binder, the higher is the strength of concrete. Hence, the higher Blaine specific surface area of RHA indicates that it would produce a good development of compressive strength in concrete. In contrast, the incorporation of RHA would cause a reduction in the flowing ability of

concrete. This is because the increase in specific surface area results in a greater water demand and reduces the amount of free water available in concrete mixture.

Table 4.5: Physical properties of rice husk ash

Property	Value
Relative density	2.07
Blaine specific surface area	2326 m^2/kg
Accelerated pozzolanic activity	122.4%

The accelerated pozzolanic activity index was 122.4%, which is much higher than 85%, the minimum requirement for silica fume (ASTM C 1240, 2004). The pozzolanic activity of RHA is generally greater than that of other supplementary cementing materials such as silica fume (Nehdi et al. 2003b). This is due to extremely high specific surface area of RHA. The specific surface area of RHA is much higher than that of fly ash and ground granulated blast-furnace slag, and even silica fume. The specific surface area of RHA by nitrogen adsorption can be about 1.5 times that of silica fume (Zhang and Malhotra 1996). Nevertheless, the high accelerated pozzolanic activity index of RHA indicates that it would accelerate the strength development at the early ages of concrete.

4.6.2 Particle size distribution

The particle size distribution of RHA is shown in Figure 4.3. It was obtained using a soil hydrometer based on the principle of Stokes' law for particle size determination. This method is widely used for obtaining an estimate of the distribution of soil particle sizes ranging from 1 to 75 μm. The range of soil particle sizes for the hydrometer analysis to be valid is approximately 0.2 to 200 μm, which also covers the size range of RHA. In addition, the dry sample is mixed with distilled water and a small amount of dispersing agent to form the suspension for use in hydrometer analysis. A similar sample preparation is also applicable for RHA since it does not react with water.

The RHA particles were well-graded with a coefficient of gradation approximately 1. About 85% of the RHA particles were smaller than 20 μm. The median particle size of RHA was 6 μm. A median diameter of RHA in the range of 6 to 15 μm is preferred with respect to workability and cohesiveness (Mehta 2002). The median particle size of RHA was 2.5 times finer than that of cement. The lower particle size of RHA contributes to reduce the bleeding

in concrete. A lower particle size increases the density of the paste, and thus lessens the bleeding in concrete by obstructing the movement of rising water. The lower particle size of RHA also improves the particle packing in binder paste, and thus the compressive of concrete. However, the lower particle size of RHA results in increased specific surface area that affects the water demand of concrete for a given flowing ability.

4.6.3 Chemical composition

The chemical composition of RHA is presented in Table 4.6. The major component of RHA is silicon dioxide or silica (SiO_2). The mass content of silica was more than 90% in RHA. This is the main oxide component that contributes to the pozzolanic reaction or secondary hydration in concrete including RHA. There were other oxides in insignificant quantities. In addition to the oxide components, negligible amounts of sulfur and carbon were present in RHA. The RHA was also tested for the chloride content. The amount of chloride found was 110 g/t (0.011%), which is acceptable. The recommended water-soluble chloride limit is typically 0.06% by mass of cementing material to avoid the risk of corrosion in concrete (ACI 222R-01, 2004).

There are no ASTM or CSA chemical requirements for RHA. However, the chemical requirements for silica fume can be applied to RHA since they are similar SCMs by chemical composition. The maximum permissible loss on ignition and the minimum amount of silica required are 6% and 85%, respectively for silica fume (CAN/CSA A3001, 2004). In case of RHA, the loss on ignition was less than 6% and the silica content was much higher than 85%. Also, the equivalent alkali content of RHA was 0.88%. An equivalent alkali content lower than 1% is specified for silica fume to counteract the reactivity of aggregates (CSA A23.2, 2004). This limit can also be applied to RHA, since its pozzolanic activity is similar to that of silica fume. Thus, the RHA was acceptable for use in concrete even with the potentially reactive aggregates.

4.7 Quality of Tap Water

The tap water did not contain any objectionable substances causing color or odor. The composition of the tap water obtained from the analysis conducted by the Regional Municipality of Waterloo (2003) is shown in Table 4.7.

Table 4.6: Chemical composition of rice husk ash*

Chemical component	Mass content (%)
Oxide composition	
Silicon dioxide or silica (SiO_2)	93.6
Aluminum oxide or alumina (Al_2O_3)	0.02
Iron oxide (Fe_2O_3)	0.80
Calcium oxide or lime (CaO)	0.38
Magnesium oxide or magnesia (MgO)	0.34
Sodium oxide (Na_2O)	0.05
Potassium oxide (K_2O)	1.26
Equivalent alkalis ($Na_2O + 0.658\ K_2O$)	0.88
Titanium oxide (TiO_2)	0.01
Phosphorous oxide (P_2O_5)	0.58
Manganese oxide (MnO)	0.14
Chromium oxide (Cr_2O_3)	0.01
Vanadium oxide (V_2O_5)	< 0.01
Others	
Sulfur (S)	< 0.01
Carbon (C)	0.15
Loss on ignition	1.90
Chloride (Cl): 110 g/t	

* Test results obtained from SGS Lakefield Research Limited, Ontario, Canada.

Table 4.7: Quality of normal tap water*

Parameter	Value contained	CSA permissible limit
Solids	430 mg/L	≤ 50000 mg/L
Chlorides (Cl^-)	80 mg/L	≤ 500 mg/L
Sulfates (SO_4^{2-})	55 mg/L	≤ 3000 mg/L
Sodium (Na^+)	30 mg/L	---
Potassium (K^+)	2.5 mg/L	---
Sodium equivalent ($Na_2O + 0.658K_2O$)	42.4 mg/L	≤ 600 mg/L
pH	7.56	---

*Test results obtained from the Regional Municipality of Waterloo.

The water was not tested to verify the acceptance criteria based on the physical tests for compressive strength and setting time, as specified in ASTM C 94/C 94M (2004). This is because the aesthetical and chemical qualities of water were excellent. The total solids, chlorides, sulfates and alkalis of water were far below the maximum permissible limit

specified by the CSA A23.1 (2004). However, the tap water was tested to determine the density required for mixture proportioning process. The density of water found was 997.28 kg/m^3. It was determined at the ambient temperature (24^{0}C) since the batching and mixing of the concretes were carried out at 24±2^{0}C.

4.8 Characteristics of Glenium 3400 NV

The results for the tested properties of Glenium 3400 NV with respect to the physical requirements specified in ASTM C 494/C 494M (2004) are presented in Table 4.8. All physical requirements for Type F (HRWR) chemical admixture were fulfilled for Glenium 3400 NV. Moreover, the relative density and solid content of Glenium 3400 NV were 1.069 and 41%, respectively. The relative density was used to compute the volume basis dosages of HRWR. Also, both relative density and solid content helped to calculate the water contribution of HRWR while adjusting the mixing water for various concrete mixtures.

Table 4.8: Physical analysis of Glenium 3400 NV*

Property	Control concrete	Concrete with Glenium 3400 NV	Change vs. control	ASTM permissible limit
Water content (kg/m^3)	137.6	121.6	88%	≤ 88%
Setting time (hr:min)				
Initial	4:12	4:10	-0:02	-1:00 to +1:30
Final	5:35	5:32	-0:03	-1:00 to +1:30
Compressive strength (MPa)				
1day	9.86	16.3	165%	≥ 140
3 days	19.6	29.2	149%	≥ 125
7 days	24.4	31.8	130%	≥ 115
28 days	32.8	40.4	123%	≥ 110
6 months	43.0	47.9	111%	≥ 100
1 year	46.8	49.9	107%	≥ 100
Flexural strength (MPa)				
3 days	3.3	4.3	130%	≥ 110
7 days	3.9	5.0	128%	≥ 100
28 days	5.0	6.1	122%	≥ 100
Shrinkage, increase over control (percentage points)	0.032	0.038	0.007	≤ 0.010
Relative durability factor	---	97%	---	≥ 80%

*Test results obtained from BASF Construction Chemicals Ltd., Brampton, Ontario, Canada.

4.9 Characteristics of Micro Air

The test results of the physical analysis of Micro Air with regard to the physical requirements specified by the ASTM (ASTM C 260, 2004) are presented in Table 4.9. All physical requirements of AEAs were fulfilled for Micro Air. Moreover, the relative density and solid content of Micro Air determined were 1.01 and 13%, respectively. The relative density of Micro Air was close to that of water, thus eased the dispersion of AEA in mixing water. The solid content was helpful to identify any unexpected solid impurities in Micro Air. Also, the relative density helped to calculate the volume basis dosages of Micro Air.

Table 4.9: Physical analysis of Micro Air*

Property	Control concrete	Concrete with Micro Air	Change vs. control	ASTM permissible limit
Bleeding (% over control)	---	0.06	---	≤ 2%
Setting time (hr:min)				
Initial	3:34	3:44	+0:10	-1:15 to +1:15
Final	4:43	5:05	+0:22	-1:15 to +1:15
Compressive strength (MPa)				
3 days	23.7	21.7	92%	≥ 90
7 days	31.0	28.8	93%	≥ 90
28 days	36.7	36.1	98%	≥ 90
Flexural strength (MPa)				
3 days	4.1	4.1	100%	≥ 90
7 days	4.4	4.6	105%	≥ 90
28 days	5.4	5.3	98%	≥ 90
Shrinkage, increase over control (percentage points)	0.038	0.039	0.001	≤ 0.006
Relative durability factor	---	99%	---	≥ 80%

*Test results obtained from BASF Construction Chemicals Ltd., Brampton, Ontario, Canada.

4.10 Characteristics of Rheomac VMA 362

The results of "harmlessness tests" are shown in Table 4.10. The results of "harmlessness tests" were justified based on several permissible limits specified in ASTM C 494/C 494M (2004). The physical requirements for length change (shrinkage) and relative durability factor are the same for all chemical admixtures mentioned in this standard specification. It can also be applied for a VEA such as Rheomac VMA 362. In addition, the compressive and flexural

strength requirements are minimum for Type B (retarding) chemical admixture whereas the setting time requirement is minimum for Type A (water reducing) chemical admixture. These requirements can also be applied to Rheomac VMA 362 to examine whether it produces any adverse effects.

The results of "harmlessness tests" exhibit that Rheomac VMA 362 was not harmful for the properties of concrete. The relative density and solid content of Rheomac VMA 362 determined were 1.002 and 0.5%, respectively. The relative density was very close to that of mixing water. It facilitated the dispersion of Rheomac VMA 362 in concrete. In addition, the relative density supported to determine the volume basis dosages of Rheomac VMA 362.

Table 4.10: Physical analysis of Rheomac VMA 362*

Property	Control concrete	Concrete with Rheomac VMA 362	Change vs. control	ASTM permissible limit
Time of setting (hr:min)				
Initial	4:36	4:45	+0:09	-1:00 to +1:30
Final	6:16	6:12	-0:04	-1:00 to +1:30
Compressive strength (MPa)				
3 days	17.0	18.3	108%	≥ 90%
7 days	22.0	24.2	110%	≥ 90%
28 days	29.6	32.0	108%	≥ 90%
6 months	38.0	39.2	103%	≥ 90%
1 year	41.6	39.3	95%	≥ 90%
Flexural strength (MPa)				
3 days	3.7	3.5	95%	≥ 90%
7 days	4.6	4.6	100%	≥ 90%
28 days	5.7	5.4	95%	≥ 90%
Shrinkage, increase over control (percentage points)	0.019	0.026	0.007	≤ 0.010
Relative durability factor	---	99%	---	≥ 80%

*Test results obtained from BASF Construction Chemicals Ltd., Brampton, Ontario, Canada.

4.11 Preparation and Testing of Aggregate Blends

Various aggregate blends were prepared using air-dry basis fine and coarse aggregates, and tested to determine compacted and uncompacted or loose bulk densities, and thus to obtain the optimum S/A ratio producing maximum bulk density.

4.11.1 Preparation of aggregate blends

The air-dry basis fine and coarse aggregates were mixed by hand using shovel and scoop to prepare the aggregate blends. The CA/FA and sand-aggregate (S/A) ratios used in the aggregate blends for determining bulk density and optimum S/A ratio are shown in Table 4.11. The size of these aggregate blends was 20 kg, which was more than 125% of the weight-basis quantity required to fill the cylindrical measure used for determining bulk density. According to ASTM C29/C 29M (2004), the size of aggregate sample should be about 125% to 200% of the quantity needed to fill the measure.

Table 4.11: Details of the aggregate blends used for testing bulk density and optimum sand-aggregate ratio.

Aggregate blend	CA/FA ratio	S/A ratio [FA/(FA+CA)]	Aggregate quantities for testing bulk density (kg)	
			Coarse aggregate	Fine aggregate
A25	0.25	0.80	4.00	16.00
A50	0.50	0.67	6.65	13.35
A75	0.75	0.57	8.60	11.40
A100	1.00	0.50	10.00	10.00
A125	1.25	0.45	11.10	8.90
A150	1.50	0.40	12.00	8.00
A175	1.75	0.36	12.75	7.25
A200	2.00	0.33	13.35	6.65

4.11.2 Test for bulk density and optimum sand-aggregate ratio

The bulk density of the aggregate blends was determined in compacted and uncompacted or loose conditions. A cylindrical metal measure or container of 7.21 liters capacity was used in the measurement. The test procedures given in ASTM C 29/C 29M (2004) were followed to determine the compacted and uncompacted bulk densities. In determining the uncompacted bulk density, the cylindrical measure was filled with aggregate blends in one layer and without any compaction. In contrast, the cylindrical measure was filled in three layers, and each layer was compacted by rodding in specified manner to obtain the compacted bulk density. In both cases, the filling operation was conducted by means of a scoop. Based on the test results for compacted and uncompacted bulk densities, the optimum S/A ratio leading to the maximum bulk density was determined.

4.12 Properties of Aggregate Blends

The properties of aggregate blends obtained were compacted, loose or uncompacted and maximum bulk densities, and optimum S/A ratio.

4.12.1 Bulk density

The compacted and uncompacted bulk densities of different aggregate blends obtained for various S/A ratios are presented in Figure 4.4.

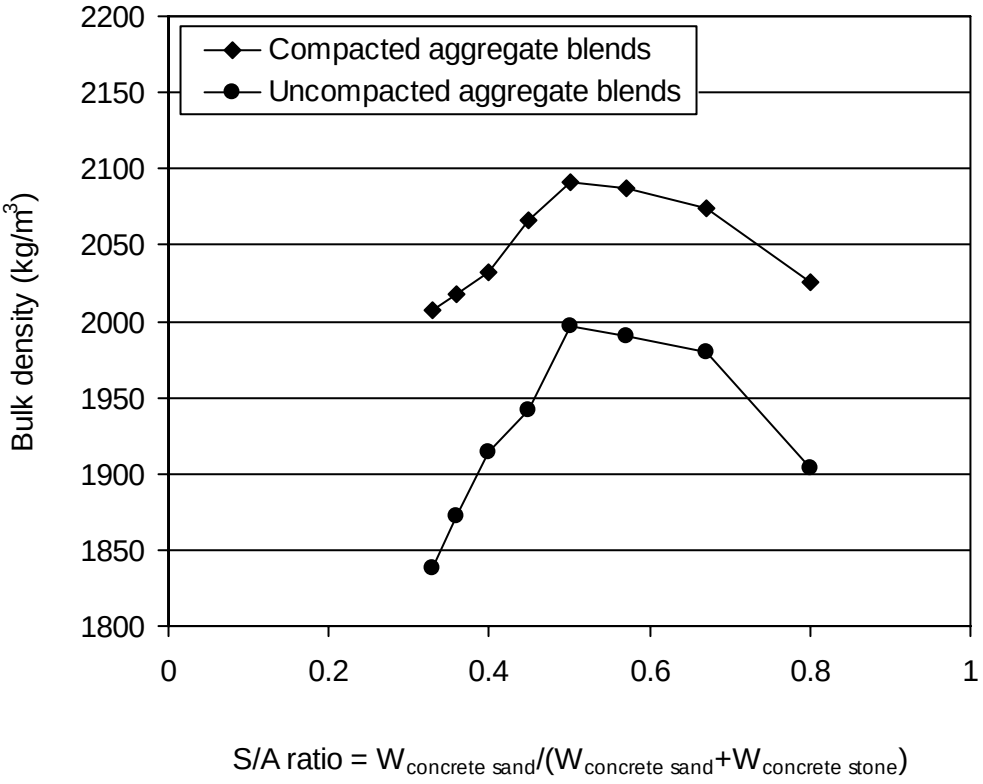

Figure 4.4: Bulk densities of different aggregate blends

Compacted bulk density:

The compacted bulk density was obtained for the compacted aggregate blends. It varied with the S/A ratios, as can be seen from Figure 4.4. The compacted bulk density gradually increased from 2007.7 to 2091.0 kg/m^3 for the S/A ratio varying in the range of 0.33 to 0.50.

Then it decreased with the increase in S/A ratio. This suggests that the extent of voids between aggregates also varied with different S/A ratios.

Uncompacted bulk density:

The uncompacted bulk density was obtained for the loose aggregate blends. Similar to compacted bulk density, it also varied with the S/A ratios, as can be seen from Figure 4.4. The uncompacted bulk density gradually increased from 1837.8 to 1997.3 kg/m^3 for the S/A ratio varying in the range of 0.33 to 0.50. Also, the curve of uncompacted bulk density obtained was below that of compacted bulk density. This is because the uncompacted bulk density was lower than the compacted bulk density for all S/A ratios. The lower uncompacted bulk density indicates the presence of greater void content in aggregate blends.

Maximum bulk density:

The bulk density of the aggregate blends reached a maximum value for a particular S/A ratio. It was called the maximum bulk density. The compacted and uncompacted maximum bulk densities obtained were 2091.0 and 1997.3 kg/m^3, respectively. The maximum bulk density is accompanied with a minimum void content in aggregate blend that contributes to produce low porosity and good compressive strength in concretes.

4.12.2 Optimum sand-aggregate ratio

The S/A ratio, which resulted in the maximum bulk density in aggregate blends was defined as the optimum S/A ratio. For both compacted and uncompacted aggregate blends, the optimum S/A ratio found was 0.50, as can be seen from Figure 4.4.

4.13 Use of Properties of Constituent Materials and Aggregate Blends

The properties of the constituent materials were used to judge their suitability for producing paste, mortar and concrete mixtures. In addition, a number of physical properties of the materials were used in determining the primary and adjusted mixture proportions of the concretes. The sieve analyses of fine and coarse aggregates were useful to identify any deviation from the gradation requirement. The chemical compositions of the cementing materials were used to check the required proportions of the component compounds, and to

examine whether any impurities are present beyond the permissible limits. The particle size analyses of the cementing materials were useful to understand their packing characteristics in the paste composition of the concretes.

The bulk density results of aggregate blends were used to determine the optimum S/A ratio. The optimum S/A ratio was beneficial to obtain the mixture proportions of various SCHPCs. The optimum S/A ratio leading to maximum bulk density was used in the concretes to produce low water absorption and porosity, high electrical resistivity and ultrasonic pulse velocity, and good compressive strength. In addition, the optimum S/A ratio lessened the amount of cementing material required for concretes, and thus made the concrete production more economic.

4.14 Conclusions

a. The constituent materials were suitable for producing the concrete mixtures, as they met the specified physical and chemical requirements.
b. The gradations of fine and coarse aggregates were in the specified range suitable for producing concrete mixtures.
c. The chemical compositions of the cementing materials exhibited that the chemical components were in specified proportions and no impurities were present above the maximum permissible limits.
d. The particle size analyses of the cementing materials revealed that both cement and RHA were well-graded suggesting good particle packing in the paste composition of concretes.
e. The maximum compacted and uncompacted bulk densities with minimum void content were obtained at the optimum S/A ratio of 0.50.
f. The optimum S/A ratio was used in the mixture proportioning of concretes to improve the hardened properties and durability of concrete.

Chapter 5

Filling Ability of Binder Pastes

5.1 General

The preparation and testing of various binder pastes, and the test results for the filling ability of the binder pastes with respect to flow time are presented and discussed in this chapter. The effects of high-range water reducer (HRWR), rice husk ash (RHA), and water-binder (W/B) ratio on the filling ability of the binder pastes are discussed. The saturation dosages and water reduction capacity of HRWR, and the water demand and suitability of RHA are highlighted. Finally, this chapter emphasizes how the paste filling ability results can be used in the concrete mixture design process.

5.2 Research Significance

The filling ability of binder pastes is useful to facilitate the mixture proportioning process of self-consolidating high performance concrete (SCHPC). The optimum combination of the cement, supplementary cementing material (SCM) and HRWR for an SCHPC mixture can be selected based on the filling ability of its binder component. The optimization of cement-admixture system reduces the volume of laboratory work involved in determining the mixture proportions of SCHPC. In addition, it is possible to predict the filling ability of SCHPC based on the filling ability of its paste component. Consequently, the whole mixture proportioning process becomes simplified, and the loss of materials is minimized. Moreover, the effectiveness and suitability of SCM and the efficiency of HRWR to be used in concretes can be examined based on the filling ability of the binder pastes.

5.3 Preparation and Testing of Binder Pastes

Different types of binder paste were prepared and tested to determine the filling ability with respect to flow time. The increased flow time correlates with a reduced filling ability of the pastes. The water reduction capacity and saturation dosage (SD) of HRWR and the water

demand of RHA were also determined based on the filling ability results of various binder pastes.

The binder pastes were designated based on the W/B ratio and RHA content used in corresponding parent concretes (Table 5.1). For example, the ‘P30R0S1’ and ‘P30R0S2’ designations were chosen for the binder pastes prepared with a W/B ratio of 0.30 and 0% RHA content, as used in corresponding parent concrete ‘C30R0A6’. In addition, the ‘S1’ and ‘S2’ components were used in the designations to categorize the binder pastes under series 1 and series 2, respectively.

5.3.1 Preparation of binder pastes

A series of binder pastes (P30R0S1 to P50R0S1), as shown in Table 5.1, was prepared to investigate the filling ability at various HRWR dosages, and thus to determine the saturation dosages of HRWR. The lower limits of HRWR dosage were selected to produce a continuous flow whereas the upper limits were chosen to obtain a flow beyond the saturation flow of pastes. The amount of the mixing water (W) for these pastes was 1.571 kg. The amounts of cement (C) and RHA were varied based on their proportions in the corresponding parent concretes. Another series of binder pastes (P30R0S2 to P50R0S2), as shown in Table 5.2, was prepared to test the filling ability for various water contents, and thus to determine the water reduction caused by HRWR and the water demand of RHA. The amounts of cement and RHA were same as in the first series. However, no HRWR was used to vary the filling ability of the pastes. Instead, the mixing water was increased incrementally to increase the filling ability of the pastes. The limits of water increment were chosen to produce a continuous flow of the pastes with successively lower flow time in the absence of HRWR.

The binder pastes were prepared using an epicyclic revolving type small mechanical mixer conforming to ASTM C 305 (2004). The mixer is shown in Figure 5.1. The nominal capacity of the mixing bowl was 4.73 liters. The cementing or binding material (cement alone or with RHA) was placed in the mixing bowl and dry mixed for 30 seconds with a stainless steel spoon. This step was omitted when RHA was not present in the binder system. The mixer was then started and the binding material was mixed with water for 30 seconds. Then the mixer was stopped, and the paste was quickly scraped from side and bottom of the mixing bowl over a period of 30 seconds. The mixer was restarted and run for 60 seconds.

The initial dosage of HRWR was added over a period of 5 to 10 seconds and the mixing was continued for 30 seconds. This step was omitted for the second series of binder pastes (P30R0S2 to P50R0S2) listed in Table 5.2. Nevertheless, the mixer was stopped again, and the paste was scraped from side and bottom of the mixing bowl to break the agglomerates over a period of 30 seconds. The mixer was restarted again and run for additional 30 seconds. Later, subsequent dosages of HRWR were used to increase the fluidity of the binder pastes (from P30R0S1 to P50R0S1) mentioned in Table 5.1. For each incremental HRWR dosage, further mixing was conducted for 60 seconds. This step was different for the binder pastes (P30R0S2 to P50R0S2) shown in Table 5.2, where the water content was increased subsequently instead of adding HRWR. In all mixing stages, the mixer was run at slow speed to minimize the entrapped air.

Table 5.1: Details of the binder pastes prepared with various dosages of HRWR (series 1)

Paste	Parent concrete*	W/B ratio	RHA (%B)	C♠ (kg)	RHA (kg)	W♣ (kg)	HRWR (%B)
P30R0S1	C30R0A6	0.30	0	5.237	0	1.571	0.25-2.00
P30R15S1	C30R15A6	0.30	15	4.451	0.786	1.571	0.75-4.00
P30R20S1	C30R20A6	0.30	20	4.190	1.047	1.571	0.75-4.00
P35R0S1	C35R0A4 C35R0A6 C35R0A8	0.35	0	4.489	0	1.571	0.25-2.00
P35R5S1	C35R5A6	0.35	5	4.265	0.225	1.571	0.25-2.00
P35R10S1	C35R10A6	0.35	10	4.040	0.449	1.571	0.50-3.00
P35R15S1	C35R15A4 C35R15A6 C35R15A8	0.35	15	3.816	0.673	1.571	0.50-4.00
P35R20S1	C35R20A4 C35R20A6 C35R20A8	0.35	20	3.591	0.898	1.571	0.75-4.00
P35R25S1	C35R25A6	0.35	25	3.367	1.122	1.571	0.75-4.50
P35R30S1	C35R30A6	0.35	30	3.142	1.347	1.571	0.75-5.00
P40R0S1	C40R0A6	0.40	0	3.928	0	1.571	0.25-2.00
P40R15S1	C40R15A6	0.40	15	3.338	0.589	1.571	0.25-2.00
P40R20S1	C40R20A6	0.40	20	3.142	0.786	1.571	0.50-2.50
P50R0S1	C50R0A2 C50R0A6	0.50	0	3.142	0	1.571	0-1.25

*Concrete designations are explained in Chapter 7; ♠Cement; ♣Water.

Table 5.2: Details of the binder pastes prepared with different increased water contents (series 2)

Paste	Parent concrete*	Initial W/B ratio	RHA (%B)	C (kg)	RHA (kg)	Initial W (kg)	Increase in water content (%W)
P30R0S2	C30R0A6	0.30	0	5.237	0	1.571	40-80
P30R15S2	C30R15A6	0.30	15	4.451	0.786	1.571	70-110
P30R20S2	C30R20A6	0.30	20	4.190	1.047	1.571	80-120
P35R0S2	C35R0A4 C35R0A6 C35R0A8	0.35	0	4.489	0	1.571	20-60
P35R5S2	C35R5A6	0.35	5	4.265	0.225	1.571	30-70
P35R10S2	C35R10A6	0.35	10	4.040	0.449	1.571	40-80
P35R15S2	C35R15A4 C35R15A6 C35R15A8	0.35	15	3.816	0.673	1.571	50-90
P35R20S2	C35R20A4 C35R20A6 C35R20A8	0.35	20	3.591	0.898	1.571	60-100
P35R25S2	C35R25A6	0.35	25	3.367	1.122	1.571	70-110
P35R30S2	C35R30A6	0.35	30	3.142	1.347	1.571	80-120
P40R0S2	C40R0A6	0.40	0	3.928	0	1.571	10-50
P40R15S2	C40R15A6	0.40	15	3.338	0.589	1.571	30-70
P40R20S2	C40R20A6	0.40	20	3.142	0.786	1.571	40-80
P50R0S2	C50R0A2 C50R0A6	0.50	0	3.142	0	1.571	0-20

*Concrete designations are explained in Chapter 7

5.3.2 Flow cone test

The filling ability of the binder pastes was investigated by flow cone test. A flow cone conforming to ASTM C 939 (2004) was used to measure the filling ability with respect to flow time. The calibration volume of the flow cone was 1.725 liters. It had a 19 mm (internal diameter) discharge tube at the bottom. The flow cone was leveled, and the discharge tube was closed using a rubber stopper. The paste was poured into the flow cone up to the calibration mark. The rubber stopper was then removed to allow the paste to flow out of the cone. Simultaneously, a stopwatch was started to record the flow time of the paste. The paste passing through the discharge tube was collected in a receiving container and transferred to the mixer bowl for further mixing with additional HRWR or water to vary the filling ability.

In the case of the binder pastes (P30R0S1 to P50R0S1) listed in Table 5.1, several incremental dosages of HRWR were added to the paste and the flow time was determined for each increment. In contrast, the water content was increased step by step for the binder pastes (P30R0S2 to P50R0S2) listed in Table 5.2, and the flow time was determined for each increase in water content. An operational stage of the flow cone test is shown in Figure 5.1.

Mixer for preparing pastes and mortars

Flow cone test for pastes

Figure 5.1: Mixer for preparing binder pastes and testing of paste filling ability

5.4 Filling Ability of Binder Pastes

The results of the flow cone test for various binder pastes under series 1 are presented in Figures 5.2 to 5.4. These figures indicate the filling ability of the binder pastes with respect to the flow time at various dosages of HRWR. In addition, the flow cone test results for various binder pastes under series 2 are shown in Figures 5.5 to 5.7. These figures exhibit the filling ability of the binder pastes with regard to flow time with increasing water content at no HRWR.

5.4.1 Effect of high-range water reducer

The effect of HRWR on the filling ability of binder pastes is evident in Figures 5.2 to 5.4. The filling ability of the binder pastes was increased, that is, the flow time was decreased with increasing dosages of HRWR. This indicates that the plastic viscosity of the binder

pastes was gradually reduced, and thus the paste fluidity was increased with greater HRWR dosages. This is mostly due to the liquefying and dispersing actions of the HRWR. In liquefying action, the HRWR improves the filling ability of the binder pastes with reduced yield stress and plastic viscosity. In dispersing action, the HRWR hinders the coagulation or flocculation of cement particles and disperses them more evenly, hence enhancing the filling ability of the binder pastes through reduced inter-particle friction.

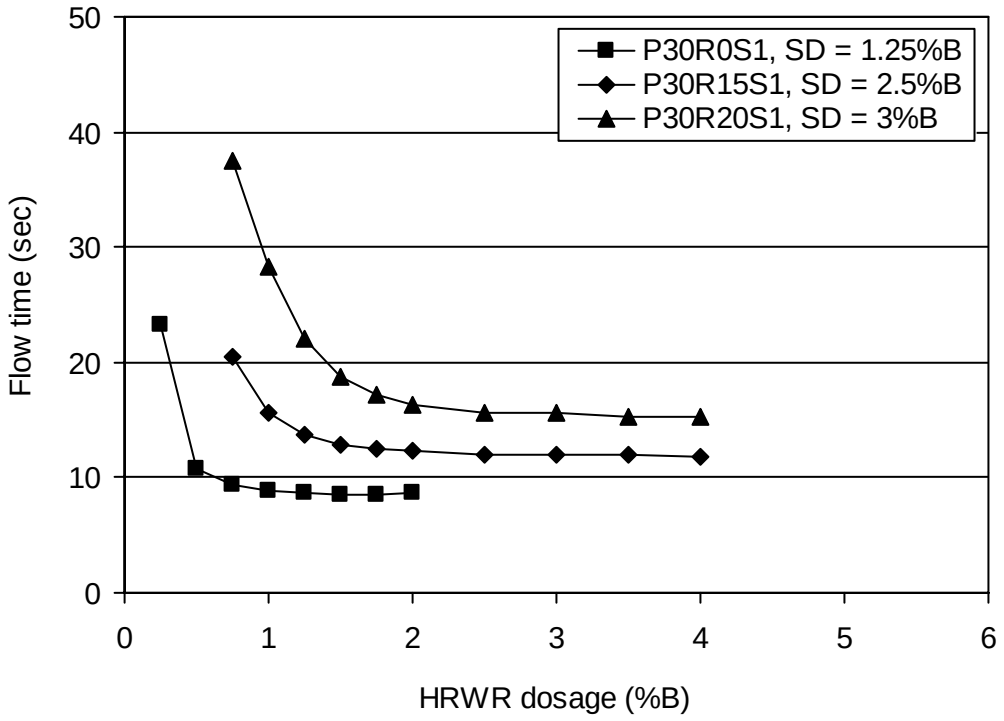

Figure 5.2: Flow time of pastes with increased HRWR dosages (W/B = 0.30)

5.4.2 Saturation dosages of high-range water reducer

The rate of increase in the filling ability, that is, the rate of decrease in the flow time of binder pastes was diminished with greater HRWR dosages. The increase in filling ability or decrease in flow time of the binder pastes was insignificant (0% to 3%) after a certain dosage, which was defined as the saturation dosage of HRWR. The flow curves became flatter at saturation dosage of HRWR. Thus, it was understood that, beyond saturation dosage, the addition of HRWR is no longer effective to increase the filling ability or to decrease the flow time of the pastes, as can be seen from Figures 5.2 to 5.4.

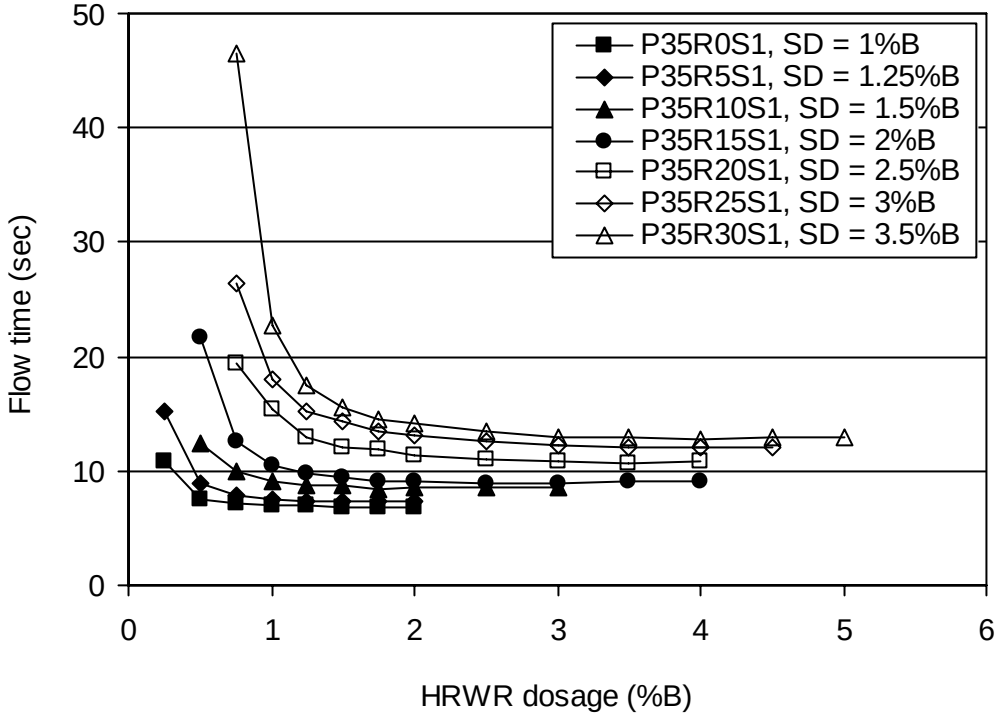

Figure 5.3: Flow time of pastes with increased HRWR dosages (W/B = 0.35)

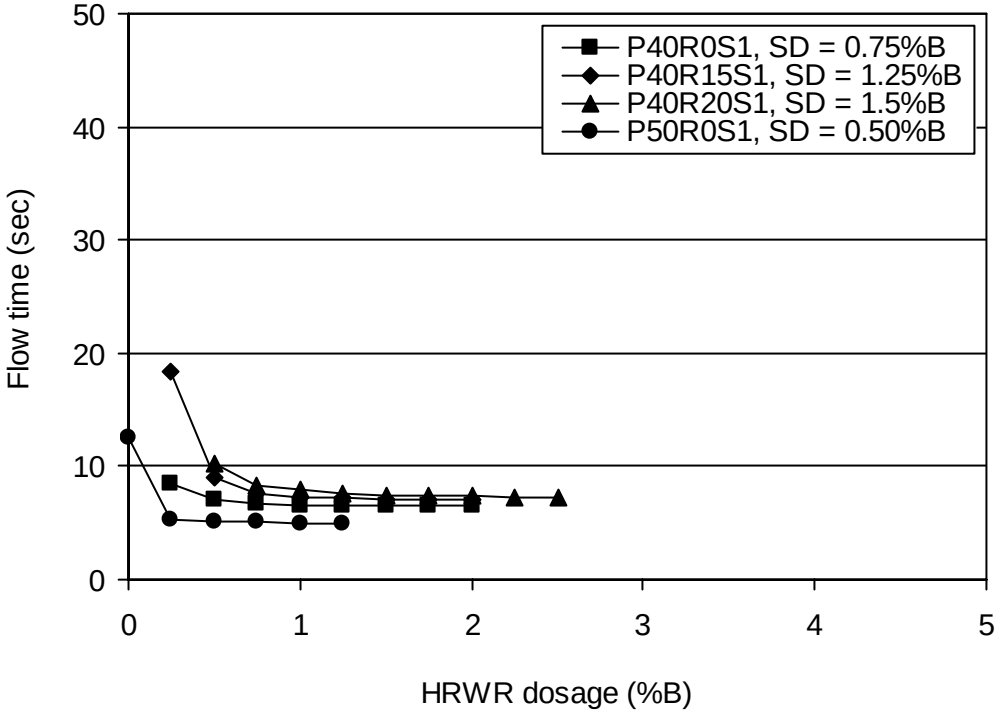

Figure 5.4: Flow time of pastes with increased HRWR dosages (W/B = 0.40 and 0.50)

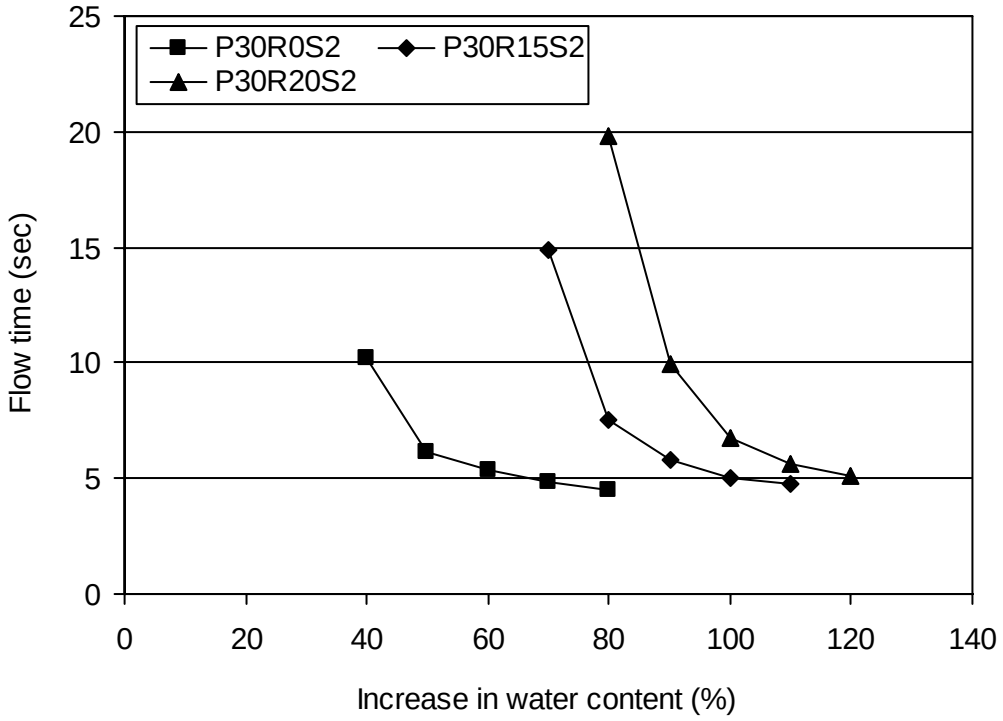

Figure 5.5: Flow time of pastes with increased water content (initial W/B = 0.30)

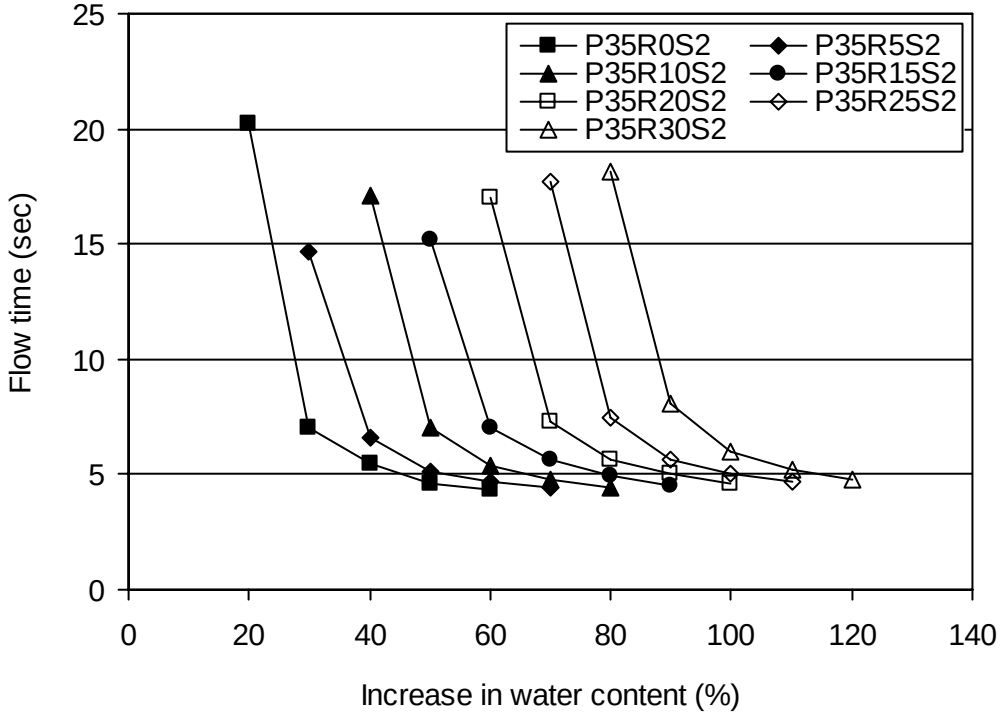

Figure 5.6: Flow time of pastes with increased water content (initial W/B = 0.35)

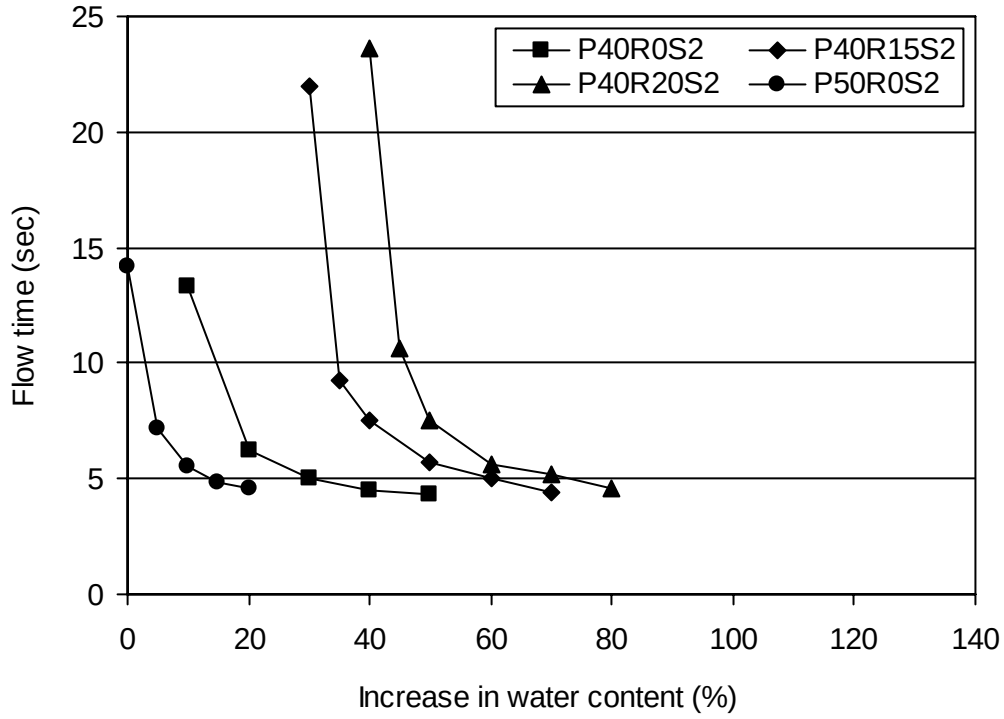

Figure 5.7: Flow time of pastes with increased water content (initial W/B = 0.40 and 0.50)

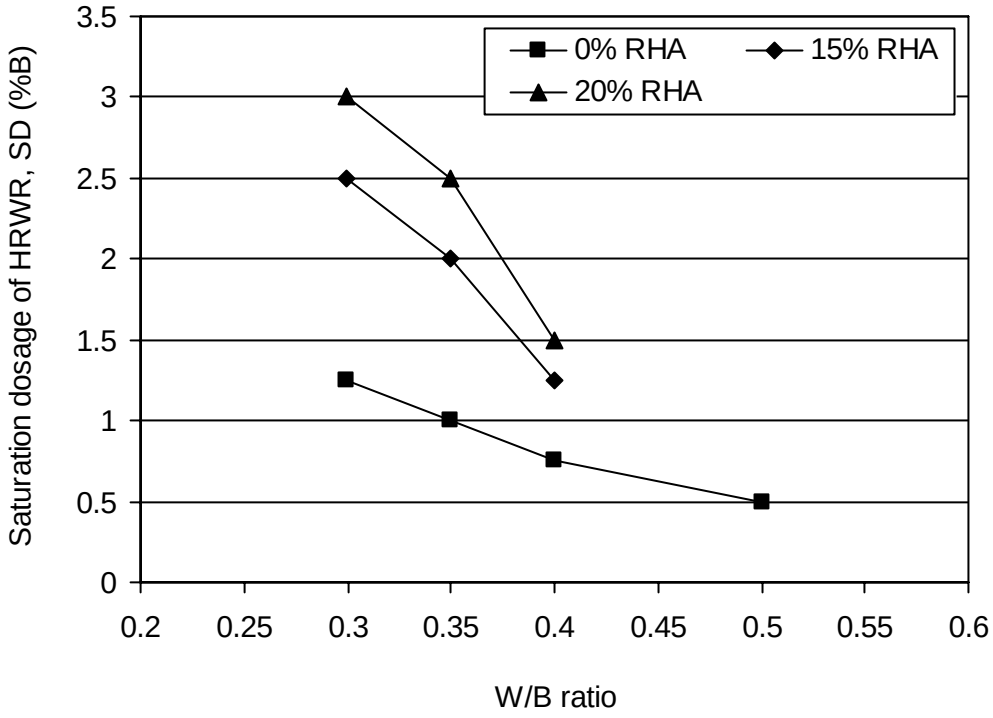

Figure 5.8: Effect of W/B ratio on the saturation dosages of high-range water reducer

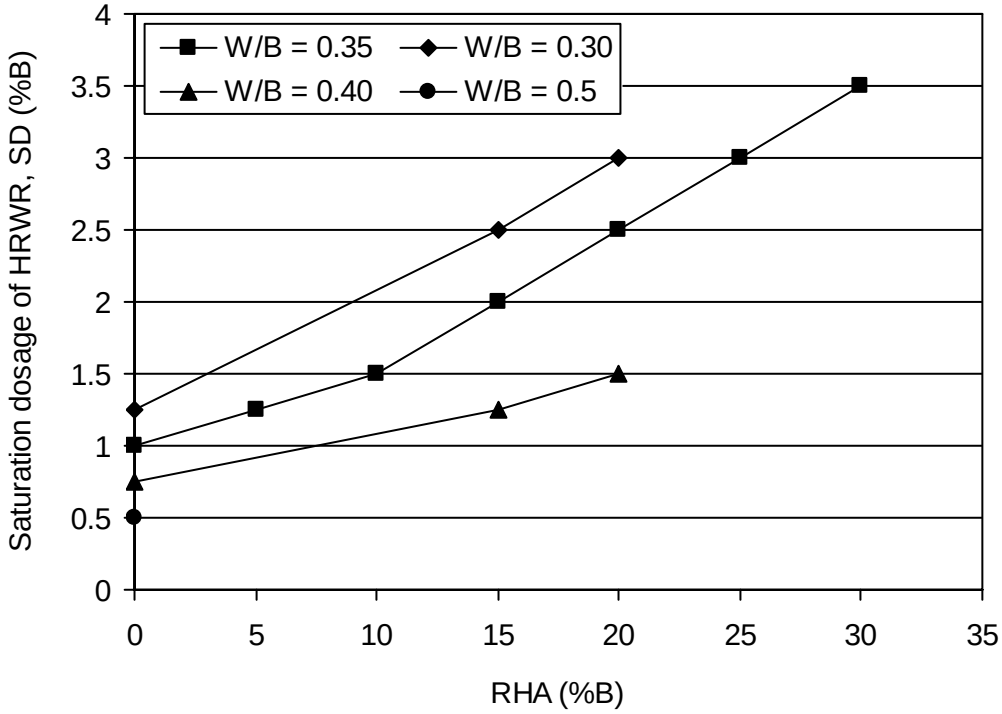

Figure 5.9: Effect of RHA on the saturation dosages of high-range water reducer

The saturation dosages of HRWR were influenced by the W/B ratio and RHA content of the binder pastes, as can be seen from Figures 5.8 and 5.9. The decreased W/B ratio and the increased RHA content required higher HRWR dosages to achieve the saturation flow of the binder pastes. The flocculation forces were greater at lower W/B ratio and higher RHA content, thus needed increased HRWR dosages for the dispersion of the cementing materials to produce saturation flow of the binder pastes.

5.4.3 Water reduction capacity of high-range water reducer

The water reduction capacity of HRWR was determined based on the flow time results presented in Figures 5.2 to 5.7. The flow time data at various saturation dosages of HRWR were obtained from the flow curves shown in Figures 5.2 to 5.4. These flow time data were superimposed in the corresponding flow curves shown in Figures 5.5 to 5.7 to obtain the increase in water content needed for producing the same paste filling ability without HRWR. Then, the water reduction capacity of HRWR was calculated from the following equation:

$$W_R = \frac{W_O - W_{HRWR}}{W_O} \times 100 \qquad \text{(Equation 5.1)}$$

where:

W_R = Water reduction capacity of HRWR (%)

W_{HRWR} = Water content for the saturation flow time in presence of HRWR

W_O = Water content needed for the same flow time without any HRWR

For example, the flow time of the binder paste with 0.30 W/B ratio and 0% RHA was 8.67 s at 1.25% saturation dosage of HRWR. In the absence of HRWR, the increase in water content needed to produce this flow time was found from Figure 5.5 by linear interpolation. The value obtained was 43.7%. Now, the water content used for preparing the binder paste with the saturation dosage of HRWR was 1571 g. It implies that (1571×1.437 = 2257.53) g of water was required to produce the same flow time without HRWR. Thus, the amount of water reduced was (2257.53 - 1571 = 686.53) g that led to (686.53×100/2257.53) = 30.4% water reduction.

The water reduction capacity of HRWR for various binder pastes is presented in Figure 5.10. The water reduction varied from 12.4% to 45.7% depending on the saturation dosage of HRWR. It is obvious from Figure 5.10 that the water reduction capacity increased with the increase in saturation dosage of HRWR. However, the efficiency of HRWR in water reduction varied with W/B ratio and RHA content. HRWR was more effective in water reduction at lower W/B ratio and higher RHA content, as can be seen from Figure 5.11. The lowest water reduction of 12.4% was obtained at the W/B ratio of 0.50 and 0% RHA content. Conversely, the water reduction was significantly high (45.7%) at the W/B ratio of 0.30 and 20% RHA content. This is perhaps due to the enhanced steric repulsion of HRWR molecules at higher volume concentration of the cementing materials.

5.4.4 Water demand of rice husk ash

The water demand of various RHA contents was computed based on the flow time data presented in Figures 5.5 to 5.7, which provided the increase in water content needed for the

binder pastes with and without RHA to produce the filling ability as given by the saturation dosage of HRWR. The following equation was used to calculate the water demand of RHA.

$$W_D = W_{IRHA} - W_{IO} \quad \text{(Equation 5.2)}$$

where:

W_D = Water demand of RHA (%)

W_{IO} = Percent increase in water content required for the binder paste without RHA

W_{IRHA} = Percent increase in water content needed for the binder paste with RHA

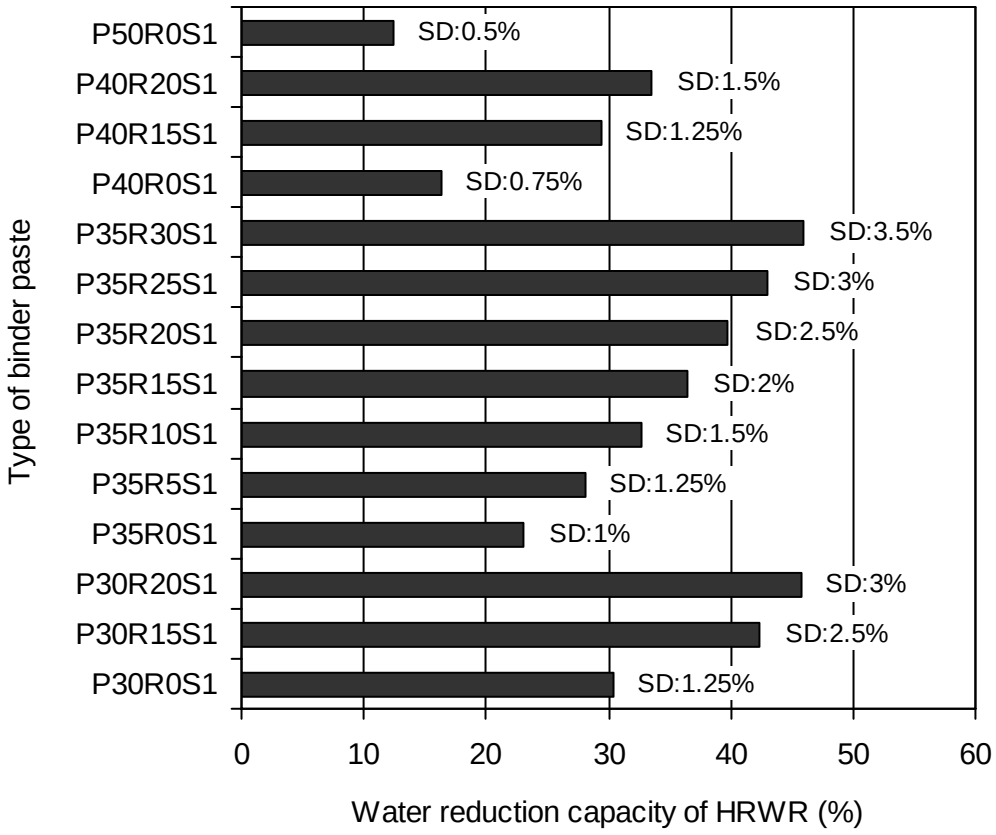

Figure 5.10: Water reduction capacity for various saturation dosages of HRWR

For example, the increase in water content needed to achieve the saturation flow time (8.67 s) in the absence of HRWR was 43.7% for the binder paste with 0.30 W/B ratio and 0% RHA, as discussed before (Section 5.4.3). Similarly, the saturation flow time for the binder

paste with 0.30 W/B ratio and 15% RHA in the presence of HRWR was obtained from Figure 5.2 as 11.95 s. The increase in water content required to attain this flow time in the absence of HRWR was found from Figure 5.5 as 73.7%. Hence, the water demand of 15% RHA was (73.6% – 43.7%) = 30%.

The water demand of various RHA contents to achieve the saturation flow is shown in Figure 5.12. It is evident from Figure 5.12 that the water demand increased with the increase in RHA content. Also, the water demand became greater at lower W/B ratio since the quantity of RHA was increased. Nevertheless, the water demand of RHA varied in the range of 0% to 55.1% depending on its content used in the binder pastes. The highest water demand (55.1%) was observed for 30% RHA content, which was incorporated in a SCHPC mixture with the W/B ratio of 0.35. The increased water demand of RHA is mainly attributed to its particle characteristics. The smaller particle size and porous honey-comb microstructure of RHA resulted in very high specific surface area that demanded a greater amount of water for saturation flow.

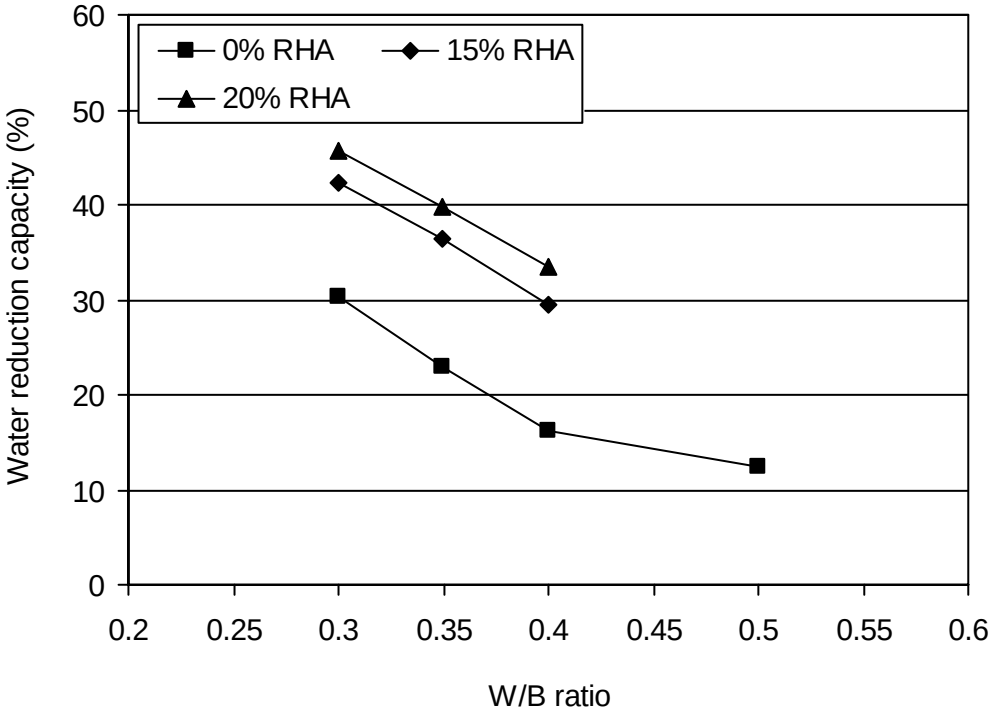

Figure 5.11: Effect of W/B ratio and RHA content on the water reduction capacity of HRWR

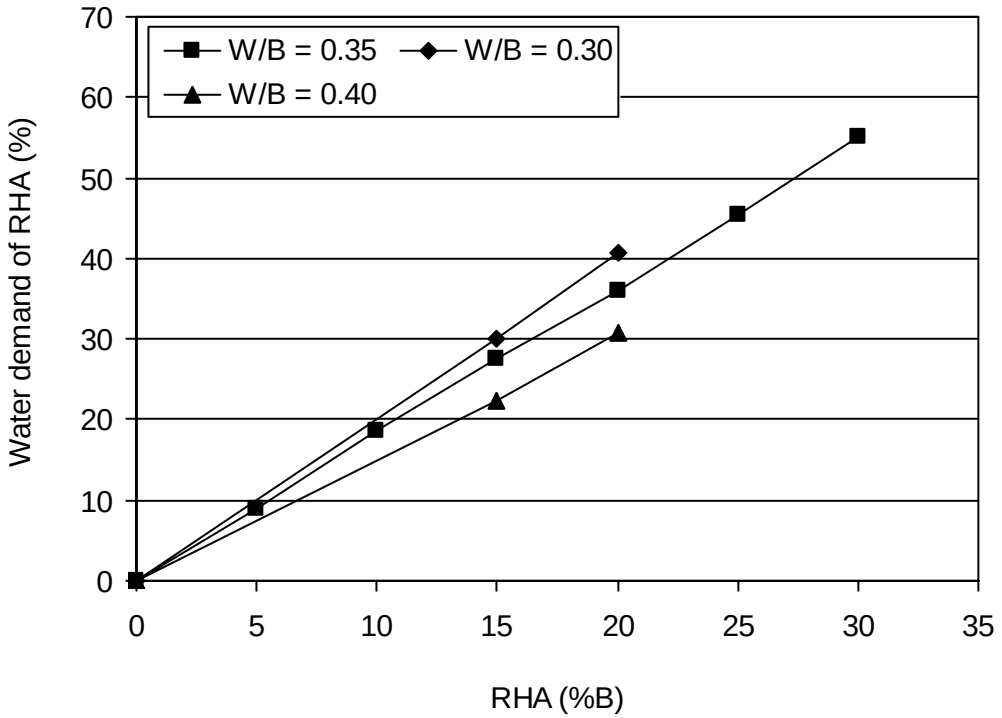

Figure 5.12: Water demand of RHA for saturation flow of binder pastes

5.4.5 Effect of rice husk ash and water-binder ratio

The flow curves presented in Figures 5.2 to 5.4 showed a shift towards the upward right-hand direction as the W/B ratio is reduced and the RHA content is increased. These trends indicate that the plastic viscosity of the binder pastes was increased with reduced W/B ratio and increased RHA content.

The effects of RHA and W/B ratio on the filling ability of the binder pastes were examined based on the saturation dosages of HRWR. The flow time values of the pastes at saturation dosages of HRWR were determined from Figures 5.2 to 5.4, and plotted in Figure 5.13. The filling ability of the binder pastes was reduced and therefore the flow time value became higher with increasing RHA content and lower W/B ratio, as evident in Figure 5.13. This is mostly due to the increased volume fraction and wettable surface area of the binder. The volume fraction of the binder was increased with lower W/B ratio and higher RHA content, which is evident from Figure 5.14. The increase in volume fraction of the binder

increases the viscosity of the binder paste. The viscosity of the paste generally increases exponentially with the increase in volume fraction of the binder (Struble and Sun 1995, Struble et al. 1998). Also, the wettable surface area of the binder affects the viscosity of the paste. The viscosity of the paste increases with greater wettable surface area of the binder (Nehdi et al. 1998). In the present study, the surface area of the binder used in different pastes was calculated based on the Blaine specific surface area of cement and RHA. The computed surface areas of the binder with various RHA contents and W/B ratios are plotted in Figure. 5.15. It can be seen from Figure 5.15 that the surface area of the binder was increased with increasing RHA content and decreasing W/B ratio. Thus, it can be inferred that the wettable surface area was increased at lower W/B ratio and higher RHA content. The increase in wettable surface area decreases the amount of free water available in the paste. Consequently, the fluidity of the paste is decreased and the viscosity becomes higher, thus causing a resistance to paste flow.

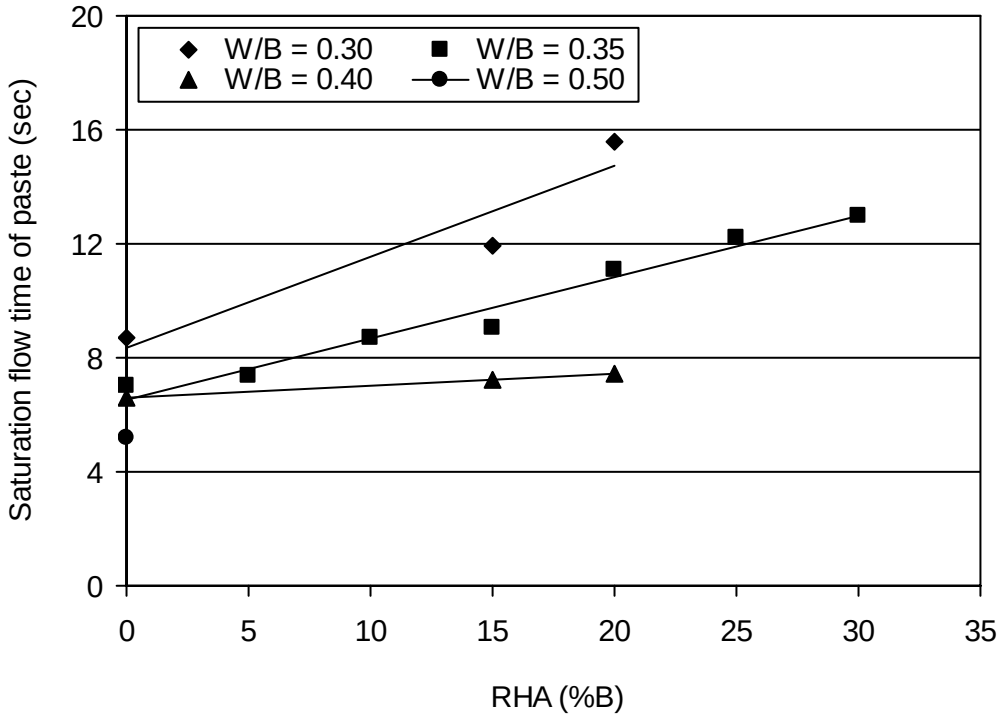

Figure 5.13: Effect of RHA and W/B ratio on the saturation flow time of binder pastes

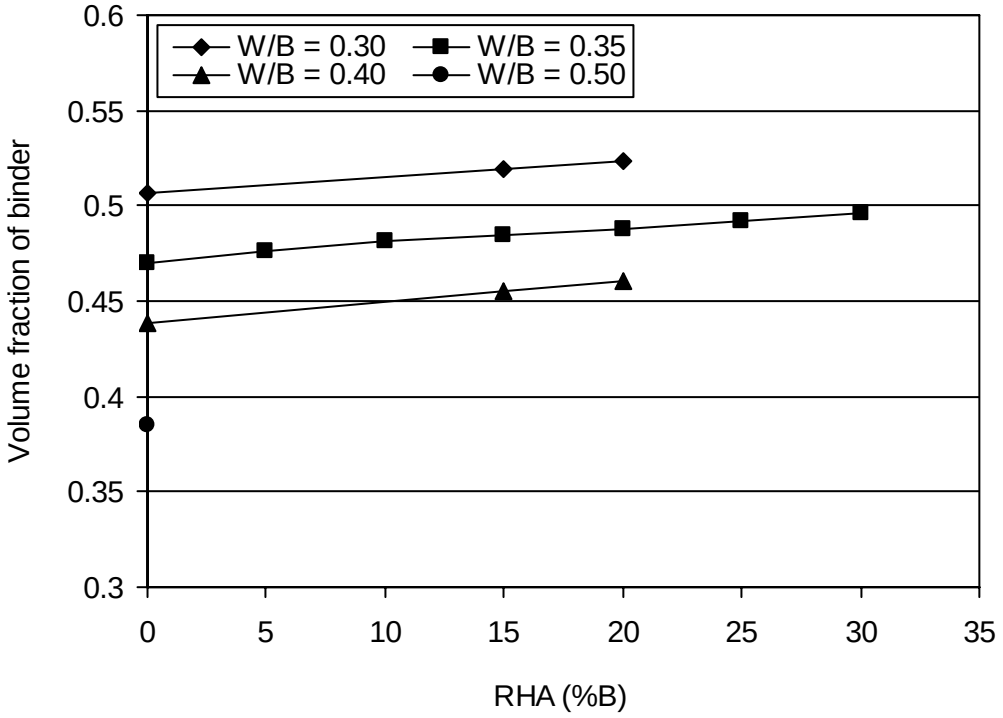

Figure 5.14: Effect of RHA and W/B ratio on the binder volume fraction of pastes

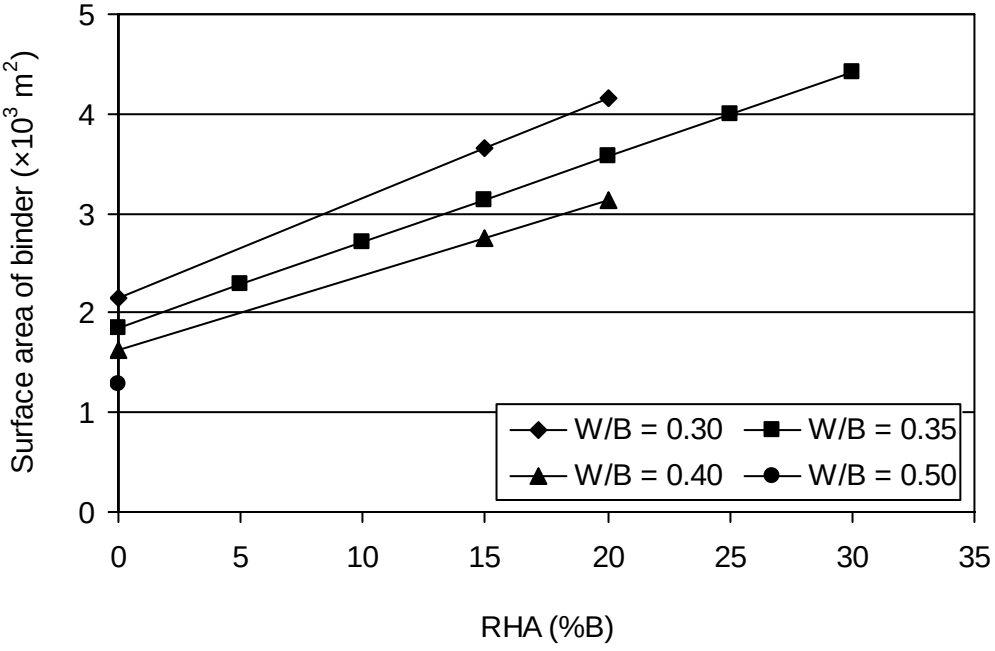

Figure 5.15: Effect of RHA and W/B ratio on the surface area of binder

The morphology (shape and surface texture) of the RHA particles was also not conducive to the filling ability of the binder pastes. The RHA particles are angular and cellular with honey-comb microstructure (Zhang and Malhotra 1996), and thus could exhibit interlocking characteristics. Therefore, the inter-particle friction becomes higher in the presence of RHA. Also, the angular and porous RHA particles require more water than rounded non-porous particles, resulting in less free water availability in the paste. Hence, the binder paste with higher RHA content exhibited a lower filling ability with greater flow time.

5.5 Suitable Content of Rice Husk Ash

The test results showed that the presence of RHA affects the filling ability of the binder pastes. The filling ability of the binder pastes was reduced with greater RHA content due to increased water demand. It was observed that the water demand of RHA became very high when its content exceeded 20%. In particular, the water demand of 25% and 30% RHA in P35R25S1 and P35R30S1 binder pastes, respectively, were higher than the water reduction capacity of the respective saturation dosage of HRWR. This can be seen from Figures 5.10 and 5.12. It indicates that the water demand of RHA was not fulfilled in P35R25S1 and P35R30S1 binder pastes, even with the saturation dosages of HRWR. Hence, the filling ability of these binder pastes can be affected. Furthermore, the saturation dosages of HRWR became much higher when the RHA content was greater than 20%, as can be seen from Figure 5.9. A HRWR dosage more than 3% is usually considered very high for SCHPC (Kwan 1999). Very high dosages of HRWR may cause cement setting problem leading to delayed hydration. In addition, mixing and handling difficulties were experienced for the binder pastes with 20% RHA at 0.30 W/B ratio, and 25 to 30% RHA at 0.35 W/B ratio. Based on these standpoints, a RHA content above 15% can be considered unsuitable for the pastes and their corresponding parent concretes.

5.6 Use of Filling Ability Results of Binder Pastes

The filling ability results of the binder pastes exhibited the effects of HRWR, RHA content and W/B ratio. The saturation dosages and water reduction capacity of HRWR, and the water demand of RHA content were helpful to fix the HRWR dosages for various SCHPC mixtures. These results were also useful to judge the suitability of RHA for use in concretes.

Moreover, the flow time results of the binder pastes indicated the filling ability of the corresponding parent concretes. They were used for establishing the correlation of paste filling ability with the filling ability of concretes.

5.7 Conclusions

a. The filling ability of the pastes was increased, and thus the flow time was decreased with greater dosages of HRWR. This is attributed to the efficient liquefying and dispersing actions of the HRWR.
b. The flow time of the pastes was increased with lower W/B ratio and higher RHA content. This is due to the increased plastic viscosity caused by a greater volume fraction and surface area of the binder.
c. The lower W/B ratio and higher RHA content increased the flocculation forces, and thus required higher dosages of HRWR to achieve the saturation flow of the binder pastes.
d. The water reduction capacity of HRWR was increased at lower W/B ratio and higher RHA content. This is mostly credited to the enhanced steric repulsion of HRWR at higher volume concentration of the binder.
e. The water demand for saturation flow was increased with higher RHA content. This is attributed to the extremely high specific surface area arising from the smaller particle size and porous honey-comb microstructure of RHA.
f. A RHA content greater than 15% of binder by weight can be considered unsuitable due to excessive water demand, and mixing and handling difficulties.
g. The optimum HRWR dosage and the suitable RHA content for concretes can be determined based on the filling ability of binder pastes, and thus the paste filling ability facilitates the mixture proportioning process of SCHPC.

Chapter 6

Filling Ability and Air Content of Mortars

6.1 General

The preparation and testing of mortars for the filling ability and air content, and their test results are presented and discussed in this chapter. The effects of high-range water reducer (HRWR), air-entraining admixture (AEA), water-binder (W/B) ratio, and rice husk ash (RHA) on the filling ability and air content of the mortars are highlighted. The acceptability of saturation dosages of HRWR and the suitability of RHA are discussed. The estimated AEA dosages for concretes are also given. Finally, this chapter focuses how the mortar filling ability and air content results are useful for the concrete mixtures.

6.2 Research Significance

The filling ability of mortars as that of binder pastes is useful to support the mixture proportioning process of self-consolidating high performance concrete (SCHPC). The suitable contents of cement and supplementary cementing material (SCM) and the required dosage of HRWR for an SCHPC mixture can be determined based on the filling ability of its mortar component. In addition, it is possible to estimate the AEA dosages for SCHPC mixtures based on the air content of the mortar components. These processes minimize the volume of laboratory work involved in finding the mixture proportions of SCHPC because the number of trial mixtures, and thus the loss of materials are greatly reduced. A wide range of variables can also be assessed using mortars in a short period. Moreover, the effectiveness of HRWR, SCM, and AEA can be observed based on the filling ability and air content of mortars.

6.3 Preparation and Testing of Mortars

Different types of mortars were prepared and tested to examine the filling ability with respect to flow spread, to verify the saturation dosages (SDs) of HRWR obtained from flow cone test of binder pastes, and to determine the air content for various dosages of AEA. The

designations of the mortars are given in Table 6.1 based on the W/B ratio and RHA content used in the corresponding parent concrete. For instance, the ‘M30R0S1’ and ‘M30R0S2’ designations were selected for the mortars prepared with a W/B ratio of 0.30 and 0% RHA content, as used in corresponding parent concrete ‘C30R0A6’. The ‘S1’ and ‘S2’ components were used in the designations to categorize the mortars under series 1 (without AEA) and series 2 (with AEA), respectively. The supplementary letter ‘a’ or ‘b’ was added right after ‘S1’ and ‘S2’ in case of several mortars formulated from the concretes with 4 and 8% design air content, respectively. Moreover, the letter ‘c’ was used after ‘S1’ for a mortar formulated from the concrete C50R0A2 (W/B: 0.50; RHA: 0%) containing 2% entrapped air content.

6.3.1 Preparation of mortars

A series of mortars (M30R0S1 to M50R0S1c), as given in Table 6.1, was prepared without AEA (no air entrainment) to investigate the filling ability at various HRWR dosages, and thus examining the effect of RHA and verifying the saturation dosages of HRWR. A second series of mortars (M30R0S2 to M50R0S2), as listed in Table 6.1, was prepared with AEA for testing air content. The primary mixture proportions of the mortars tested for filling ability and air content are shown in Table 6.1. These proportions were calculated based on the primary mixture proportions of the corresponding parent concretes.

The volume of the mortars prepared was 3 liters in both series. The dosages of HRWR for the mortars under series 1 were varied in the vicinity of saturation dosages obtained from the flow cone test of binder pastes. No AEA was used in the series 1 mortars. The dosages of HRWR used for the mortars under series 2 were fixed at the saturation dosages. The AEA was added to these mortars to produce the entrained air-voids. For each mortar, the dosages of AEA were varied with additional mixing. The limits of AEA dosages were chosen to produce the mortar air content in the range of 3.7% to 19.4%, which is equivalent to the concrete air content ranging from 2.5% to 12.9%.

Before batching, the water correction was determined considering the absorption of fine aggregate (natural pit sand) and the water contribution of HRWR. Accordingly, the proportions of fine aggregate and water were adjusted. These adjustments were required since air-dry pit sand and liquid HRWR were used in preparing the mortars. The adjusted

mixture proportions of the mortars under series 1 and series 2 are presented in Table 6.2 and Table 6.3, respectively.

Table 6.1: Primary mixture proportions of the mortars tested for filling ability and air content (series 1 and series 2)

Mortar type	Parent concrete*	FA♠ (kg)	C♥ (kg)	RHA (kg)	W♦ (kg)
M30R0S1, M30R0S2	C30R0A6	4.030	2.358	0	0.707
M30R15S1, M30R15S2	C30R15A6	3.914	1.985	0.350	0.701
M30R20S1, M30R20S2	C30R20A6	3.875	1.862	0.465	0.698
M35R0S1, M35R0S2	C35R0A6	4.246	2.057	0	0.720
M35R0S1a, M35R0S2a	C35R0A4	4.305	2.024	0	0.708
M35R0S1b, M35R0S2b	C35R0A8	4.186	2.092	0	0.732
M35R5S1, M35R5S2	C35R5A6	4.212	1.949	0.102	0.718
M35R10S1, M35R10S2	C35R10A6	4.178	1.841	0.204	0.716
M35R15S1, M35R15S2	C35R15A6	4.143	1.734	0.306	0.714
M35R15S1a, M35R15S2a	C35R15A4	4.202	1.706	0.301	0.702
M35R15S1b, M35R15S2b	C35R15A8	4.082	1.763	0.311	0.726
M35R20S1, M35R20S2	C35R20A6	4.109	1.627	0.407	0.712
M35R20S1a, M35R20S2a	C35R20A4	4.169	1.601	0.401	0.701
M35R20S1b, M35R20S2b	C35R20A8	4.048	1.654	0.414	0.724
M35R25S1, M35R25S2	C35R25A6	4.075	1.521	0.507	0.710
M35R30S1, M35R30S2	C35R30A6	4.041	1.416	0.607	0.708
M40R0S1, M40R0S2	C40R0A6	4.414	1.824	0	0.730
M40R15S1, M40R15S2	C40R15A6	4.321	1.539	0.271	0.724
M40R20S1, M40R20S2	C40R20A6	4.290	1.445	0.361	0.723
M50R0S1, M50R0S2	C50R0A6	4.646	1.493	0	0.746
M50R0S1c♣	C50R0A2	4.440	1.589	0	0.794

*Designations are given in Chapter 7; ♣Tested for filling ability only; ♠Fine aggregate; ♥Cement; ♦Water

The mortars were prepared using an epicyclic revolving type small mechanical mixer used for the binder pastes (Figure 5.1, Chapter 5). The fine aggregate and cementing material (cement alone or with RHA) were taken in the mixing bowl, and dry-mixed for 60 seconds using a stainless spoon. The mixing water was added into the bowl and a rest period of 30 seconds was allowed for absorption by the fine aggregate. In case of series 2 mortars, this step was followed using the initial dosage of AEA. Then the mixer was started and the initial dosage of HRWR was gradually added followed by mixing for 60 seconds. This step was

followed using the saturation dosage of HRWR for the second series of mortars (M30R0S2 to M50R0S2) mentioned in Table 6.3. Later the mixer was stopped, and the mortar was quickly scraped from the side and bottom of the mixing bowl over a period of 30 seconds. The mixer was restarted and run for 60 seconds. Again, the mixer was stopped, the mortar from the bottom and side of the bowl was scraped, and the mortar agglomerates were broken if any over a period of 30 seconds. The mixer was restarted again and the mixing was continued for 60 seconds. Later, the subsequent dosages of HRWR were used to vary the fluidity of the mortars (M30R0S1 to M50R0S1c) mentioned in Table 6.2. For each incremental HRWR dosage, further mixing was conducted for 60 seconds. This step was different for the mortars (M30R0S2 to M50R0S2) mentioned in Table 6.3, for which additional AEA was added instead of HRWR and the mixing was continued for 120 seconds for each incremental AEA dosage.

Table 6.2: Adjusted mixture proportions of the mortars tested for filling ability by flow mould (series 1)

Mortar type	Parent concrete	FA (kg)	C (kg)	RHA (kg)	W (kg)	HRWR (% B)
M30R0S1	C30R0A6	3.994	2.358	0	0.726	1.00-2.00
M30R15S1	C30R15A6	3.879	1.985	0.350	0.702	1.50-3.00
M30R20S1	C30R20A6	3.840	1.862	0.465	0.692	2.00-4.00
M35R0S1	C35R0A6	4.208	2.057	0	0.746	0.75-1.50
M35R0S1a	C35R0A4	4.267	2.024	0	0.734	0.75-1.50
M35R0S1b	C35R0A8	4.149	2.092	0	0.757	0.75-1.50
M35R5S1	C35R5A6	4.174	1.949	0.102	0.741	0.75-1.75
M35R10S1	C35R10A6	4.141	1.841	0.204	0.735	1.00-2.00
M35R15S1	C35R15A6	4.106	1.734	0.306	0.727	1.25-2.50
M35R15S1a	C35R15A4	4.164	1.706	0.301	0.716	1.25-2.50
M35R15S1b	C35R15A8	4.046	1.763	0.311	0.738	1.25-2.50
M35R20S1	C35R20A6	4.072	1.627	0.407	0.719	1.50-3.00
M35R20S1a	C35R20A4	4.132	1.601	0.401	0.708	1.50-3.00
M35R20S1b	C35R20A8	4.012	1.654	0.414	0.729	1.50-3.00
M35R25S1	C35R25A6	4.039	1.521	0.507	0.710	1.75-3.50
M35R30S1	C35R30A6	4.005	1.416	0.607	0.702	2.50-4.50
M40R0S1	C40R0A6	4.375	1.824	0	0.761	0.50-1.25
M40R15S1	C40R15A6	4.282	1.539	0.271	0.750	1.00-2.00
M40R20S1	C40R20A6	4.252	1.445	0.361	0.745	1.50-2.50
M50R0S1	C50R0A6	4.605	1.493	0	0.783	0.25-1.00
M50R0S1c	C50R0A2	4.400	1.589	0	0.829	0.25-1.00

6.3.2 Flow mould test

The flow mould test was conducted to investigate the filling ability of the mortars at various dosages of HRWR. A standard flow mould conforming to ASTM C 230/C 230M (2004) was used to determine the filling ability with respect to flow spread. The flow mould used is shown in Figure 6.1. The mould was placed over a leveled plexiglass plate. The mortar was placed into the mould in one layer and without any compaction. Then the mould was raised vertically without any disturbance, and the mortar was allowed to flow over the plexiglass plate. The diameter of the mortar spread was measured at two pairs of right-angle locations that divided the flow patty into eight equal segments. The average diameter was used to express the flow spread of mortar. An operational stage of the flow mould test is shown in Figure 6.1.

Table 6.3: Adjusted mixture proportions of the mortars tested for air content by Chace indicator (series 2)

Mortar type	Parent concrete	FA (kg)	C (kg)	RHA (kg)	W (kg)	HRWR (% B)	AEA (ml)
M30R0S2	C30R0A6	3.994	2.358	0	0.726	1.25	1.0-4.0
M30R15S2	C30R15A6	3.879	1.985	0.350	0.702	2.50	1.0-4.0
M30R20S2	C30R20A6	3.840	1.862	0.465	0.692	3.00	1.0-4.0
M35R0S2	C35R0A6	4.208	2.057	0	0.746	1.00	1.0-4.0
M35R0S2a	C35R0A4	4.267	2.024	0	0.734	1.00	1.0-4.0
M35R0S2b	C35R0A8	4.149	2.092	0	0.757	1.00	1.0-4.0
M35R5S2	C35R5A6	4.174	1.949	0.102	0.741	1.25	1.0-4.0
M35R10S2	C35R10A6	4.141	1.841	0.204	0.735	1.50	1.0-4.0
M35R15S2	C35R15A6	4.106	1.734	0.306	0.727	2.00	1.0-4.0
M35R15S2a	C35R15A4	4.164	1.706	0.301	0.716	2.00	1.0-4.0
M35R15S2b	C35R15A8	4.046	1.763	0.311	0.738	2.00	1.0-4.0
M35R20S2	C35R20A6	4.072	1.627	0.407	0.719	2.50	1.0-4.0
M35R20S2a	C35R20A4	4.132	1.601	0.401	0.708	2.50	1.0-4.0
M35R20S2b	C35R20A8	4.012	1.654	0.414	0.729	2.50	1.0-4.0
M35R25S2	C35R25A6	4.039	1.521	0.507	0.710	3.00	1.0-4.0
M35R30S2	C35R30A6	4.005	1.416	0.607	0.702	3.50	1.0-4.0
M40R0S2	C40R0A6	4.375	1.824	0	0.761	0.75	1.0-4.0
M40R15S2	C40R15A6	4.282	1.539	0.271	0.750	1.25	1.0-4.0
M40R20S2	C40R20A6	4.252	1.445	0.361	0.745	1.50	1.0-4.0
M50R0S2	C50R0A6	4.605	1.493	0	0.783	0.5	0.5-2.0

6.3.3 Chace indicator test

The Chace indicator test was carried out to determine the air content of the mortars at various dosages of AEA. The Chace indicator used is shown in Figure 6.2. The standard procedure given in AASHTO T 199 (2004) was followed in determining the air content except for filling the brass cup; the mortar was placed into the brass cup without any rodding by thin stiff wire. An operational stage of the Chace indicator test is shown in Figure 6.2.

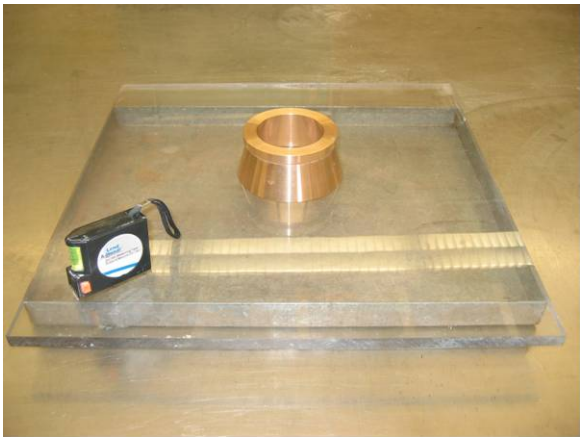

Flow mould used for determining the flow spread of mortars

An operational stage to determine the flow spread of mortars

Figure 6.1: Test setup and testing of mortar filling ability with respect to flow spread

Chace indicator used for determining the air content of mortars

An operational stage to determine the air content of mortars

Figure 6.2: Test setup and testing of mortars for air content

6.4 Filling Ability of Mortars

The results of the flow mould test for various mortars are illustrated in Figures 6.3 to 6.7. These figures exhibit the filling ability of the mortars with respect to the flow spread at various dosages of HRWR. The flow spread varied in the range of 195 to 325 mm for all mortars. The bottom diameter of the mortar samples was 100 mm at the start of the test. Thus, the mortars spread by 95 to 225 mm for different HRWR dosages. For saturation HRWR dosages, the flow spread of the mortars formulated from various SCHPC mixtures differed in the range of 238 mm to 317 mm. A mortar flow spread in the range of 275 to 335 mm generally suggests a slump flow of 550 to 850 mm for SCHPC (Jin and Domone 2002).

The flow spread of the mortars is controlled by their rheological properties; yield stress and plastic viscosity. The flow spread increases with reduced yield stress and plastic viscosity (Tanigawa and Mori 1989). The mixture parameters that might affect the yield stress and plastic viscosity, and thus the flow spread of mortar are listed in Table 6.4. These parameters were computed based on the saturated surface-dry basis mixture proportions of the mortars used in the present study.

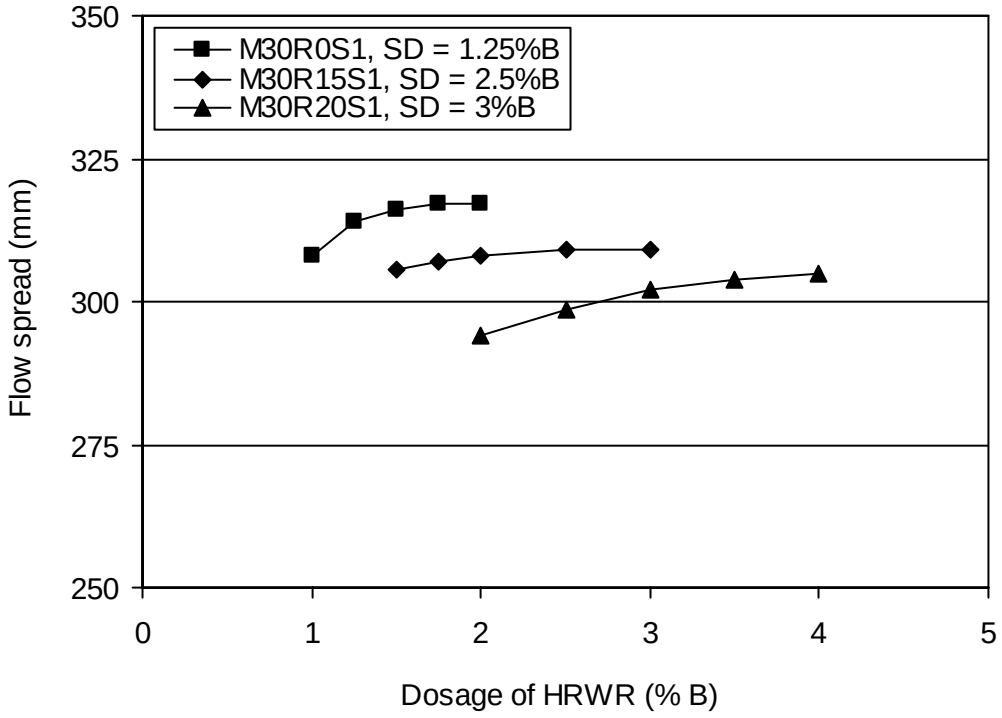

Figure 6.3: Flow spread of various mortars (W/B = 0.30, concrete air content = 6%)

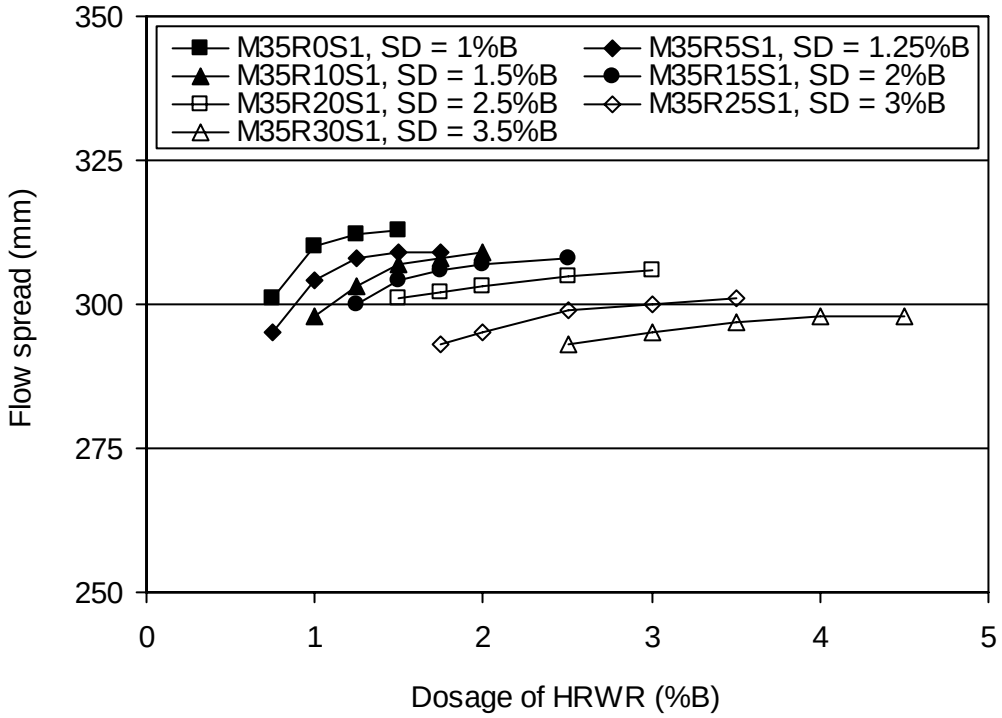

Figure 6.4: Flow spread of various mortars (W/B = 0.35, concrete air content = 6%)

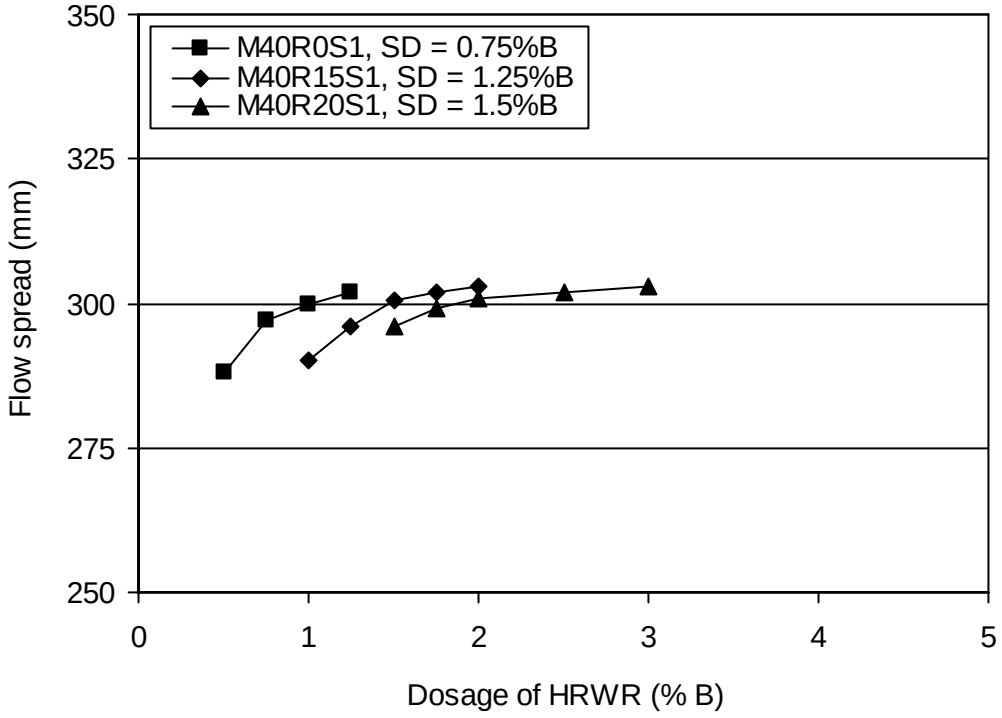

Figure 6.5: Flow spread of various mortars (W/B = 0.40, concrete air content = 6%)

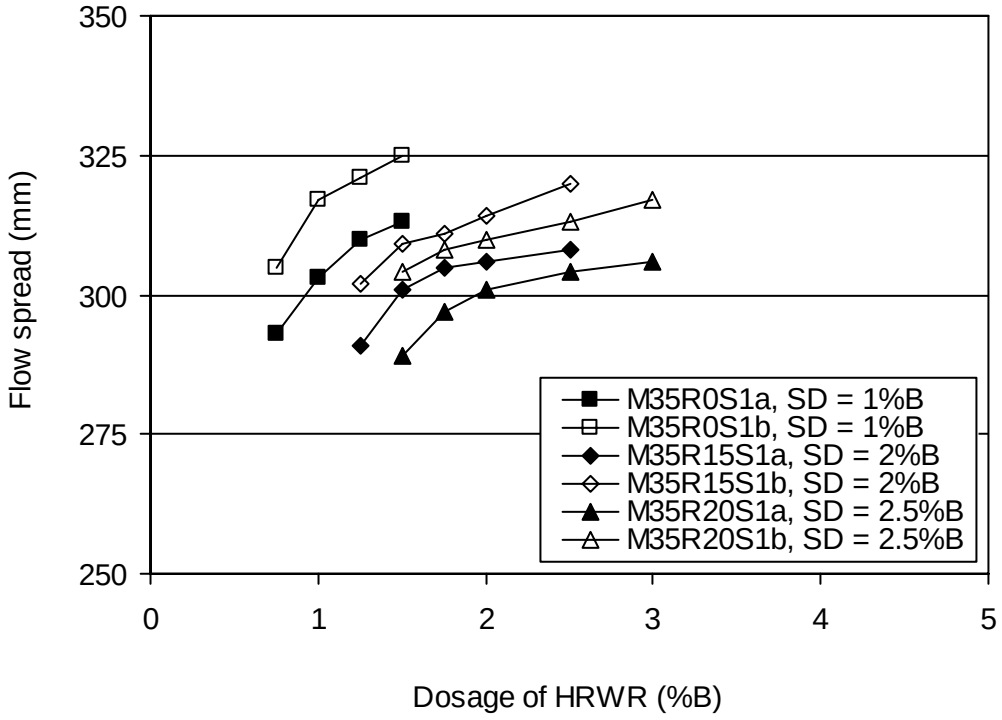

Figure 6.6: Flow spread of various mortars (W/B = 0.35, concrete air content = 4% and 8%)

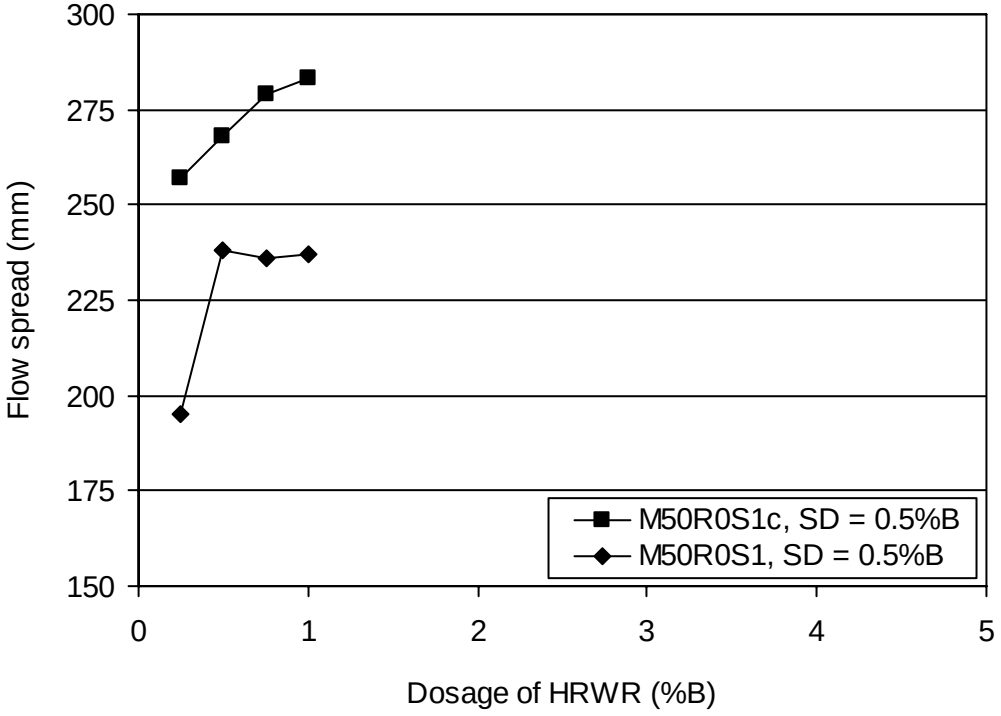

Figure 6.7: Flow spread of various mortars (W/B = 0.50, concrete air content = 2% and 6%)

The flow curves presented in Figures 6.3 to 6.5 represent the mortars formulated from the concretes with 6% design air content. It was observed that these curves progressively shifted towards the downward right-hand and downward direction showing a reduction in flow spread. It indicates that the yield stress and plastic viscosity of the mortars represented were gradually increased. This is mostly due to the increases in the volume fraction of total solids, and specific surface area and volume fraction of binder (Banfill 1994, Vom Berg 1979, Westerholm 2006).

Table 6.4: Various mixture parameters of the mortars tested for filling ability and air content

Mortar type	Volume fraction of total solids (m^3/m^3)	Volume fraction of sand (m^3/m^3)	Binder volume fraction (m^3/m^3)	Binder surface area ($\times 10^3$ m^2/m^3)	Volume fraction of paste (m^3/m^3)
M30R0S1, M30R0S2	0.764	0.514	0.249	323.833	0.486
M30R15S1, M30R15S2	0.766	0.499	0.266	543.973	0.501
M30R20S1, M30R20S2	0.766	0.494	0.272	616.243	0.506
M35R0S1, M35R0S2	0.759	0.542	0.218	282.493	0.458
M35R0S1a, M35R0S2a	0.763	0.549	0.214	277.963	0.451
M35R0S1b, M35R0S2b	0.755	0.534	0.221	287.303	0.466
M35R5S1, M35R5S2	0.760	0.537	0.223	346.747	0.463
M35R10S1, M35R10S2	0.761	0.533	0.228	411	0.467
M35R15S1, M35R15S2	0.761	0.529	0.233	475.387	0.471
M35R15S1a, M35R15S2a	0.765	0.536	0.229	467.667	0.464
M35R15S1b, M35R15S2b	0.757	0.521	0.237	483.247	0.479
M35R20S1, M35R20S2	0.762	0.524	0.238	539.003	0.476
M35R20S1a, M35R20S2a	0.766	0.532	0.234	530.780	0.468
M35R20S1b, M35R20S2b	0.758	0.516	0.242	548.137	0.484
M35R25S1, M35R25S2	0.763	0.520	0.243	601.977	0.480
M35R30S1, M35R30S2	0.763	0.516	0.248	665.090	0.484
M40R0S1, M40R0S2	0.756	0.563	0.193	250.497	0.437
M40R15S1, M40R15S2	0.758	0.551	0.207	421.470	0.449
M40R20S1, M40R20S2	0.758	0.547	0.211	478.343	0.453
M50R0S1, M50R0S2	0.751	0.593	0.158	205.040	0.407
M50R0S1c	0.734	0.566	0.168	218.223	0.434

The flow curves illustrated in Figures 6.6 and 6.7 represent the mortars, which were formulated from the concretes with different air content. These curves exhibit that M35R0S1b, M35R15S1b, M35R20S1b and M50R0S1c provided higher flow spread than

M35R0S1a, M35R15S1a, M35R20S1a and M50R0S1, respectively. In particular, the flow spread of M50R0S1 was significantly lower than that of M50R0S1c for all HRWR dosages. Also, bleeding and a larger sand pile (due to segregation of fine aggregates) appeared at and after the saturation dosage of HRWR, and no increase in flow spread was observed. Therefore, the mortar M50R0S1 exhibited a different trend in flow curve beyond the saturation dosage of HRWR, as evident in Figure 6.7. The increase in the flow spread of M35R0S1b, M35R15S1b, M35R20S1b and M50R0S1c is possibly due to the combined effect of greater paste volume, lower total solids, and reduced sand content. The decrease in total solids and sand content, and the increase in paste volume contribute to reduce the yield stress and plastic viscosity (Banfill 1994, Westerholm 2006), leading to increased flow spread. Moreover, the sand content affects the amount of free water in mortars. The sand particles confine some of the mixing water in mortars. The amount of confined water is approximately proportional to the volume content of sand (Okamura and Ozawa 1995). It means that a lesser amount of water is confined at reduced sand content. Consequently, a greater amount of free water was available in M35R0S1b, M35R15S1b, M35R20S1b and M50R0S1c containing lower sand content to improve the filling ability of the mortars.

6.4.1 Effect of high-range water reducer

The effect of HRWR on the filling ability of the mortars is evident from Figures 6.3 to 6.7. In general, the filling ability, that is, the flow spread of the mortars increased with increasing dosages of HRWR, and this trend was in agreement with other research findings (Chandra and Björnström 2002, Domone 2006). It indicates that the yield stress and plastic viscosity of the mortars were reduced and therefore the mortar deformability increased with higher dosages of HRWR. This is mainly credited to the liquefying and dispersing actions of the HRWR, as discussed in Chapter 5.

The effect of HRWR on the flow spread of the mortars was also examined by visual inspection. The excessive HRWR dosage (equal to or greater than saturation dosage) was not conducive to the flow spread of the mortars since it caused bleeding, and bleed water appeared at the periphery of the spread for the majority of the mortars, as can be seen from Table 6.5. In few cases such as for M50R0S1 and M50R0S1c, the sand pile appeared at the centre of the flow spread.

Table 6.5: Results of visual inspection of the flow spread of mortars during flow mould test

Mortar type	Parent concrete	Saturation dosage of HRWR (%B)*	Dosage of HRWR used (%B)	Observation on flow spread of mortar
M30R0S1	C30R0A6	1.25	1.00-2.00	Bleeding at and after 1.5% HRWR
M30R15S1	C30R15A6	2.5	1.50-3.00	No bleeding
M30R20S1	C30R20A6	3	2.00-4.00	No bleeding
M35R0S1	C35R0A6	1	0.75-1.50	Bleeding at and after 1.25% HRWR
M35R0S1a	C35R0A4	1	0.75-1.50	Bleeding at and after 1.25% HRWR
M35R0S1b	C35R0A8	1	0.75-1.50	Bleeding at and after 1% HRWR
M35R5S1	C35R5A6	1.25	0.75-1.75	Bleeding at and after 1.50% HRWR
M35R10S1	C35R10A6	1.5	1.00-2.00	Bleeding at 2% HRWR
M35R15S1	C35R15A6	2	1.25-2.50	Bleeding at 2.5% HRWR
M35R15S1a	C35R15A4	2	1.25-2.50	Bleeding at 2.5% HRWR
M35R15S1b	C35R15A8	2	1.25-2.50	Bleeding at 2.5% HRWR
M35R20S1	C35R20A6	2.5	1.50-3.00	No bleeding
M35R20S1a	C35R20A4	2.5	1.50-3.00	No bleeding
M35R20S1b	C35R20A8	2.5	1.50-3.00	No bleeding
M35R25S1	C35R25A6	3	1.75-3.50	No bleeding
M35R30S1	C35R30A6	3.5	2.50-4.50	No bleeding
M40R0S1	C40R0A6	0.75	0.50-1.25	Bleeding at and after 0.75% HRWR
M40R15S1	C40R15A6	1.25	1.00-2.00	Bleeding at and after 1.75% HRWR
M40R20S1	C40R20A6	1.5	1.50-3.00	Bleeding at and after 2.5% HRWR
M50R0S1	C50R0A6	0.5	0.25-1.00	Bleeding and bigger sand pile at and after 0.5% HRWR
M50R0S1c	C50R0A2	0.5	0.25-1.00	Bleeding and smaller sand pile at and after 0.5% HRWR

*Obtained from flow cone test of binder pastes mentioned in Chapter 5

6.4.2 Verification of saturation dosages of high-range water reducer

The saturation dosages obtained from the flow cone test of the binder pastes were verified based on the flow spread of the mortars. In general, the increase in flow spread was

insignificant (0% to 5.6%) beyond the saturation dosages of HRWR. Furthermore, the bleeding occurred in most cases when the HRWR dosages exceeded the saturation dosage. This observation justifies the acceptability of the saturation dosages of HRWR obtained from the flow cone test of the binder pastes. However, a slight bleeding was even observed for the saturation dosages of HRWR in few cases such as for the mortars designated as M35R0S1b, M40R0S1, M50R0S1 and M50R0S1c. In addition, a sand pile appeared in the flow spread of M50R0S1 and M50R0S1c due to the segregation of fine aggregates. The overall observations suggest that the use of HRWR at or above saturation dosage should be avoided to prevent bleeding and segregation, and thus to improve the uniformity of mortars.

6.4.3 Effect of water-binder ratio

The effect of W/B ratio on the filling ability of the mortars was examined based on the flow spreads obtained at the saturation dosages of HRWR. The saturation flow spread of the mortars corresponding to the parent concretes with 6% design air content were noted from Figures 6.3 to 6.5 and 6.7, and plotted in Figure 6.8. It can be seen from Figure 6.8 that the saturation flow spread was greater for lower W/B ratio. This is due to larger paste volume and reduced sand content. At lower W/B ratio, the paste volume was increased simultaneously with the reduced sand content, as can be seen from Table 6.4. The increased paste volume and the reduced sand content decrease the yield stress and plastic viscosity of the mortars (Banfill 1994, Westerholm 2006), leading to greater flow spread. Also, the dispersion of the sand particles was enhanced with reduced sand content and increased paste volume. The increased paste volume pushed the sand particle away from each other with greater coating thickness of paste (Noguchi and Tomosawa 1999, Yen et al. 1999). Thus, the friction among sand particles became lower with higher inter-particle distance, and a greater kinetic energy was available to spread the mortar.

6.4.4 Effect of rice husk ash

The presence of RHA removed the bleeding from the mortars at saturation and higher dosages of HRWR, as can be seen from Table 6.5. But the flow spread of the mortars was decreased in the presence of RHA, which is obvious from Figure 6.9. Hence, the greater HRWR dosages were required at higher RHA contents to obtain the saturation flow spread.

For similar reason, the flow curves presented in Figures 6.3 to 6.5 generally showed a shift towards the downward right-hand direction, as the RHA content was increased. Such trends indicate that the yield stress and plastic viscosity of the mortars were increased with increasing RHA content. This is mostly due to the increased volume fraction and surface area of the binder caused by RHA. In particular, the surface area of the binder was increased predominantly in the presence of RHA. Both yield stress and viscosity of the mortars are increased with increasing surface area of the binder (Vom Berg 1979, Westerholm 2006). This is linked with the increased water demand of greater surface area that decreases the amount of free water available in mortar mixtures.

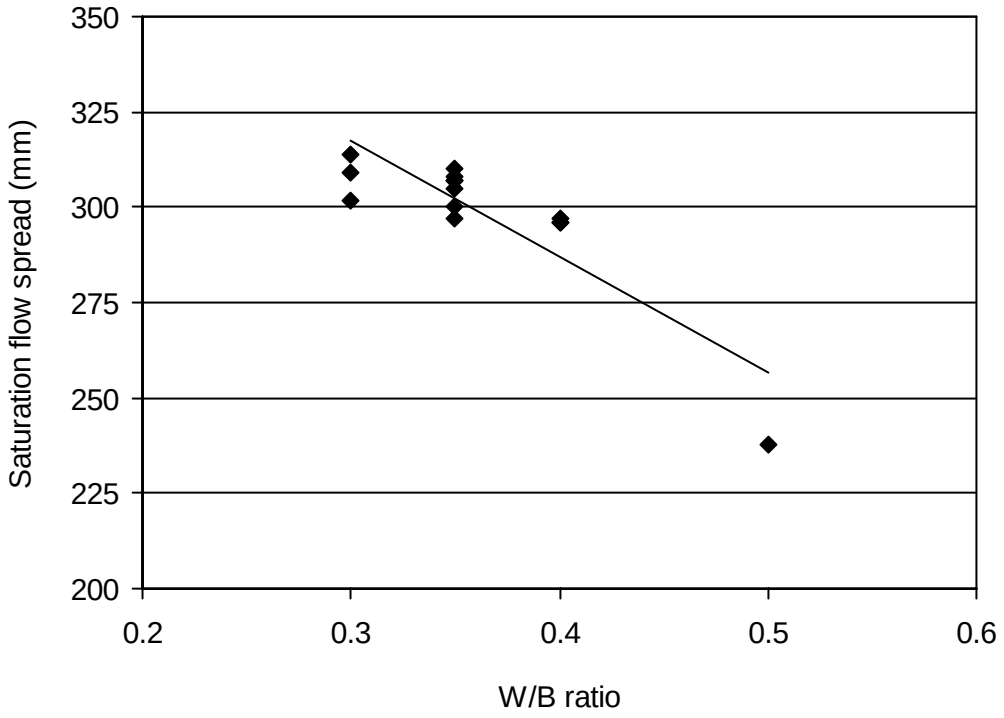

Figure 6.8: Effect of water-binder ratio on the flow spread of mortars

6.5 Air Content of Mortars

The results of the air content for different mortars are presented in Figures 6.10 to 6.13. The air content curves presented in Figures 6.10, 6.11 and 6.13 are for the mortars formulated from the concretes with 6% design air content. In contrast, the air content curves shown in Figure 6.12 are for the mortars formulated from the concretes with 4 and 8% design air contents. In general, the measured air content of the mortars varied from 3.7 to 19.4% for the

AEA dosages used in the range of 0.5 to 4 mL. Also, the air content curves shifted to the downward direction with increasing RHA content and lower W/B ratio, indicating the increased demand of AEA for a given air content.

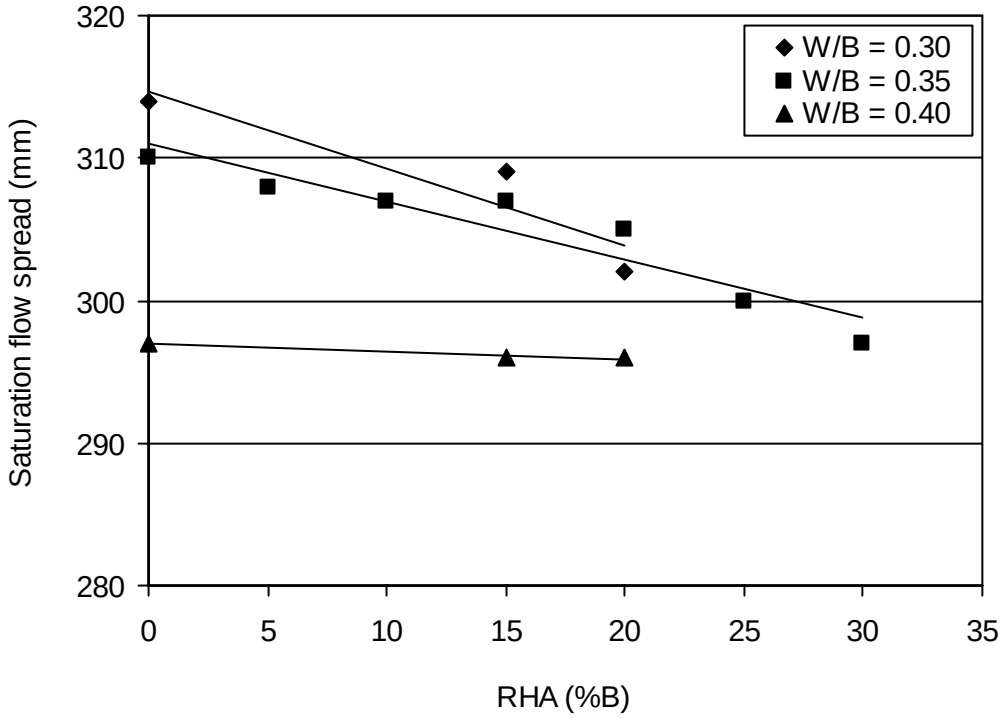

Figure 6.9: Effect of rice husk ash on the flow spread of mortars

The variation in the air content of different mortars, as observed in Figures 6.10 to 6.13, occurred due to the differences in W/B ratios and RHA contents along with AEA dosages. Moreover, the variation in the air content of the mortars presented in Figure 6.12 was caused by the changes in sand content. The sand content of M35R0S2a, M35R15S2a and M35R20S2a was greater than that of M35R0S2b, M35R15S2b, M35R20S2b, respectively, as can be seen from Table 6.3. The increase in sand content results in increased yield stress and viscosity (Banfill 1994), which reduce the air content. Also, it was observed that the former mortars provided lower flow spread than the latter mortars. A reduction in flow spread might reduce the air content for a given AEA dosage (Siebel 1989) possibly due to the enhanced interaction of the sand particles. Hence, the air content of M35R0S2a, M35R15S2a and M35R20S2a was about 1.5 to 2.5% lower than that of M35R0S2b, M35R15S2b and M35R20S2b, respectively, as can be seen in Figure 6.12.

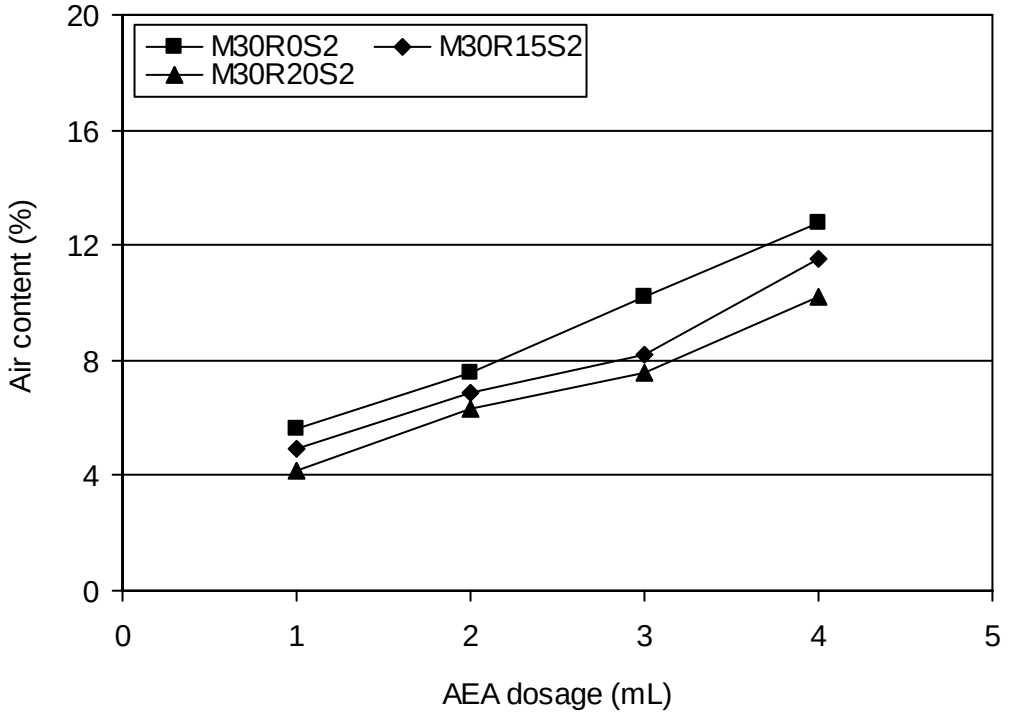

Figure 6.10: Air content of various mortars (W/B = 0.30, concrete air content = 6%)

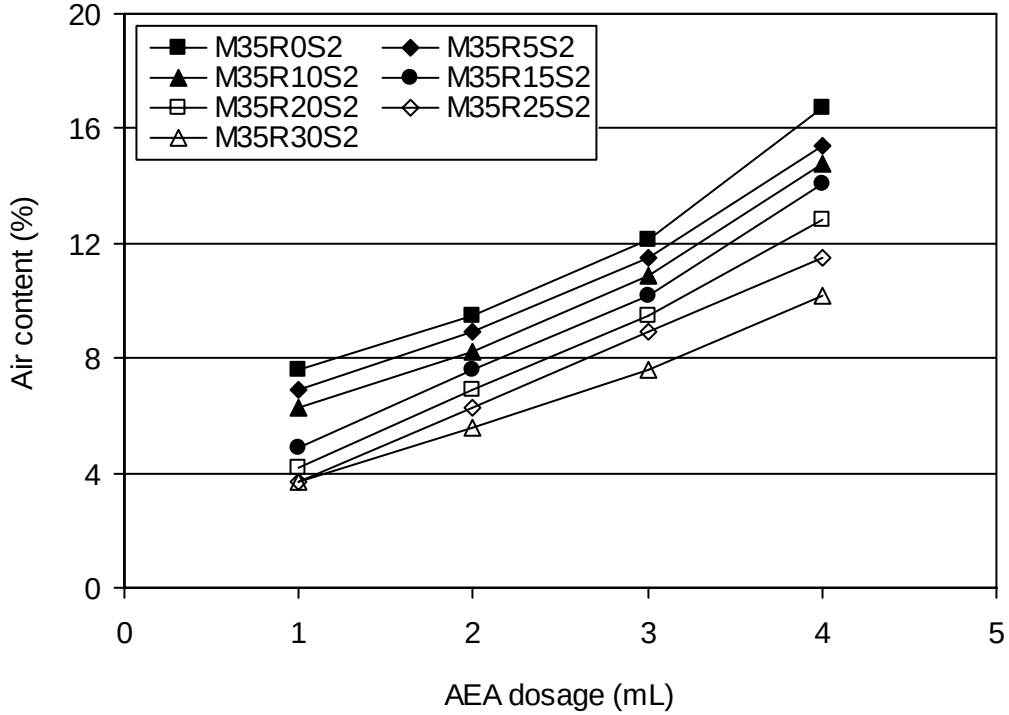

Figure 6.11: Air content of various mortars (W/B = 0.35, concrete air content = 6%)

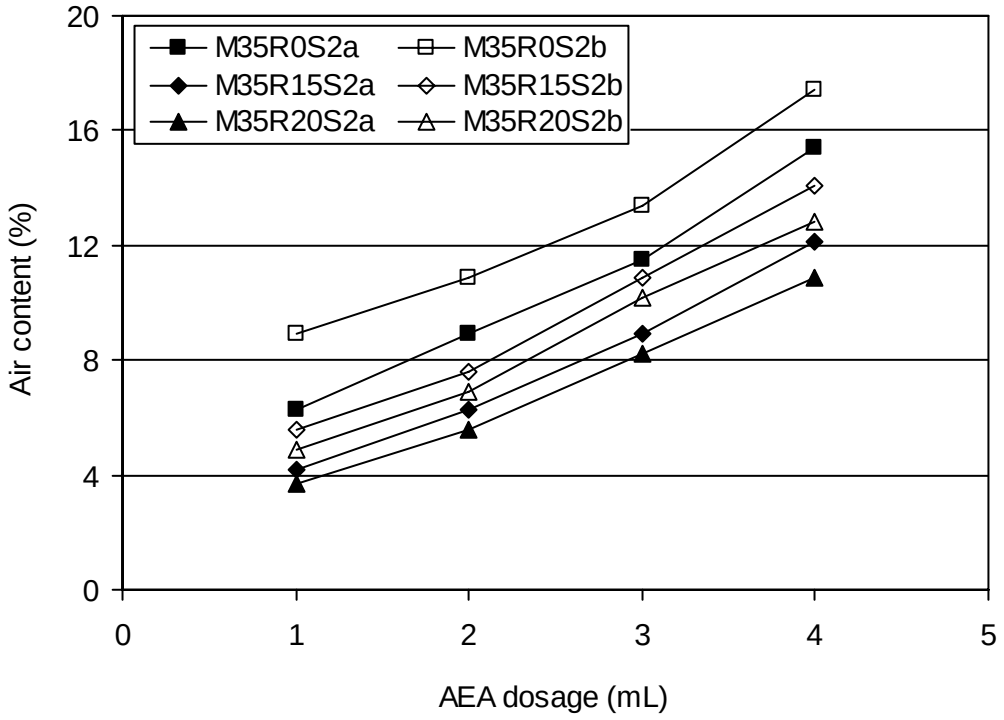

Figure 6.12: Air content of various mortars (W/B = 0.35, concrete air content = 4% and 8%)

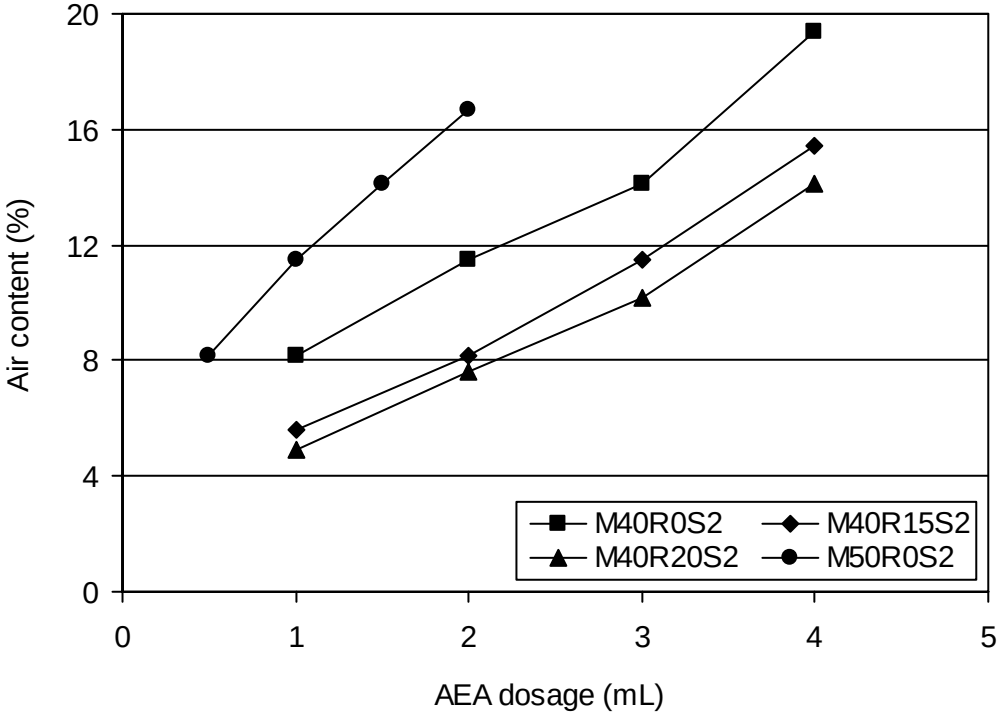

Figure 6.13: Air content of various mortars (W/B = 0.40 and 0.50, concrete air content = 6%)

6.5.1 Effect of air-entraining admixture

The air content of the mortars increased with increasing AEA dosages, as can be seen from Figures 6.10 to 6.13. The rate of increase was generally greater for the AEA dosages at 3 mL and above indicating the formation of more air-voids. It is reflected with the slope of the curves that became steeper in most cases at higher AEA dosages between 3 and 4 mL. This is perhaps due to the reduced loss of AEA through absorption in sand particles and binding materials that occurs at the early stage of mixing. Furthermore, additional air-voids can also be produced from the previous dosages with increased mixing time (Kosmatka et al. 2002), leading to a greater total air content.

6.5.2 Effect of water-binder ratio

The air content of the mortars was decreased linearly with lower W/B ratio for all AEA dosages, which is obvious from Figure 6.14. This is caused by the increased cement content at lower W/B ratio (ACI 212.3R-04, 2004; Whiting and Nagi 1998). An increase in the amount of cementing material results in a higher surface area that enhances the yield stress and plastic viscosity of paste, and thus causes some loss of air-voids leading to a reduction in air content.

6.5.3 Effect of rice husk ash

The air content of the mortars decreased with the increased RHA content for all AEA dosages. In general, the mortar air content was reduced linearly with increasing RHA content, as can be seen from Figure 6.15. Also, the reduction in air content due to RHA followed a similar trendline for all AEA dosages. The reduction in air content is mostly due to the increased surface area of the binder in the presence of RHA. The increased surface area of the binder intensifies the viscosity of the paste that tends to collapse some of the air-voids with increased internal pressure (Khayat and Assaad 2002). In addition, the increased RHA content required higher dosages of HRWR. The HRWR molecules impede the attachment of entrained air-voids onto the binding materials by reducing the attachment sites (Khayat and Assaad 2002). Thus, the air content of the mortars can be reduced with increased RHA content.

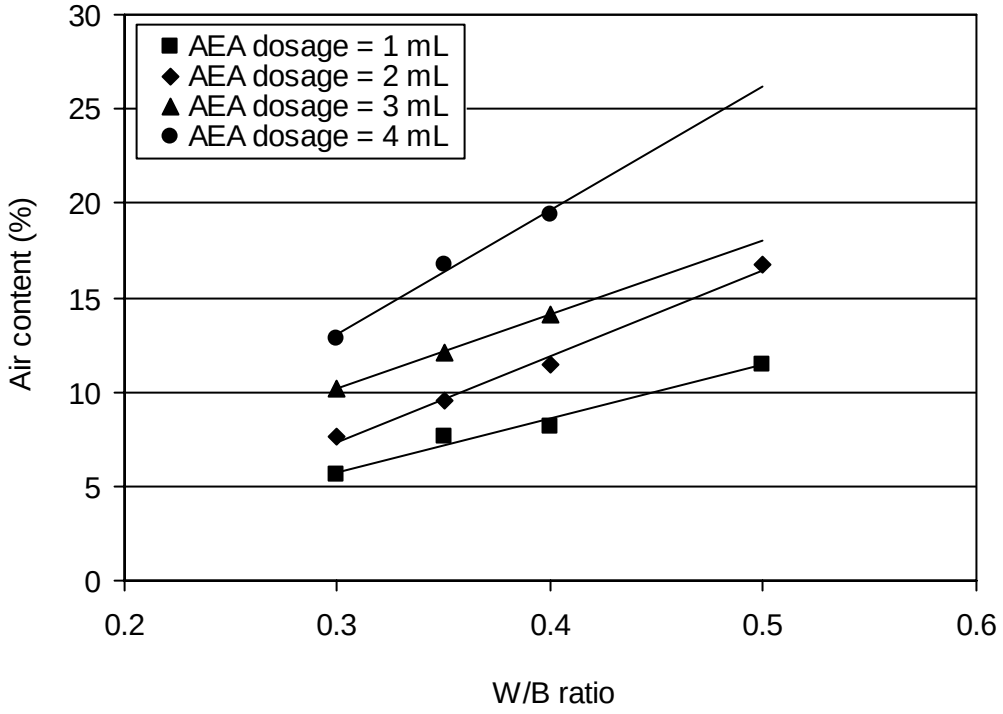

Figure 6.14: Effect of W/B ratio on the air content of mortars

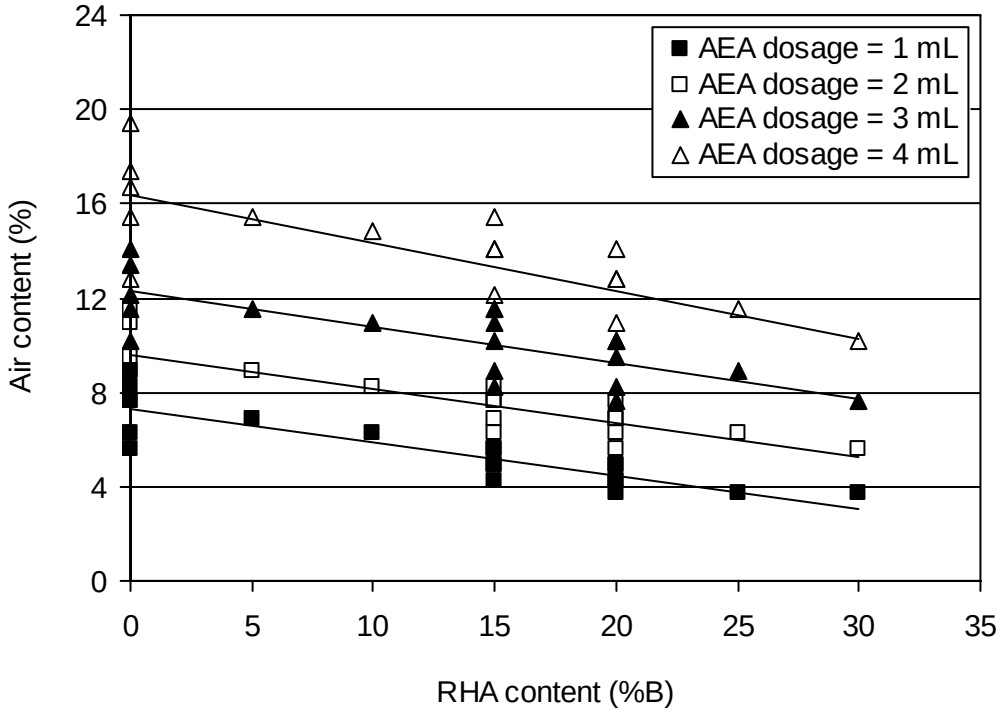

Figure 6.15: Effect of RHA content on the air content of mortars

6.6 Suitable Content of Rice Husk Ash

The reduction in the filling ability of the mortars was significant for a RHA content greater than 20% although it practically eliminated the bleeding. However, it depended on the W/B ratio of the mortars. The water demand for 20% RHA was higher at lower water W/B ratio. For this reason, 20% RHA caused a significant reduction in the flow spread of mortars at 0.30 and 0.35 W/B ratios. In comparison, the minimum reduction in flow spread was observed at 0.40 W/B ratio, as can be seen from Figures 6.5 and 6.9. Also, it can be inferred based on Figures 6.4 and 6.9 that the yield stress and plastic viscosity became very high at 25 and 30% RHA, resulting in a significant reduction in the flow spread of mortar. Therefore, relatively high HRWR dosages were required to achieve the saturation flow spread for these two cases. The overall flow spread results suggest that a RHA content greater than 20% is not effective for the filling ability of mortar. In addition, the demand for the AEA dosages for a given air content was comparatively high for 20% and greater RHA contents. Also, handling and mixing difficulties were experienced for the mortars with a RHA content higher than 15%, particularly at lower W/B ratios. Therefore, a RHA content greater than 15% may not be suitable to achieve the target filling ability of mortars and their corresponding parent concretes.

6.7 Estimated Dosages of Air-entraining Admixture for Concretes

The dosages of AEA required to produce a given air content in concretes were estimated based on the air content results of the mortars. For this, the concrete air content was converted into the equivalent mortar air content. Since the entrapped air content of the concrete is not produced from the AEA dosage, it was deducted from the specified concrete air content. The entrapped air content of concretes generally varies in the range of 1 to 3% (Kosmatka et al. 2002). Therefore, an average amount of entrapped air (2%) was subtracted from the specified concrete air content before converting it into equivalent mortar air content. Also, the entrapped air content of the mortars was not included while computing the equivalent mortar air content since the entrapped air is minimized when the mortars are produced at the slow speed of the mixer (Kim and Robertson 1997). The following equation was used to determine the equivalent mortar air content of the concretes (ASTM C231, 2004):

$$A_{me} = \frac{100 A_c V_c}{100 V_m + A_c (V_c - V_m)} \quad \text{(Equation 6.1)}$$

where:

A_{me} = Equivalent air content of the mortar (%)

A_c = Entrained air content of the concrete (%)

V_c = Air-free absolute volume of the concrete (m^3)

V_m = Air-free absolute volume of the mortar component of concrete (m^3)

The AEA dosages needed for the equivalent mortar air contents were calculated using the air content curves presented in Figures 6.10 to 6.13. These AEA dosages are applicable for the pure mortars, which were prepared separately instead of taking them from the concrete mixtures during testing of the air content by Chace indicator. Hence, they were corrected by multiplying with the actual air-free volume fraction of the mortar present in concrete. Equation 6.2 was applied to estimate the AEA dosages for the concretes. The estimated AEA dosages are shown in Table 6.6.

$$D_{ce} = \frac{D_{me} R_d}{1000 B} \times \phi_{mc} \times 100 \quad \text{(Equation 6.2)}$$

where:

B = Binder content of mortar (kg)

D_{ce} = Estimated AEA dosage for the specified air content of concrete (%B)

D_{me} = AEA dosage for the equivalent air content of mortar (mL)

R_d = Relative density of AEA

ϕ_{mc} = Volume fraction of the mortar component in concrete (m^3/m^3)

6.8 Use of Filling Ability and Air Content Results of Mortars

The filling ability results primarily revealed the effects of HRWR, RHA content, and W/B ratio or binder content on the flow spread of mortars. In addition, the flow spread of several mortars showed the effect of sand content. These results were useful to verify the saturation

dosages of HRWR obtained from the flow cone test of the binder pastes, and to decide the HRWR dosages for various SCHPC mixtures. It was understood that a HRWR dosage less than its saturation dosage usually should be used to improve the uniformity of concretes without any bleeding and segregation of coarse aggregates. Therefore, the HRWR dosages in the range of 70 to 80% of saturation dosages were selected for use in SCHPC mixtures except for C50R0A2 and C50R0A6. The saturation dosage was intentionally used in C50R0A2 to investigate the performance of segregation column apparatus. The flow spread results of the mortars were also helpful to observe the effectiveness of HRWR and the suitability of RHA for the required filling ability of concretes. On the other hand, the air content results of the mortars were used to estimate the AEA dosages for various air-entrained SCHPC mixtures. These processes minimized the number of trial mixtures involved in the mixture design of concretes.

Table 6.6: Estimated AEA dosages for various concrete mixtures

Concrete type	W/B ratio	Binder content (kg/m^3)	RHA content (%B)	Design air content (%)	AEA dosage (%B)
C30R0A6	0.30	492.7	0	6	0.030
C30R15A6	0.30	492.7	15	6	0.045
C30R20A6	0.30	492.7	20	6	0.052
C35R0A6	0.35	422.3	0	6	0.022
C35R0A4	0.35	422.3	0	4	0.015
C35R0A8	0.35	422.3	0	8	0.031
C35R5A6	0.35	422.3	5	6	0.026
C35R10A6	0.35	422.3	10	6	0.030
C35R15A6	0.35	422.3	15	6	0.043
C35R15A4	0.35	422.3	15	4	0.023
C35R15A8	0.35	422.3	15	8	0.072
C35R20A6	0.35	422.3	20	6	0.051
C35R20A4	0.35	422.3	20	4	0.027
C35R20A8	0.35	422.3	20	8	0.078
C35R25A6	0.35	422.3	25	6	0.060
C35R30A6	0.35	422.3	30	6	0.070
C40R0A6	0.40	369.5	0	6	0.013
C40R15A6	0.40	369.5	15	6	0.041
C40R20A6	0.40	369.5	20	6	0.049
C50R0A6	0.50	296.8	0	6	0.008

6.9 Conclusions

a. The filling ability of the mortars with respect to flow spread was increased with greater dosages of HRWR, which improved the deformability of mortar by its liquefying and dispersing actions.
b. The increase in mortar flow spread was not significant beyond the saturation dosages of HRWR obtained from the flow cone test of binder pastes. In most cases the bleeding and in few cases the sand pile appeared when the HRWR dosage used was equal to and higher than saturation dosage.
c. Excessive dosages of HRWR caused bleeding, which was minimized or eliminated in the presence of RHA that reduced the amount of free water available in mortar mixture due to increased water demand.
d. The filling ability, that is, the flow spread of the mortars was increased with lower W/B ratio due to larger paste volume and reduced sand content.
e. The filling ability of the mortars with regard to flow spread was decreased with higher RHA content due to the increased volume fraction and surface area of the binder.
f. A RHA content greater than 20% reduced the flow spread of mortar significantly, suggesting it might be unsuitable to achieve the required filling ability of concrete. Also, the demand for the AEA dosages for a given air content was relatively high for 20% and greater RHA contents.
g. The filling ability and air content of the mortars were influenced by their mixture composition, particularly, the sand and cement contents affected the flow spread and air content of the mortars by affecting their yield stress and plastic viscosity.
h. The air content of the mortars increased with the increase in AEA dosage due to the formation of greater air-voids, and decreased with lower W/B ratio and higher RHA content due to the increases in binder content, binder surface area and HRWR dosage.
i. The filling ability and air content of the mortars facilitate the mixture proportioning process of concretes to set the necessary HRWR dosages, to estimate the required AEA dosages, and to select a suitable RHA content.

Chapter 7

Mixture Proportions of Concretes

7.1 General

The design of self-consolidating high performance concrete (SCHPC) mixtures including the variables and constraints are presented and discussed in this chapter. In addition, this chapter presents the design approach, describes different types of SCHPC, and gives their primary and adjusted mixture proportions and the dosages of various chemical admixtures such as high-range water reducer (HRWR), air-entraining admixture (AEA) and viscosity-enhancing admixture (VEA).

7.2 Design of Concrete Mixtures

Different types of SCHPC mixtures were designed with various water-binder (W/B) ratios and rice husk ash (RHA) contents. All SCHPC mixtures designed were air-entrained except for one. The non-air-entrained concrete was mainly designed for using in the development of segregation column apparatus.

7.2.1 Design variables and constraints

The variables and constraints for different concrete mixtures are shown in Table 7.1. The major design variables for the concrete mixtures were W/B ratio or binder (cement plus RHA) content, RHA content and air content. The other variables were the dosages of HRWR and AEA, and the mixing time of concrete. The dosages of HRWR were varied for different concrete mixtures to achieve a slump flow in the range of 600 to 800 mm. The HRWR dosages were mainly dependent of the W/B ratio or binder content and RHA content used. The dosages of AEA also varied for different concrete mixtures, depending on the required air content and the W/B ratio and RHA content used.

The major constraints for the concrete mixtures were the slump and slump flow. A minimum slump of 250 mm and a minimum slump flow of 600 mm were considered to produce the SCHPC mixtures. The optimum sand-aggregate (S/A) ratio was also used in all

concrete mixtures. The type and source of the constituent materials and the nominal maximum size of fine and coarse aggregates were kept unchanged. A minimum total air content of 4% and a minimum 28 days compressive strength of 40 MPa were considered for all air-entrained concrete mixtures. In addition, a maximum sieve segregation of 18%, and a maximum column segregation of 20% were set for the acceptable static segregation resistance of the concrete mixtures.

Table 7.1: Variables and constraints for different types of concrete mixture

Variables
a. W/B ratios: 0.30, 0.35, 0.40, 0.50 by weight
b. Binder content: 295 to 495 kg/m^3
c. RHA content: 0 to 30% of total binder by weight
d. Total air content: 2 to 8%
e. HRWR dosage: 0.50 to 2.45% of binder by weight
f. AEA dosage: 0 to 0.085% of binder by weight
g. VEA dosage: 0 to 1.00% of binder by weight
h. Net mixing time: 7 to 13 minutes
Constraints
a. Type and source of the constituent materials of concrete
b. Nominal maximum size of fine aggregates: 4.75 mm
c. Nominal maximum size of coarse aggregates: 19 mm
d. Minimum slump: 250 mm
e. Minimum slump flow: 600 mm
f. Minimum total air content for fresh air-entrained concrete: 4%
g. Minimum compressive strength at 28 days: 40 MPa
h. Optimum S/A ratio: 0.50
i. Maximum sieve segregation: 18%
j. Maximum column segregation: 20%

7.2.2 Design approach

The SCHPC mixtures were designed using the W/B ratios of 0.30, 0.35, 0.40 and 0.50 to achieve the target compressive strength in the range of 40 to 100 MPa. These W/B ratios were selected based on the recommendation of Lessard et al. (1995) for mixture design of air-entrained high performance concrete. The RHA was used in SCHPC mixtures as a supplementary cementing material substituting 0 to 30% of cement by weight. The design air content was 6% for the majority of SCHPC mixtures. The design air content was 4 to 8% for the SCHPC mixtures tested for air-void stability. In addition, 2% design air content

(entrapped air content) was considered for the non-air-entrained SCHPC mixture with 0.50 W/B ratio and 0% RHA content.

The quantity of the mixing water for SCHPC mixtures with 0.30 to 0.40 W/B ratios was estimated and adjusted based on the ACI guideline for mixture design of high strength concrete given in ACI 211.4R-93 (2004). In this case, a minimum slump of 75 to 100 mm specified without any HRWR was considered for the first estimate of mixing water requirement. The mixing water for the SCHPC mixtures with 0.50 W/B ratio was estimated according to the CAC guideline (Kosmatka et al. 2002). In this case a minimum slump of 25 to 50 mm was considered for the first estimate of mixing water prior to the addition of any HRWR. In addition, the optimum S/A ratio of 0.50, as obtained from the testing of various aggregate blends, was used to design the SCHPC mixtures. The HRWR was used in all concretes to obtain the required filling ability and passing ability. The AEA was incorporated to obtain the concrete air content in the range of 4% to 8%. Moreover, the VEA was used in a limited number of concrete mixtures to improve their stability with increased segregation resistance.

7.2.3 Various types of concrete mixture

In total, twenty one different types of SCHPC mixtures were designed. The designation and description of the concrete mixtures are presented in Table 7.2. The concrete mixtures were designated based on the W/B ratio, RHA content, and design air content used. For example, the ‘C30R0A6’ designation was used for a concrete prepared with a W/B ratio of 0.30, 0% RHA content, and 6% design air content.

7.3 Mixture Proportions

The mixture proportions of various SCHPCs were determined based on the absolute volume method. At first, the primary mixture proportions were determined considering the design air content and the absolute volumes of fine and coarse aggregates, binder (cement pus RHA), and water. Then, the dosages of chemical admixtures (HRWR, AEA and VEA) were decided, the water correction was done, and finally the adjusted mixture proportions were determined for concrete batching.

7.3.1 Primary mixture proportions

The primary mixture proportions of various SCHPCs were determined based on the following procedure:

Step 1: Deciding the W/B ratio based on the expected compressive strength.

Step 2: Estimation of the mixing water requirement for concretes.

Step 3: Computation of the quantity of binder from W/B ratio and mixing water.

Step 4: Calculation of the cement and RHA contents based on the quantity of total binder and the weight replacement level of cement by RHA.

Step 5: Determination of the relative proportions of concrete stone and concrete sand in total aggregates based on the optimum S/A ratio.

Step 6: Calculation of the quantity of total aggregates, and thus the proportions of concrete stone and sand using absolute volume method.

Table 7.2: Designation and description of the concrete mixtures

Concrete type	W/B ratio	Binder (B)		Design air content (%)
		C* (%B)	RHA (%B)	
C30R0A6	0.30	100	0	6
C30R15A6	0.30	85	15	6
C30R20A6	0.30	80	20	6
C35R0A6	0.35	100	0	6
C35R0A4	0.35	100	0	4
C35R0A8	0.35	100	0	8
C35R5A6	0.35	95	5	6
C35R10A6	0.35	90	10	6
C35R15A6	0.35	85	15	6
C35R15A4	0.35	85	15	4
C35R15A8	0.35	85	15	8
C35R20A6	0.35	80	20	6
C35R20A4	0.35	80	20	4
C35R20A8	0.35	80	20	8
C35R25A6	0.35	75	25	6
C35R30A6	0.35	70	30	6
C40R0A6	0.40	100	0	6
C40R15A6	0.40	85	15	6
C40R20A6	0.40	80	20	6
C50R0A6	0.50	100	0	6
C50R0A2	0.50	100	0	2

*Normal portland cement

The absolute volumes of the HRWR, AEA and VEA were not taken into account to calculate the primary mixture proportions. This is because these chemical admixtures were used as additives to the primary concrete mixtures. The primary mixture proportions of the concretes are shown in Table 7.3.

Table 7.3: Details of the primary concrete mixture proportions

Concrete type	CA* (kg/m^3)	FA♣ (kg/m^3)	C (kg/m^3)	RHA (kg/m^3)	W♠ (kg/m^3)
C30R0A6	846.3	842.2	492.7	0	147.8
C30R15A6	829.9	825.8	418.8	73.9	147.8
C30R20A6	824.4	820.3	394.2	98.5	147.8
C35R0A6	876.1	871.8	422.3	0	147.8
C35R0A4	902.7	898.3	422.3	0	147.8
C35R0A8	849.4	845.2	422.3	0	147.8
C35R5A6	871.4	867.1	401.2	21.1	147.8
C35R10A6	866.7	862.4	380.1	42.2	147.8
C35R15A6	862.0	857.8	359.0	63.3	147.8
C35R15A4	888.6	884.2	359.0	63.3	147.8
C35R15A8	835.3	831.2	359.0	63.3	147.8
C35R20A6	857.3	853.1	337.8	84.5	147.8
C35R20A4	883.9	879.5	337.8	84.5	147.8
C35R20A8	830.6	826.5	337.8	84.5	147.8
C35R25A6	852.6	848.4	316.7	105.6	147.8
C35R30A6	847.9	843.7	295.6	126.7	147.8
C40R0A6	898.4	894.0	369.5	0	147.8
C40R15A6	886.0	881.7	314.1	55.4	147.8
C40R20A6	881.9	877.6	295.6	73.9	147.8
C50R0A6	928.3	923.7	296.8	0	148.4
C50R0A2	940.1	935.5	334.8	0	167.4

*Coarse aggregate; ♣Fine aggregate; ♠Normal tap water

7.3.2 Dosages of chemical admixtures

The dosages of chemical admixtures such as HRWR, AEA and VEA were selected to produce the required flowing ability (filling ability and passing ability), air content, and segregation resistance, respectively. The HRWR dosages for the concretes were set based on the saturation dosages (SDs) of HRWR. The saturation dosages of HRWR were obtained from the filling ability test results of the pastes, as discussed in Chapter 5. The AEA dosages

needed for the concretes were fixed based on the estimated AEA dosages obtained from the air content test results of the mortars, as shown in Chapter 6. In addition, the dosages of VEA were selected for the limited number of concrete mixtures according to the guideline of the manufacturer. The dosages of HRWR, AEA and VEA used for the concretes are shown in Table 7.4. The dosages of the chemical admixtures shown were applied as a single addition except for the HRWR dosages used for C35R0A4, C35R0A8, C35R15A4, C35R15A8, C35R20A4, and C35R20A8, which were tested for the air-void stability in fresh concretes. For these concretes, the HRWR dosages were used as several split additions to maintain similar slump and slump flow during different test stages so that their effects on the air content of concrete were minimized.

Table 7.4: Various mass dosages of HRWR, AEA and VEA

Concrete type	Dosage of HRWR		Dosage of AEA (%B)	Dosage of VEA (%B)
	%SD*	%B		
C30R0A6	70	0.875	0.026	---
C30R15A6	70	1.75	0.047	---
C30R20A6	70	2.10	0.056	---
C35R0A6	70	0.70	0.020	---
C35R0A4	70+10×3	0.70+0.10×3	0.016	---
C35R0A8	70+10×3	0.70+0.10×3	0.026	---
C35R5A6	70	0.875	0.025	---
C35R10A6	70	1.05	0.035	0 - 0.923
C35R15A6	70	1.40	0.045	0 - 0.923
C35R15A4	70+10×3	1.4+0.20×3	0.031	---
C35R15A8	70+10×3	1.4+0.20×3	0.072	---
C35R20A6	70	1.75	0.054	---
C35R20A4	70+10×3	1.75+0.25×3	0.036	---
C35R20A8	70+10×3	1.75+0.25×3	0.083	---
C35R25A6	70	2.10	0.070	---
C35R30A6	70	2.45	0.080	---
C40R0A6	80	0.60	0.011	---
C40R15A6	80	1.00	0.040	---
C40R20A6	80	1.20	0.051	---
C50R0A6	100	0.50	0.006	---
C50R0A2	100	0.50	0	---

*Saturation dosage of HRWR

7.3.3 Adjusted mixture proportions

The primary mixture proportions of fine and coarse aggregates obtained were on the basis of saturated surface-dry condition. However, the air-dry basis fine and coarse aggregates were used in preparing the concrete mixtures. Therefore, they absorbed some mixing water during concrete batching. In addition, the liquid HRWR contributed some water to the mixing water. Thus, the water corrections were made considering the absorption of aggregates and the water contribution of HRWR to obtain the accurate proportion of the mixing water. Moreover, the proportions of fine and coarse aggregates were adjusted based on their absorption and moisture content. The adjusted mixture proportions of the concretes are shown in Table 7.5.

Table 7.5: Details of the adjusted concrete mixture proportions

Concrete type	CA (kg/m^3)	FA (kg/m^3)	C (kg/m^3)	RHA (kg/m^3)	W (kg/m^3)
C30R0A6	834.7	834.7	492.7	0	163.4
C30R15A6	818.4	818.4	418.8	73.9	159.4
C30R20A6	813.0	813.0	394.2	98.5	157.8
C35R0A6	864.0	864.0	422.3	0	165.2
C35R0A4	890.3	890.3	422.3	0	165.7
C35R0A8	837.7	837.7	422.3	0	164.5
C35R5A6	859.4	859.4	401.2	21.1	164.5
C35R10A6	854.7	854.7	380.1	42.2	163.8
C35R15A6	850.1	850.1	359.0	63.3	162.4
C35R15A4	876.4	876.4	359.0	63.3	162.9
C35R15A8	823.8	823.8	359.0	63.3	161.9
C35R20A6	845.5	845.5	337.8	84.5	161.1
C35R20A4	871.7	871.7	337.8	84.5	161.6
C35R20A8	819.2	819.2	337.8	84.5	160.4
C35R25A6	840.8	840.8	316.7	105.6	159.7
C35R30A6	836.2	836.2	295.6	126.7	158.3
C40R0A6	886.0	886.0	369.5	0	166.6
C40R15A6	873.8	873.8	314.1	55.4	165.2
C40R20A6	869.8	869.8	295.6	73.9	163.4
C50R0A6	915.5	915.5	296.8	0	169.4
C50R0A2	927.2	927.2	334.8	0	187.6

7.4 Concluding Remarks

The concrete mixtures were designed using the W/B ratios varying from 0.30 to 0.50, RHA content ranging from 0 to 30% of binder by weight, and an optimum S/A ratio of 0.50. The primary mixture proportions were computed based on the absolute volumes of the constituent materials. The dosages of HRWR were fixed based on the saturation dosages obtained from the flow cone test of binder pastes. The dosages of AEA were estimated using the air content results of the mortar components of corresponding parent concretes. The VEA dosages were fixed based on the manufacture's guideline.

Chapter 8

Properties of Freshly Mixed Self-consolidating High Performance Concretes

8.1 General

This chapter describes the preparation and testing of various freshly mixed self-consolidating high performance concretes (SCHPCs). The test results for various fresh properties of different SCHPCs, and for the air void-stability in several freshly mixed SCHPCs are also presented and discussed. A simplified single-operator inverted slump cone apparatus including the performance criteria for filling ability and passing ability has been introduced. The effects of water-binder (W/B) ratio, rice husk ash (RHA), high-range water reducer (HRWR), and air content are highlighted. The effects of re-mixing and filling ability on the air-void stability are also discussed. In addition, a number of correlations for the flow times of paste and concrete, flow spread of mortar and slump flow of concrete, various filling ability and passing ability properties, and estimated and actual dosages of AEA are shown. This chapter also provides an empirical model for the filling ability with regard to slump flow, and discusses its validity and application. Finally, this chapter gives the optimum RHA content of SCHPC.

8.2 Research Significance

The filling ability and passing ability are two essential properties of SCHPC. They must be carefully maintained in concretes to achieve self-consolidation capacity (self-compactability). The air-void stability in SCHPC is also essential to provide sufficient freeze-thaw resistance. The performance of various SCHPCs incorporating RHA was investigated with respect to different fresh properties, particularly filling ability and passing ability. In addition to several known techniques, a simplified single-operator inverted slump cone apparatus was proposed to assess the filling ability and passing ability. The correlations for different filling ability and passing ability properties are highlighted. Also, the air-void stability in fresh SCHPC is

discussed. The test results give the effect of RHA on various fresh properties and air-void stability, and suggest an optimum RHA content for SCHPC. Based on the slump flow results, a filling ability model was developed to facilitate the mixture design of SCHPC. The research findings will be of special interest to the construction industry regarding the use of SCHPC in different structural and non-structural applications.

8.3 Preparation of Fresh Concretes

The fresh SCHPC mixtures were prepared using a revolving pan type mixer conforming to ASTM C 192/C 192M (2004). The nominal capacity of the pan was 50 liters. The pan mixer used is shown in Figure 8.1.

8.3.1 Batching procedure

The batch volume of the concrete mixtures was calculated before batching. The batch quantity of the fresh concrete taken was at least 15% more than the required to compensate the loss during mixing and testing. The amounts of the primary constituent materials for each concrete batch were determined based on the adjusted mixture proportions shown in Table 7.5 (Chapter 7). The aggregates, cement and RHA were taken on weight basis. But the quantities of the mixing water and all chemical admixtures such as HRWR, air-entraining admixture (AEA) and viscosity-enhancing admixture (VEA) required for a concrete batch were measured on volume basis. The volume dosages of the chemical admixtures were determined based on the mass dosages shown in Table 7.4 (Chapter 7).

8.3.2 Mixing method

The coarse and fine aggregates were charged first into the mixer and mixed with one-quarter of the mixing water for 60 seconds. Then the dosage of AEA dispensed in the second-quarter of the mixing water was added and the mixing was continued for 60 seconds. This step was followed in absence of AEA in non-air-entrained SCHPC mixture. The mixer was stopped thereafter and the cementing material (cement alone or with RHA) was charged into the mixer. Immediately, the mixer was restarted and the mixing was continued for 120 seconds with the addition of third-quarter of the mixing water. After that, the mixer was stopped, and the concrete materials in the pan were covered with a piece of wet burlap and allowed to rest

for 180 seconds. The rest period was intended to allow the air-dry aggregates to absorb some of the mixing water, thus minimizing the likelihood for absorption of HRWR by the aggregates. Then the mixer was restarted and the mixing was continued for 180 seconds with the addition of HRWR dispensed in fourth-quarter of the mixing water.

8.4 Testing of Fresh Concretes

The fresh SCHPC mixtures were tested for slump and slump flow with and without J-ring, unit weight and air content, orimet flow with and without J-ring, and inverted slump cone flow with and without J-ring. Some of the SCHPC mixtures were also tested for the air-void stability. The overall test program for various fresh concretes is shown in Table 8.1.

Table 8.1: Test program for different types of fresh SCHPC

Concrete designation*	Type of tests
C30R0A6, C30R15A6, C30R20A6	Slump and slump flow
	Slump and slump flow with J-ring
C35R0A6, C35R5A6, C35R10A6, C35R15A6, C35R20A6, C35R25A6, C35R30A6	Orimet flow
	Orimet flow with J-ring
	Inverted slump cone flow
	Inverted slump cone flow with J-ring
C40R0A6, C40R15A6, C40R20A6	Unit weight
C50R0A2, C50R0A6	Air content
C35R0A4, C35R0A8, C35R15A4, C35R15A8, C35R20A4, C35R20A8	Air-void stability
	Air content
	Slump and slump flow
	Unit weight

*Concrete designations are given in Chapter 7

8.4.1 Slump and slump flow test

The slump and slump flow were determined using an Abram's slump cone (ASTM C 143/C 143M, 2004). The fresh concrete was poured into the slump cone in one layer and without any consolidation. Then the slump cone was raised vertically in 3 to 5 seconds to allow the fresh concrete to deform over the surface of a steel pan or sheet. The vertical drop of the concrete sample from its original position was measured and reported as the slump. An operational stage of the slump test is shown in Figure 8.1.

Pan mixer used for preparing concretes

Measurement of slump

Measurement of slump flow

Measurement of slump with J-ring

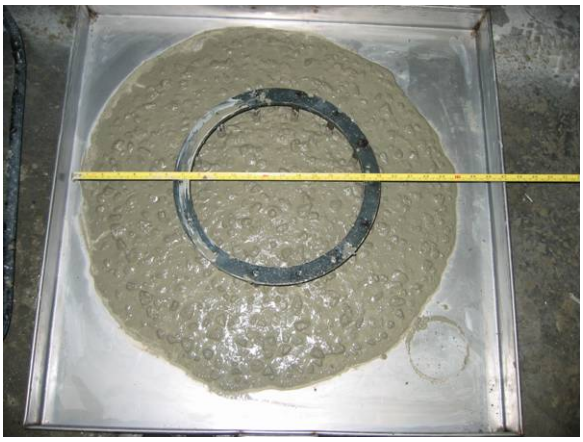

Measurement of slump flow with J-ring

Flow spread in orimet flow test

Figure 8.1: Pan mixer, slump and slump flow with and without J-ring, and orimet flow spread

The slump flow was measured from the same test conducted for determining the slump. The diameter of the concrete spread was measured at four positions that divided the flow patty into eight equal segments. The average diameter was used to express the slump flow of the concrete. An operational stage of the slump flow test is also shown in Figure 8.1.

8.4.2 Slump cone – J-ring flow test

The slump cone – J-ring flow test was conducted to determine the slump and slump flow with J-ring. The J-ring was built using 10-mm deformed reinforcing bars. The spacing of the bars was 57 mm (3 times the maximum size of concrete stone), which is greater than the minimum recommended bar spacing. The minimum recommended bar spacing for J-ring is 2.5 times higher than the maximum size of coarse aggregate (Brameshuber and Uebachs 2001). The details of the J-ring are shown in Figure 8.2. The slump cone was placed at the centre of the J-ring and filled with concrete in one layer without any consolidation. Then the slump cone was raised vertically and the concrete was allowed to deform. The vertical drop of the concrete sample was measured in presence of J-ring and reported as the slump with J-ring. An operational stage of the slump measurement in the presence of J-ring is shown in Figure 8.1. In addition, the diameter of the concrete spread through the J-ring was measured in a similar way as mentioned in case of slump flow. The average diameter was recorded as the slump flow with J-ring. An operational stage for the slump flow measurement in the presence of J-ring is shown in Figure 8.1.

8.4.3 Orimet flow test

The orimet flow was determined using an orimet, as shown in Figure 8.3. This apparatus is used in Europe to examine the filling ability of SCHPC (EFNARC 2002). It has a 120 mm diameter × 600 mm long vertical pipe section, which is welded with a 60 mm high conical orifice at the bottom end. The outlet diameter of the orifice can be varied. The orimet used in this study had an orifice with the outlet diameter of 80 mm. The level of the orifice outlet was fixed at a height of 430 mm from the floor. During testing, the fresh concrete was placed into the pipe section of the orimet without any consolidation, while keeping the trap door closed. Then the door was opened and the concrete was allowed to flow through the orifice. Simultaneously, a stopwatch was used to record the flow time. In addition, the diameter of

the deformed concrete was measured at four right-angle positions that divided the flow patty into eight equal segments. The average diameter was recorded as the orimet flow spread. An operational stage of the orimet flow test is shown in Figure 8.1.

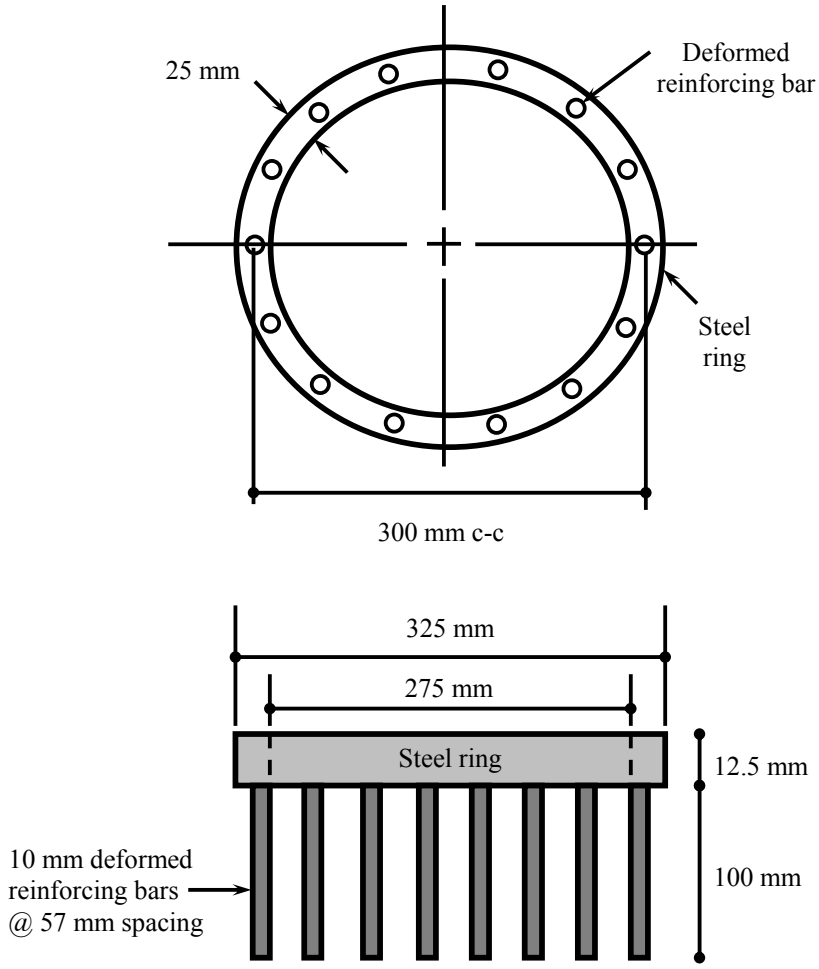

Figure 8.2: Details of the J-ring

8.4.4 Orimet – J-ring flow test

The orimet – J-ring flow test was conducted to determine the orimet flow spread with J-ring. The orimet was placed over the J-ring and the orifice of the orimet was centralized with the J-ring. The concrete was placed in the cast pipe of the orimet in one layer and without any consolidation. The trap door was opened, and the concrete was allowed to fall and deform through the J-ring. The diameter of the concrete spread through the J-ring was measured in a similar way as mentioned in case of orimet flow spread. The average diameter was recorded

as the orimet flow spread with J-ring. An operational stage of the orimet – J-ring flow test is shown in Figure 8.4.

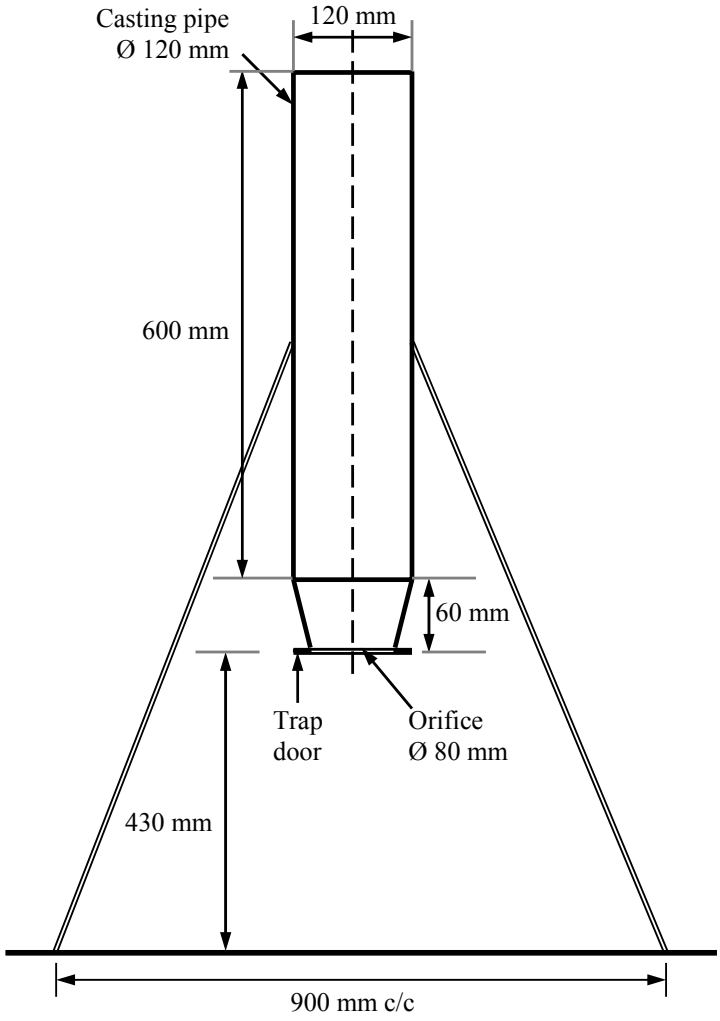

Figure 8.3: Details of the orimet apparatus

8.4.5 Inverted slump cone flow test

The inverted slump cone flow was determined using the Abram's slump cone in its inverted position. The details of the inverted slump cone apparatus are shown in Figure 8.5. A wooden rigid frame was built to hold the inverted slump cone, and a trap door was attached at the bottom of the inverted slump cone. The constricted end of the inverted slump cone was at a height of 430 mm from the floor. The conical shape (the diameter is reduced from 200 to 100 mm over a depth of 300 mm) produced some resistance to the concrete flow. The fresh

concrete was placed into the inverted slump cone in one layer while keeping the trap door closed at the bottom. No means of consolidation was used during concrete placement. Immediately after filling of the inverted slump cone, the trap door was opened to allow the concrete to flow. At the same time, a stopwatch was used to record the flow time of the concrete. In addition, the diameter of the concrete spread was measured at four right-angle positions that divided the flow patty into eight equal segments. The average diameter was recorded as the inverted slump cone flow spread. An operational stage of the inverted slump cone flow test is shown in Figure 8.4.

8.4.6 Inverted slump cone – J-ring flow test

The inverted slump cone – J-ring flow test was conducted to determine the inverted slump cone flow spread with J-ring. The test was carried out by using the inverted slump cone apparatus along with a J-ring. The inverted slump cone apparatus was placed above the J-ring with the lower opening of the cone vertically centralized with the J-ring. The trap door was closed and the concrete was placed in the inverted slump cone in one layer and without any consolidation. Then the trapped door was opened, and the concrete was allowed to fall and flow through the J-ring. The diameter of the deformed concrete was measured in the presence of J-ring. The measurement was taken in a similar way as mentioned in case of inverted slump cone flow spread. The average diameter was reported as the inverted slump cone flow spread with J-ring. An operational stage of the inverted slump cone – J-ring flow test is shown in Figure 8.4.

8.4.7 Test for unit weight

The unit weight of various fresh concretes was determined using the measuring bowl of the air meter. The measuring bowl was calibrated prior to testing to determine the volume. The procedure stated in ASTM C 138/C 138M (2004) was followed with some exceptions for filling and consolidation. Specifically, the measuring bowl was filled in one layer instead of three, and no means of consolidation was used during concrete filling. The weight of the concrete contained in the measuring bowl was determined. Later, the unit weight was computed from known weight and volume of concrete. An operational stage of unit weight measurement is shown in Figure 8.4.

Orimet – J-ring flow

Inverted slump cone flow

Inverted slump cone – J-ring flow

A measurement for unit weight

Type B air meter

Measurement of air content

Figure 8.4: Orimet – J-ring flow, inverted slump cone flow with and without J-ring, unit weight, and air content tests for various concretes

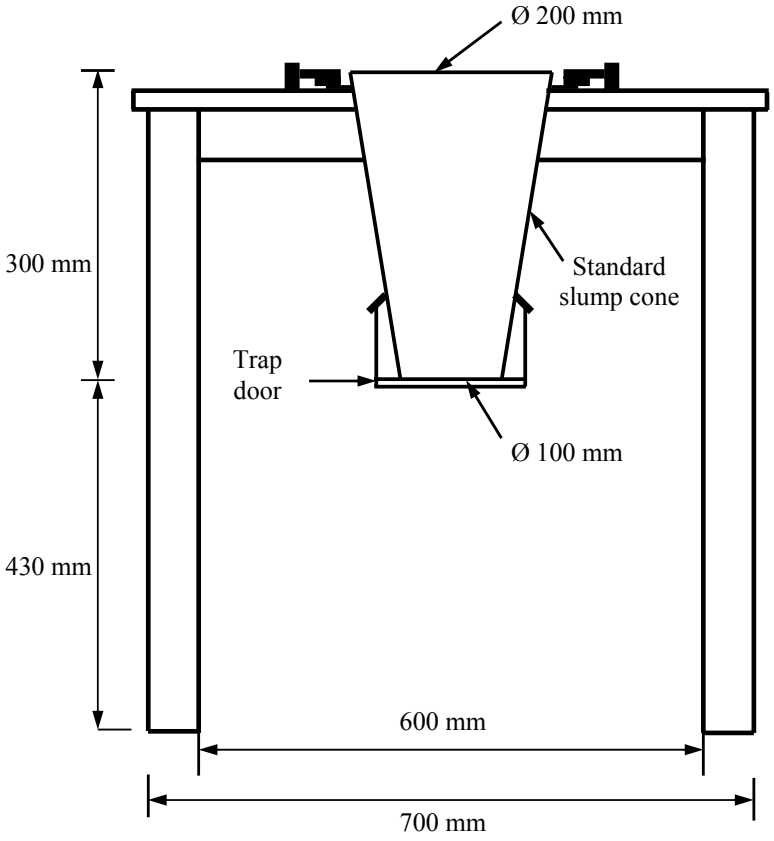

Figure 8.5: Details of the inverted slump cone apparatus

8.4.8 Test for air content

The air content of the fresh concretes was determined by a Type B air meter (ASTM C 231, 2004), as shown in Figure 8.4. The pressure method was used with some exceptions for pouring and consolidation. Specifically, the measuring bowl of the air meter was filled with the fresh concrete in one layer and without any means of consolidation. The air content obtained from the air meter was corrected for the aggregate content of the concrete to obtain the actual air content. An operational stage of the air content test is shown in Figure 8.4.

8.4.9 Test for air-void stability

Several SCHPC mixtures (C35R0A4 to C35R20A8), as mentioned in Table 8.1 were tested to examine the air-void stability in fresh concretes. The details of these concretes including

the mixture proportions and dosages of HRWR and AEA are given in Tables 7.2 to 7.5 (Chapter 7). The concrete mixtures were prepared following the same procedure as described in Section 8.3. However, the saturation dosage (SD) of HRWR was used by splitting to produce the required filling ability. The saturation dosage was split into four parts such as 70, 10, 10 and 10%, and added sequentially into concrete mixture to maintain similar slump and slump flow during different test stages as shown in Figure 8.6. The initial dosage of HRWR was 70% of the saturation dosage. The remaining three parts of the saturation dosage of HRWR were added to the concrete mixture during re-mixing at different test stages.

The air-void stability was investigated with respect to the changes in fresh air content over time. The total testing time of 60 to 90 minutes was chosen based on the transportation time of concrete from ready-mixed concrete plant to the jobsite. The lower testing time (60 minutes) was chosen for the concretes with 4% design air content whereas the higher testing time (90 minutes) was selected for the concretes with 8% design air content. The entire testing was comprised of four stages as shown in Figure 8.6. At the end of Stage 1, the concrete mixtures were tested after 15 minutes from the start of initial mixing to determine the air content. Then the concrete mixtures were covered with wet burlap and allowed for rest. The subsequent rest period varied from 10 to 25 minutes depending on the testing time as shown in Figure 8.6. Before testing the air content at the end of Stages 2 to 4, the concrete mixtures were re-mixed. The re-mixing was employed to simulate intermittent agitation of concrete during transportation. The re-mixing was conducted for 6 minutes in total and applied at 3 stages for all concretes. In each stage, the re-mixing time was 2 minutes. The subsequent measurement for air content was taken after 30, 45 and 60 minutes for the concretes with 4% design air content (C35R0A4, C35R15A4, and C35R20A4). These measurements were carried out after 30, 60 and 90 minutes for the concretes with 8% design air content (C35R0A8, C35R15A8, and C35R20A8). The air content of all fresh concretes was determined following the test procedure mentioned in Section 8.4.8.

8.5 Filling Ability of Concretes

The filling ability results of various SCHPC mixtures were obtained with respect to slump and slump flow, inverted slump cone flow time and spread, and orimet flow time and spread. They are discussed below.

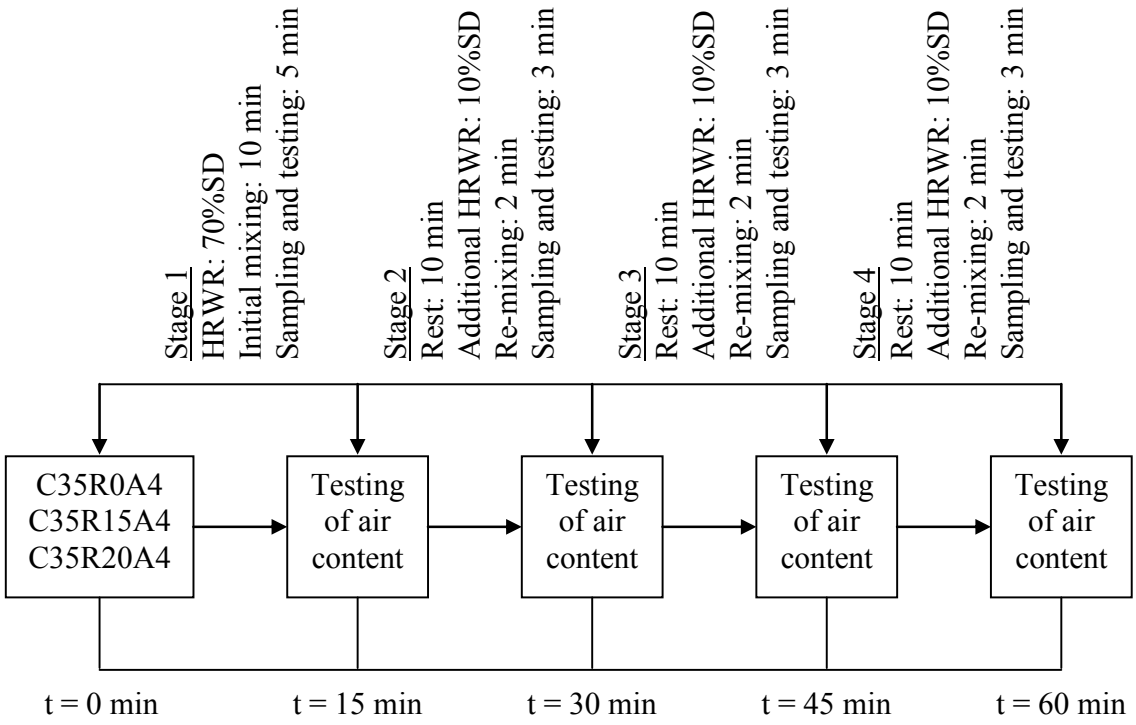

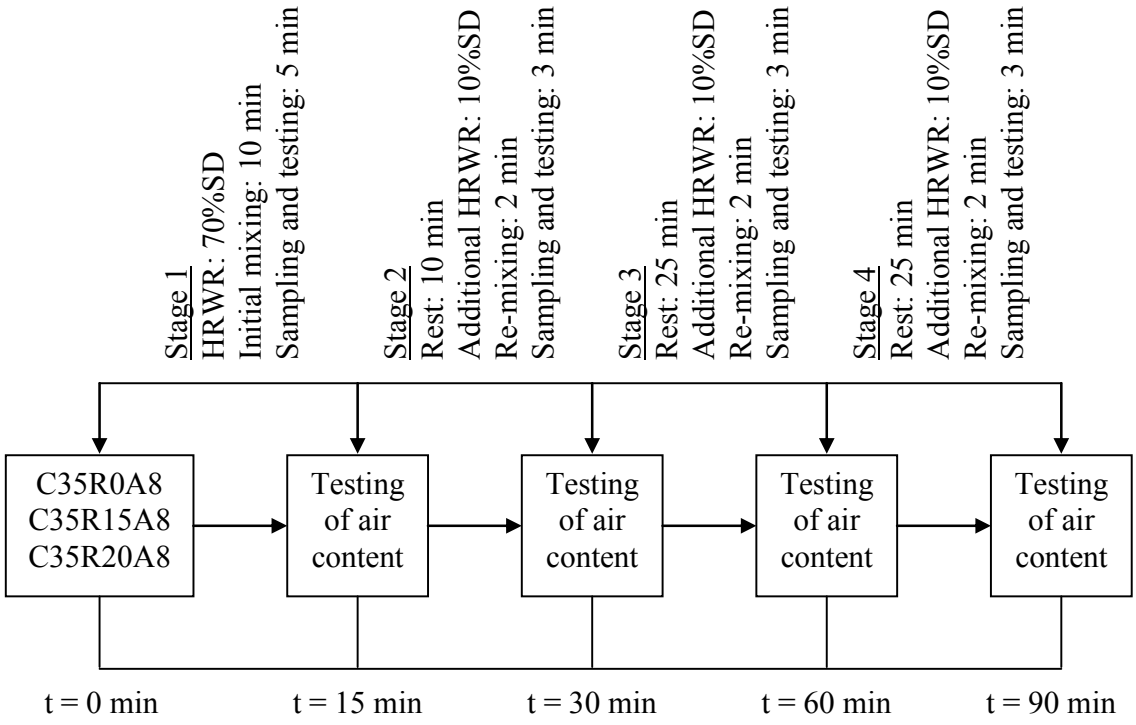

Figure 8.6: Details of air-void stability test

8.5.1 Slump and slump flow

The slump varied in the range of 260 to 280 mm, which is consistent with the slump values reported in the literature (Ferraris et al. 2000). However, the measured slump values did not exhibit any significant relative differences among the filling ability of the concretes, since the variation of the slump was marginal. The slump mainly depends on the yield stress of the concrete. When the yield stress is low, the slump becomes very high (Tanigawa and Mori 1989). The yield stress is greatly reduced in SCHPC due to the higher dosages of HRWR. The yield stress of SCHPC is less than 60 Pa (Bonen and Shah 2005), and typically ranges between 20 and 50 Pa (Cyr and Mouret 2003). For this low range of yield stress, the variation in the slump of SCHPC mixtures becomes insignificant, suggesting that slump is not a suitable criterion to assess the filling ability of SCHPC.

The slump flow of the concretes varied in the range of 600 to 770 mm, which indicates an excellent filling ability of SCHPC. Usually, the slump flow of SCHPC varies from 550 to 850 mm (EFNARC 2002, Khayat 2000, SCCEPG 2005). Unlike slump, the slump flow results exhibited the relative differences in the filling ability of the concretes with some variation in the flow spread. Hence, the slump flow is recommended instead of slump to assess the filling ability of SCHPC.

8.5.2 Orimet flow time and spread

The orimet flow time of different SCHPC mixtures varied in the range of 1.8 to 11.5 sec. The maximum acceptable limit for orimet flow time is 9 sec (Grünewald et al. 2004). The orimet flow time of several concretes with higher RHA content (greater than 15 to 20%) at lower W/B ratios was slightly above this maximum limit. Furthermore, the orimet flow spread varied from 615 to 800 mm for different concretes. The variation in the orimet flow spread followed a similar trend as observed for the slump flow of different concretes. It was also observed that the orimet flow spreads were greater than the slump flow values by 15 to 40 mm. Thus, it was understood that more kinetic energy was involved in the orimet flow spread of concrete. This is mainly due to a greater amount of concrete used in orimet test. In addition, the concrete dropped from a height of 430 mm, which is higher than the sample height (300 mm) used in slump flow test.

8.5.3 Inverted slump cone flow time and spread

The inverted slump cone flow time of different SCHPC mixtures varied in the range of 1.1 to 6.2 sec and the inverted slump cone flow spread ranged from 550 to 725 mm for different concretes. The variation in the inverted slump cone flow time followed a similar trend as observed for the orimet flow time of the concretes. In addition, the variation in the inverted slump cone flow spread followed a similar trend as observed for the slump flow and orimet flow spread of the concretes. It was also observed that the inverted slump cone flow spreads were lower than the slump flow values by 15 to 50 mm. It indicates that less kinetic energy was available in the inverted slump cone flow spread although the concrete quantity was the same and the falling height was greater than the sample height as used in the slump flow test. This suggests that some loss of energy occurred due to the resistance caused by the constricted end of the inverted slump cone and owing to the impact of concrete on the pan.

8.5.4 Effect of water-binder ratio and rice husk ash on flow time

The orimet and inverted slump cone flow times were influenced by the W/B ratio and RHA content of the concretes, as can be seen from Figure 8.7. The flow times increased with lower W/B ratio and greater RHA content, thus indicating an increase in the plastic viscosity of the concretes. The reasons are the same as discussed for the filling ability of the binder pastes (Chapter 5). The volume fraction and surface area of binder were increased with lower W/B ratio and higher RHA content, as can be seen from Table 8.2. The increased volume fraction and surface area of the binder increase the viscosity of concretes, and hence increase the flow time of concretes (Kim et al. 1997). However, the aggregate content of concretes was reduced and the paste volume was increased simultaneously with the lower W/B ratio and greater RHA content. The reduced aggregate content and the increased paste volume decrease the plastic viscosity of the concretes (Struble et al. 1998, EFNARC 2002). Based on the data given in Table 8.2, it was understood that the proportional reduction in aggregate content and increase in paste volume were not as significant as the proportional increases in volume fraction and surface area of binder. Therefore, the net effect was to increase the plastic viscosity of concrete as indicated from the flow time results of the orimet and inverted slump cone flow tests. Nevertheless, the viscosity remained low enough to sustain uninterrupted concrete flow during the orimet and inverted slump cone flow tests.

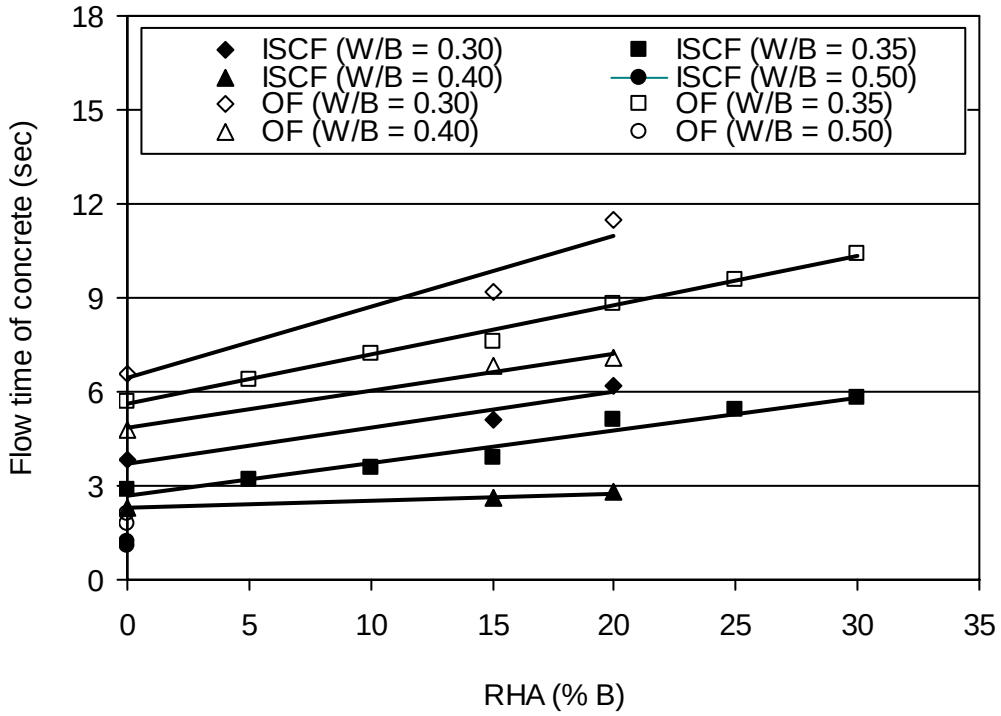

Figure 8.7: Effect of W/B ratio and RHA content on the orimet and inverted slump cone flow times of concrete

8.5.5 Effect of water-binder ratio and rice husk ash on slump and flow spreads

The slump flow, orimet flow spread, and inverted slump cone flow spread increased considerably with lower W/B ratio and higher RHA content, as can be seen from Figures 8.8 to 8.10. This is attributed to the increased paste volume and decreased aggregate content of concrete. The paste volume of the concretes was increased with lower W/B ratio and higher RHA content, as can be seen from Table 8.2. In addition, the aggregate content was decreased at lower W/B ratio and higher RHA content, as evident from Tables 7.3, 7.5 (Chapter 7) and 8.2. The slump flow increases with increased paste volume and decreased aggregate content of the concrete (Bonen and Shah 2005, Yen et al. 1999). A similar effect is expected for orimet and inverted slump cone flow spreads. The increased paste volume and decreased aggregate content enhance the deformability of the concrete, as the collision between aggregates is greatly reduced with higher inter-particle distance. However, the increased paste volume at lower W/B ratio and higher RHA content did not produce any significant influence on the slump of the concretes, as can be seen from Figure 8.11. This is

because the relationship between slump and yield stress becomes less dependent on the paste volume in highly workable concretes such as SCHPC (Wallevik 2006).

Table 8.2: Variations of volume fractions of aggregates, binder, RHA and paste, and surface area of the binder for different SCHPCs

Concrete	Volume fraction of aggregates (m^3/m^3)	Volume fraction of RHA (m^3/m^3)	Volume fraction of binder (m^3/m^3)	Surface area of binder ($\times 10^3$ m^2/m^3)	Volume fraction of paste* (m^3/m^3)
C30R0A6	0.635	0	0.156	202.78	0.365
C30R15A6	0.622	0.036	0.169	344.06	0.378
C30R20A6	0.615	0.047	0.172	388.92	0.385
C35R0A6	0.661	0	0.135	174.72	0.339
C35R0A4	0.674	0	0.133	172.99	0.326
C35R0A8	0.635	0	0.134	173.34	0.365
C35R5A6	0.655	0.010	0.138	214.70	0.345
C35R10A6	0.654	0.021	0.142	256.00	0.346
C35R15A6	0.650	0.031	0.145	296.15	0.351
C35R15A4	0.662	0.031	0.144	292.94	0.338
C35R15A8	0.624	0.031	0.144	293.41	0.376
C35R20A6	0.646	0.041	0.149	336.74	0.354
C35R20A4	0.657	0.041	0.147	332.43	0.343
C35R20A8	0.616	0.041	0.146	331.44	0.384
C35R25A6	0.637	0.051	0.151	374.48	0.363
C35R30A6	0.636	0.061	0.155	415.78	0.364
C40R0A6	0.673	0	0.117	151.76	0.328
C40R15A6	0.668	0.027	0.127	259.45	0.332
C40R20A6	0.664	0.036	0.130	294.52	0.336
C50R0A6	0.702	0	0.095	123.10	0.298
C50R0A2	0.706	0	0.106	138.00	0.294

* Includes the measured air content

8.5.6 Effect of high-range water reducer on filling ability

The liquefying and dispersion actions and the resulting water reduction capacity of HRWR contributed to improve the filling ability of concretes. The adequate dosage of HRWR improved the deformability of concrete and thus resulted in high slump and slump flow, and good orimet flow and inverted slump cone flow spreads. In addition, the adequate dosage of HRWR contributed to achieve an optimum viscosity, and therefore an uninterrupted concrete flow with lower flow time was maintained.

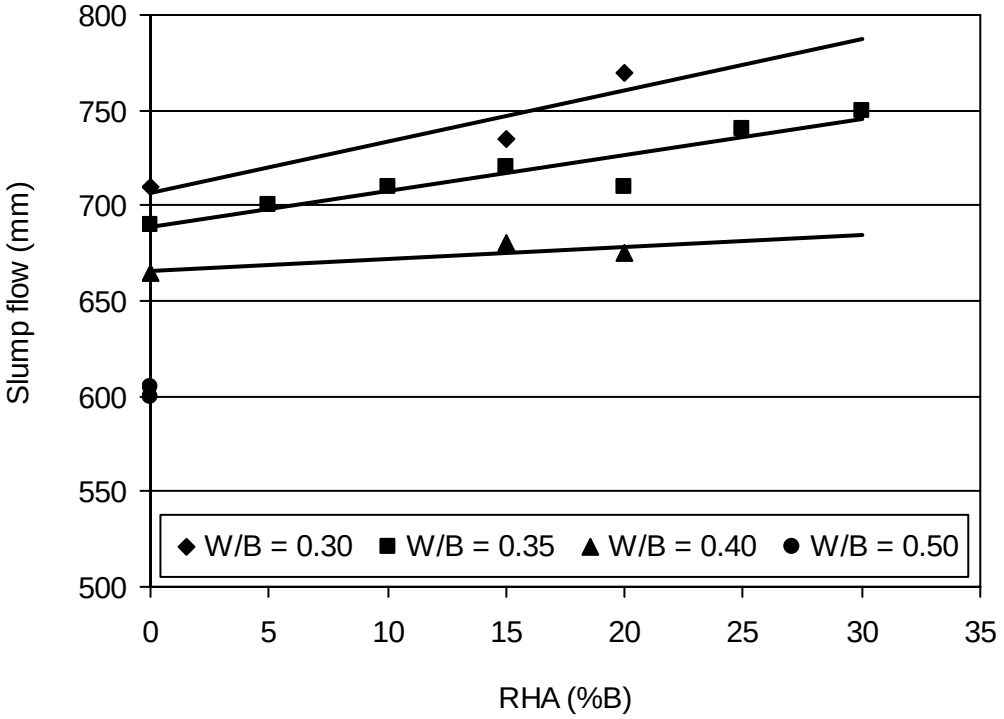

Figure 8.8: Effect of W/B ratio and RHA content on the slump flow of concretes

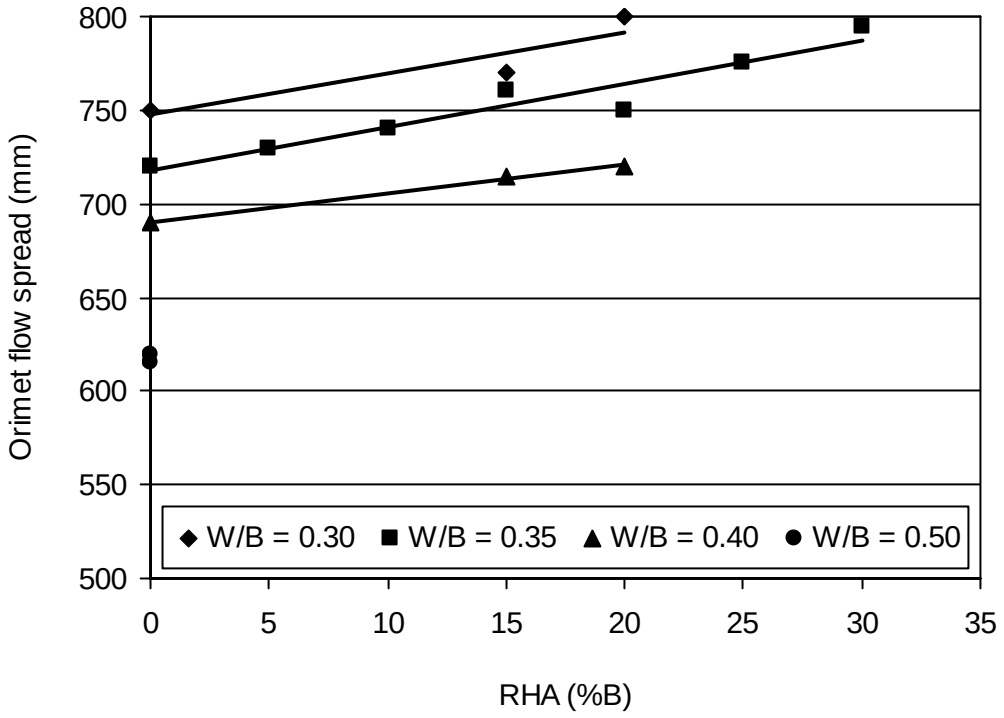

Figure 8.9: Effect of W/B ratio and RHA content on the orimet flow spread of concretes

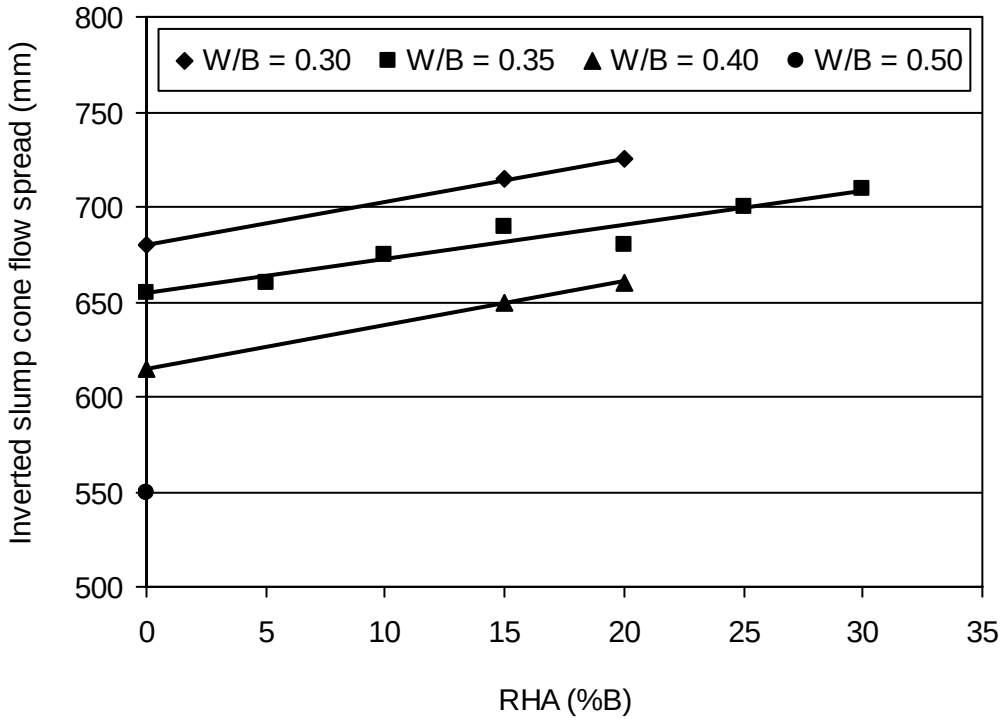

Figure 8.10: Effect of W/B ratio and RHA content on the inverted slump cone flow spread of concretes

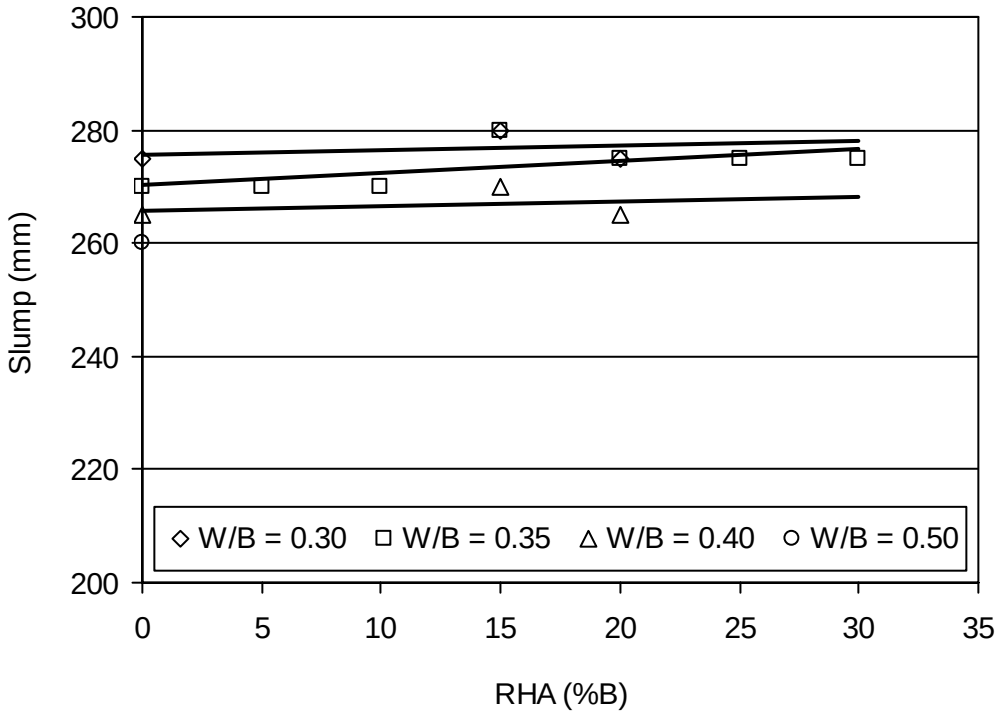

Figure 8.11: Effect of W/B ratio and RHA content on the slump of concretes

8.5.7 Effect of air-entraining admixture on filling ability

The AEA induced microscopic air-bubbles which acted like ball-bearing to increase the filling ability of concretes. Therefore, the use of AEA decreased the water demand of concrete for a given filling ability. This is obvious from the mixture proportions of C50R0A2 and C50R0A2 given in Tables 7.3 and 7.5 (Chapter 7). Despite the lower water and binder contents, the filling ability properties of C50R0A6 were similar to those of C50R0A2 due to the presence of AEA.

8.6 Correlations for Different Filling Ability Properties

The correlations for the flow times of pastes and concretes, and the flow spread of mortars and slump flow of concretes were determined. The correlations for the orimet and inverted slump cone flow times, slump flow and orimet flow spread, slump flow and inverted slump cone flow spread, and orimet and inverted slump cone flow spread of the concretes were also determined.

8.6.1 Flow times of pastes and concretes

The inverted slump cone and orimet flow times of the concretes were plotted versus the paste flow time. The flow time of the concretes was strongly correlated with the flow time of the pastes, as can be seen from Figure 8.12. In both cases, the relationship was linear. The coefficient of determination (R^2) reveals that at least 88 to 96% of the flow time data were accounted for in the linear relationship. The correlation coefficient (R) for concrete orimet flow time and paste flow time was 0.939, while the correlation coefficient for concrete inverted slump cone flow time and paste flow time was 0.979. The excellent correlations were obtained since the changes in viscosity due to various W/B ratios and RHA contents followed similar trends in pastes and concretes. Also, the flow times of concrete and paste are highly dependent of the paste viscosity (Kim et al. 1997, Schwartzentruber et al. 2006).

8.6.2 Flow spread of mortars and slump flow of concretes

The slump flow of concretes was plotted versus the flow spread of mortars to determine the correlation. A good correlation with a linear relationship between the slump flow of concrete and the flow spread of mortar was obtained in the absence of RHA, as can be seen from

Figure 8.13. The coefficient of determination was 0.953 and the correlation coefficient was 0.976. The good correlation was obtained because both mortar flow spread and concrete slump flow were increased similarly without RHA at lower W/B ratio. In contrast, a poor correlation was observed between mortar flow spread and concrete slump flow when both mortars and concretes contained the RHA. This is because the mortar flow spread was decreased but the concrete slump flow was increased in the presence of RHA. The opposite behavior of RHA in mortars and concretes is possibly related to the volume fraction and surface area of the binder. The volume fraction and surface area of the binder were significantly greater in mortars as compared to concretes, as can be seen from Table 6.4 (Chapter 6) and Table 8.2. Increased surface area and volume fraction of binder significantly increase the yield stress and plastic viscosity of mortars (Banfill 1994, Westerholm 2006), and thus may decrease the mortar flow spread despite the increased paste volume. In addition, the mortars did not contain any entrained air content, while the concretes containing RHA had an air content in the range of 4.2 to 8.6%, which can reduce the required water content by 10 to 12% (Kosmatka et al. 2002). Hence, the air content improved the filling ability of the concretes for a given water content, and resulted in greater slump flow.

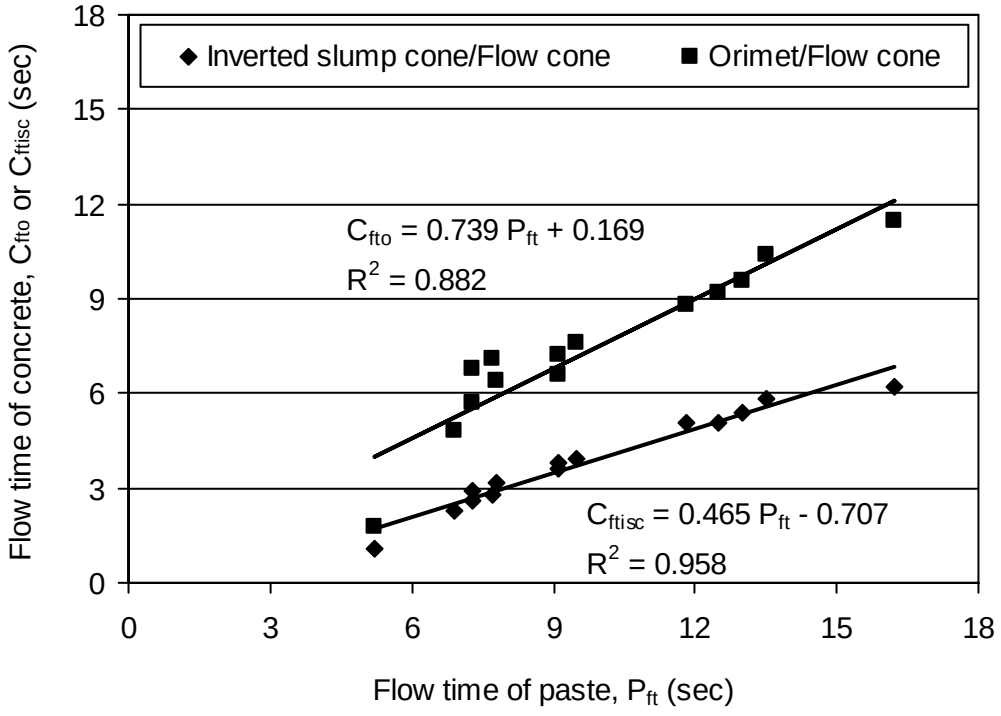

Figure 8.12: Correlation between flow times of pastes and concretes

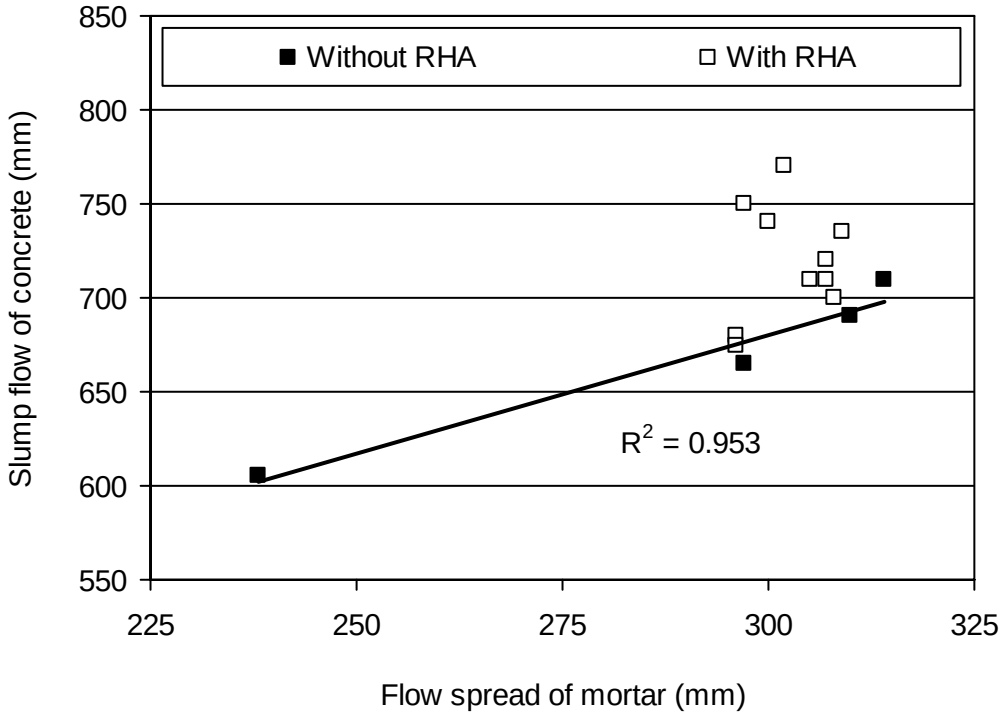

Figure 8.13: Correlation between mortar flow spread and concrete slump flow

8.6.3 Orimet and inverted slump cone flow times

The orimet and inverted slump cone flow times were well-correlated with a linear relationship, as can be seen from Figure 8.14. The coefficient of determination was 0.918 and the correlation coefficient was 0.958. The good correlation was obtained because both orimet and inverted slump cone flow time varied similarly with the W/B ratio and RHA content. In addition, both orimet and inverted slump cone flow time were similarly related to the plastic viscosity of the paste component of concrete.

8.6.4 Inverted slump cone flow spread and slump flow

The slump flow and inverted slump cone flow spread of the concretes were well-correlated with a linear relationship, as can be seen from Figure 8.15. This is because both inverted slump cone flow spread and slump flow varied similarly with the W/B ratio and RHA content of concrete. The coefficient of determination was 0.946 and the correlation coefficient was 0.973. The strong correlation also indicated that both inverted slump cone flow spread and slump flow were similarly related to the yield stress of concrete.

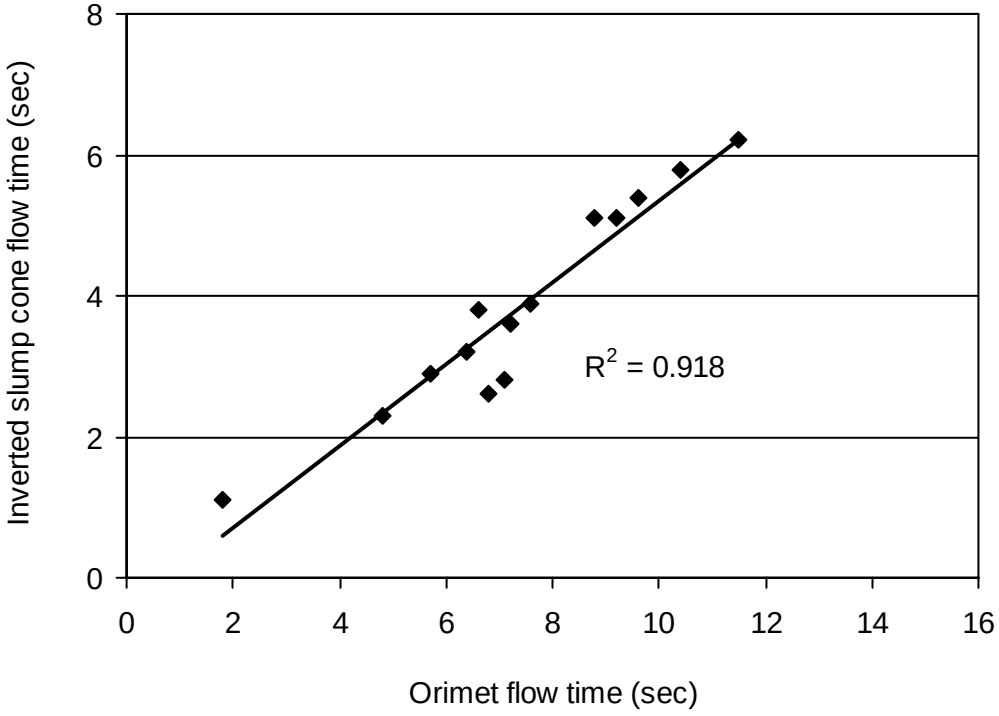

Figure 8.14: Correlation between orimet and inverted slump cone flow times

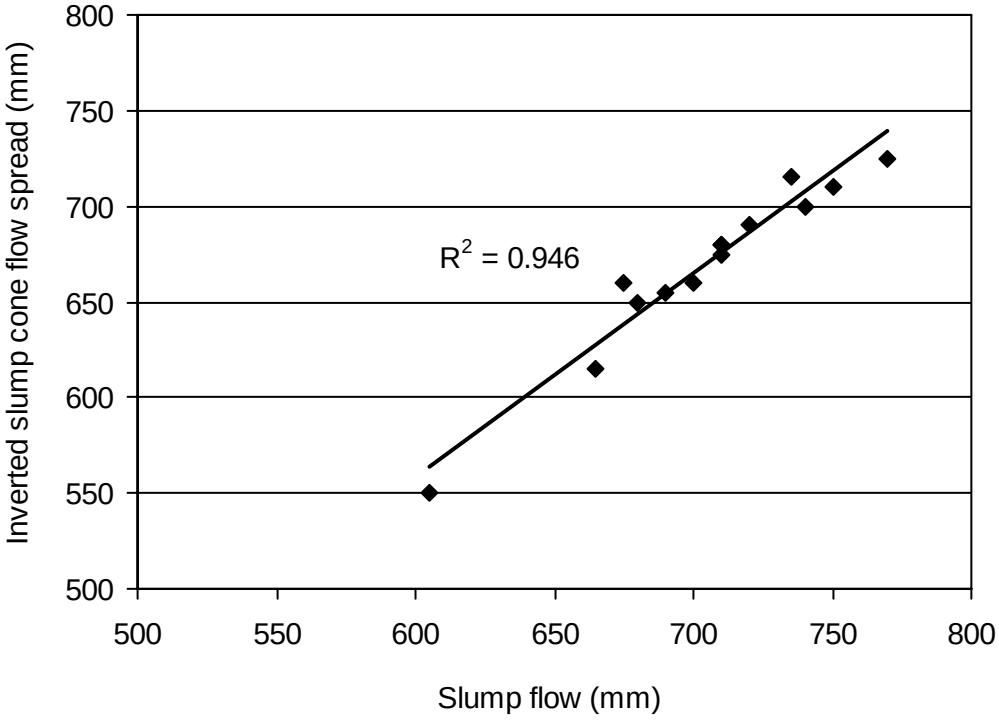

Figure 8.15: Correlation between inverted slump cone flow spread and slump flow

8.6.5 Orimet flow spread and slump flow

The slump flow and inverted slump cone flow spread of the concretes were well-correlated with a linear relationship, as can be seen from Figure 8.16. The coefficient of determination was 0.979 and the correlation coefficient was 0.989. The excellent correlation was due to similar trend of variation of orimet flow spread and slump flow with the W/B ratio and RHA content of concrete. It was also understood from the relationship that both orimet flow spread and slump flow were similarly related to the yield stress of concrete.

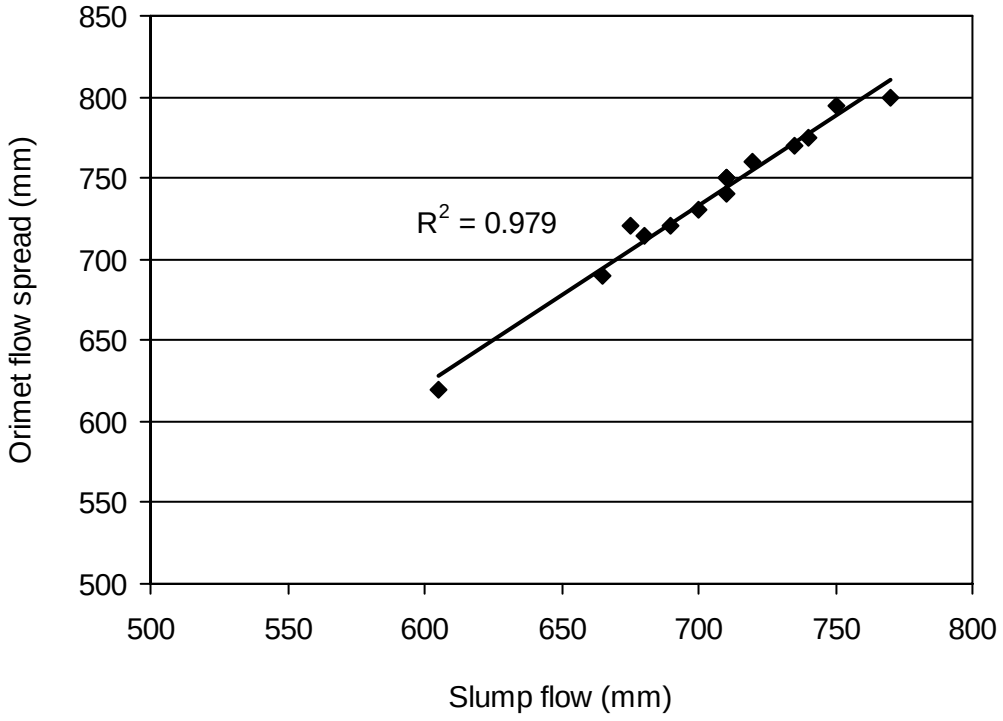

Figure 8.16: Correlation between orimet flow spread and slump flow

8.6.6 Orimet and inverted slump cone flow spreads

The orimet and inverted slump cone flow spreads of the concretes were well-correlated. The best-fit curve was a straight line, as can be seen from Figure 8.17. The coefficient of determination and the correlation coefficient was 0.975 and 0.987, respectively. The strong correlation is attributed to similar trend of variation of inverted slump cone and orimet flow spreads with the W/B ratio and RHA content of concrete. Also, both inverted slump cone and orimet flow spreads were similarly related to the slump flow, which is highly dependent of the yield stress of concrete (Murata 1984, Saak et al. 2004).

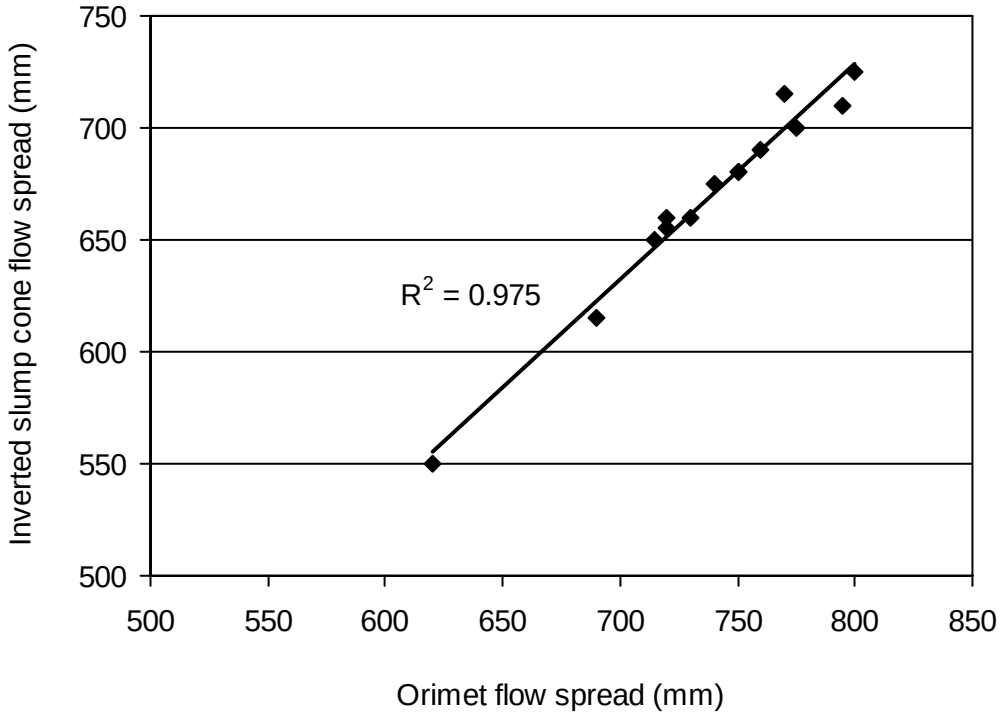

Figure 8.17: Correlation between orimet and inverted slump cone flow spreads

8.7 Performance Criteria for Inverted Slump Cone Flow

The performance criteria for the inverted slump cone flow time and spread can be determined based on the known criteria for orimet flow time and slump flow. The acceptable range of the flow time of SCHPC measured by the orimet having an orifice with 80 mm outlet diameter is 2.5 to 9 sec (Grünewald et al. 2004). Using this orimet flow time range, the performance criterion for the inverted slump cone flow time was determined based on the correlation between inverted slump cone and orimet flow times. For 2.5 to 9 sec orimet flow time, the corresponding inverted slump cone flow time was 1 to 4.8 sec. Thus, the performance criterion for the inverted slump cone flow time can be set at 1 to 5 sec.

The slump flow of SCHPC generally varies in the range of 550 to 850 mm (EFNARC 2002, Khayat 2000, SCCEPG 2005). Using this slump flow range, the performance criteria for the inverted slump cone flow spread was determined based on the correlation between inverted slump cone flow spread and slump flow. For 550 to 850 mm slump flow, the corresponding inverted slump cone flow spread was 505 to 824 mm. Thus, the performance criterion for the inverted slump cone flow spread can be set at 500 to 825 mm.

8.8 Advantages of Inverted Slump Cone Apparatus

The inverted slump cone apparatus will be useful to measure the filling ability of SCHPC. In addition, it can be used with the J-ring to measure both filling ability and passing ability of concrete simultaneously. It might also qualitatively indicate the segregation resistance of concrete whether it is used alone or with J-ring. Thus a single test apparatus will provide information on three key properties of SCHPC. The inadequacy of filling ability, passing ability and segregation resistance will be detected during concrete flow.

The inverted slump cone apparatus would provide several benefits over some of the existing methods. For example, the standard slump and slump flow test does not provide any information on the viscosity unless the slumping or slump flow time is measured. The inverted slump cone apparatus can be used to obtain information on both yield stress and plastic viscosity from the same test. The flow time relates the viscosity where as the flow spread indicates the yield stress of concrete. Moreover, it has the advantage of being a dynamic test and thus reflects the concrete placement in practice. In comparison with other apparatus such as slump cone and orimet, the inverted slump cone ideally does not require two operators. It can be easily handled by a single operator. In addition, it requires about 27% less concrete than the orimet and thus saves both concrete quantity and operation time. The whole test takes about 2 to 3 minutes to conduct. Because of simplicity, it can be used comfortably and quickly in laboratory and field.

The construction of inverted slump cone apparatus is not difficult as compared to other apparatus such as U-box. The construction cost is also minimal since it uses Abram's slump cone, which is not expensive. The cone used in inverted slump cone apparatus can be separated easily. Therefore, the same cone can also be used to conduct the slump and slump flow test.

8.9 Model for Filling Ability of Concretes

An empirical model has been developed for the filling ability of SCHPC based on the slump flow and paste volume of the concretes. In a slump flow test, the deformation of the fresh concrete is mainly caused by gravity. The deformation continues until the equilibrium is established and the fresh concrete achieves it final slump flow spread. In equilibrium, the

applied shear stress is equal to the yield stress. Based on the force balance approach given by Murata (1984), the yield stress (τ_y) of the concrete can be calculated as follows:

$$\tau_y = \frac{\rho g V}{2\pi\left(S_f / 2\right)^2} = \alpha \frac{\rho}{S_f^2} \qquad \text{(Equation 8.1)}$$

where:

ρ is the density or unit weight of concrete (kg/m^3), g is the gravitational acceleration (9.806 m/s^2), V is the volume of fresh concrete that equals the volume of slump cone (0.0055 m^3), S_f is the slump flow (diameter of spread) of concrete (m), and α is a constant that substitutes ($2gV/\pi$).

Equation 8.1 is based on the assumption that the concrete behaves as an incompressible material and no flow exists between the layers of concrete. It is obvious from Equation 8.1 that the second power of the slump flow is inversely proportional to the yield stress of concrete. The yield stress is a major rheological parameter of concrete. Tomas (1961) performed a comprehensive experimental investigation on the non-Newtonian laminar-flow properties of flocculated suspension and reported a relationship for the yield stress. Based on a wide range of data fitted satisfactorily with the Bingham plastic model, he concluded that the yield stress is directly proportional to the cube of the volume fraction of solids (S_v) for any given suspension. That is,

$$\tau_y \propto S_v^3 \qquad \text{(Equation 8.2)}$$

The SCHPC mixture can be considered as a flocculated suspension (coarse and fine aggregates suspended in a matrix of binder paste). In addition, it is well-known that the SCHPC mixture behaves like a Bingham (non-Newtonian) fluid. Hence, the following relationship can be assumed for SCHPC:

$$\tau_y \propto S_v^n \qquad \text{(Equation 8.3)}$$

where:

n is an empirical constant and S_v is the volume fraction of coarse and fine aggregates (concrete stone and sand). Assuming the air-voids and HRWR dosage as a part of the binder paste, for 1 m^3 of concrete, S_v can be expressed in the following form with respect to the paste volume of concrete (V_p).

$$S_v = 1 - V_p \qquad \text{(Equation 8.4)}$$

Now from Equations 8.1, 8.3 and 8.4, the following relationship can be obtained for the slump flow and paste volume of concrete.

$$\frac{\rho}{S_f^2} = \beta(1 - V_p)^n \qquad \text{(Equation 8.5)}$$

where:

β is an empirical constant. Both β and n were determined based on the experimental results obtained from the slump flow test of various concretes. In order to determine β and n, Equation 8.5 was reformed as follows:

$$\ln\frac{\rho}{S_f^2} = \ln\{\beta(1 - V_p)^n\} = n\ln(1 - V_p) + \ln\beta \qquad \text{(Equation 8.6)}$$

The paste volume was computed based on the proportions of cement and water, the dosages of HRWR and the air content or volume of air-voids in concrete. The logarithmic data of ρ/S_f^2 were plotted versus the logarithmic ($1-V_p$) data for various concretes. The best-fit plot was a straight line, as can be seen from Figure 8.18.

The value of n was determined as the slope of the straight line whereas the value of β was found based on the intercept of the $y = \ln(\rho/S_f^2)$ axis. The values of β and n obtained were 15873, and 2.84, respectively. Thus, Equation 8.5 can be expressed in the following form:

$$\frac{\rho}{S_f^2} = 15873(1 - V_p)^{2.84} \qquad \text{(Equation 8.7)}$$

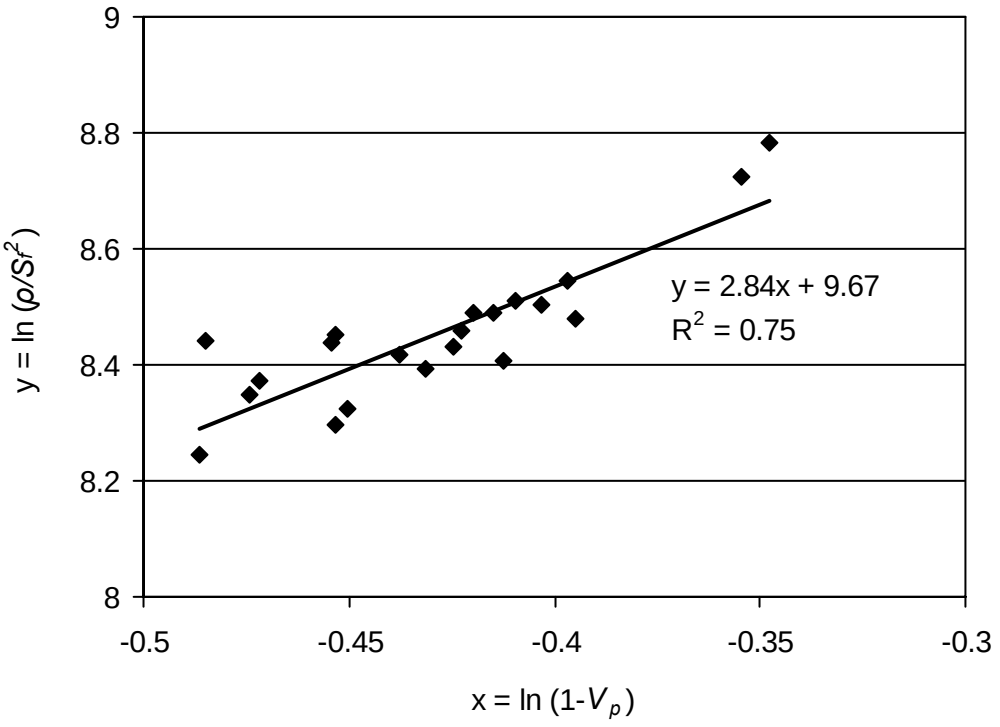

Figure 8.18: Relationship between (ρ/S_f^2) and ($1-V_p$) for various concrete mixtures

Equation 8.7 can be modified by replacing ρ by the relative density (ρ_r) of fresh concrete ($\rho_r = \rho/\rho_w$, where ρ_w is the density of water at 24^0C, 997.28 kg/m^3). Hence, the following equation can be obtained.

$$\frac{\rho_r}{S_f^2} = 15.92(1 - V_p)^{2.84} \qquad \text{(Equation 8.8)}$$

where:

ρ_r = Relative density of concrete

S_f = Slump flow of concrete (m)

V_p = Paste volume of concrete (m^3/m^3)

8.9.1 Validity of the model

The filling ability model (Equation 8.8) is applicable for SCHPC mixtures possessing a paste volume in the range of 0.29 to 0.39 m^3/m^3. The paste volume of SCHPC typically ranges from 0.28 to 0.40 m^3/m^3 (ACI Committee 211H, 2006; Koehler and Fowler 2006, SCCEPG 2005). In addition, this model is valid for both air-entrained and non-air-entrained SCHPC with and without RHA. The model was derived based on the slump flow varying from 600 to 800 mm in the absence of any VEA. The slump flow in such range was achieved by using 70 to 80% of the saturation dosages of a polycarboxylate-based HRWR. However, the model can be used for the slump flow range of 550 to 850 mm, which is common for SCHPC (SCCEPG 2005).

The suitability, type and proportions of the constituent materials, particularly the type and dosage of HRWR and the binder-HRWR compatibility may affect the generalization of the model. The dosage of HRWR could influence the slump flow significantly without any considerable change in the paste volume. Similarly, the incompatibility of HRWR with the binder may reduce the slump flow without any change in the paste volume of concrete. Nevertheless, the model was used to calculate the slump flow of various SCHPC mixtures produced in the present study. In addition, the model was applied for a number of SCHPC mixtures selected from the literature. The paste volume of these concretes ranged from 0.30 to 0.40 m^3/m^3. Some of these concretes contained ground granulated blast-furnace slag and/or different types fly ash. The slump flows of these concretes were computed using the model. The computed slump flows were compared with the measured values as shown in Figure 8.19. The computed and measured slump flows of the concretes were within ±7.6% error. The best-fit line for the measured and computed slump flows had a coefficient of determination of 0.741 (correlation coefficient: 0.861) indicating that at least 74% of the measured slump values were accounted for with the derived model.

8.9.2 Application of the model

The filling ability model (Equation 8.8) will be helpful to determine the paste volume needed for a given slump flow of concrete, and thus to facilitate the mixture design of SCHPC. This is because the water and binder contents of a concrete mixture can be determined for a chosen W/B ratio if the paste volume is known. Also, the water content for a given binder

content or the binder content for a given water content can be found based on the paste volume of concrete. In addition, the filling ability model would be useful to assess the passing ability of SCHPC because the passing ability is well-correlated with the filling ability of concrete, as discussed in Section 8.12.

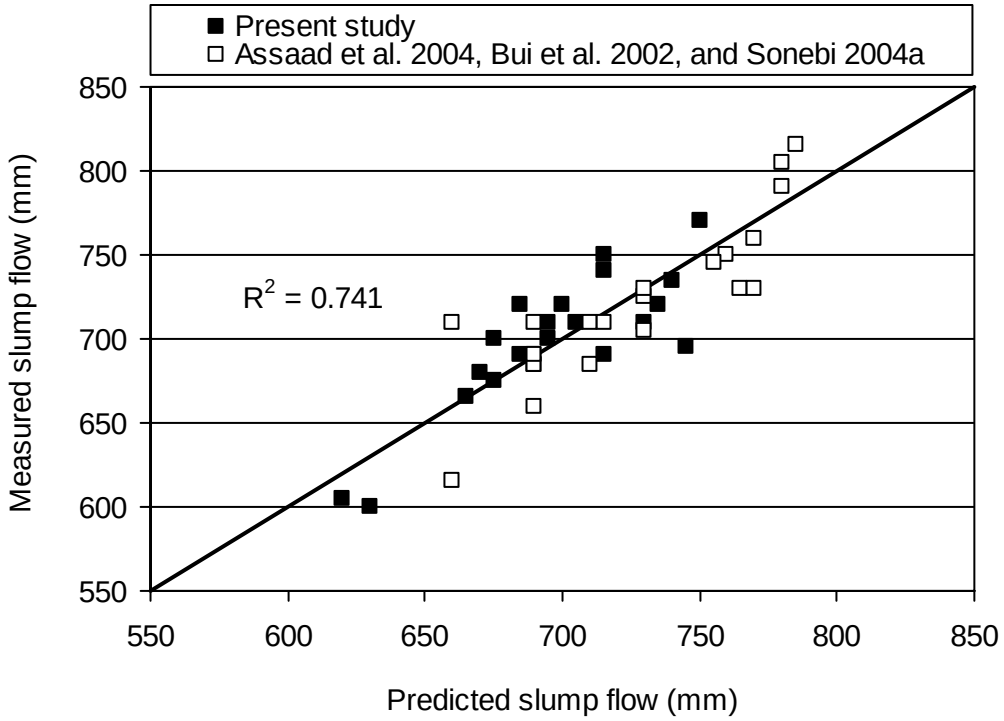

Figure 8.19: Comparison between computed and measured slump flows of various SCHPCs

8.10 Passing Ability of Concretes

The passing ability results of various SCHPC mixtures were obtained with respect to slump and slump flow with J-ring, orimet – J-ring flow, and inverted slump cone – J-ring flow. They are presented and discussed below.

8.10.1 Slump and slump flow with J-ring

The slump with J-ring varied in the range of 250 to 270 mm for various concretes, as can be seen from Figure 8.20. Similar to the slump, the slump with J-ring also varied in a narrow range indicating its unsuitability for measuring the passing ability of SCHPC. The reason is the same as discussed in case of slump. Unlike the slump with J-ring, the slump flow with J-ring varied in a wide range of 575 to 740 mm, as can be seen from Figure 8.21. The

minimum slump flow with J-ring was observed for the SCHPCs with 0.50 W/B ratio and without any RHA. But the highest slump flow with J-ring was attained for the SCHPC with 0.30 W/B ratio and 20% RHA. The trend was similar as observed in case of slump flow. However, the slump flow was reduced by 15 to 30 mm. The maximum reduction in slump flow in the presence of J-ring should not greater than 50 mm to maintain good passing ability (Brameshuber and Uebachs 2001). The slump flow with J-ring was about 96 to 98% of the slump flow without J-ring. Thus, the slump flow results in the presence of J-ring exhibited a good passing ability of the concretes.

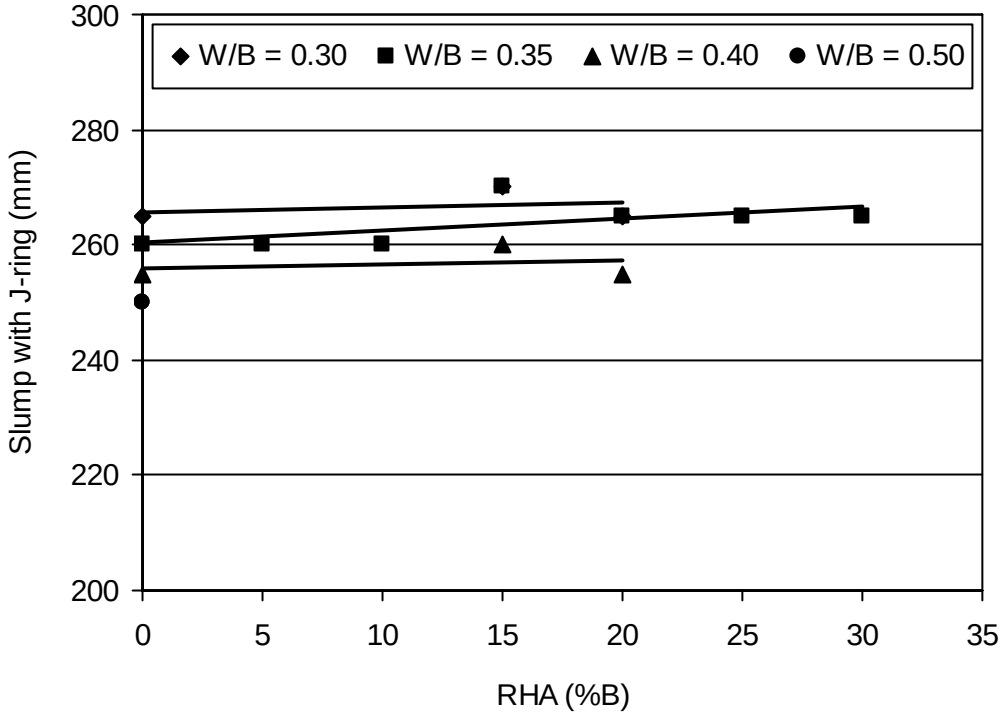

Figure 8.20: Effect of W/B ratio and RHA content on the slump with J-ring for various concretes

8.10.2 Orimet – J-ring flow

The orimet – J-ring flow (orimet flow spread in presence of J-ring) varied from 590 to 775 mm, as can be seen from Figure 8.22. The variation in orimet – J-ring flow followed a trend similar to that observed in orimet flow spread. However, the presence of J-ring decreased the orimet flow spread by 15 to 40 mm. Similar to the slump flow with J-ring, the lowest orimet – J-ring flow was observed for the SCHPC mixtures with 0.50 W/B ratio and without any

RHA. The highest orimet – J-ring flow was obtained for the SCHPC with 0.30 W/B ratio and 20% RHA. In general, the orimet – J-ring flow was 94 to 98% of the orimet flow spread, and thus indicated a good passing ability of the concretes.

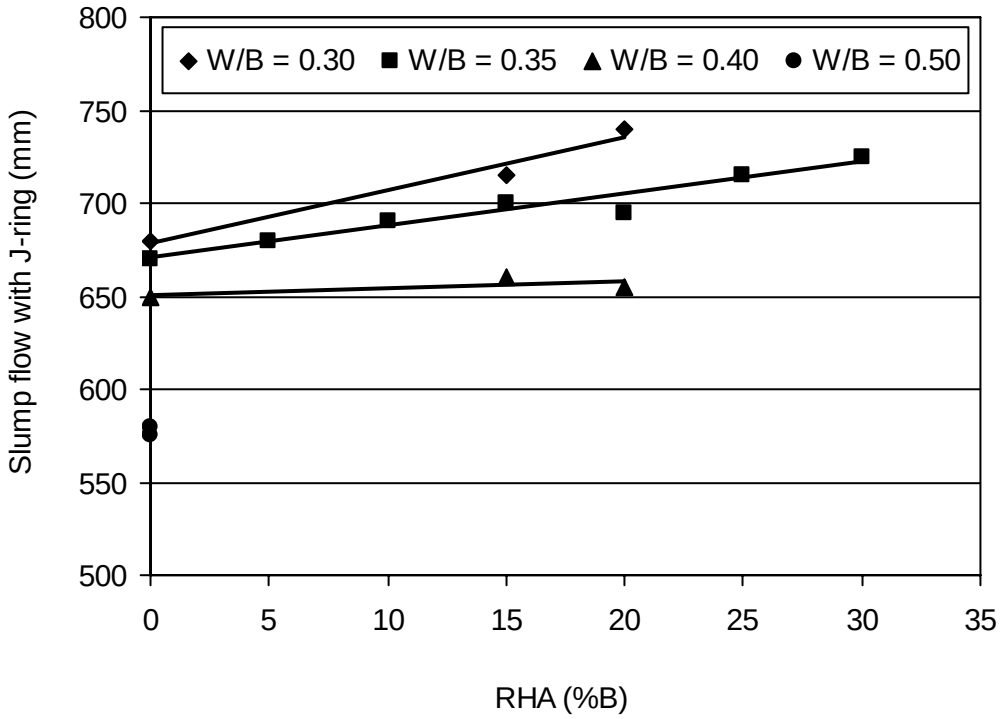

Figure 8.21: Effect of W/B ratio and RHA content on the slump flow with J-ring for various concretes

8.10.3 Inverted slump cone – J-ring flow

The inverted slump cone – J-ring flow of various SCHPC mixtures ranged from 525 to 710 mm, as can be seen from Figure 8.23. Similar to the slump flow with J-ring and orimet – J-ring flow, the lowest inverted slump cone – J-ring flow was obtained for the SCHPCs with 0.50 W/B ratio and no RHA whereas the highest inverted slump cone – J-ring flow was achieved for SCHPC mixture with 0.30 W/B ratio and 20% RHA. Moreover, the trend of variation in the inverted slump cone – J-ring flow was similar to that of inverted slump cone flow spread. But the spread of the concretes was reduced in the presence of J-ring. The difference between the inverted slump cone – J-ring flow and inverted slump cone flow spread was about 15 to 30 mm. However, the inverted slump cone – J-ring flow was about 95 to 98% of the inverted slump cone flow spread, and thus exhibited a good passing ability of the concretes.

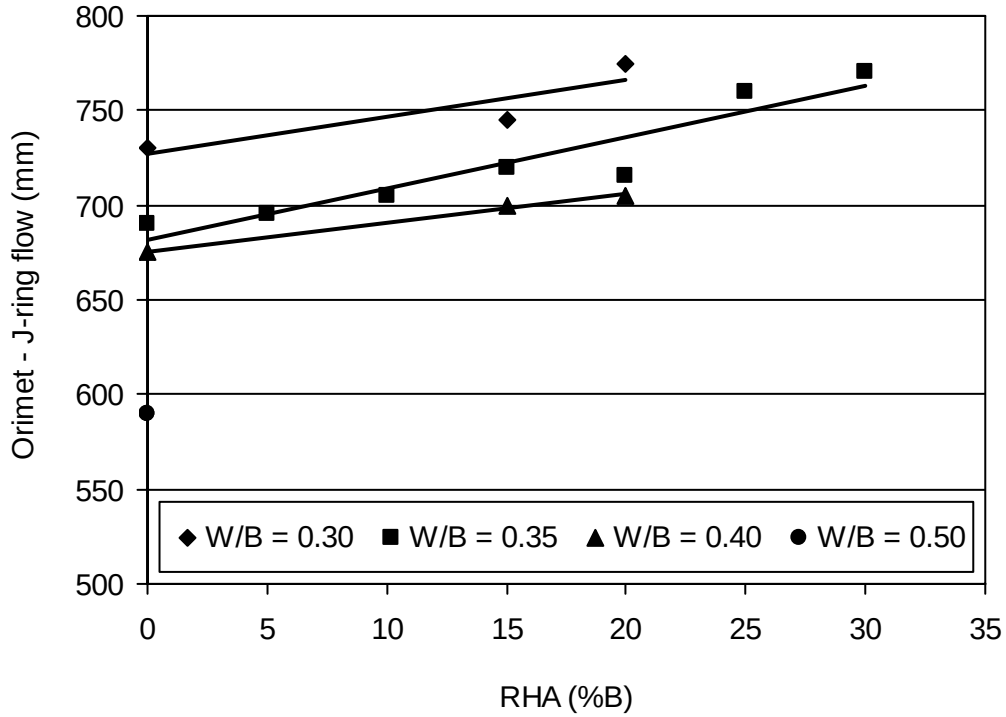

Figure 8.22: Effect of W/B ratio and RHA content on the orimet – J-ring flow of various concretes

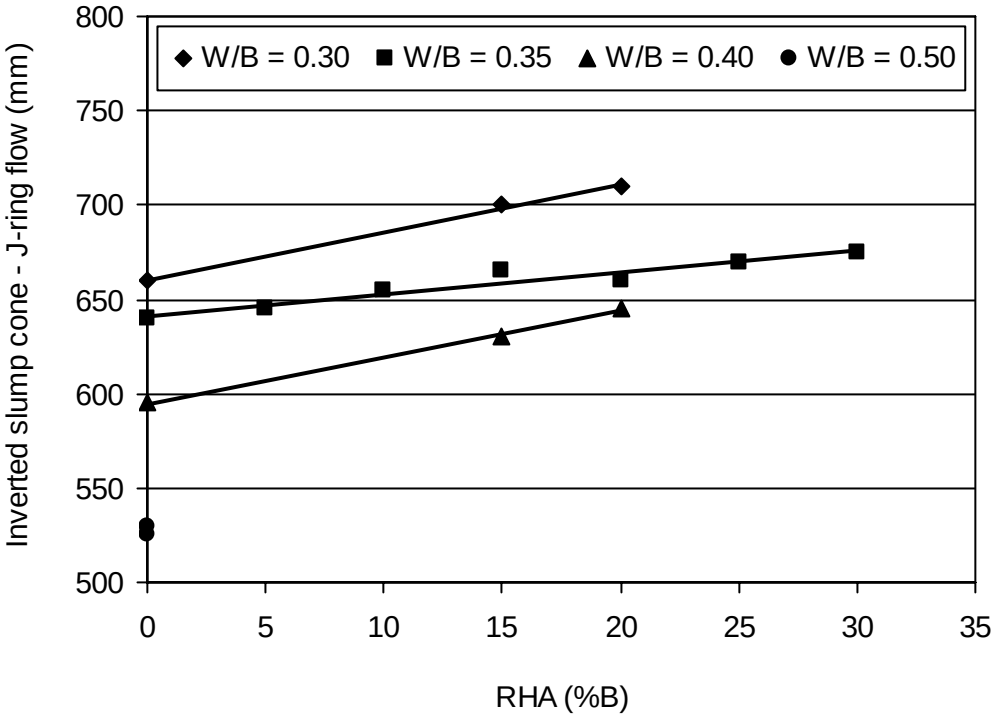

Figure 8.23: Effect of W/B ratio and RHA content on the inverted slump cone – J-ring flow of various concretes

8.10.4 Effect of water-binder ratio and rice husk ash on passing ability

The slump and slump flow with J-ring, orimet – J-ring flow, and inverted slump cone – J-ring flow were affected by the W/B ratio and RHA content of the concretes. The slump and slump flow with J-ring, orimet – J-ring flow, and inverted slump cone – J-ring flow increased with lower W/B ratio and greater RHA content, as evident from Figures 8.20 to 8.23. This is due to increased paste volume and decreased aggregate content as discussed in case of the filling ability properties of the concretes with respect to flow spreads (Section 8.5.5). However, the effects of W/B ratio and RHA content on the slump with J-ring were marginal, as evident from Figure 8.20. A similar trend was observed for the slump without J-ring.

8.10.5 Effect of high-range water reducer on passing ability

The HRWR influenced the passing ability of concretes by influencing filling ability. The adequate dosage of HRWR improved the filling ability, and thus maintained a good passing ability for the concretes. Therefore, a significant amount of concrete passed though the J-ring in all cases, as discussed before.

8.10.6 Effect of air-entraining admixture on passing ability

The AEA improved the passing ability of concrete in a similar way as it did in case of filling ability (Section 8.5.7). The effect of AEA is evident from the passing ability properties of C50R0A2 and C50R0A6. Despite lower water and binder contents, the passing ability properties of C50R0A6 were similar to those of C50R0A2 due to the presence of AEA.

8.11 Correlations for Different Passing Ability Properties

The correlations for slump flow with J-ring and orimet – J-ring flow, slump flow with J-ring and inverted slump cone – J-ring flow, and orimet – J-ring flow and inverted slump cone – J-ring flow are expressed in Figures 8.24 to 8.26.

8.11.1 Slump flow with J-ring and orimet – J-ring flow

The orimet – J-ring flow and slump flow with J-ring were well-correlated with a linear relationship, as be seen from Figure 8.24. The coefficient of determination was 0.921, and the correlation coefficient was 0.960. The strong correlation is due to similar trends of

variation of orimet – J-ring flow and slump flow with J-ring with the W/B ratio and RHA content. Also, the presence of J-ring produced similar effects to reduce the spread of concrete during slump cone – J-ring and orimet – J-ring tests.

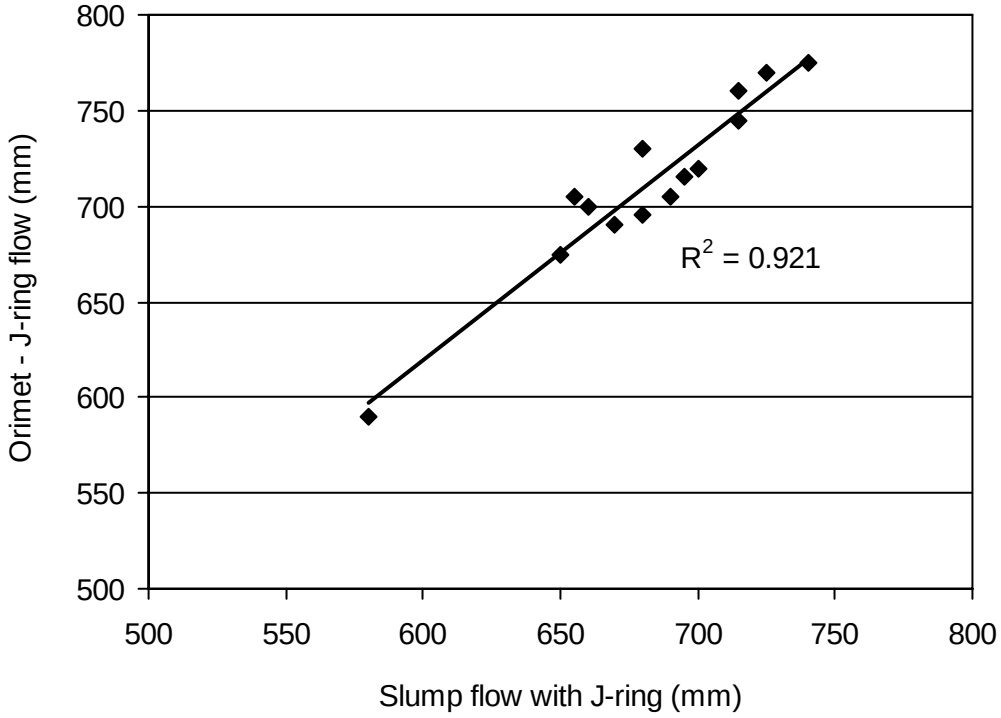

Figure 8.24: Correlation between orimet – J-ring flow and slump flow with J-ring for various concretes

8.11.2 Inverted slump cone – J-ring flow and slump flow with J-ring

The inverted slump cone – J-ring flow and slump flow with J-ring were well-correlated with a linear relationship, as can be seen from Figure 8.25. The best-fit line had a coefficient of determination of 0.914 and a correlation coefficient of 0.956. The strong correlation was obtained because both inverted slump cone – J-ring flow and slump flow with J-ring varied similarly with the W/B ratio and RHA content of concrete. In addition, the presence of J-ring produced similar effects for the reduction in the spread of concretes during slump cone – J-ring and inverted slump cone – J-ring tests.

8.11.3 Inverted slump cone – J-ring flow and orimet – J-ring flow

The inverted slump cone – J-ring flow and orimet – J-ring flow showed a good correlation with a linear relationship, as obvious from Figure 8.26. The coefficient of determination was

0.892 and the correlation coefficient was 0.944. The strong correlation obtained is attributed to similar variations of inverted slump cone – J-ring flow and orimet – J-ring flow with the W/B ratio and RHA content of concrete. Also, both inverted slump cone – J-ring flow and orimet – J-ring flow are similarly related to the yield stress and plastic viscosity that influence the spread of concrete.

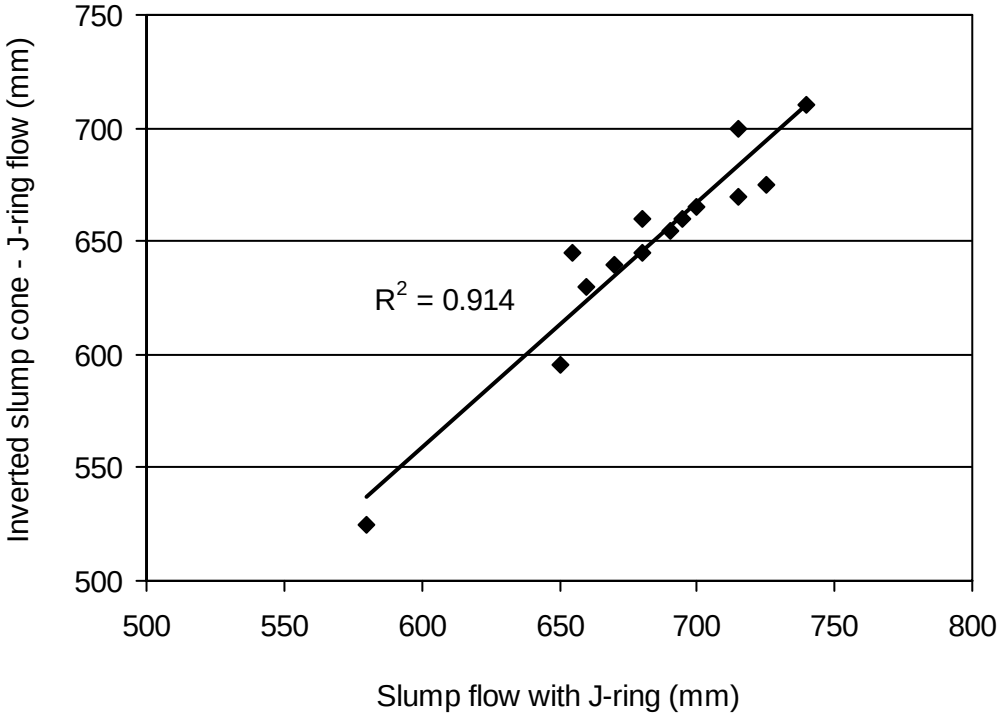

Figure 8.25: Correlation between inverted slump cone – J-ring flow and slump flow with J-ring for various concretes

8.12 Correlations between Filling Ability and Passing Ability Properties

The correlations between filling ability properties (slump and slump flow, orimet flow spread, and inverted slump cone flow spread) and passing ability properties (slump and slump flow with J-ring, orimet – J-ring flow, and inverted slump cone – J-ring flow) were established. The filling ability properties exhibited strong linear correlations with the passing ability properties, as can be seen from Figures 8.27 to 8.34. The coefficient of determination ranged from 0.904 to 1, and the correlation coefficient varied in the range of 0.951 to 1. Strong correlations were obtained because the filling ability and passing ability properties varied similarly with various W/B ratios and RHA contents of the concretes.

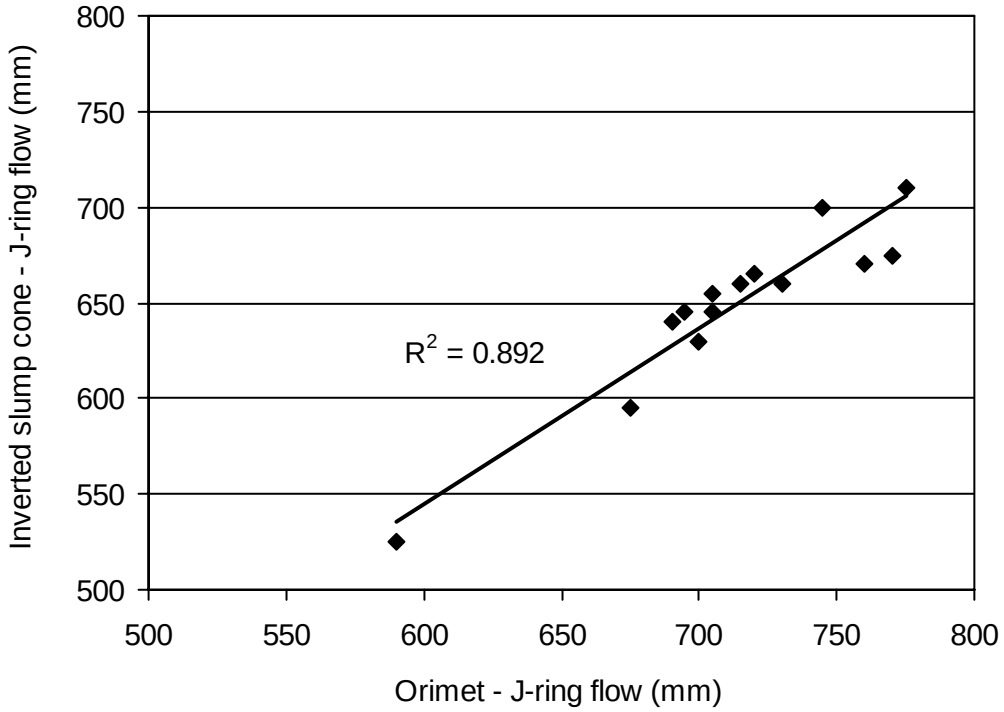

Figure 8.26: Correlation between inverted slump cone – J-ring flow and orimet – J-ring flow for various concretes

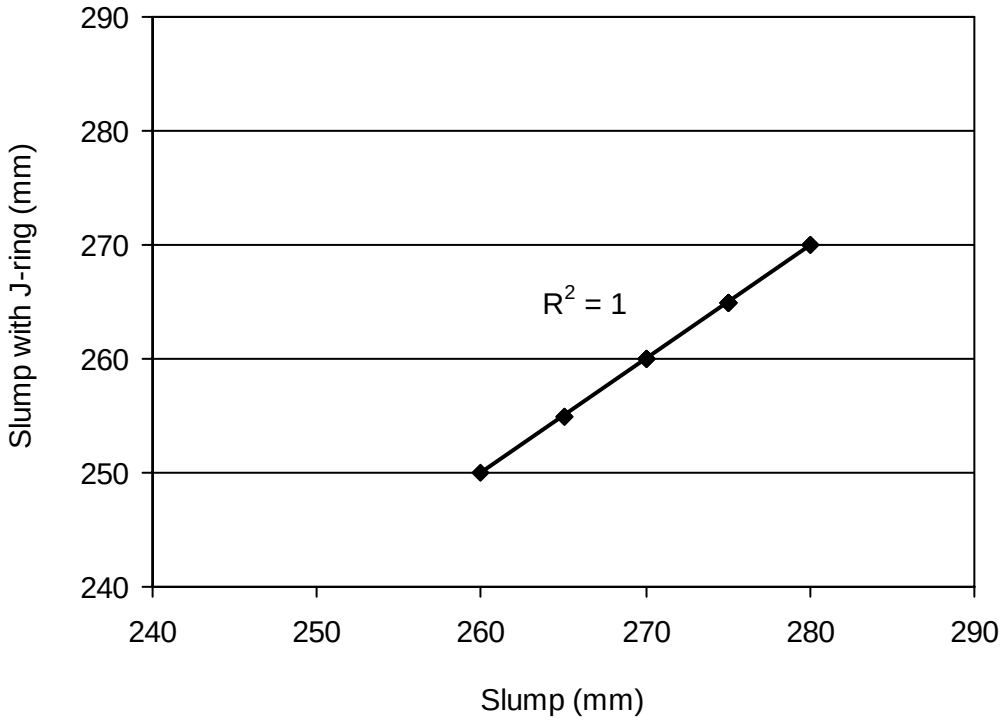

Figure 8.27: Correlation between slump with and without J-ring for various concretes

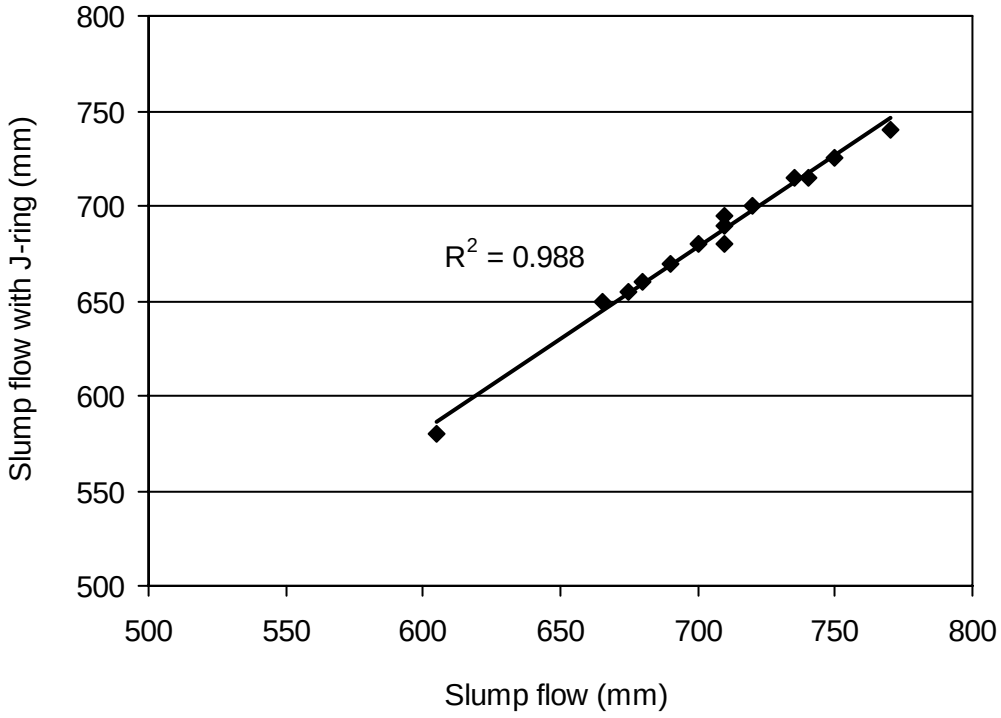

Figure 8.28: Correlation between slump flow with and without J-ring for various concretes

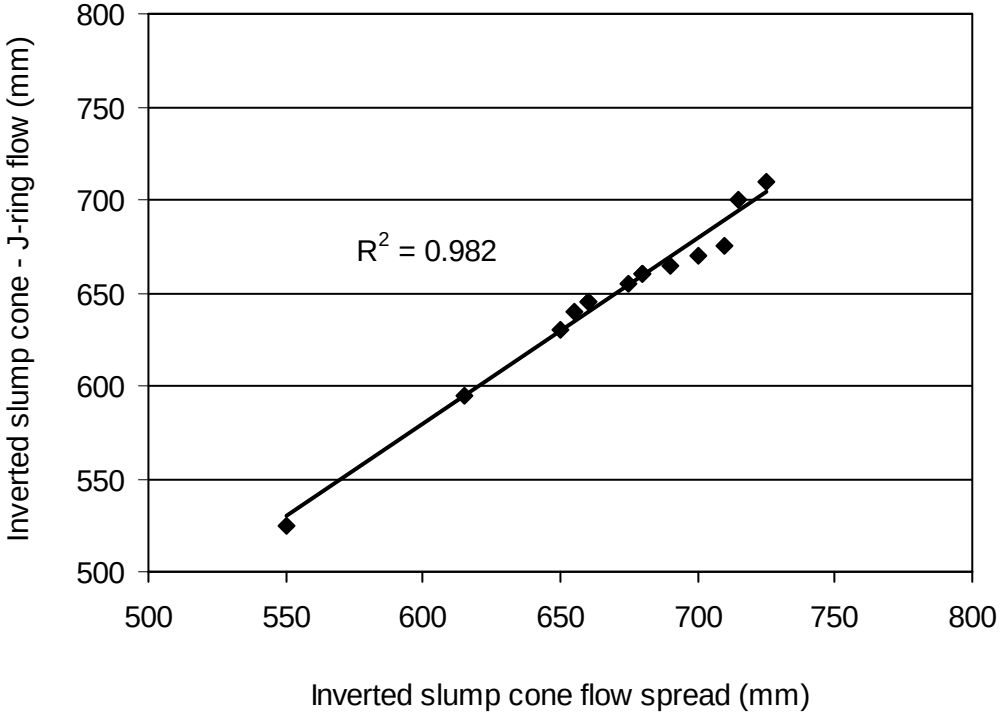

Figure 8.29: Correlation between inverted slump cone flow spread with and without J-ring for various concretes

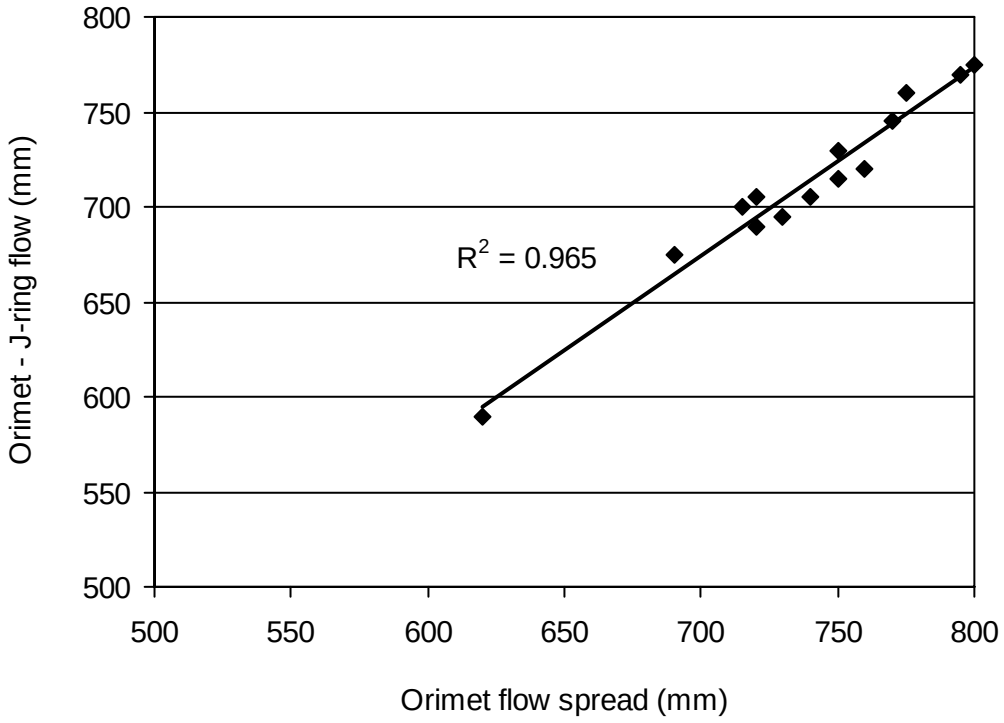

Figure 8.30: Correlation between orimet flow spread with and without J-ring for various concretes

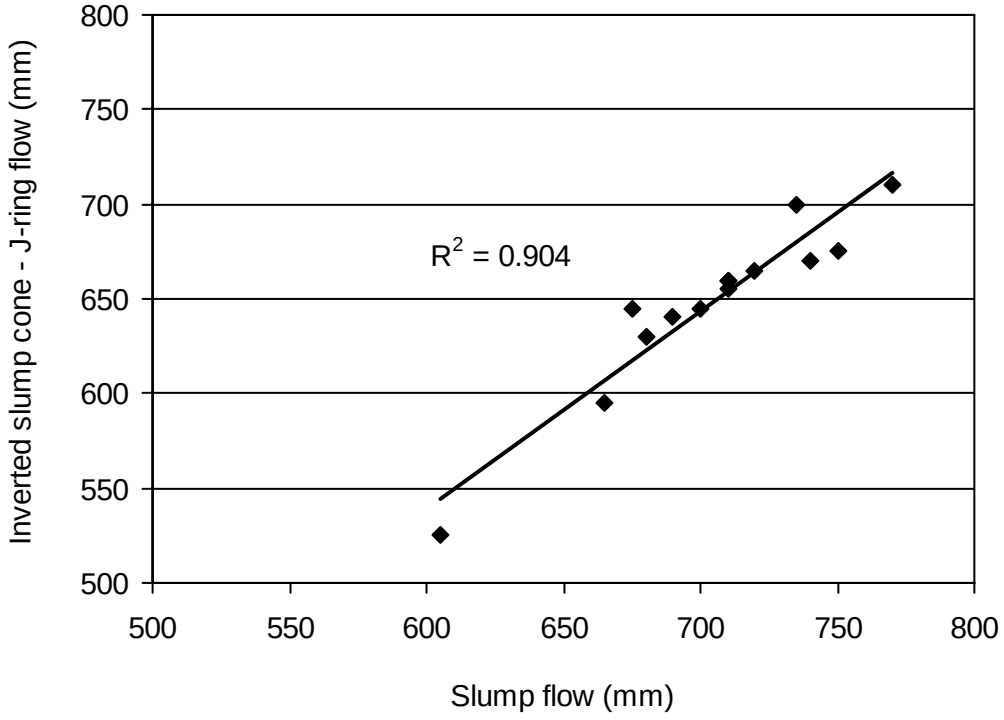

Figure 8.31: Correlation between inverted slump cone – J-ring flow and slump flow for various concretes

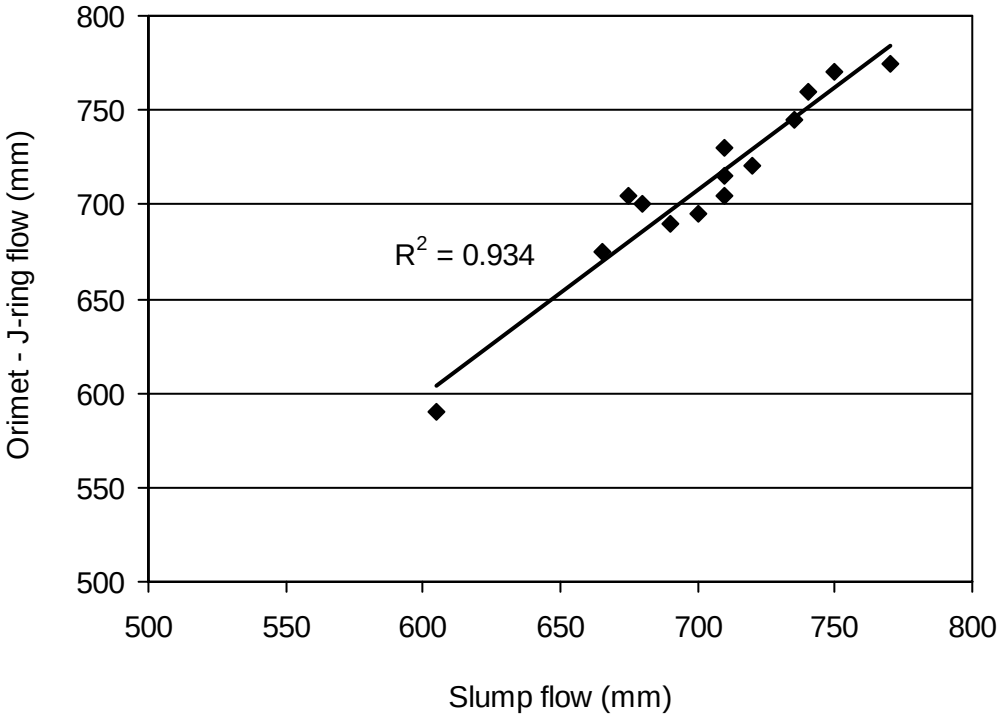

Figure 8.32: Correlation between orimet – J-ring flow and slump flow for various concretes

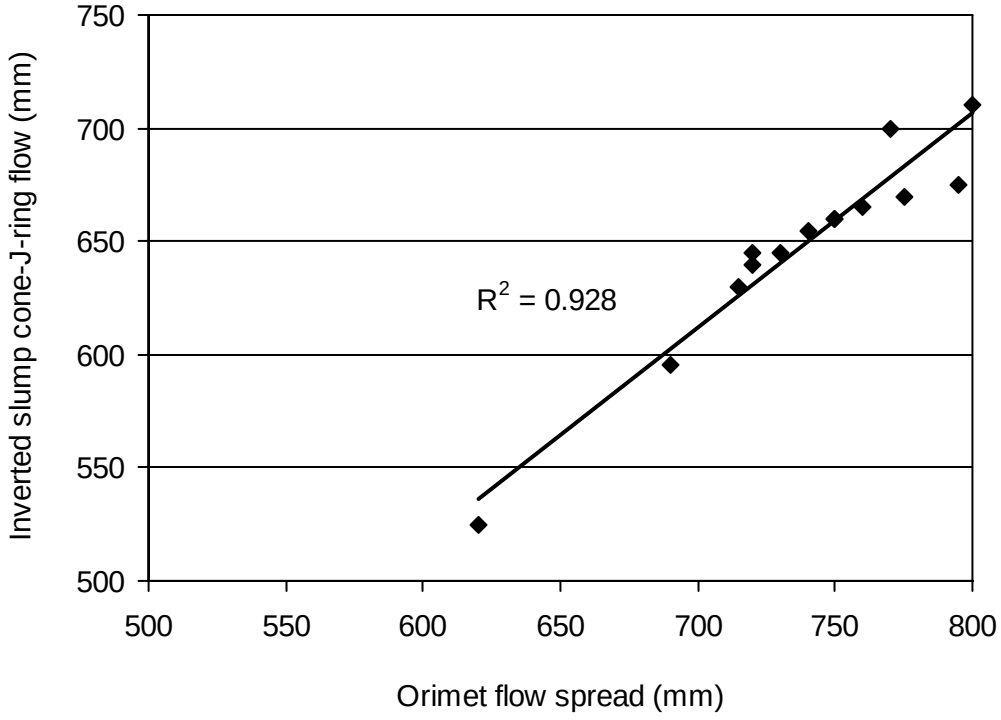

Figure 8.33: Correlation between inverted slump cone – J-ring flow and orimet flow spread for various concretes

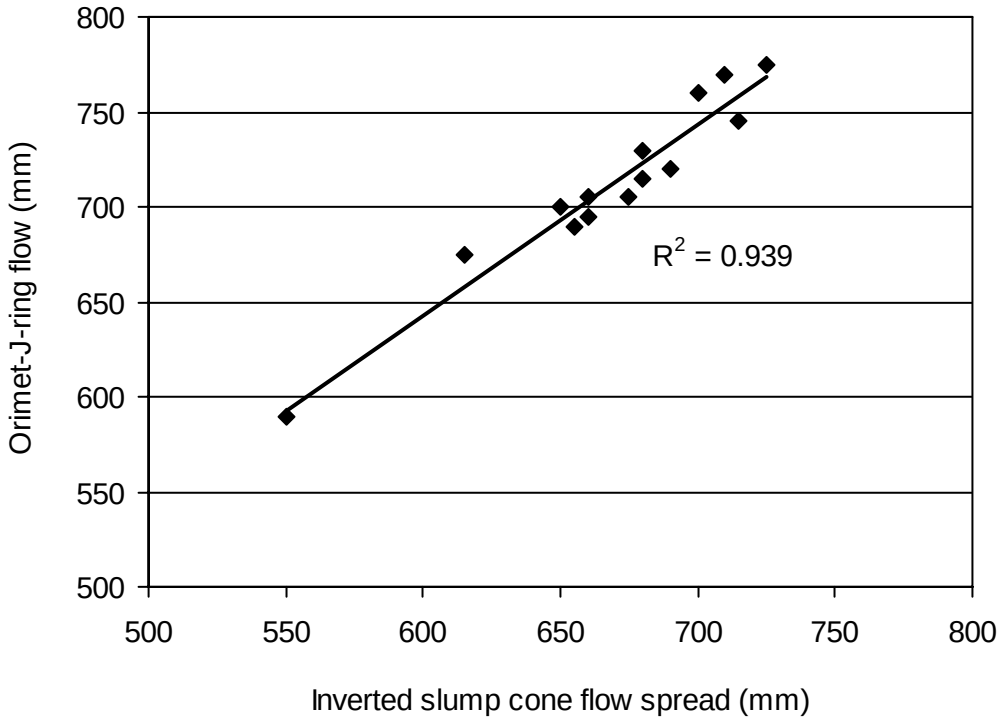

Figure 8.34: Correlation between orimet – J-ring flow and inverted slump cone flow spread for various concretes

8.13 Performance Criterion for Inverted Slump Cone – J-ring Flow

The performance criterion for the inverted slump cone – J-ring flow can be determined based on the known criterion for slump flow, which is widely used to measure the filling ability of SCHPC. The slump flow of SCHPC is generally specified in the range of 550 to 850 mm (EFNARC 2002, Khayat 2000, SCCEPG 2005). Using this slump flow range, the performance criterion for the inverted slump cone – J-ring flow can be determined based on the correlation between inverted slump cone – J-ring flow and slump flow, as shown in Figure 8.31. The corresponding inverted slump cone – J-ring flow obtained for 550 to 850 mm slump flow was 487 to 801 mm. Thus, the performance criterion for the inverted slump cone – J-ring flow spread can be fixed in the range of 475 to 800 mm.

8.14 Unit Weight of Concretes

The results of unit weight for different concretes are presented in Table 8.3. The unit weight of the concretes varied in the range of 2230 to 2355 kg/m^3 depending on the W/B ratio, RHA content and air content. Based on the measured air content of concrete and the batch weight

of constituent materials, the unit weights for various SCHPCs were also estimated. The difference between the estimated and measured unit weights was negligible (1 to 3%), as can be seen from Table 8.3.

Table 8.3: Unit weight and air content of various fresh concretes

Concrete	W/B ratio	RHA (%B)	Air content (%)		Unit weight (kg/m^3)	
			Design	Measured	Estimated	Measured
C30R0A6	0.30	0	6	5.7	2290	2325
C30R15A6	0.30	15	6	5.3	2265	2280
C30R20A6	0.30	20	6	5.7	2245	2260
C35R0A6	0.35	0	6	5.3	2285	2315
C35R0A4	0.35	0	4	4.3	2310	2355
C35R0A8	0.35	0	8	8.1	2160	2230
C35R5A6	0.35	5	6	5.5	2275	2310
C35R10A6	0.35	10	6	5.1	2275	2310
C35R15A6	0.35	15	6	5.1	2265	2290
C35R15A4	0.35	15	4	4.2	2290	2320
C35R15A8	0.35	15	8	8.0	2190	2240
C35R20A6	0.35	20	6	5.0	2255	2280
C35R20A4	0.35	20	4	4.3	2280	2315
C35R20A8	0.35	20	8	8.6	2170	2235
C35R25A6	0.35	25	6	5.6	2235	2255
C35R30A6	0.35	30	6	5.2	2235	2255
C40R0A6	0.40	0	6	6.1	2260	2275
C40R15A6	0.40	15	6	5.2	2255	2280
C40R20A6	0.40	20	6	5.3	2245	2260
C50R0A2	0.50	0	2	1.8	2300	2350
C50R0A6	0.50	0	6	5.2	2215	2250

8.14.1 Effect of water-binder ratio

The unit weight of the concretes without RHA was slightly reduced with higher W/B ratio for a given air content, as can be seen from Table 8.3. The binder weight was lower at higher W/B ratio, which is evident from Tables 7.3 and 7.5 (Chapter 7). However, the aggregate weight increased at higher W/B ratio. But the percent increase in aggregate weight was much lower than the percent reduction in binder weight per unit volume of concrete. Therefore, the unit weight of concrete was decreased at higher W/B ratio.

8.14.2 Effect of rice husk ash

The unit weight of most concretes decreased slightly with higher RHA content, as evident from Table 8.3. This is because RHA was lighter than cement. Also, the fine and coarse aggregate contents decreased as the paste volume increased in the presence of RHA. However, the decrease in the unit weight of concrete caused by RHA was marginal (1.7 to 2.8%). This is perhaps attributed to the improved physical packing of the fresh concretes due to the finer particle size of RHA as compared to cement.

8.14.3 Effect of air content

The unit weight of the concretes varied with the air content. The higher unit weight was obtained at lower air content, as can be seen from Table 8.3. This is due to the increased aggregate contents. At lower air content, the amounts of both fine and coarse aggregates were increased for a given W/B ratio (fixed contents of binder and water), as can be seen from Tables 7.3 and 7.4 (Chapter 7).

8.15 Air Content of Concretes

The results of air content for various SCHPC mixtures are shown in Table 8.3. The measured air contents were within ±1.0% of the design air content, which is acceptable. The maximum acceptable tolerance for air content measurement can be in the range of ±1.5% (ACI 201.2R-01, 2004).

8.15.1 Effect of water-binder ratio and rice husk ash

The air content was prone to decrease with lower W/B ratio and higher RHA content due to the same reasons as discussed in Sections 6.5.2 and 6.5.3 (Chapter 6). Therefore, the demand for AEA was increased progressively with lower W/B ratio and higher RHA content for a given design air content, as illustrated in Table 7.4 (Chapter 7).

8.15.2 Correlation of estimated and actual dosages of air-entraining admixture

The correlation between actual and estimated AEA dosages of concretes was established. The estimated AEA dosages for various concretes were obtained based on the air content of their mortar components (Chapter 6). The actual and estimated AEA dosages were well-

correlated with a correlation coefficient of 0.96. The relationship was linear, as can be seen from Figure 8.35. Some variations in estimated and actual AEA dosages occurred possibly due to the differences in ambient environment, batch volume, mixture composition and type of mixer. However, the observed correlation suggests that the AEA dosages required for air-entrained SCHPC mixtures can be estimated based on the air content results of their corresponding mortar components.

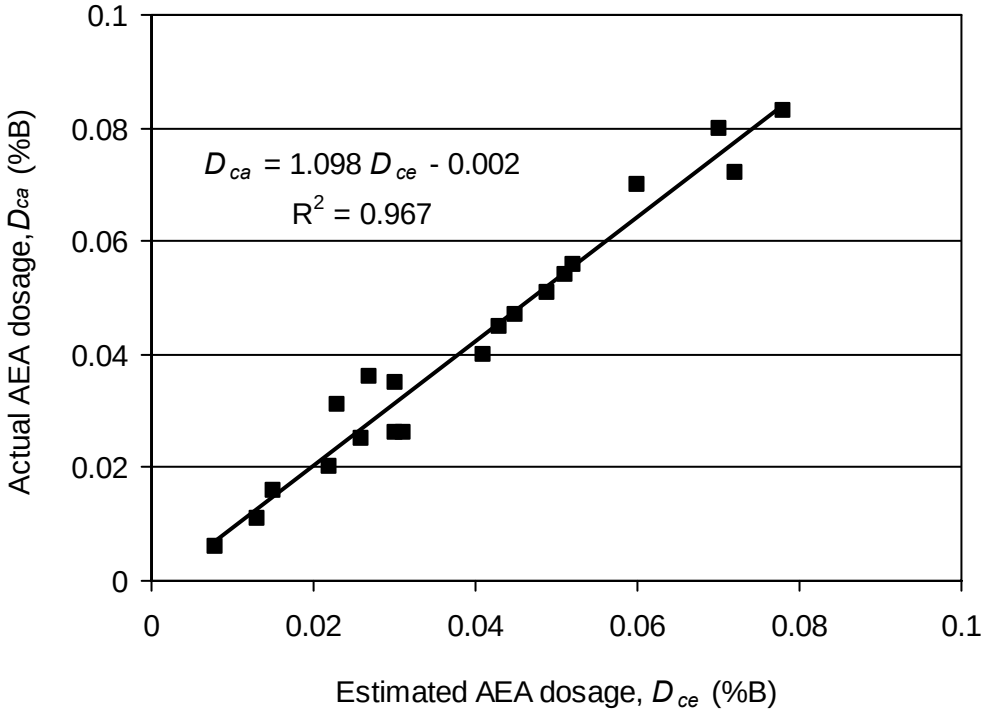

Figure 8.35: Correlation between estimated and actual AEA dosages for various concretes

8.16 Air-void Stability of Concretes

The air-void stability was observed in several fresh SCHPCs with respect to the changes in air content over time. The results for air content of the SCHPCs tested at different stages are presented in Figures 8.36 and 8.37. It can be seen from Figure 8.36 that the air content varied from 3.5 to 4.3% for the concretes with 4% design air content. Conversely, the air content ranged from 7.5 to 8.6% for the concretes with 8% design air content, as can be seen from Figure 8.37. Hence, the actual air contents deviated from the design air contents (4 and 8%) within the range of ±0.6%, which is less than the acceptable tolerance of ±1.5% for air

content measurement (ACI 201.2R-01, 2004). In a few cases, the air content observed during the second stage of testing at 30 minutes from concrete batching was slightly higher than the initial air content. This is possibly due to enhanced dispersion of the entrained air under more mixing action. The overall test results indicate that the air-void stability in all fresh SCHPC mixtures was good. The maximum loss of air content over the period of 60 and 90 minutes was less than 1.0% for all concretes. This is below the air loss of 1 to 2% that generally occurs due to the transportation of concrete (Kosmatka et al. 2002).

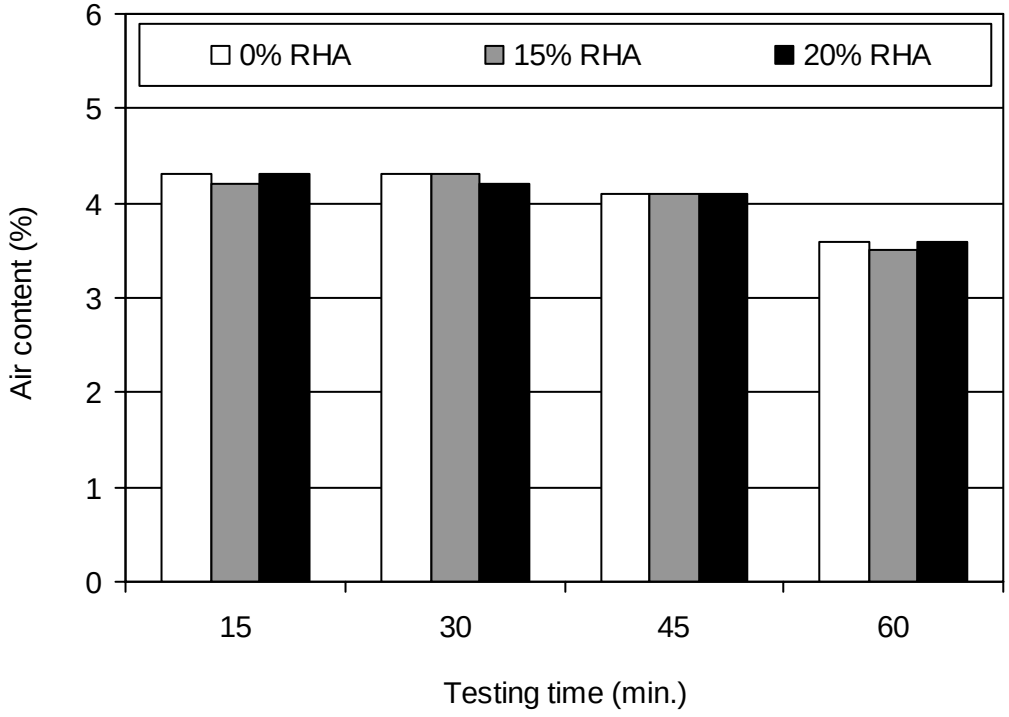

Figure 8.36: Variation of air content in self-consolidating high performance concretes with 4% design air content

The air-void stability observed in various fresh SCHPC mixtures is attributed to the relatively high binder content, low W/B ratio and high S/A ratio. These properties are not only conducive to the filling ability of the concretes, but also enhance the air-void stability (Khayat and Assaad 2002). In the present study, the concretes tested for air-void stability were prepared using a relatively low coarse aggregate content with a higher amount of binder. In addition, the saturation dosages of HRWR dispersed the binding materials and

maintained a good fluidity in the concrete mixtures. As a result, the inter-particle friction and collision of aggregates were reduced during mixing, handling and placement, which might produce more stable air-voids in fresh concretes.

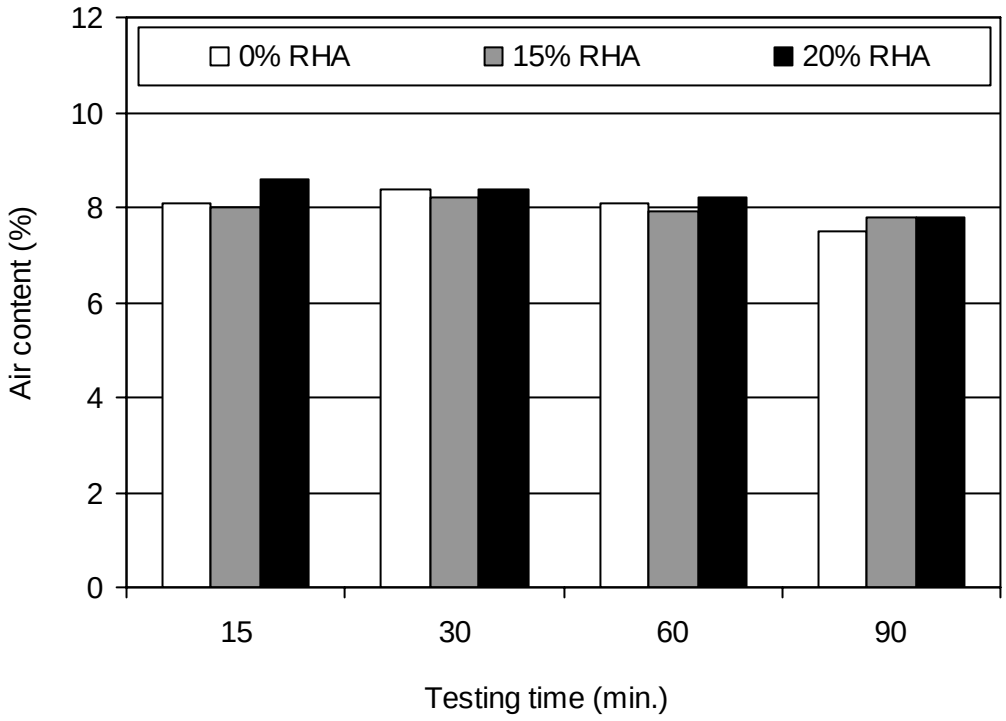

Figure 8.37: Variation of air content in self-consolidating high performance concretes with 8% design air content

8.16.1 Effect of re-mixing

The re-mixing was used at different stages as shown in Figure 8.6 to simulate the intermittent agitation of concrete during transport. No significant loss of air content occurred due to re-mixing at different test stages, as can be seen from Figures 8.36 and 8.37. Also, there was no significant difference in loss of air content between first and second groups of concretes, which were intermittently re-mixed and tested at several stages extended to 60 and 90 minutes, respectively. This suggests that the concrete placement can be delayed up to 60 to 90 minutes from the time of batching, while maintaining the desirable air content. This time is adequate for the transport of concrete from the ready-mixed plant to the construction site.

8.16.2 Effect of filling ability

The air-void stability can be affected by the filling ability of the concretes. The ability of AEA to reduce the surface tension is generally decreased at lower filling ability (Khayat and Assaad 2002). Thus, bigger and less stable air-voids could be produced. Also, the reduction in filling ability (slump and slump flow) tends to lower the total air content of fresh concrete (Baalbaki and Aïtcin 1994). These drawbacks were eliminated in the current study since the filling ability of the concretes was almost the same at all test stages. The measured slump and slump flow of the concretes tested for air-void stability are presented in Tables 8.4 and 8.5, respectively. It can be seen from Table 8.4 that the slump was always consistent for each concrete. The variation in slump at different test stages was -1.8 to 0%. Moreover, Table 8.5 shows that the slump flow was also consistent for each concrete. The variation in slump flow at different test stages was -3.5 to 4.5%.

Table 8.4: Variation of slump at different test stages for various SCHPCs

Concrete	RHA (%B)	Slump (mm)			
		T = 15 min.	T = 30 min.	T = 45 min.	T = 60 min.
C35R0A4	0	275	275	275	270
C35R15A4	15	280	275	275	275
C35R20A4	20	275	275	275	275
		T = 15 min.	T = 30 min.	T = 60 min.	T = 90 min.
C35R0A8	0	275	275	275	275
C35R15A8	15	280	275	275	275
C35R20A8	20	275	275	275	270

8.16.3 Effect of high-range water reducer

The HRWR was used by splitting its saturation dosages to maintain similar filling ability over the testing duration for all concretes tested for air-void stability. The initial (70% of SD) and successive dosages (10% of SD) of HRWR worked very well to provide the consistent slump and slump flow throughout the testing periods, as can be seen from Tables 8.4 and 8.5. Thus, the spilt dosages of HRWR minimized the drawbacks of different filling ability (slump and slump flow) as discussed in Section 8.16.2. However, the additional dosages may slightly increase the air content of concrete through interaction with the AEA (Baalbaki and Aïtcin 1994). It can be assumed that this effect was minimized in the present study since a minimum additional dosage of HRWR (only 10% of SD) was used at later stages. Indeed, a

previous research reported that the total air content of fresh concrete is relatively unaffected by the split addition of HRWR (Schemmel et al. 1994).

Table 8.5: Variation of slump flow at different test stages for various SCHPCs

Concrete	RHA (%B)	Slump flow (mm)			
		T = 15 min.	T = 30 min.	T = 45 min.	T = 60 min.
C35R0A4	0	700	700	700	680
C35R15A4	15	720	705	700	700
C35R20A4	20	690	695	700	695
		T = 15 min.	T = 30 min.	T = 60 min.	T = 90 min.
C35R0A8	0	670	680	700	695
C35R15A8	15	720	700	710	695
C35R20A8	20	695	690	695	690

8.16.4 Effect of rice husk ash

The air-void stability in fresh concretes was not affected by the presence of RHA. This is evident from Figures 8.36 and 8.37. However, the presence of RHA increased the demand of AEA for a given range of air content. It can be seen from Table 7.4 (Chapter 7) that greater AEA dosages were required for concretes with 15 and 20% RHA at 4 and 8% design air content. This is mostly due to the increased paste viscosity and reduced attachment site of entrained air-voids, as discussed in case of mortar air content (Chapter 6). In addition, some AEA molecules could also be adsorbed or absorbed in the porous and honeycomb microstructure of RHA. Thus, a lower amount of AEA will be available for air-void formation and stabilization. The steric repulsion of polycarboxylate-based HRWR with long grafted side chains (Mindess et al. 2003) may further reduce the attachment of air-voids on cement and RHA particles. Hence, some air-voids could become less stable and combine to seep out of the concrete mixture, resulting in a higher demand for AEA. Both attachment site reduction and steric repulsion effects of HRWR can be more pronounced in case of 15 and 20% RHA, since greater dosages were used to obtain the desired filling ability in concretes.

8.17 Optimum Content of Rice Husk Ash

The optimum content of RHA was determined based on the consideration of several factors, and was found to depend on the W/B ratio of the concretes. The RHA content above 15% caused a high viscosity in the concrete with 0.30 W/B ratio and thus the orimet flow time

exceeded the maximum acceptable criterion for filling ability. In contrast, the orimet flow time was within the acceptable range when 20% RHA was used in concretes with 0.35 and 0.40 W/B ratios. However, the viscosity became higher for 25 and 30% RHA contents used in concretes with 0.35 W/B ratio and therefore the orimet flow time also exceeded the maximum acceptable criterion in these two cases. In addition, the RHA content greater than 15% required high dosages of HRWR to achieve the required filling ability and passing ability, particularly at lower W/B ratios. In case of 20 to 30% RHA, the HRWR dosages required were much higher than the maximum dosage recommended by the manufacturer. A high dosage of HRWR may cause concrete setting problem and thus could delay the hydration process. Handling and mixing difficulties were also experienced for the concretes including a RHA content greater than 15%. Nevertheless, obtaining the required filling ability, passing ability and air content was not problematic in the presence of 15% RHA. Moreover, no adverse effect on the air-void stability in fresh concrete was observed for 15% RHA. The overall test results suggest that 15% RHA can be selected as the optimum content for use in SCHPC.

8.18 Conclusions

a. The slump flow, inverted slump cone flow spread, and orimet flow spread with and without J-ring increased at lower W/B ratio and higher RHA content due to the increased paste volume of concrete.
b. The dosages of HRWR required to achieve adequate filling ability and passing ability increased with lower W/B ratio and higher RHA content mostly due to the increased content and surface area of the binder.
c. The filling ability and passing ability criteria were fulfilled for all SCHPCs except few concretes with a lower W/B ratio and a RHA content greater than 15 and 20% that exhibited high viscosity mostly due to the excessive surface area of rice husk ash.
d. The orimet and inverted slump cone flow times increased with lower W/B ratio and higher RHA content, and thus indicated the increased viscosity of concrete. This is greatly attributed to the increased volume fraction and surface area of the binder used in concrete.

e. The filling ability model is applicable to various air-entrained and non-air-entrained SCHPC mixtures containing a paste volume in the range of 0.29 to 0.40 m^3/m^3, and providing a slump flow between 550 and 850 mm.

f. The filling ability model provided the slump flows close to the measured slump flow values. The computed and measured slump flows were within ±7.6% error.

g. Strong correlations were observed for the flow times of all pastes and concretes. The mortar flow spread was also well correlated with the slump flow of concrete in the absence of RHA. Strong correlations were also seen for various filling ability and passing ability properties of concrete.

h. The inverted slump cone apparatus can be used in laboratory and field comfortably by a single operator with and without J-ring to assess the filling ability and passing ability of SCHPC based on the performance criteria derived.

i. The air-void stability in various SCHPC mixtures was not affected by the presence of RHA and re-mixing, as the maximum loss of air content over the period of 60 to 90 minutes remained less than 1%.

j. The unit weight of concrete slightly increased at lower W/B ratio due to greater binder content. The unit weight of concrete also increased with lower air content due to increased aggregate quantity and reduced void content. Conversely, the unit weight marginally decreased with higher RHA content due to the increased paste volume.

k. The measured air contents were within ±1.0% of the design air contents. The dosages of AEA for achieving a given air content increased with lower W/B ratio and greater RHA content mostly due to higher plastic viscosity of the concretes.

l. The estimated and actual AEA dosages for different SCHPC mixtures were well-correlated. Hence, the AEA dosage needed for a concrete air content can be fixed based on the AEA dosage used for the equivalent mortar air content.

m. The optimum RHA content was 15% based on the results of filling ability and passing ability properties at lower W/B ratios of 0.30 and 0.35. It was dependent of the W/B ratio used in concrete. An increased optimum content can be obtained at higher W/B ratios.

Chapter 9

Properties of Hardened Self-consolidating High Performance Concretes

9.1 General

The preparation of hardened test specimens, the test procedures, and the test results for various hardened properties of self-consolidating high performance concretes (SCHPCs) are presented in this chapter. The effects of water-binder (W/B) ratio, rice husk ash (RHA) and air content are discussed, and the correlations among different hardened properties are shown. This chapter also presents a model for the compressive strength of concretes, and discusses it validity and application.

9.2 Research Significance

The cost-effective SCHPCs with good hardened properties and durability are desirable in construction industry. The SCHPCs have been produced using several supplementary cementing materials (SCMs) such as silica fume, ground granulated blast-furnace slag, and fly ash. However, silica fume is an expensive SCM. Presently, slag and fly ash are also sold in North America as a commercial commodity. In developing countries, the use of SCM such as silica fume may be cost-prohibitive. Therefore, it is important to use an alternative less expensive SCM such as RHA to produce cost-effective SCHPC. Like silica fume, RHA offers similar benefits with regard to hardened properties and durability of concrete. This study incorporated RHA in various SCHPCs as an SCM. The performance of RHA was investigated with respect to several hardened properties. Both destructive and non-destructive tests were performed to obtain key hardened properties of different SCHPCs and an empirical model for compressive strength was developed. Some of the properties tested were indicative of concrete durability. The test results obtained for the hardened properties of the concretes can be beneficial to the construction industry regarding the use of RHA in SCHPC. Also, the strength model will be useful for the mixture design of SCHPC.

9.3 Preparation of Test Specimens

The specimens required for testing the hardened properties of concrete were prepared through several steps such as molding, de-molding, and curing. In addition, grinding and cutting operations were performed when necessary. The cylinder specimens of different sizes, as shown in Figure 9.1, were used in conducting the tests for hardened properties. The details of the test specimens are shown in Table 9.1. The cylinder specimens required for testing the compressive strength, ultrasonic pulse velocity, and electrical resistivity of hardened concretes were molded in single-use plastic moulds. The ASTM standard practice (ASTM C 192/C 192M, 2004) was followed with some exceptions for molding the test specimens; the fresh concrete was poured into the cylinder moulds in one layer, and no vibration or rodding was used for consolidation. The cylinder specimens were sealed immediately using the lids and left undisturbed at room temperature. The specimens were de-molded, marked and transferred to the fog room for wet curing at the age of 24±4 hours. The wet curing was carried out until the day of testing. The ASTM standard practice (ASTM C 192/C 192M, 2004) was followed for curing. The curing temperature was 23 ± 2^0C and the relative humidity was above 95%.

100D×200H mm de-moulded cylinders

100D×50H mm cut cylinders

Figure 9.1: Cylinder specimens used for determining the hardened properties of concretes

The cylinder (100D×200H mm) specimens were always kept saturated during the testing of electrical resistivity to minimize the differential drying effects. Also, the top faces

of the molded cylinders were smoothened by grinding to make the ends plane and parallel before testing ultrasonic pulse velocity and compressive strength. It facilitated good coupling during the ultrasonic pulse velocity test. It also ensured the perpendicularity of end faces to the axis of specimen during the compression test.

Table 9.1: Details of the test specimens

Type of test	Type of specimens	Size of specimens
Compression	Medium cylinders	100D*×200H♣ mm
Ultrasonic pulse velocity	Medium cylinders	100D×200H mm
Electrical resistivity	Medium cylinders	100D×200H mm
Water absorption and total porosity	Small cylinders	100D×50H mm

*Diameter; ♣Height

The test specimens (100D×50H mm small cylinders) required for determining the water absorption and total porosity were prepared by cutting a required number of molded and cured cylinders. While cutting operation, thin sections from both ends of the cylinders were discarded to minimize the end effects. Three 100D×50H mm small cylinder specimens were prepared from each 100D×200H mm parent cylinder.

9.4 Test Procedures for Hardened Concretes

The hardened specimens of various SCHPCs were tested to determine compressive strength, ultrasonic pulse velocity, water absorption and total porosity, and true electrical resistivity. The details of the test program are shown in Table 9.2.

9.4.1 Compression test

The compression test was carried out to determine the compressive strength of the concretes. ASTM standard (ASTM C 39/C 39M, 2004) was followed to conduct the compression test at the ages of 3, 7, 28 and 56 days. Triplicate 100D×200H mm medium cylinders were tested at each age. During testing, unbonded metal (steel) caps with neoprene elastometric pads were used on the end faces of the cylinders to ensure uniaxial loading. An operational stage of the compression test is shown in Figure 9.2. The compression was applied and the maximum or

ultimate load carried by the specimen was recorded. The compressive strength was calculated based on the ultimate load and the cross-sectional area of the cylinder, and averaged from the results of three specimens.

Table 9.2: Test program for different types of hardened concrete

Concrete type*	Type of test	Test age (days)	Specimens number tested at each age
C30R0A6, C30R15A6, C30R20A6	Compression	3, 7, 28, 56	3
	Ultrasonic pulse velocity	28, 56	3
C35R0A6, C35R5A6, C35R10A6, 35R15A6, C35R20A6, 35R25A6, C35R30A6	Electrical resistivity	28, 56	3
	Water absorption and total porosity	28, 56	3
C40R0A6, C40R15A6, C40R20A6			
C50R0A2, C50R0A6			

*Concrete designations are given in Chapter 7

9.4.2 Test for ultrasonic pulse velocity

The test for ultrasonic pulse velocity of concretes was carried out in accordance with ASTM C 597 (2004). An operational stage of the ultrasonic pulse velocity test is shown in Figure 9.2. The test was conducted at the ages of 28 and 56 days. Triplicate 100D×200H mm cylinders were tested at each age. The specimens were air-dried at room temperature (23 ± 2^0C) for 24 hours prior to testing. The drying process helped to obtain good coupling between transducers and specimen. The average path length of the specimens was determined by taking the measurement at four quaternary longitudinal locations. A CNS portable ultrasonic non-destructive digital indicating tester, PUNDIT plus (CNS Farnell 2000) was used for determining the ultrasonic pulse velocity. Before using the PUNDIT, the transducers were zeroed by placing them face to face with water-soluble coupling gel. During testing, the transducers were coupled firmly to the specimen ends and the transit time was recorded. The ultrasonic pulse velocity was determined from measured transit time and path length and averaged based on the results of three specimens.

Compression test (before loading)

Compression test (after failure)

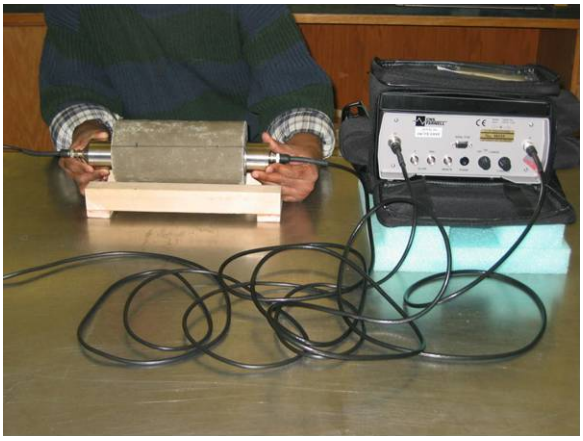

Ultrasonic pulse velocity test

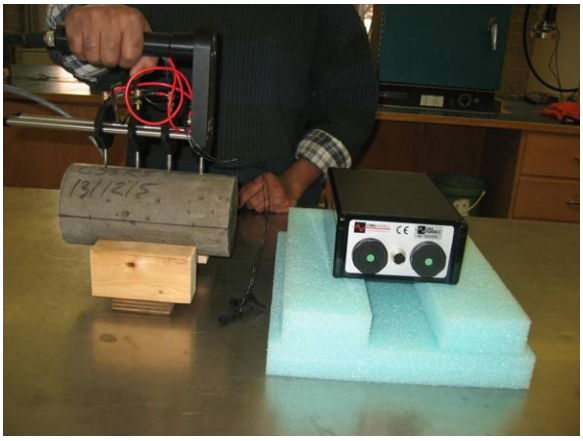

Electrical resistivity test

Water absorption and total porosity test (vacuum saturation)

Water absorption and total porosity test (determination of buoyant mass)

Figure 9.2: Different tests for determining the hardened properties of concretes

9.4.3 Test for electrical resistivity

The electrical resistivity test for concretes was carried out by the four-point Wenner array probe technique. The Florida test method FM 5-578 was followed for determining the resistivity of various concretes (Florida Department of Transportation 2004). A CNS RM MKII concrete resistivity meter (CNS Farnell 2004) was used to measure the surface resistivity at the ages of 28 and 56 days. The probe array spacing used was 40 mm. An operational stage of the electrical resistivity test is shown in Figure 9.2. Triplicate 100D×200H mm saturated cylinders were used at each test age. The resistivity measurements were taken at four quaternary longitudinal locations of the specimen, and repeated once for each location to obtain 8 readings per specimen. Hence, 24 resistivity readings were obtained in total for three specimens. These readings were averaged to get the electrical resistivity of the concrete. The resistivity obtained was the apparent electrical resistivity of concrete. Therefore, a correction factor was applied to obtain the true electrical resistivity. The correction factor was determined based on the procedure described by Morris et al. (1996). The true electrical resistivity of the concretes was determined by dividing the apparent resistivity with the correction factor.

9.4.4 Test for water absorption and total porosity

A test method based on the vacuum saturation technique was employed to determine the water absorption and total porosity of the concretes from saturated, suspended and oven-dry masses of the specimens. A schematic of the vacuum saturation technique is shown in Figure 9.3. The 100D×50H mm cylinder specimens were vacuum saturated at the ages of 28 and 56 days. Triplicate specimens were used at each testing age. The specimens were placed in a vacuum pycnometer with both end faces being exposed. There was a movable air-tight collar attached to the lid of this pycnometer. The collar was used to connect or disconnect the vacuum and water lines with the pycnometer holding test specimens. Cool tap water was poured in another vacuum pycnometer. Both pycnometers were covered by the lid and sealed using vacuum grease. The pycnometers were then connected to a vacuum pump through a water trap by means of a vacuum line connector. A pressure gage was attached to the vacuum line connector. Another pressure gage was attached to the vacuum pycnometer holding water to ensure the required vacuum pressure. The vacuum pump was started and run for 3 hours at

a pressure of -97 kPa (-28.5 in. Hg). With the vacuum pump still running, the stopcock for the pycnometer containing water was closed and the vacuum was released. Immediately, the vacuum line of the pycnometer holding test specimens was disconnected by turning the collar to the air-tight position, the water line was attached, and a sufficient amount of de-aired water was drained to entirely cover the specimens. Then the water line was disconnected while keeping the collar in air-tight position, the vacuum line was connected, and the specimens covered with de-aired water were further vacuumed for two hours. An operational stage of the vacuum saturation technique is shown in Figure 9.2. After 5 hours of vacuum operation, the pump was turned off and the air was allowed to enter the pycnometer containing test specimens. The specimens were soaked under water keeping them in vacuum pycnometer for 19 hours and then the saturated surface-dry and buoyant masses were determined. An operational stage of the buoyant mass measurement is shown in Figure 9.2. Then the specimens were oven-dried at 105 ± 5^0C for 48 hours. The oven-drying was conducted after vacuum saturation to eliminate the effect of microstructural damage. Later the specimens were removed from the oven, cooled in dry air to a room temperature of 23 ± 2^0C, and then weighed to obtain the oven-dry mass. Finally, the water absorption and total porosity of the concretes were calculated using Equation 9.1 and Equation 9.2, respectively, and averaged based on the results of three specimens.

$$W_a = \frac{M_s - M_d}{M_d} \times 100\% \qquad \text{(Equation 9.1)}$$

$$P_t = \frac{M_s - M_d}{M_s - M_b} \times 100\% \qquad \text{(Equation 9.2)}$$

where:

P_t = Total porosity (volume %)

W_a = Water absorption (mass %)

M_b = Buoyant mass of the saturated specimen in water

M_d = Oven-dry mass of the specimen in air

M_s = Saturated surface-dry mass of the specimen in air

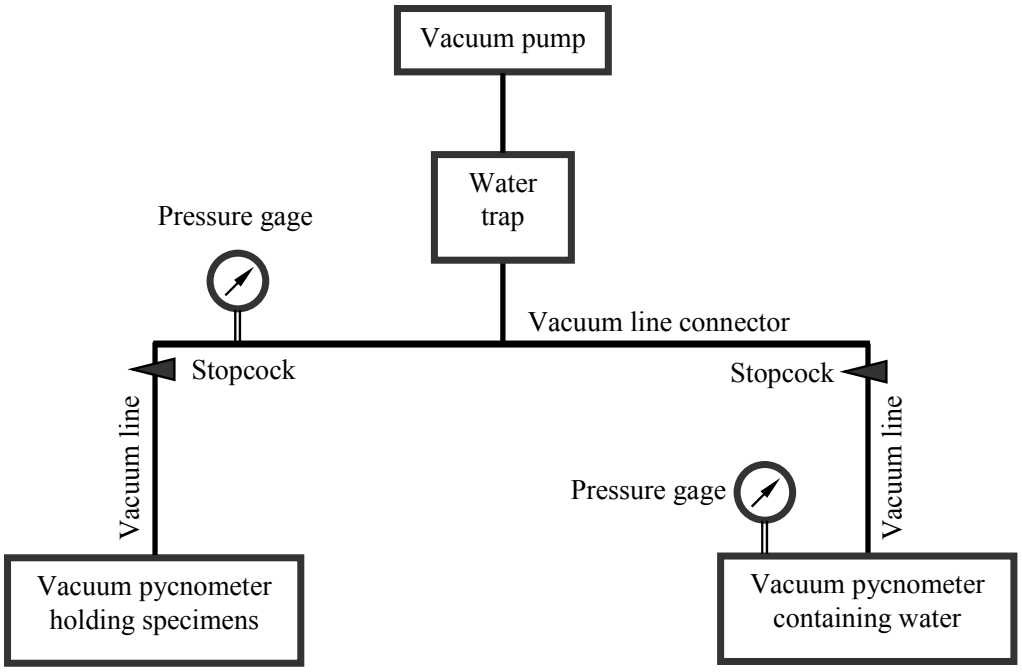

Figure 9.3: Schematic of test setup for determining water absorption and total porosity

9.5 Test Results for Hardened Properties

The hardened properties of the concretes tested were the compressive strength, ultrasonic pulse velocity, water absorption, total porosity, and electrical resistivity. The results are presented and discussed below.

9.5.1 Compressive strength

The detailed results for compressive strength including the average strength with standard deviation are given in Tables 9.3 and 9.4. The average compressive strengths of the concretes are presented in Figures 9.4 to 9.6. The gain in compressive strength continued to occur until the age of 56 days where the highest strength was achieved for all concretes due to greater hydration of cementing materials. However, the largest strength development happened between 3 and 28 days, as can be seen from Figures 9.4 to 9.6. The compressive strength at the age of 28 days was in the range of 42.7 to 94.1 MPa for different concretes. In addition, the compressive strength of concretes at the age of 56 days varied from 44.9 to 98.4 MPa.

Table 9.3: Compressive strength of various concretes (W/B = 0.30, 0.40, and 0.50)

Concrete Mixture	Compressive strength (MPa)			
	3D	7D	28D	56D
C30R0A6	S1: 53.8 S2: 53.8 S3: 52.6 Average: 53.4 σ*: 0.69	S1: 62.4 S2: 61.8 S3: 61.2 Average: 61.8 σ: 0.60	S1: 68.9 S2: 68.8 S3: 68.6 Average: 68.8 σ: 0.16	S1: 71.0 S2: 71.3 S3: 71.6 Average: 71.3 σ: 0.30
C30R15A6	S1: 55.7 S2: 56.3 S3: 55.7 Average: 55.9 σ: 0.35	S1: 68.5 S2: 69.2 S3: 70.4 Average: 69.4 σ: 0.96	S1: 88.4 S2: 87.5 S3: 86.9 Average: 87.6 σ: 0.76	S1: 92.1 S2: 91.5 S3: 91.8 Average: 91.8 σ: 0.30
C30R20A6	S1: 56.9 S2: 57.5 S3: 56.3 Average: 56.9 σ: 0.60	S1: 71.6 S2: 72.2 S3: 72.8 Average: 72.2 σ: 0.60	S1: 92.4 S2: 93.0 S3: 91.2 Average: 92.2 σ: 0.92	S1: 96.4 S2: 94.8 S3: 95.8 Average: 95.7 σ: 0.81
C40R0A6	S1: 42.2 S2: 42.2 S3: 41.6 Average: 42.0 σ: 0.35	S1: 50.2 S2: 50.2 S3: 49.5 Average: 49.9 σ: 0.41	S1: 59.7 S2: 59.3 S3: 59.1 Average: 59.4 σ: 0.31	S1: 62.4 S2: 61.5 S3: 61.8 Average: 61.9 σ: 0.46
C40R15A6	S1: 43.5 S2: 42.8 S3: 42.9 Average: 43.1 σ: 0.38	S1: 52.0 S2: 50.8 S3: 53.2 Average: 52.0 σ: 1.20	S1: 67.0 S2: 64.6 S3: 65.5 Average: 65.7 σ: 1.21	S1: 68.5 S2: 70.1 S3: 69.2 Average: 69.3 σ: 0.80
C40R20A6	S1: 44.6 S2: 42.8 S3: 44.1 Average: 43.8 σ: 0.38	S1: 56.9 S2: 55.7 S3: 54.5 Average: 55.7 σ: 1.2	S1: 71.0 S2: 71.9 S3: 70.4 Average: 71.1 σ: 0.76	S1: 74.7 S2: 73.7 S3: 74.1 Average: 74.2 σ: 0.51
C50R0A6	S1: 30.0 S2: 29.4 S3: 29.7 Average: 29.7 σ: 0.30	S1: 36.1 S2: 35.2 S3: 34.6 Average: 35.3 σ: 0.76	S1: 41.6 S2: 43.1 S3: 43.4 Average: 42.7 σ: 0.96	S1: 45.3 S2: 44.7 S3: 44.7 Average: 44.9 σ: 0.35
C50R0A2	S1: 36.1 S2: 37.0 S3: 36.7 Average: 36.6 σ: 0.46	S1: 45.3 S2: 44.7 S3: 44.1 Average: 44.7 σ: 0.60	S1: 56.6 S2: 54.5 S3: 56.0 Average: 55.7 σ: 1.08	S1: 57.8 S2: 56.6 S3: 57.5 Average: 57.3 σ: 0.62

*Standard deviation

Table 9.4: Compressive strength of various concretes (W/B = 0.35)

Concrete Mixture	Compressive strength (MPa)			
	3D	7D	28D	56D
C35R0A6	S1: 47.8 S2: 47.1 S3: 47.2 Average: 47.4 σ: 0.38	S1: 56.9 S2: 56.9 S3: 56.3 Average: 56.7 σ: 0.35	S1: 66.4 S2: 64.9 S3: 65.5 Average: 65.6 σ: 0.76	S1: 68.3 S2: 67.9 S3: 68.6 Average: 68.3 σ: 0.35
C35R5A6	S1: 48.3 S2: 49.0 S3: 48.9 Average: 48.7 σ: 0.38	S1: 58.1 S2: 58.7 S3: 57.5 Average: 58.1 σ: 0.60	S1: 71.6 S2: 70.4 S3: 72.8 Average: 71.6 σ: 1.2	S1: 74.6 S2: 75.0 S3: 72.2 Average: 73.9 σ: 1.5
C35R10A6	S1: 49.6 S2: 49.0 S3: 50.2 Average: 49.6 σ: 0.60	S1: 59.7 S2: 60.3 S3: 60.0 Average: 60.0 σ: 0.30	S1: 75.0 S2: 73.7 S3: 75.9 Average: 74.9 σ: 1.11	S1: 76.2 S2: 77.7 S3: 78.4 Average: 77.5 σ: 1.13
C35R15A6	S1: 49.9 S2: 50.2 S3: 50.5 Average: 50.2 σ: 0.30	S1: 61.9 S2: 61.8 S3: 62.5 Average: 62.1 σ: 0.38	S1: 78.5 S2: 78.3 S3: 78.9 Average: 78.6 σ: 0.31	S1: 80.7 S2: 81.1 S3: 81.6 Average: 81.1 σ: 0.55
C35R20A6	S1: 50.8 S2: 51.4 S3: 50.8 Average: 51.0 σ: 0.35	S1: 64.9 S2: 66.1 S3: 65.5 Average: 65.5 σ: 0.60	S1: 85.1 S2: 85.6 S3: 85.6 Average: 85.4 σ: 0.29	S1: 89.9 S2: 89.9 S3: 89.3 Average: 89.7 σ: 0.35
C35R25A6	S1: 52.1 S2: 52.1 S3: 50.8 Average: 51.7 σ: 0.75	S1: 66.7 S2: 67.3 S3: 69.2 Average: 67.7 σ: 1.31	S1: 88.1 S2: 90.6 S3: 90.0 Average: 89.6 σ: 1.31	S1: 95.2 S2: 93.0 S3: 94.2 Average: σ: 1.10
C35R30A6	S1: 51.7 S2: 52.0 S3: 52.3 Average: 52.0 σ: 0.30	S1: 69.1 S2: 70.7 S3: 69.8 Average: 69.9 σ: 0.80	S1: 92.4 S2: 95.2 S3: 94.8 Average: 94.1 σ: 1.51	S1: 98.2 S2: 98.5 S3: 98.5 Average: 98.4 σ: 0.17

The highest level of later-age compressive strength was achieved for C35R30A6, which contained 30% RHA at the W/B ratio of 0.35. Conversely, the lowest level of compressive strength at all ages was obtained for C50R0A6, which was produced with a

W/B ratio of 0.50 and without any RHA. Nevertheless, the requirements for the early-age and later-age compressive strengths of high performance concrete, as listed in Table 2.2 (Chapter 2) were fulfilled for all SCHPCs. The development of good compressive strength is due to the use of optimum sand-aggregate (S/A) ratio and high-range water reducer (HRWR) that resulted in dense concretes with minimum voids.

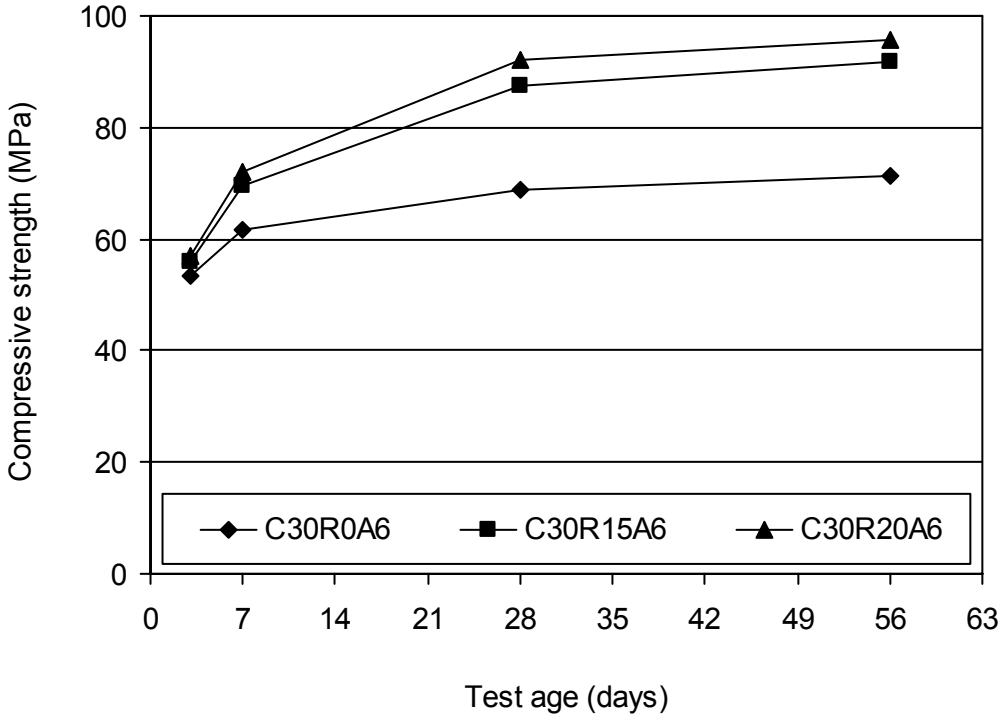

Figure 9.4: Compressive strength development of various concretes (W/B = 0.30)

9.5.1.1 Effect of water-binder ratio

The compressive strength of the concretes increased significantly with lower W/B ratio, as evident from Tables 9.3 and 9.4, and from Figures 9.7 and 9.8. The increase in compressive strength is directly related to the reduction in concrete porosity (Neville 1996, Neville and Brooks, 1999). In the present study, the total porosity of concrete decreased with lower W/B ratio. Hence, it can be inferred that the microstructure of concrete was improved in both bulk paste matrix and interfacial transition zone. Also, the cement content became higher at lower W/B ratio since the water content was kept constant for all concretes. It was deduced that the increased cement content improved the physical packing of aggregates and produced a greater amount of calcium silicate hydrate (CSH) leading to a higher compressive strength.

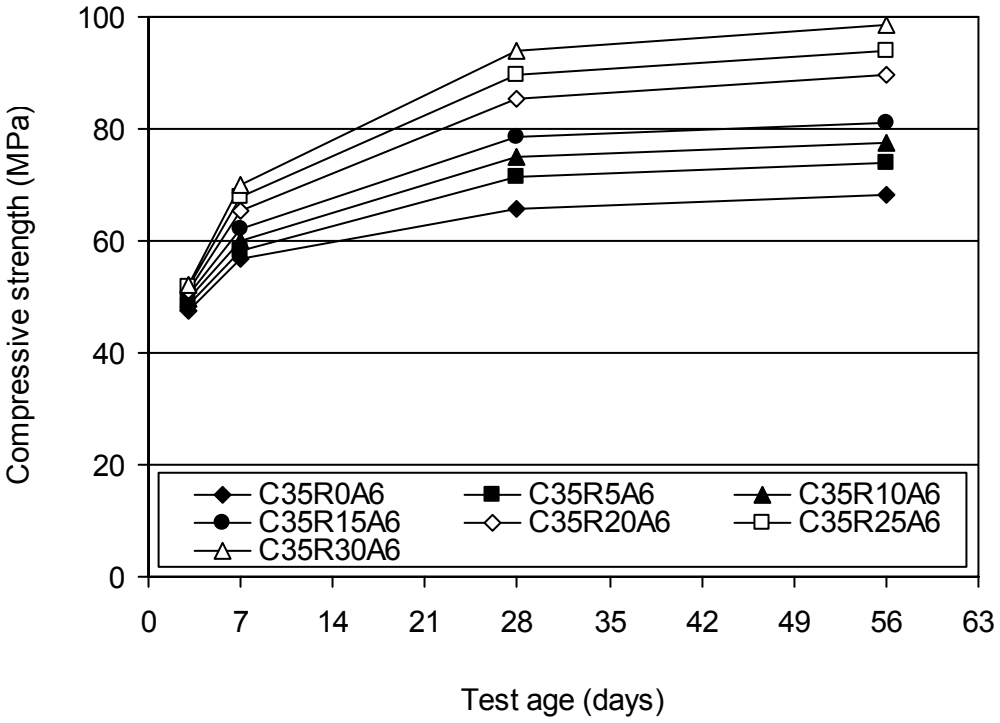

Figure 9.5: Compressive strength development of various concretes (W/B = 0.35)

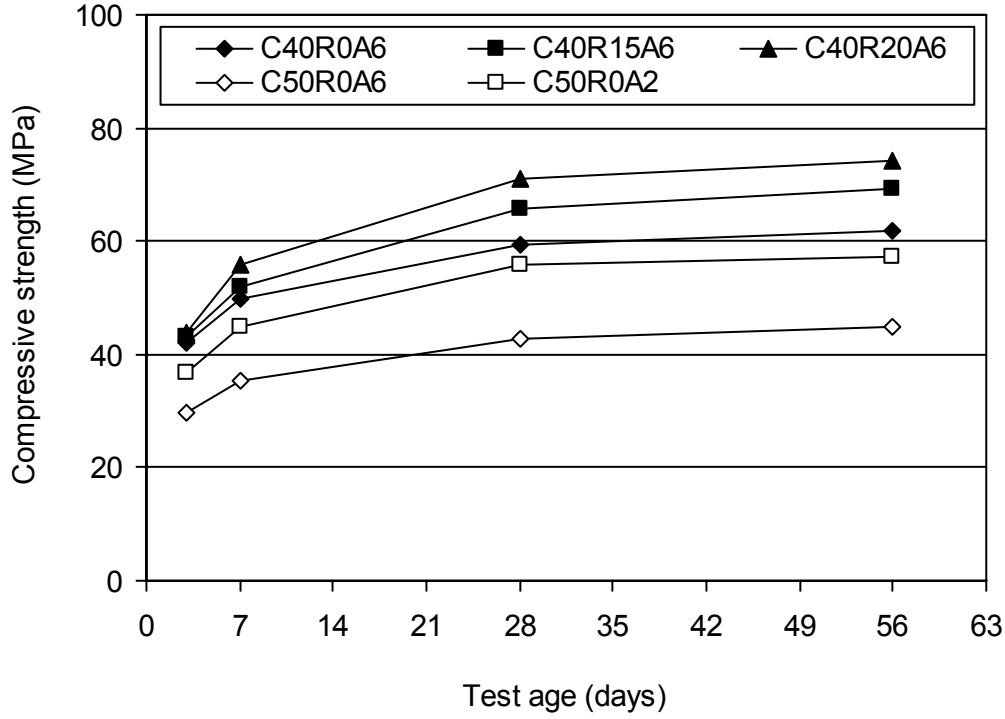

Figure 9.6: Compressive strength development of various concretes (W/B = 0.40 and 0.50)

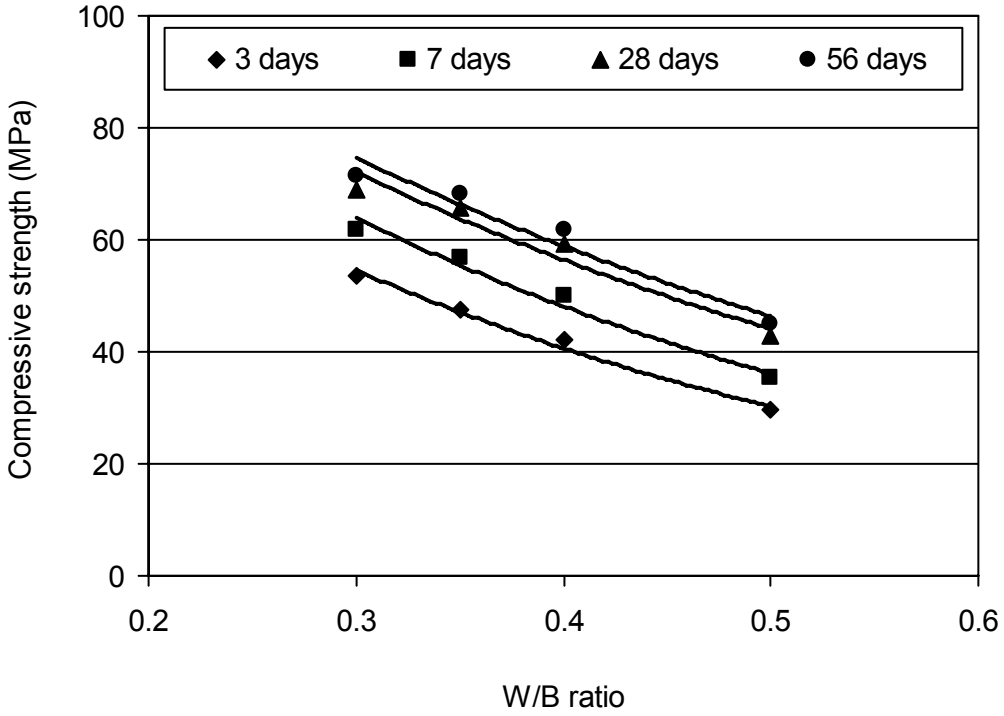

Figure 9.7: Effect of W/B ratio on the compressive strength of concretes without RHA

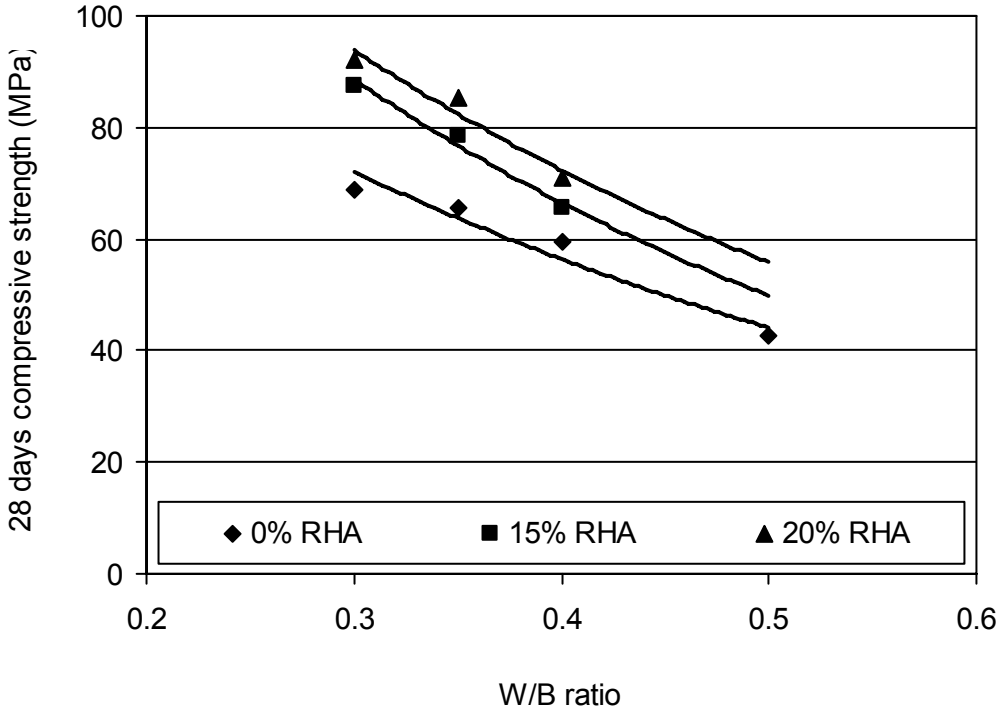

Figure 9.8: Effect of W/B ratio on the 28 days compressive strength of concretes with RHA

9.5.1.2 Effect of rice husk ash

The RHA significantly increased the compressive strength of concretes at the ages of 7, 28 and 56 days, as evident from Tables 9.3 to 9.4 and Figure 9.8. The improvement of compressive strength is mostly due to the microfilling ability and pozzolanic activity of RHA (see Section 2.9.5.3). With a smaller particle size, the RHA can fill the micro-voids within the cement particles. Also, the RHA readily reacts with water and calcium hydroxide, a by-product of cement hydration and produces additional calcium silicate hydrate or CSH (Yu et al. 1999). The additional CSH increases the compressive strength of concrete since it is a major strength-contributing compound. Also, the additional CSH reduces the porosity of concrete by filling the capillary pores, and thus improves the microstructure of concrete in bulk paste matrix and transition zone leading to increased compressive strength.

9.5.1.3 Effect of air content

The increased air content decreased the compressive strength of concretes. This is obvious from the compressive strength development in concretes 'C50R0A2' and 'C50R0A6', as presented in Figure 9.6. The air content of C50R0A2 was 1.8% whereas C50R0A6 had an air content of 5.2%. For 3.4% increase in air content, the reduction in 28 days compressive strength was 13.0 MPa. Thus, the compressive strength was reduced by 3.82 MPa per 1% increase in air content. The decrease in compressive strength with increased air content is due to the reason that the entrained air-voids increase the void content of concrete (Neville 1996).

9.5.2 Ultrasonic pulse velocity

The average test results for the 28 and 56 days ultrasonic pulse velocity of the concretes are presented in Figures 9.9 to 9.11. The ultrasonic pulse velocity varied in the range of 4.730 to 5.097 km/s, thus indicated an excellent physical condition of the concretes. This is because an ultrasonic pulse velocity higher than 4.575 km/s generally indicates an excellent quality of concrete (Demirboğa et al. 2004, Leslie and Cheeseman 1949). The excellent ultrasonic pulse velocity attained was mostly due to the improved pore structure of concretes resulting from optimum S/A ratio and enhanced filling ability. Also, the ultrasonic pulse velocity of all concretes at 56 days was greater than that at 28 days, which is due to reduced porosity resulting from continued hydration of the cementing materials.

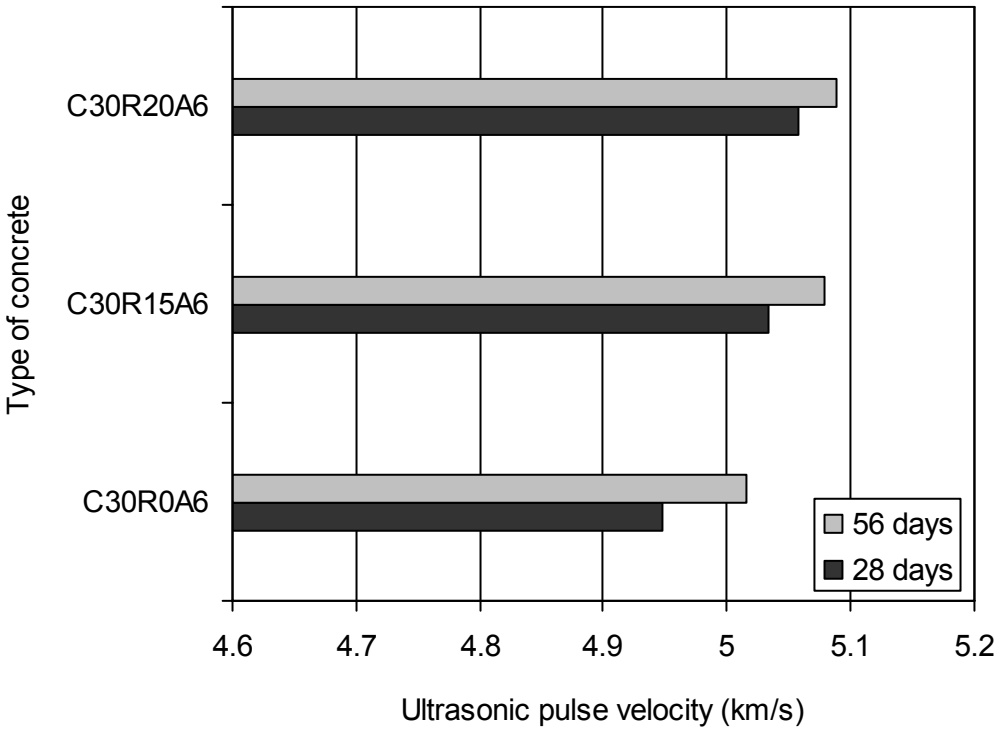

Figure 9.9: Ultrasonic pulse velocity of various concretes (W/B = 0.30)

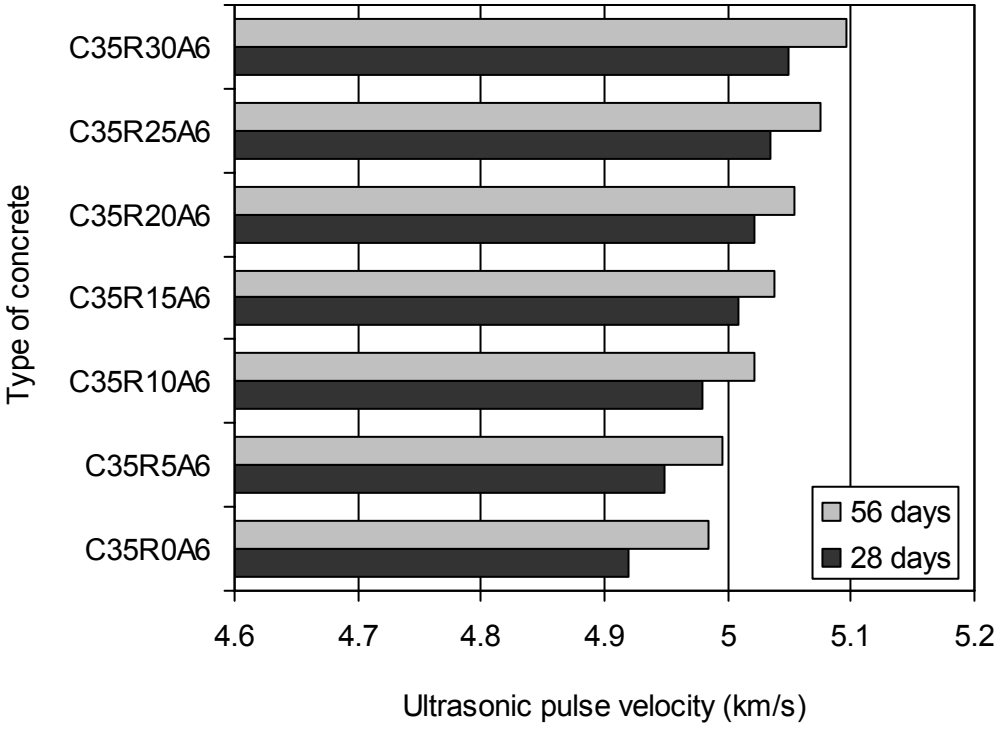

Figure 9.10: Ultrasonic pulse velocity of various concretes (W/B = 0.35)

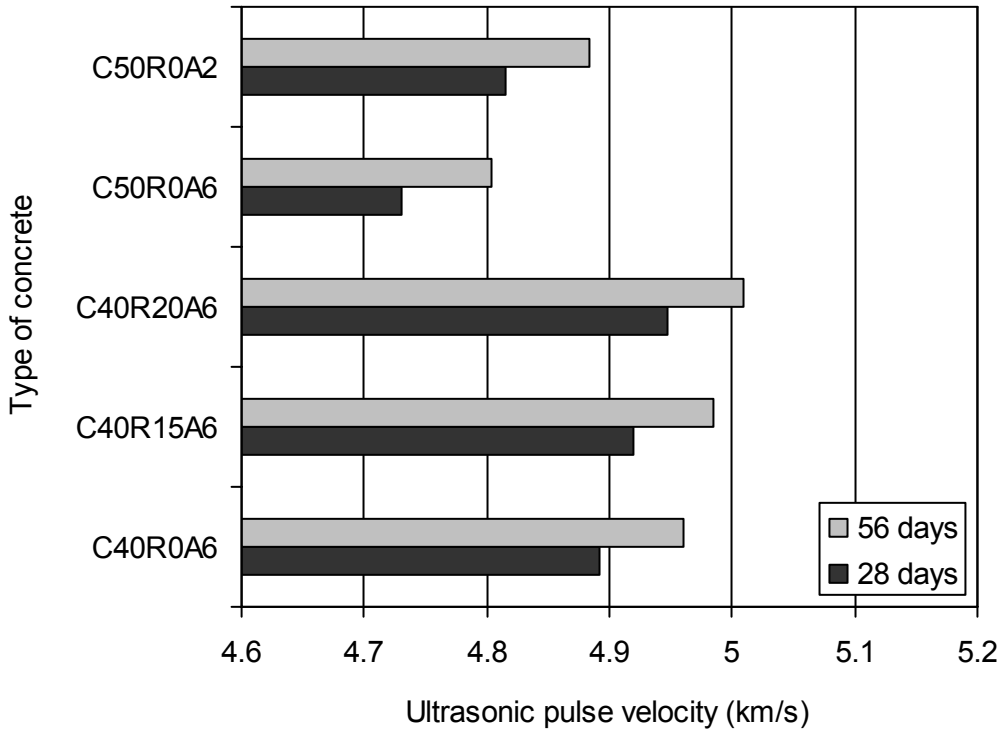

Figure 9.11: Ultrasonic pulse velocity of various concretes (W/B = 0.40 and 0.50)

9.5.2.1 Effect of water-binder ratio

The ultrasonic pulse velocity of the concretes was increased with lower W/B ratio, as evident from Figures 9.12 and 9.13. A similar effect was noticed in an earlier study (Lin et al. 2003). In the present study, the maximum increase in pulse velocity was 4.61%. The highest level of ultrasonic pulse velocity was achieved for the concretes prepared with the W/B ratio of 0.30 due to reduced porosity of concrete resulting from greater volume of hydration products (Section 9.5.4.1). In contrast, the lowest level of ultrasonic pulse velocity was obtained for the two concretes produced with a W/B ratio of 0.50 due to increased porosity. However, the range of ultrasonic pulse velocity (4.730 to 4.884 km/s > 4.575 km/s) obtained for this W/B ratio still represents an excellent physical quality of concrete. This is possibly due to the reason that the aggregate content was increased at higher W/B ratios, as evident from Tables 7.3 and 7.5 (Chapter 7). The higher aggregate content accelerates the propagation of the pulse through concrete and therefore the ultrasonic pulse velocity is increased for the same strength level (Naik and Malhotra 1991, Shetty 2001).

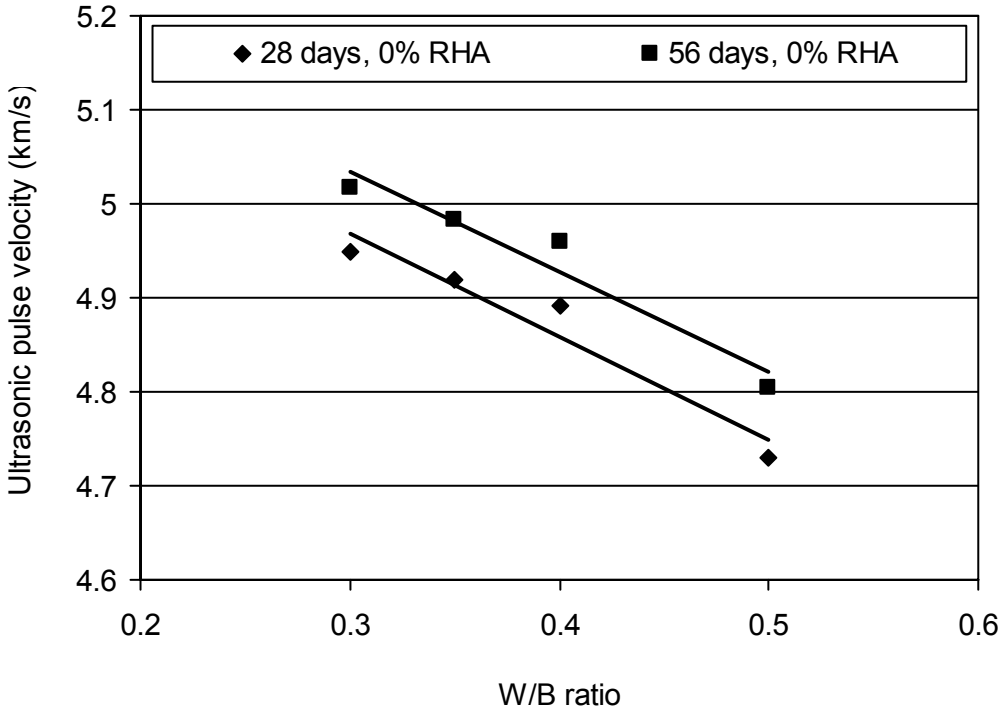

Figure 9.12: Effect of W/B ratio on the ultrasonic pulse velocity of concretes

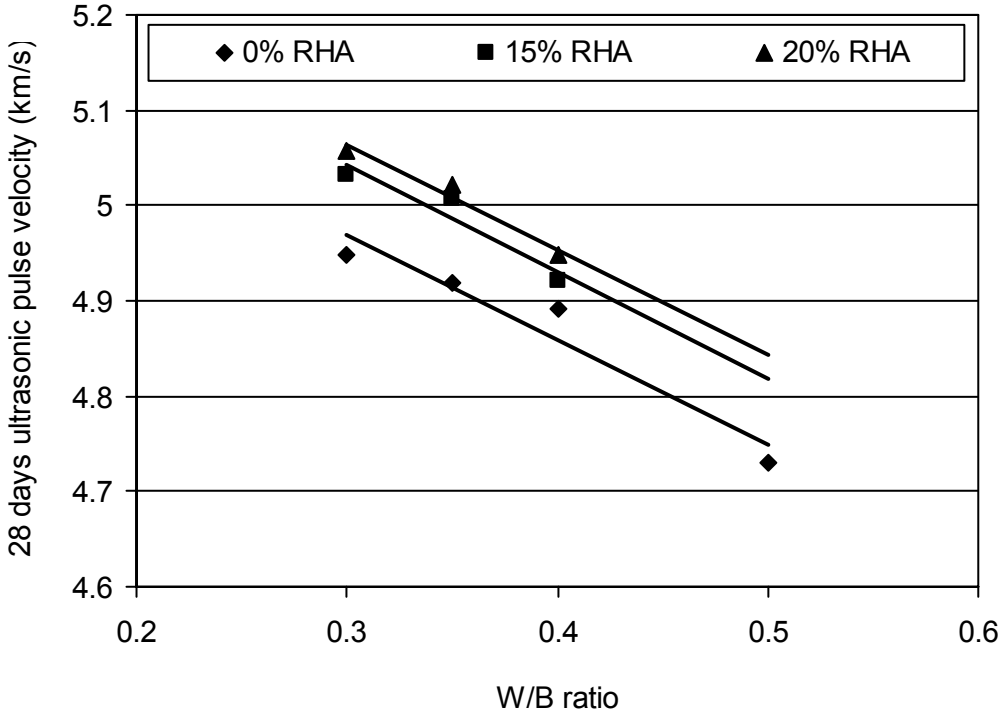

Figure 9.13: Effect of W/B ratio and RHA content on the 28 days ultrasonic pulse velocity of concretes

9.5.2.2 Effect of rice husk ash

The presence of RHA increased the ultrasonic pulse velocity, as can be seen from Figures 9.9 to 9.11, and Figure 9.13. It suggests that the use of RHA improved the quality of concrete through reduced porosity and densification of its pore structure. The physical and chemical modification of the pore structure of concrete occurs in the presence of RHA due to its microfilling and pozzolanic effects (see Section 9.5.1.2). This results in pore refinement and porosity reduction leading to a dense pore structure in both bulk paste matrix and transition zone of concrete that contributes to increase the ultrasonic pulse velocity. However, the increase in ultrasonic pulse velocity with increased RHA content was not as significant as the increase in compressive strength. The maximum increase in ultrasonic pulse velocity was about 2.66%. It indicates that the ultrasonic pulse velocity is less sensitive to the micro-porosity of concrete. Also, the aggregate content was slightly decreased with the increase in RHA content, as can be seen from Tables 7.3 and 7.5 (Chapter 7). This can reduce the positive effect of RHA on the ultrasonic pulse velocity of concrete since a reduction in aggregate content decreases the ultrasonic pulse velocity of concrete (Naik and Malhotra 1991, Shetty 2001).

9.5.2.3 Effect of air content

The ultrasonic pulse velocity of the non-air-entrained concrete was higher than that of air-entrained concrete produced with the same W/B ratio, as can be seen from Figure 9.11. At both 28 and 56 days, the concrete 'C50R0A2' containing 1.8% entrapped air content provided higher ultrasonic pulse velocity than the concrete 'C50R0A6', which had 5.2% total air content. This indicates that the presence of entrained air-voids delayed the propagation of the pulse leading to a lower ultrasonic pulse velocity. This is probably due to greater number of pores and CSH gel/pore interfaces in the presence of entrained air-voids that may influence the passage of the ultrasonic pulse, and hence its velocity through concrete.

9.5.3 Water absorption

The average test results for the water absorption of the concretes are illustrated in Figures 9.14 to 9.16. The lower water absorption was obtained at 56 days for all concretes. The reason is the same as discussed in Sections 9.5.1 and 9.5.2. Nevertheless, the water

absorption varied from 2.89% to 5.97%, which is relatively low. The water absorption of SCHPC generally varies in the range of 3 to 6%, as mentioned in Table 2.2 (Chapter 2). The non-RHA concretes provided higher water absorption than the RHA concretes. For example, the concretes with higher W/B ratio and without any RHA such as 'C50R0A2' and 'C50R0A6' provided a water absorption close to 5% at both ages, as can be seen from Figure 9.16. In addition, the concrete 'C40R0A6' provided 5.25% and 5% water absorption at 28 and 56 days, respectively. The lowest level of water absorption was obtained for the concrete 'C35R30A6', which provided 3.03% and 2.89% water absorption at the age of 28 and 56 days, respectively. In contrast, the highest level of water absorption was found for the concrete 'C50R0A2', which provided 5.97% and 5.85% water absorption at the age of 28 and 56 days, respectively. The low range of water absorption (2.89 to 5.97%) obtained was due to the limited pore connectivity and reduced porosity of the concretes. The water absorption of concrete becomes low when the capillary porosity is less than 15%, since most of the pores appear to be discontinuous (Bentz and Haecker 1999, Parrott 1992) and thus the flow channels for the water movement are reduced.

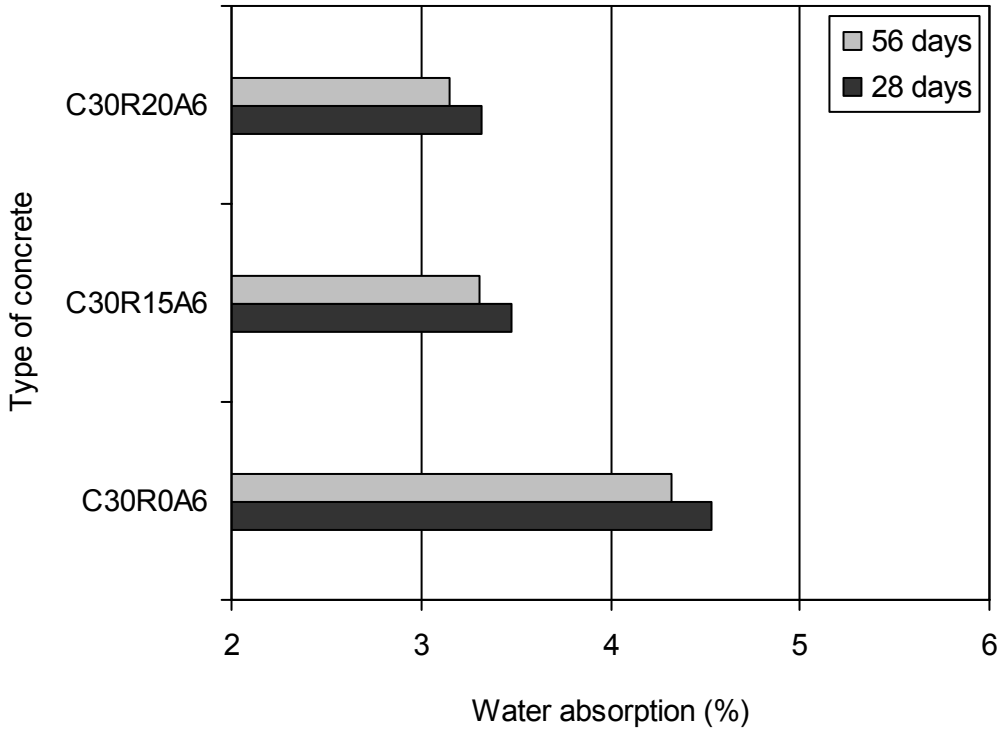

Figure 9.14: Water absorption of various concretes (W/B = 0.30)

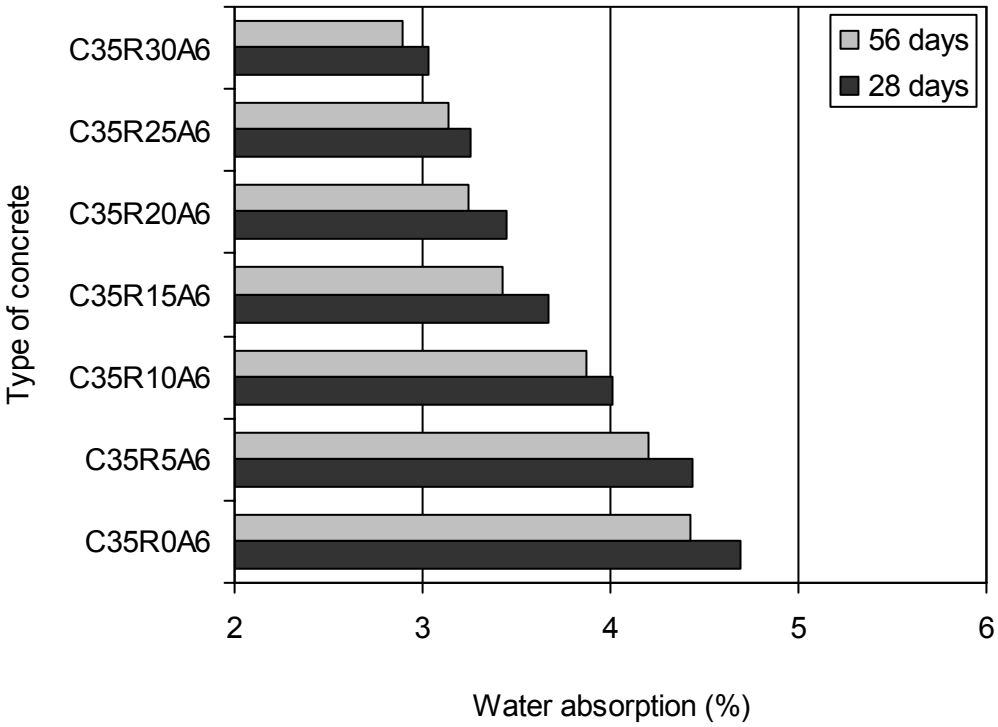

Figure 9.15: Water absorption of various concretes (W/B = 0.35)

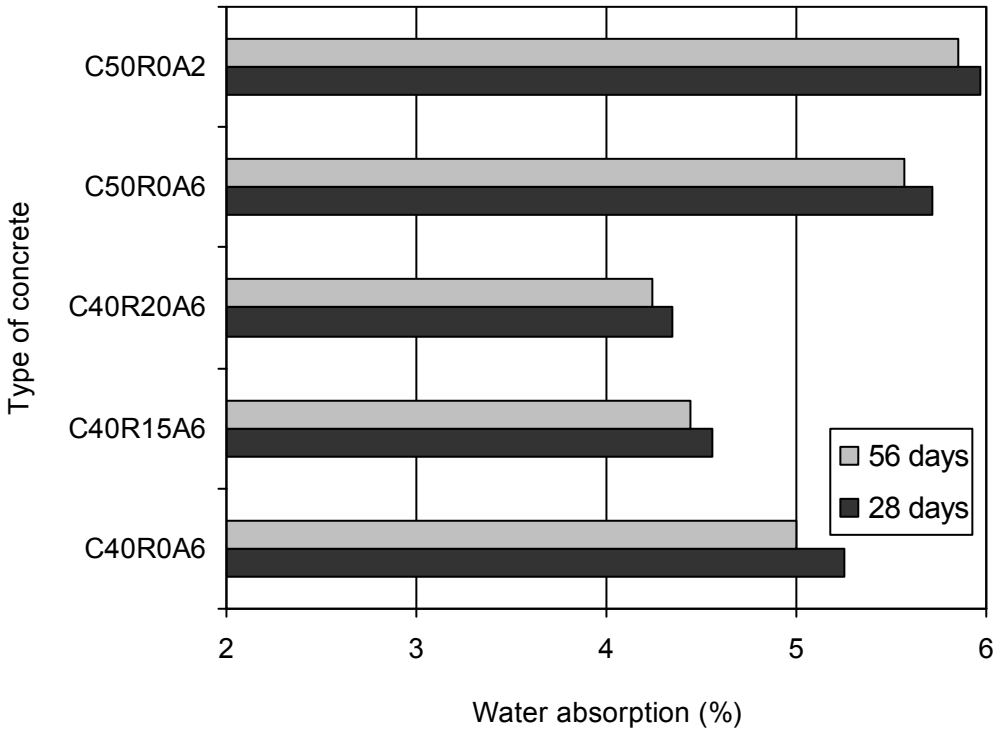

Figure 9.16: Water absorption of various concretes (W/B = 0.40 and 0.50)

9.5.3.1 Effect of water-binder ratio

The water absorption of the concretes at both ages of 28 and 56 days varied linearly with the W/B ratios. It was reduced with lower W/B ratio, as can be seen from Figures 9.17 and 9.18. In the absence of RHA, the highest level of water absorption was obtained for the concretes prepared with the W/B ratio of 0.50. Conversely, the lowest level of water absorption was achieved for the concrete produced with the W/B ratio of 0.30. In the case of non-RHA concretes, the reduction in water absorption at the W/B ratio of 0.30 was about 25% in comparison with the W/B ratio of 0.50. In the presence RHA, the water absorption of concrete was also decreased with lower W/B ratio, as evident from Figure 9.18. The reasons are the same as discussed in Sections 9.5.1.1 and 9.5.2.1.

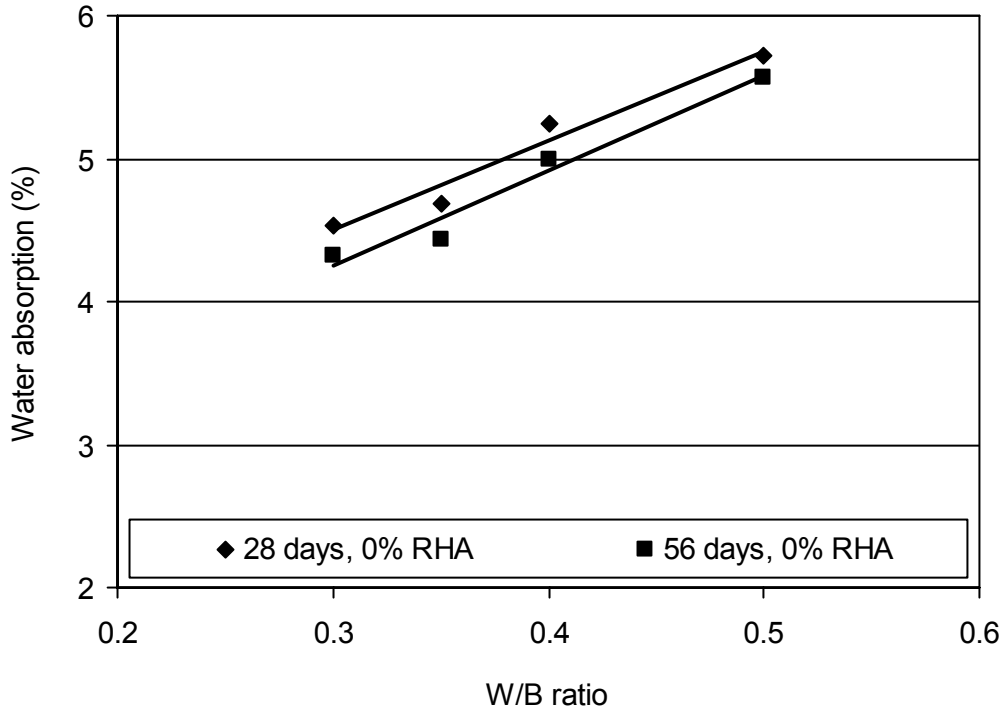

Figure 9.17: Effect of W/B ratio on the water absorption of concretes

9.5.3.2 Effect of rice husk ash

The water absorption of the concretes was decreased with greater RHA content, as can be seen from Figure 9.18. This is also evident from Figures 9.14 to 9.16. Similar results were reported by Coutinho (2003) and Mahmud et al. (2004) for medium and high strength

concretes. In the present study, the RHA produced a higher degree of reduction in water absorption for different W/B ratios. This is evident from the steeper slope of the lines representing the RHA concretes in Figure 9.18. The lowest level of water absorption was attained for 30% RHA used in the concrete 'C35R30A6', which provided about 35% reduced water absorption than C35R0A6 at 28 and 56 days. The significant reduction in water absorption obtained is primarily credited to the reduced porosity of the concretes at higher RHA content, as discussed in Sections 9.5.1.2 and 9.5.2.2.

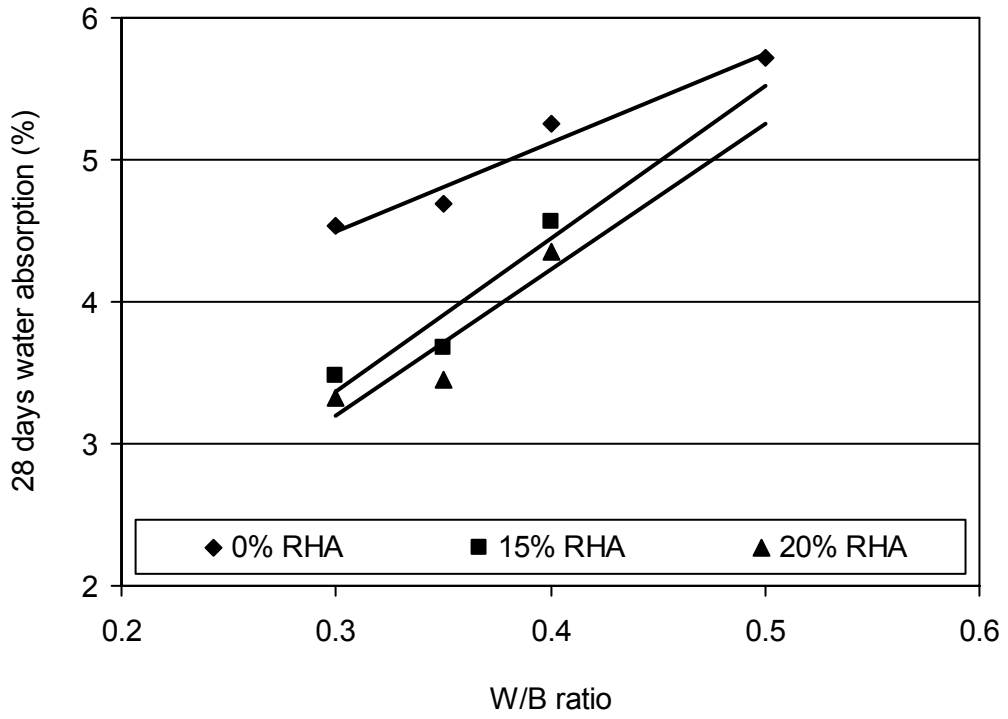

Figure 9.18: Effect of W/B ratio and RHA content on the 28 days water absorption of concretes

9.5.3.3 Effect of air content

The water absorption of concrete was slightly reduced in the presence of entrained air-voids. It can be seen from Figure 9.16 that the concrete 'C50R0A2' containing 1.8% entrapped air provided higher water absorption than the concrete 'C50R0A6' containing 5.2% total air content. Similar results were obtained by Dhir et al. (1987). The reason is that the porosity of C50R0A6 was reduced due to the presence of entrained air-voids (see Section 9.5.4.3).

9.5.4 Total porosity

The average test results for the total porosity of concretes are illustrated in Figures 9.19 to 9.21. The total porosity ranged from 6.77 to 13.71%. The lowest level of porosity was obtained for the concrete 'C35R30A6', with the total porosity of 7.07% and 6.77%, respectively, at 28 and 56 days. In contrast, the highest level of porosity was attained for the concrete 'C50R0A2', which provided a total porosity of 13.71% and 13.38% at 28 and 56 days, respectively. The overall test results of total porosity suggest that the quality of the concretes was good. The total porosity of high-quality concrete is about 7% whereas that of average-quality concrete is 15% (Hearn et al. 1994). The lowest level of total porosity was obtained for all concretes at the age of 56 days for the same reasons as discussed before. In addition, the pore structure of the concretes was improved due to the use of HRWR. The HRWR induces high consistency in concrete, and thus improves the packing in the range of the fines. Also, the HRWR enhances the hydration process by dispersing the cement grains (Collepardi and Massidda 1976). Thus, both total porosity and pore diameter are reduced in concretes.

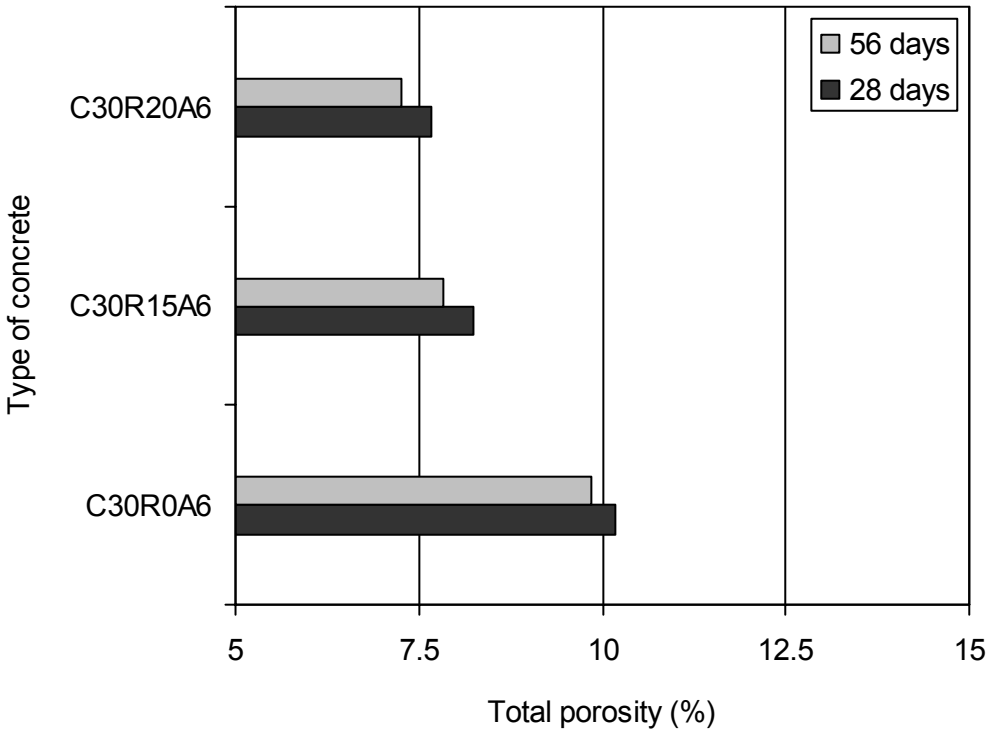

Figure 9.19: Total porosity of various concretes (W/B = 0.30)

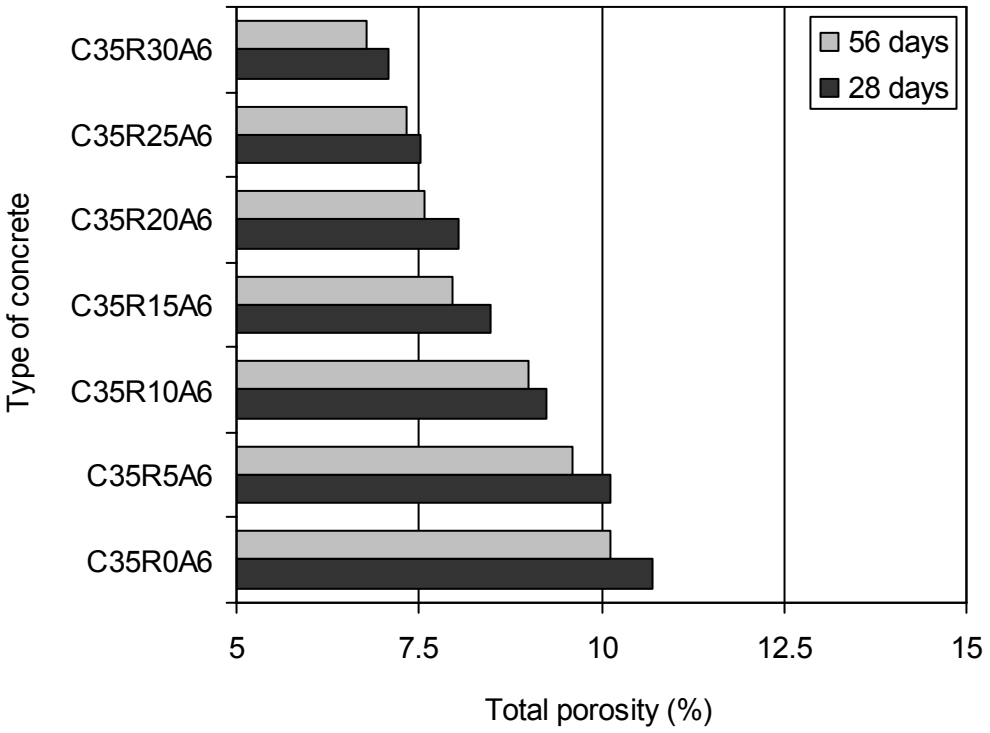

Figure 9.20: Total porosity of various concretes (W/B = 0.35)

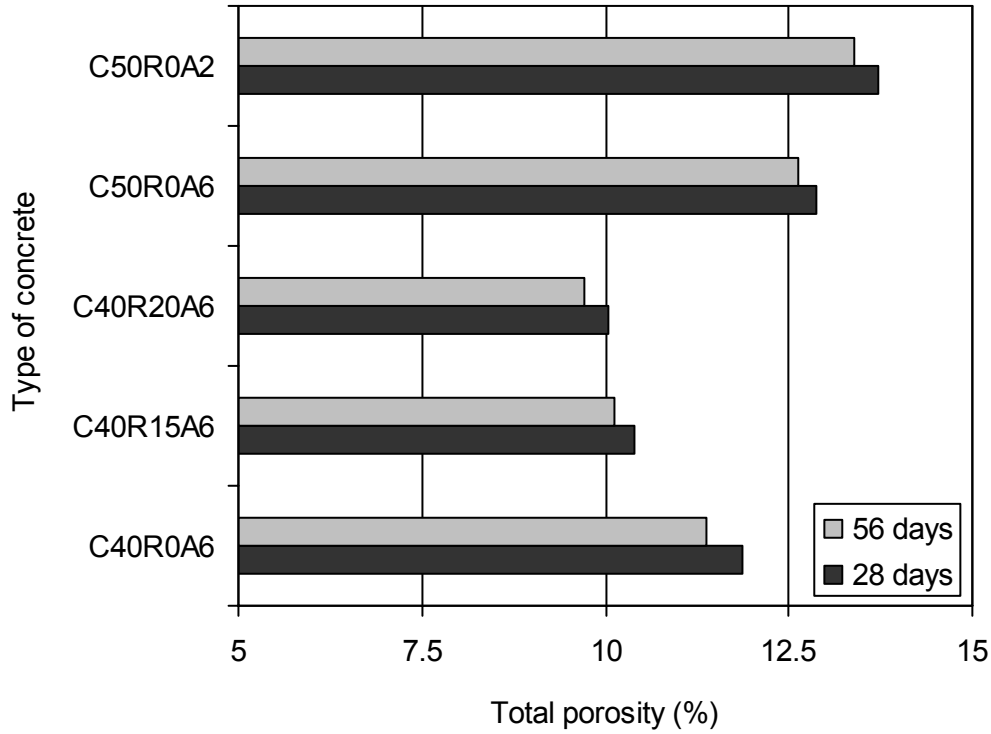

Figure 9.21: Total porosity of various concretes (W/B = 0.40 and 0.50)

9.5.4.1 Effect of water-binder ratio

The total porosity of the concretes was increased with higher W/B ratio, as can be seen from Figures 9.22 and 9.23. A similar effect of W/B ratio on porosity was observed by other researchers in case of normal and high performance concretes (Roy 1994, Maeda et al. 2001). The reasons are discussed in Sections 9.5.1.1 and 9.5.2.1. Furthermore, the total porosity of the concretes was relatively high at the W/B ratio of 0.50. This is possibly due to the reason that the W/B ratio was higher than the minimum W/B ratio needed to eliminate the capillary pores. For a W/B ratio greater than 0.38, the bulk volume of CSH gel is not sufficient to fill all water-filled pores and therefore some capillary pores still remain in binder paste even after complete hydration (Hearn et al. 1994, Neville 1996). Thus, the total porosity appears to be higher at the W/B ratio of 0.50.

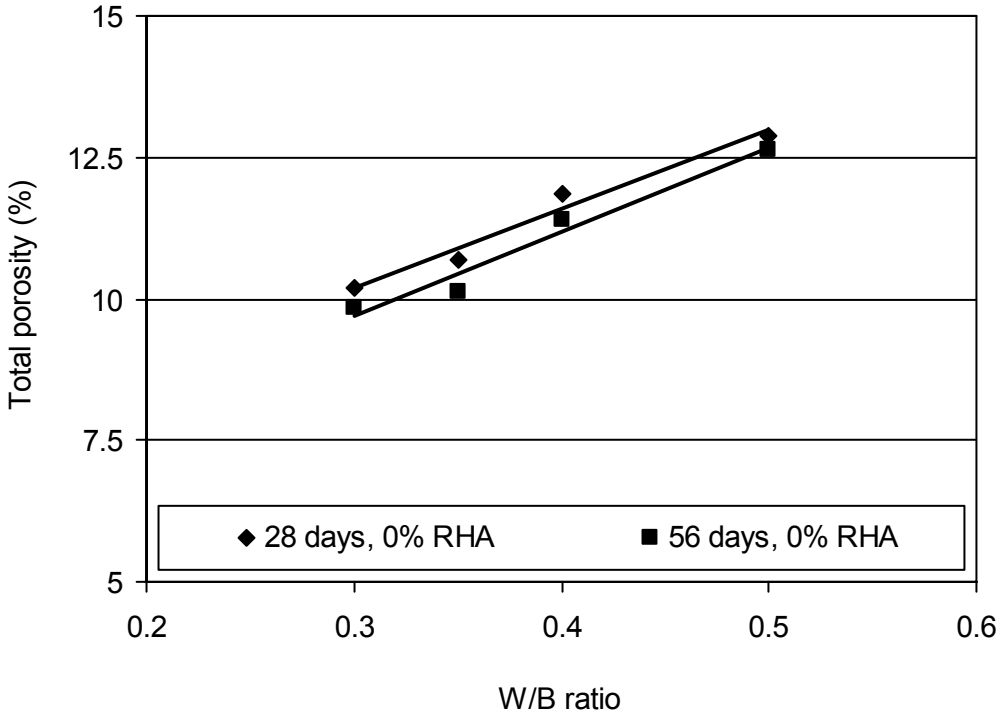

Figure 9.22: Effect of W/B ratio on the total porosity of concretes

9.5.4.2 Effect of rice husk ash

The total porosity of the concretes was decreased with greater RHA content, as evident from Figures 9.19 to 9.21, and Figure 9.23. A similar effect of RHA on porosity was observed in

previous research for normal and high performance concretes (Maeda et al. 2001, Sugita et al. 1997). In the present study, the total porosity of concrete was decreased by 5% to 35% for various RHA contents. Thus, it was understood that the physical and chemical effects of RHA modified the open channels at the cement paste matrix and transition zone of concrete leading to a discontinuous pore structure with reduced total porosity. Indeed, the presence of RHA contributes to produce a dense pore structure in concrete by decreasing the amount and average size of the pores (Sugita et al. 1997, Zhang et al. 1996).

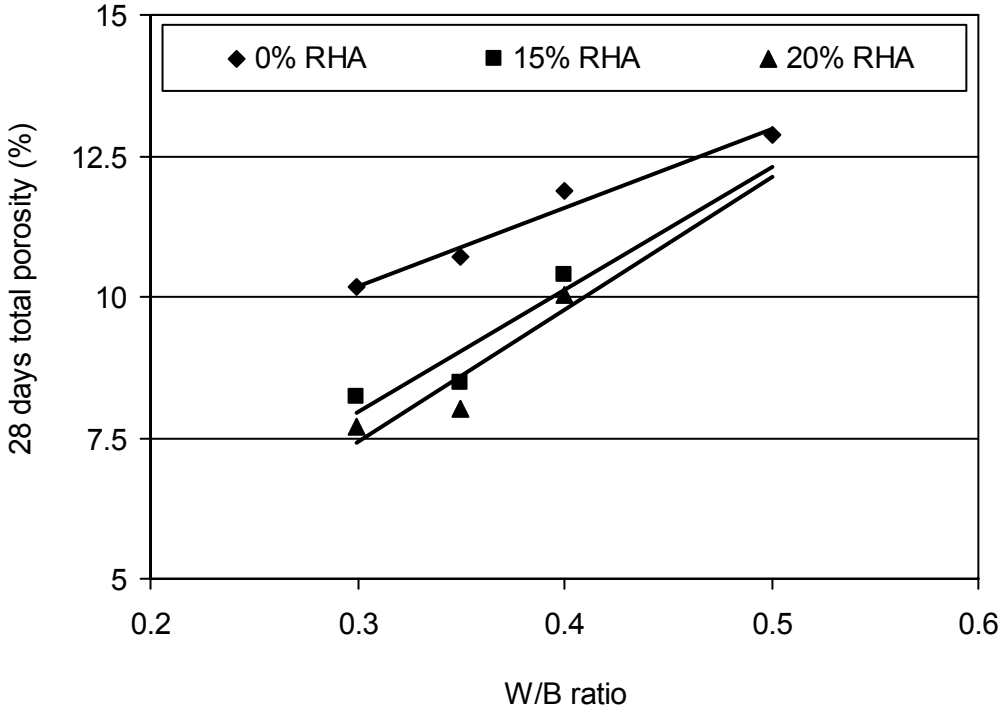

Figure 9.23: Effect of W/B ratio and RHA content on the 28 days total porosity of various concretes

9.5.4.3 Effect of air content

The air-entrained concrete 'C50R0A6' provided lower total porosity than the non-air-entrained concrete 'C50R0A2', as can be seen from Figure 9.21. This is due to the combined effect of reduced water content and non-connectivity of the air-voids (Dhir et al. 1987). Also, the total volume of capillary pores becomes lower in air-entrained concrete since a part of the gross volume of hardened cement paste is entrained air (Neville 1996).

9.5.5 Electrical resistivity

The average test results for the true electrical resistivity of various concretes are presented in Figures 9.24 to 9.26. The true electrical resistivity of the concretes varied in the range of 4.1 to 121.2 kΩ-cm for different types of concrete. The true resistivity of concretes must be greater than 5 kΩ-cm, since the corrosion rate can be high below this limit (Hearn 1996). The concrete exhibits moderate to low corrosion rate when its true resistivity is between 5 and 10 kΩ-cm, whereas good corrosion resistance is obtained when the true resistivity is above 10 kΩ-cm (Hearn 1996, Neville 1996). All RHA concretes provided an electrical resistivity higher than 10 kΩ-cm. In contrast, the non-RHA concretes exhibited the electrical resistivity in the range of 4.1 to 8.9 kΩ-cm. Moreover, the true electrical resistivity of all concretes was higher at the age of 56 days. The true resistivity at 56 days was about 9.8% to 92.7% higher than that at 28 days for various concretes. A similar effect of curing age was noticed in an earlier research (Hossain 2005). This is due to the reduced porosity at the later age. Also, the ionic concentration in pore solution decreases at later age due to enhanced pozzolanic reaction, and consequently the resistivity is increased (Selvaraj et al. 2003).

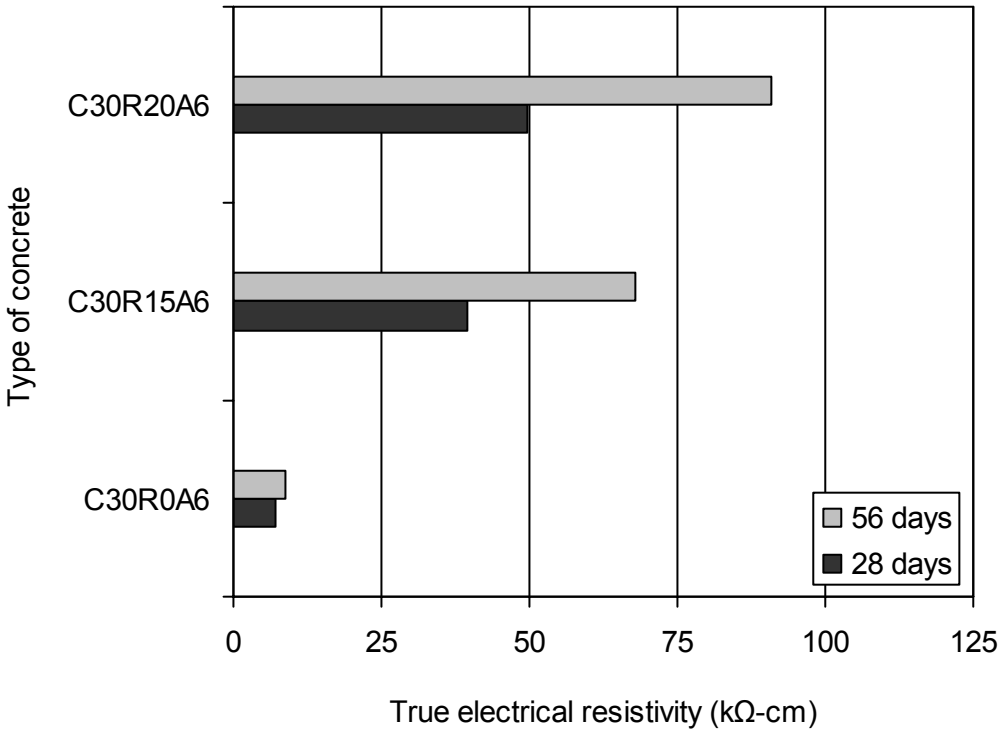

Figure 9.24: True electrical resistivity of various concretes (W/B = 0.30)

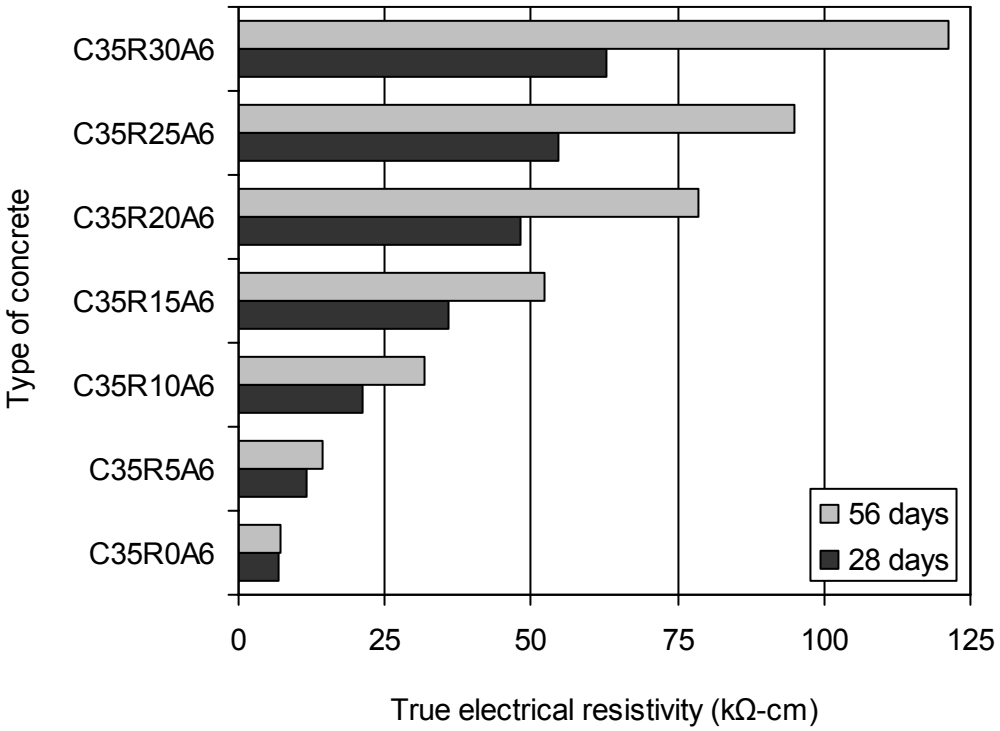

Figure 9.25: True electrical resistivity of various concretes (W/B = 0.35)

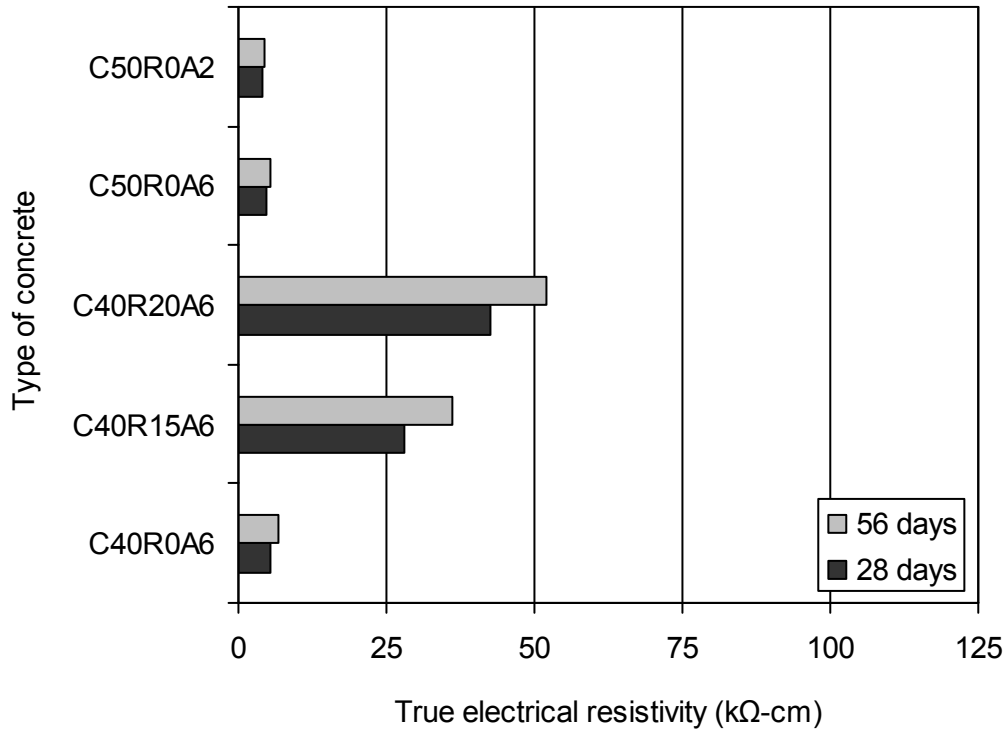

Figure 9.26: True electrical resistivity of various concretes (W/B = 0.40 and 0.50)

9.5.5.1 Effect of water-binder ratio

The true electrical resistivity of concrete was increased with lower W/B ratio, as can be seen from Figures 9.27 and 9.28. In the absence of RHA, the highest level of resistivity was observed at the W/B ratio of 0.30. This is due to the densification of the paste microstructure with reduced porosity. Conversely, the lowest level of resistivity was obtained for the non-RHA concretes with the W/B ratio of 0.50. This is because the higher W/B ratio increases the porosity and thus enhances the ionic movement resulting in reduced electrical resistivity. A similar effect of W/B ratio on electrical resistivity of concrete was reported by Roper (1994).

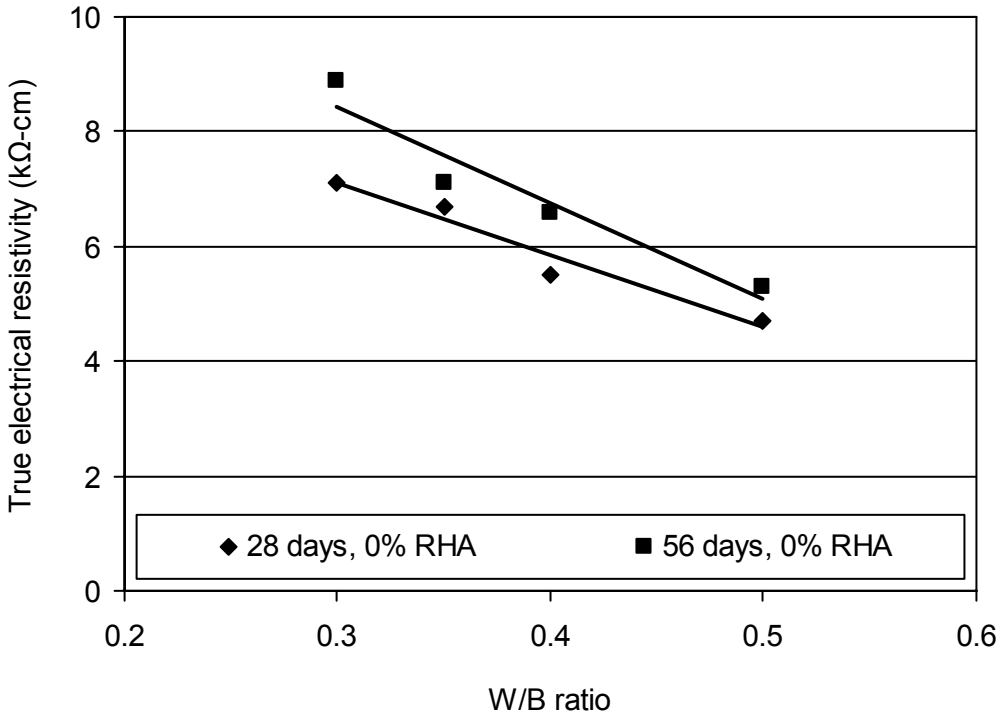

Figure 9.27: Effect of W/B ratio on the true electrical resistivity of concretes

9.5.5.2 Effect of rice husk ash

The presence of RHA increased the true electrical resistivity of concretes, as can be seen from Figures 9.24 to 9.26, and Figure 9.28. It is due to the reduced porosity and pore refinement produced by RHA. The resistivity usually increases with lower porosity and smaller pore size (Hossain 2005, Tumidajski 2005), as the flow of ions through the pore

spaces is hindered. In addition, the use of RHA reduces the amount of hydroxyl and alkali ions, which are the main ions that carry charge (Claisse 2005). Therefore, the electrical resistivity was greatly increased in the presence of RHA. Also, the RHA resulted in substantially high resistivity at 56 days. In particular, the increase was relatively high as compared to other properties such as compressive strength. This is probably due to the combined effect of porosity reduction and pozzolanic reaction. A pozzolanic material generally exhibits high resistivity despite its contribution to the compressive strength of concrete (Ampadu and Torii 2002, Roper 1994).

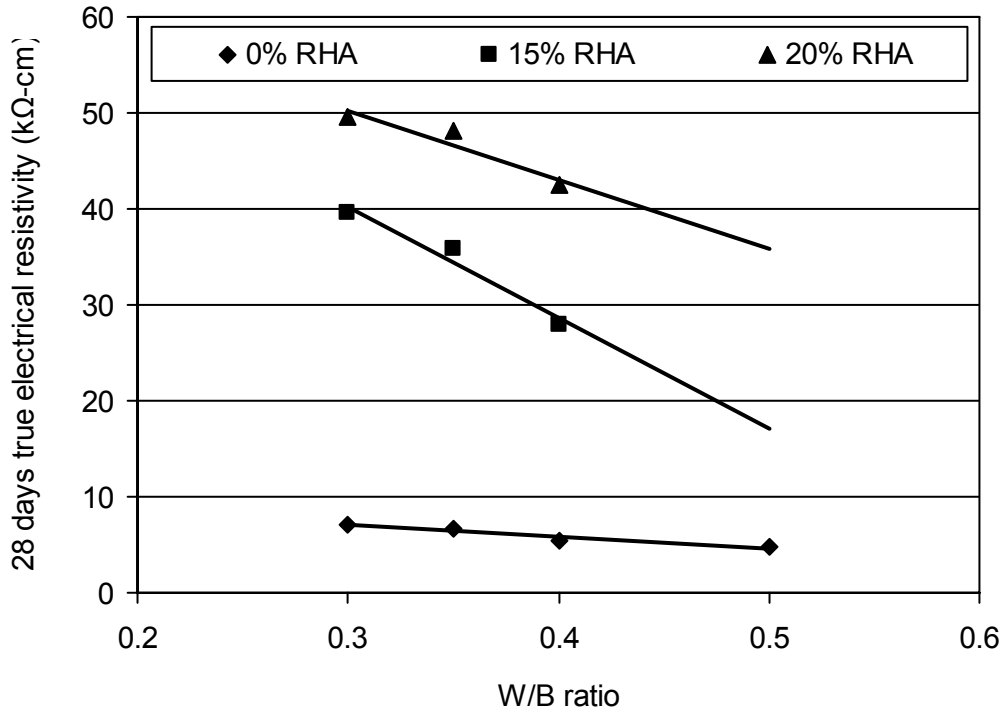

Figure 9.28: Effect of W/B ratio and RHA content on the 28 days true electrical resistivity of concretes

9.5.5.3 Effect of air content

The electrical resistivity of concrete was increased in the presence of entrained air-voids. It can be seen from Figure 9.26 that the concrete 'C50R0A6' with 5.2% total air content provided slightly greater resistivity than the concrete 'C50R0A2' containing 1.8% entrapped air content. This is related to the total porosity of these two concretes. The concrete 'C50R0A6' provided lower total porosity than the concrete 'C50R0A2'. Moreover, the

capillary porosity is decreased in the presence of entrained air-voids as discussed before. Consequently, the ionic movement was reduced and the resistivity became higher.

9.6 Concrete Durability

The durability of the concretes was not tested directly in the present study. However, the hardened properties determined indicated a good durability for the majority of concretes. The ultrasonic pulse velocity and compressive strength results exhibited the excellent physical condition or quality of concretes with a reduced porosity, and thus pointed to good durability. In addition, the low range of water absorption and total porosity, and the high level of electrical resistivity obtained for most concretes suggested that they would show good durability. This is because the reduction in porosity enhances the freeze-thaw durability (Litvan 1973, Claisse 2005), decreases the water and gas permeability (Coppola et al. 2004), and increases the resistance to acid attack, carbonation and chloride penetration (Sugita et al. 1997). A lower range of water absorption indicates the reduced penetration of chlorides and other deleterious agents into concretes (McCarter et al. 1992). Also, the concretes with a true electrical resistivity higher than 10 kΩ-cm exhibit low chloride ion permeability (Chini et al. 2003, Kessler et al. 2005) and reduced corrosion rate (ACI 222R-01, 2004).

9.7 Correlations among Various Hardened Properties

The correlations for the compressive strength and ultrasonic pulse velocity, compressive strength and total porosity, ultrasonic pulse velocity and total porosity, and true electrical resistivity and total porosity were determined. They are presented and discussed below.

9.7.1 Compressive strength and ultrasonic pulse velocity

An exponential relationship was observed between the compressive strength and ultrasonic pulse velocity of all concretes, as can be seen from Figure 9.29. This relationship was found for the compressive strength ranging from 42.7 to 98.4 MPa and for the ultrasonic pulse velocity varying from 4.730 to 5.097 km/s. The coefficient of determination (R^2) for the best-fit curve was 0.929, and the correlation coefficient (R) was 0.964, which indicates an excellent relationship. This correlation was obtained for both later ages (28 and 56 days) of concretes. Thus, it was understood that the relationship between compressive strength and

ultrasonic pulse velocity is independent of the concrete age. A similar correlation was observed by Demirboğa et al. (2004) for the concretes including fly ash and slag. This is due to the reason that both compressive strength and ultrasonic pulse velocity are increased with the curing age of concretes (Naik and Malhotra 1991, Kaplan 1958). However, the variation in ultrasonic pulse velocity was insignificant as compared to the compressive strength of concrete.

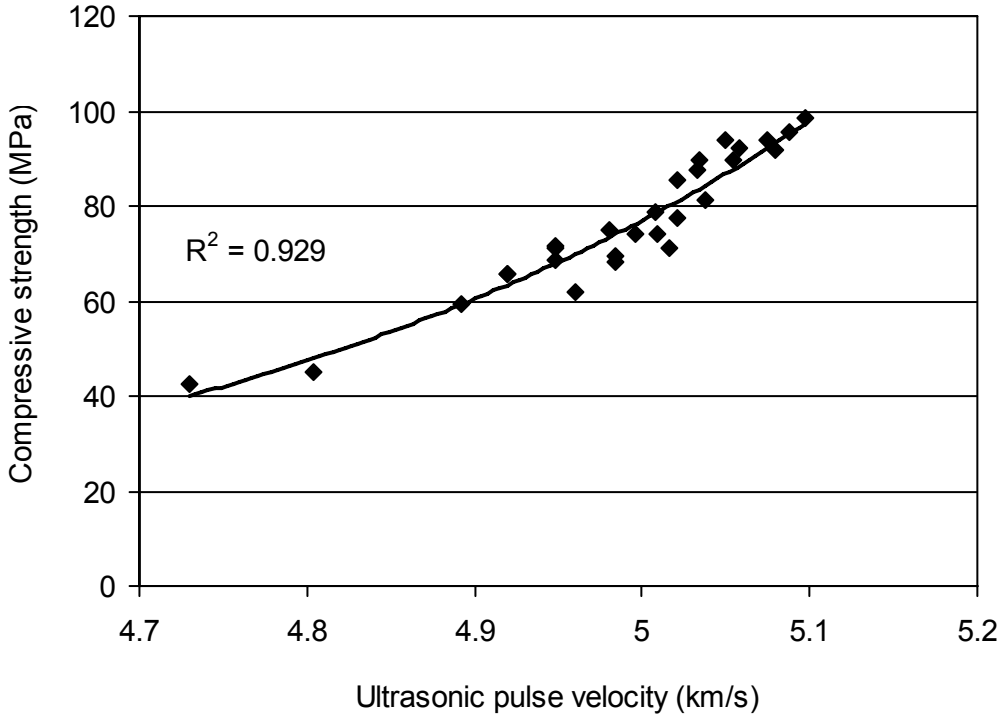

Figure 9.29: Correlation between compressive strength and ultrasonic pulse velocity

9.7.2 Compressive strength and total porosity

The compressive strength was well-correlated with the total porosity of concretes, as can be seen from Figure 9.30. The best-fit line exhibited a linear relationship between the compressive strength ranging from 42.7 to 98.4 MPa and the total porosity varying from 6.77 to 13.71%. The coefficient of determination for the best-fit line was 0.970, and the correlation coefficient was 0.985, which indicates an excellent relationship. A similar relationship between the compressive strength and total porosity of paste and concrete was noticed by other researchers (Al-Amoudi et al. 1996, Neville 1996). A single good correlation between compressive strength and total porosity was obtained for both ages of

concretes. Therefore, the relationship between compressive strength and total porosity was also independent of the curing age of concrete.

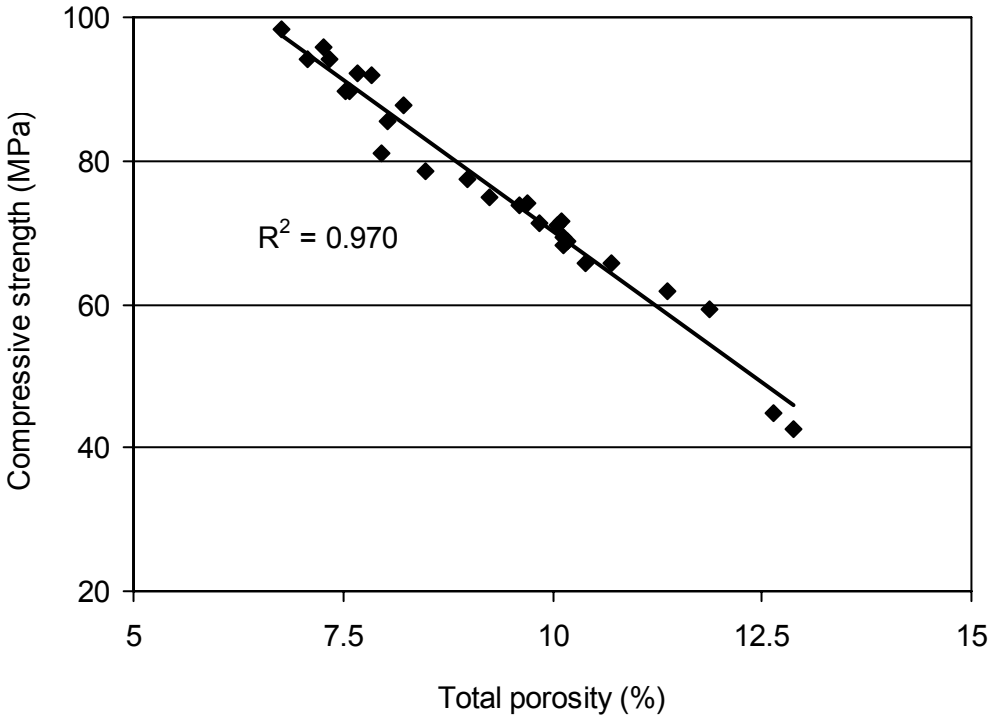

Figure 9.30: Correlation between compressive strength and total porosity

9.7.3 Ultrasonic pulse velocity and total porosity

The ultrasonic pulse velocity was well-correlated with the total porosity of concretes, as can be seen from Figure 9.31. The best-fit line exhibited a second-order polynomial relationship between the ultrasonic pulse velocity varying from 4.730 to 5.097 km/s and the total porosity ranging from 6.77 to 13.71%. The best-fit curve had a coefficient of determination of 0.901, and a correlation coefficient of 0.949, which indicates an excellent relationship. Also, the relationship was independent of the curing age of concrete since one single good correlation was valid for both ages.

9.7.4 Electrical resistivity and total porosity

The true electrical resistivity and total porosity of concretes were well-correlated, as evident from Figure 9.32. This relationship was obtained for the electrical resistivity ranging from

4.1 to 121.2 kΩ-cm and for the total porosity varying from 6.77 to 13.71%. The best-fit curve showed a power relationship with a coefficient of determination of 0.794 and a correlation coefficient of 0.891, which indicates a good relationship. However, the RHA concretes with relatively high W/B ratio such as C40R15A6 and C40R20A6 tended to deviate from this relationship. This is because the electrical resistivity of these two concretes significantly increased at higher RHA content where as the total porosity was relatively high due to increased capillary pores at the W/B ratio greater than 0.38.

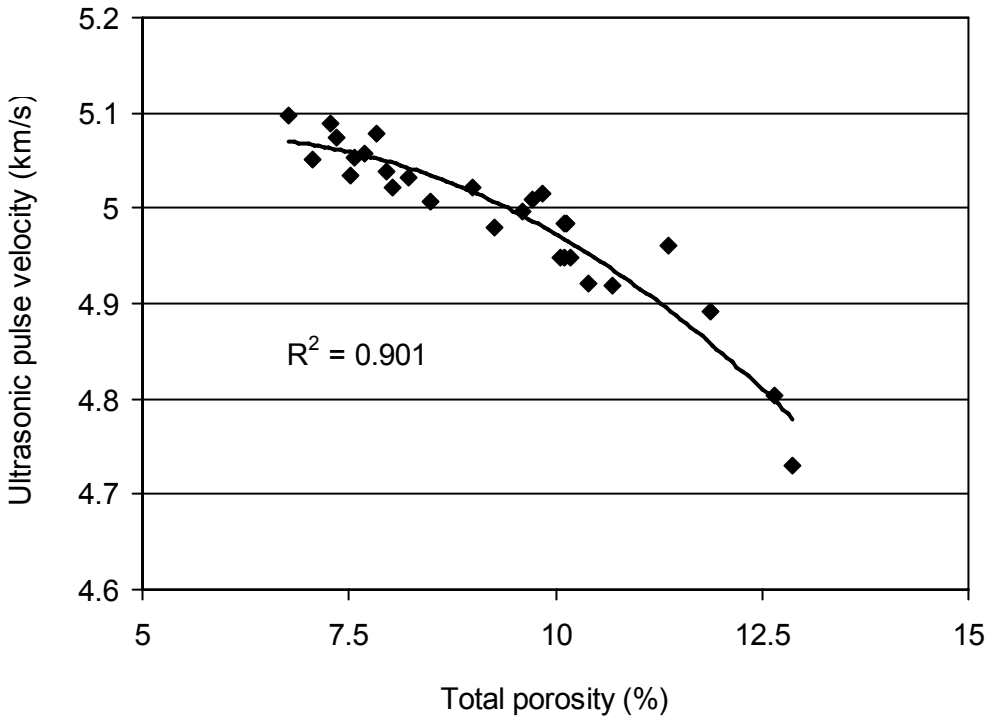

Figure 9.31: Correlation between ultrasonic pulse velocity and total porosity

The nature of the best-fit curve indicates that the true electrical resistivity appears to be very low when the total porosity of concrete is beyond 12.5%. Conversely, the true electrical resistivity becomes very high when the total porosity is below 7.5%. Furthermore, a single good correlation was valid for both 28 and 56 days curing ages. Thus, it was understood that the relationship between true electrical resistivity and total porosity is also independent of concrete age.

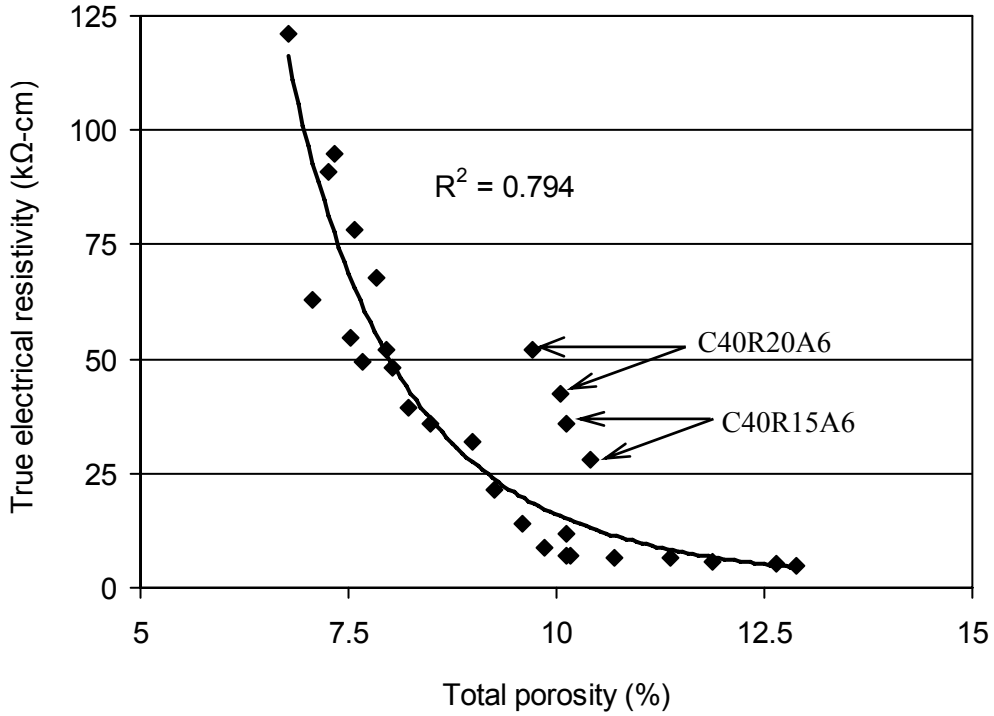

Figure 9.32: Correlation between true electrical resistivity and total porosity

9.8 Model for Compressive Strength

An empirical model for the compressive strength of SCHPC can be developed by combining a function for the strength development with time, and a second function correlating the specific strength with W/B ratio and RHA content, as presented in the equation below.

$$f_c(t) = f(t, t_s) \times f_{cs}\left(\frac{W}{B}, RHA\right) \qquad \text{(Equation 9.3)}$$

where:

$f_c(t)$ is the compressive strength at any time t (days), $f(t, t_s)$ is a strength-time function with $f(t_s, t_s) = 1$ at 28 days, and f_{cs} is the specified compressive strength of concrete. The 28 days strength 'f_{c28}' is most commonly used in practice to specify the compressive strength of concrete. Also, the strength increase at 56 days was only about 3 to 6% in the present study. Thus, replacing f_{cs} by 'f_{c28}', Equation 9.3 can be reformed as follows:

$$f_c(t) = f(t, 28) \times f_{c28}\left(\frac{W}{B}, RHA\right) \quad \text{(Equation 9.4)}$$

The strength-time function, *f (t, 28)* for a concrete can be expressed as follows (ACI 209R-92, 2004):

$$f(t, 28) = \frac{f_c(t)}{f_{c28}} = \frac{t}{\alpha + \beta t} \quad \text{(Equation 9.5)}$$

where:

α and β are constants that depend on the type of cement, concrete and curing method; $f_c(t)$, f_{c28}, and t have been explained before.

The constants α and β were determined using the results of compressive strength development with curing age and by plotting *1/f(t, 28)* over 1/t as shown in Figure 9.33. In determining α and β, the total strength-time data for all concretes with and without RHA were considered for simplification of the model. The influence of this simplification on the validity of the model is discussed in Section 9.8.1. The calculated value of α was 1.86 and that of β was 0.94. The values of α and β usually range from 0.05 to 9.25 and from 0.67 to 0.98, respectively (ACI 209R-92, 2004). Nevertheless, substituting α and β with the obtained values, Equation 9.5 can be reformed as follows:

$$f(t,28) = \frac{t}{1.86 + 0.94t} \quad \text{(Equation 9.6)}$$

The compressive strength of the concretes for different ages varied exponentially with the W/B ratios, as can be seen from Figure 9.7. In the absence of RHA, the following relationship was obtained using the trendline (see Figure 9.7) for the W/B ratio and 28 days compressive strength (f_{c028}) of concretes:

$$f_{c028} = 151\, e^{-2.46\frac{W}{B}}$$ (Equation 9.7)

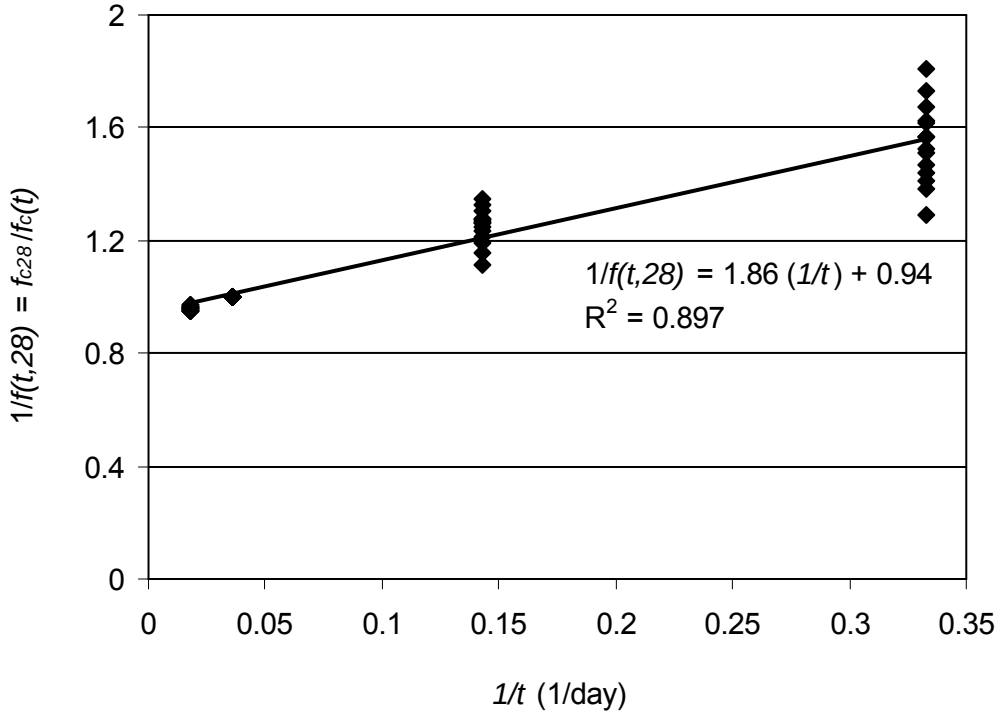

Figure 9.33: Relationship between *1/f(t,28)* and *1/t*

The 28 days compressive strength was increased in the presence of RHA. The increase in strength varied linearly with the increase in RHA content, as can be seen from Figure 9.34. The linear relationship between RHA content and its contribution towards 28 days compressive strength is shown in Equation 9.8.

$$f_{ccr28} = K_c \left(P_{rha}\right)$$ (Equation 9.8)

where:

K_c is the strength contribution factor of RHA, P_{rha} is the percent amount of RHA in total binder or cementing materials (by weight), and f_{ccr28} is the strength contribution of RHA towards 28 days compressive strength of concrete.

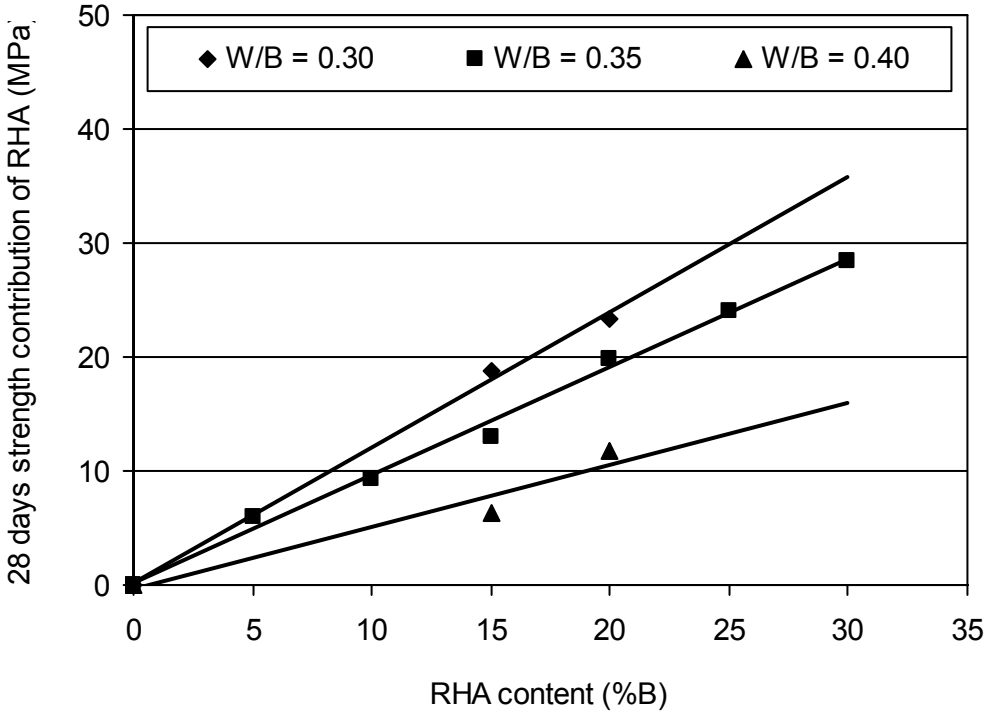

Figure 9.34: Contribution of RHA towards 28 days compressive strength of concretes

The strength contribution factor of RHA (K_c) varied linearly with the W/B ratio of the concretes, as can be seen from Figure 9.35. The linear relationship is expressed in the following equation:

$$K_c = -6.42\frac{W}{B} + 3.14 \qquad \text{(Equation 9.9)}$$

Combining Equations 9.7 to 9.9, the second function of Equation 9.4 can be expressed as follows:

$$f_{c28}\left(\frac{W}{B}, RHA\right) = 151\, e^{-2.46\frac{W}{B}} - 6.42\left(\frac{W}{B}\right)P_{rha} + 3.14\,(P_{rha}) \qquad \text{(Equation 9.10)}$$

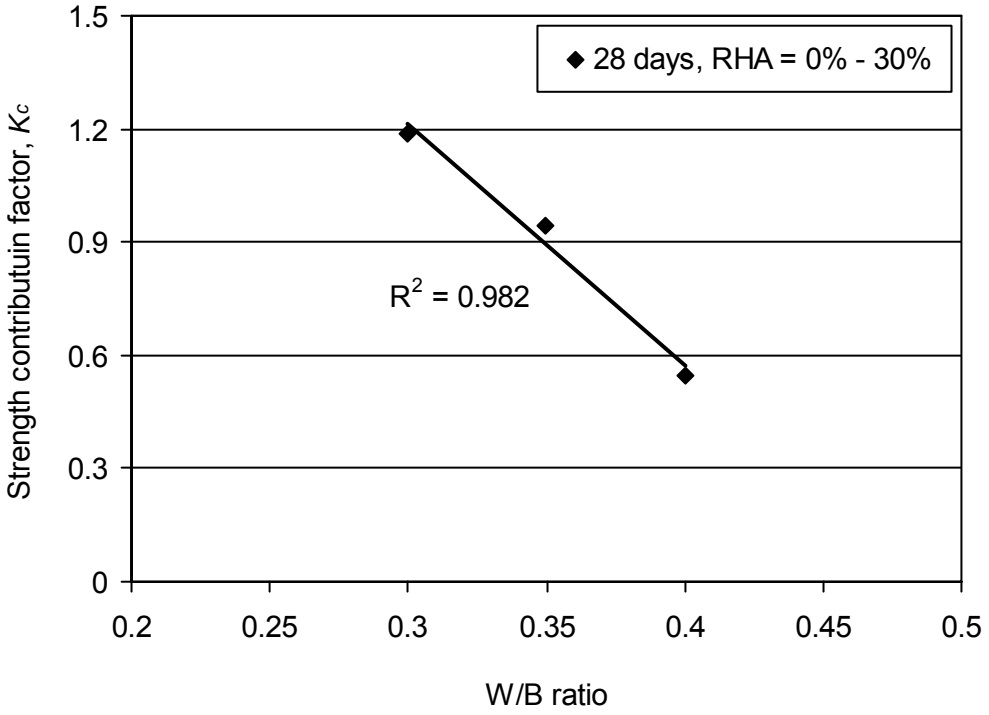

Figure 9.35: Relationship between strength contribution factor and W/B ratio

Finally, substituting Equation 9.6 and Equation 9.10 in Equation 9.4, the following expression for the compressive strength of concretes can be obtained:

$$f_c(t) = \frac{t}{1.86 + 0.94t}\left[151\, e^{-2.46\frac{W}{B}} - 6.42\left(\frac{W}{B}\right)P_{rha} + 3.14\,(P_{rha})\right] \qquad \text{(Equation 9.11)}$$

where:

$f_c(t)$ = Compressive strength of concrete at any age (MPa)

t = Age of concrete (days)

P_{rha} = Percent RHA content of concrete (%B)

W/B = Water-binder ratio (by weight)

9.8.1 Validity of the model

The model (Equation 9.11) was used to compute the compressive strength of the concretes at different curing ages. The computed compressive strength was compared with the measured

strength values, as shown in Figures 9.36 to 9.38. The computed and measured compressive strengths varied in the range of +11.60% to -13.81% with the maximum error occurring in case of 3 days strength. The errors between computed and measured compressive strengths at 28 and 56 days were in the range of +3.79% to -6.66%. The maximum error in case of 3 days compressive strength was due to the fact that the strength gain function over time was calibrated for all concretes independent of W/B ratio and RHA content. The coefficient of determination (R^2) and correlation coefficient (R) for the computed and measured compressive strengths was 0.955 and 0.977, respectively. The high coefficient of determination indicates that at least 95% of the measured values can be accounted for by using the strength model.

The strength model is valid for the air-entrained SCHPC mixtures whose W/B ratio ranges from 0.30 to 0.50, and which include RHA as a partial replacement of cement in the range of 0% to 30%. Big differences between predicted and measured compressive strengths can be found for W/B ratios over 0.50. Also, this model is applicable for a given type and size of aggregates, which were used with an optimum S/A ratio to minimize the void content in the aggregate skeleton of concretes. In addition, this model is valid for the water-cured concretes produced with normal portland (ASTM Type I or CSA Type GU) cement, and for a RHA whose pozzolanic activity index and silica content are about 120% and 95%, respectively.

9.8.2 Application of the model

The compressive strength of ordinary concretes can be estimated with good accuracy based on the strength charts. However, the strength development in SCHPC becomes complicated in the presence of SCMs, since it now depends upon the combined effects of cement hydration, dilution, microfilling, and pozzolanic reaction. The derived model can be used to estimate the compressive strength of the SCHPC mixtures where RHA is used as a partial replacement of cement. Thus, the model will be useful in the design process of concretes incorporating RHA to estimate the average compressive strength. In addition, the model can be used to determine the level of cement replacement by RHA for a given compressive strength with higher W/B ratio.

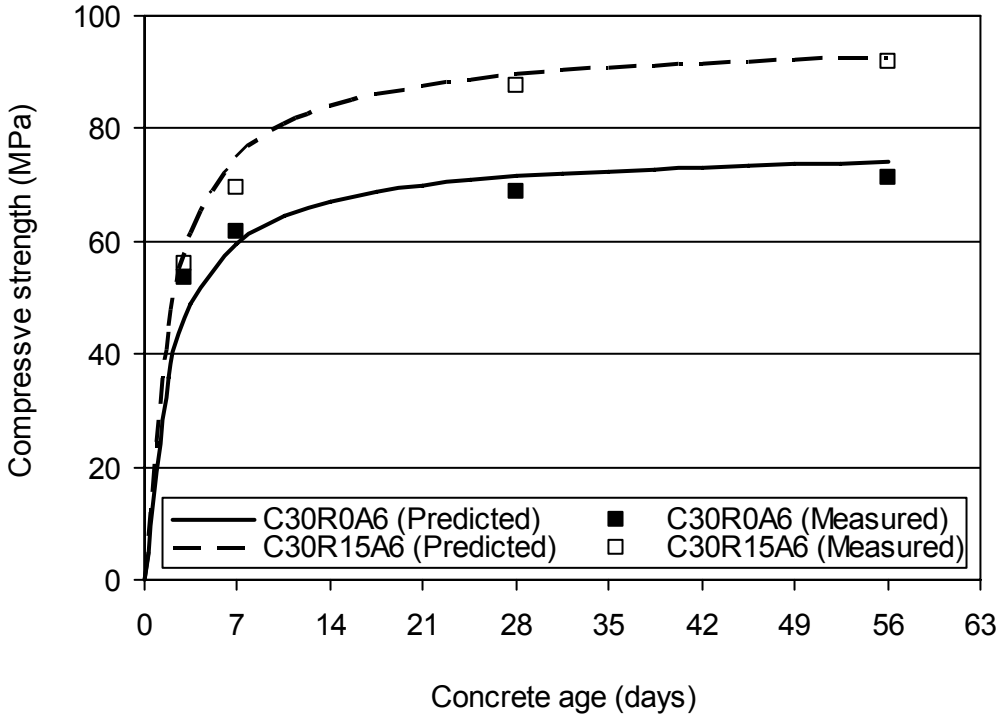

Figure 9.36: Predicted and measured compressive strengths of concretes (W/B = 0.30)

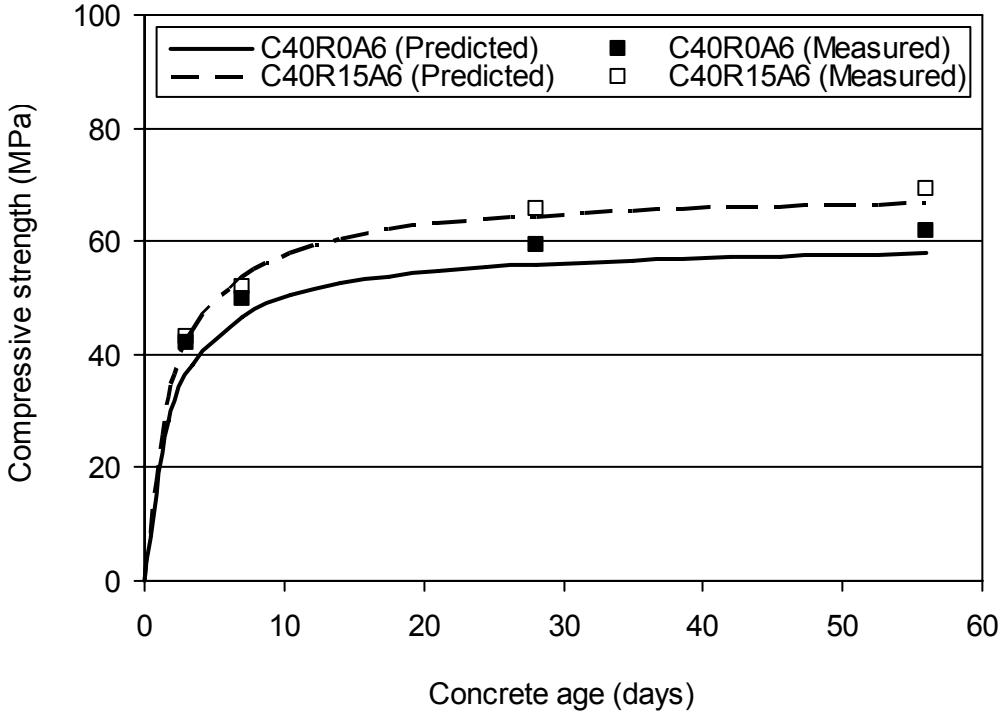

Figure 9.37: Predicted and measured compressive strengths of concretes (W/B = 0.40)

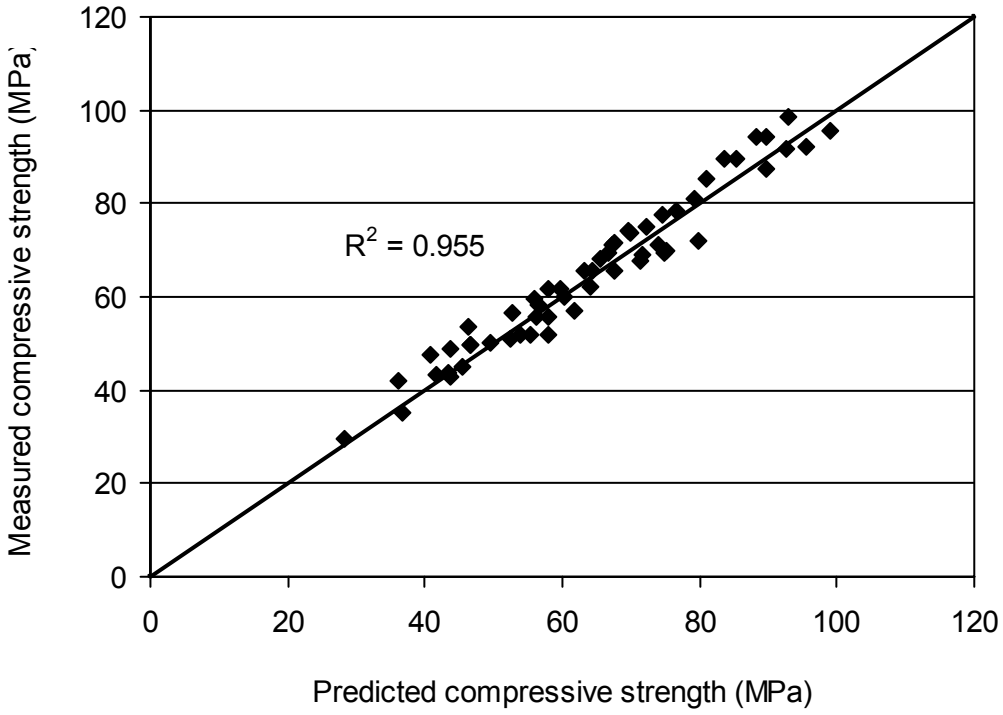

Figure 9.38: Comparison between predicted and measured compressive strength of concretes

9.9 Optimum Content of Rice Husk Ash

The hardened properties of the concretes were improved gradually with the increased RHA content. All concretes including RHA fulfilled the performance criteria for the tested hardened properties. However, excellent hardened properties were achieved for the concretes with 15 and 20% RHA. At the ages of 28 and 56 days, the improvement in the concrete properties, except for true electrical resistivity was less than 6% for each 5% increase beyond 20% RHA content. The true electrical resistivity was increased by 14% to 28% for 5% increase in RHA content. In contrast, the increase in electrical resistivity became almost double (25% to 52%) when the RHA content was increased from 15% to 20%. Hence, 15 to 20% RHA can be considered as the optimum content. However, a RHA content greater than 15% caused mixing and handling difficulties due to excessive cohesiveness or stickiness, particularly at lower W/B ratios. Therefore, 15% RHA content can be recommended as the optimum RHA content for SCHPC.

9.10 Conclusions

a. The hardened properties of the SCHPCs were improved at later ages such as 28 and 56 days due to greater hydration of cement and enhanced pozzolanic activity of RHA.
b. The hardened properties of the SCHPCs were improved with lower W/B ratio due to improved paste densification resulting from greater hydration products in the presence of higher binder content.
c. The hardened properties of the SCHPCs were improved with higher RHA content due to the microfilling and pozzolanic effects of rice husk ash.
d. The total porosity of the SCHPCs was decreased with lower W/B ratio and higher RHA content, and thus it increased the compressive strength, ultrasonic pulse velocity and electrical resistivity, and decreased the water absorption of concrete.
e. The hardened properties of the SCHPCs were progressively improved with the increase in RHA content. However, the performance criteria for all targeted hardened properties were fulfilled at 15%, which was also suitable for the fresh properties of SCHPC except for static segregation resistance.
f. The increased air content decreased the compressive strength of SCHPC since the air-voids increased the void content of concrete. Also, the increase in air content decreased the ultrasonic pulse velocity of SCHPC, as the increased amount of air-voids delayed the propagation of ultrasonic pulse.
g. The higher air content decreased the total porosity of SCHPC to some extent probably due to the reduced capillary porosity in the presence of entrained air-voids, and thus provided lower water absorption and higher electrical resistivity in concrete.
h. The test results for the compressive strength, total porosity, ultrasonic pulse velocity, water absorption and true electrical resistivity of the SCHPCs including RHA indicated good durability.
i. Good correlations were observed among the hardened properties of SCHPC and these correlations were independent of the curing age of concrete.
j. The compressive strength computed based on the derived model varied in the range of +11.6% to -13.81% as compared to the measured strength of the SCHPCs. At least 95% of the measured compressive strengths were accounted for with the derived model.

Chapter 10

Segregation Resistance of Self-consolidating High Performance Concrete

10.1 General

The preparation of fresh concretes and hardened test specimens, the development of a simplified segregation column apparatus, and the test procedures are presented in this chapter. The test results for the segregation resistance of various self-consolidating high performance concretes (SCHPCs) are also presented and discussed. The performances of sieve and column segregation apparatus are compared. In addition, this chapter discusses the effects of water-binder (W/B) ratio, rice husk ash (RHA) and viscosity-enhancing admixture (VEA), and suggests the suitable RHA content to produce segregation-resistant SCHPC.

10.2 Research Significance

SCHPC must possess adequately high segregation resistance during and after placement. Such phenomenon should be properly assessed by a simple and reliable test method. A proper assessment of segregation resistance is helpful for the mixture proportioning and quality control of SCHPC. The present study reports the development of a simplified segregation column apparatus with test procedure and performance criteria, and demonstrates its usage for several SCHPCs. The segregation column apparatus developed is simple to use in laboratory or field with a single operator. This study also compares the performances of sieve and column apparatus, discusses the effects of W/B ratio, RHA and VEA, and shows how the segregation resistance of SCHPC can be improved. The research findings will be useful for the construction industry to control segregation in SCHPC.

10.3 Preparation of Fresh Concretes

The fresh concretes were prepared for use in the development of column apparatus and for evaluating static and dynamic segregation resistances. Similar batching and mixing steps as

described in Chapter 8 were followed except for the addition of VEA. The VEA was added with the initial mixing water for a limited number of concrete mixtures. The mixture proportions of the concretes are given in Chapter 7.

10.4 Development of Segregation Column Apparatus

The segregation column apparatus for measuring the static segregation resistance of concrete was developed through trial and error by testing several batches of the non-air-entrained SCHPC (C50R0A2) prepared with a W/B ratio of 0.50. The experimental investigation was carried out to establish the column size, test procedure and performance criteria.

10.4.1 Different types of segregation column

The column size (height and diameter) and the number of column sections were varied, as shown in Table 10.1. The circular shape was selected for all columns to minimize the corner effects. The maximum column height of 600 mm was chosen to minimize the susceptibility of dynamic segregation, since the separation of coarse aggregates may occur when the concrete is discharged from a height greater than 600 mm (ACI 304R-00, 2004). The diameter of the columns was also varied because the lateral dimension may be related to concrete blocking and aggregate settlement. The material for all columns was poly-vinyl chloride (PVC). Different types of segregation column are shown in Figure 10.1.

Table 10.1: Different types of segregation column and methods of filling

Column designation	Column size	Number of sections	Method of filling	Comments
C_{13}	100D*×450H♣	3	Scooping	H/D: 4.5
C_{23}	150D×450H	3	Scooping	H/D: 3.0
C_{33}	100D×600H	3	Scooping	H/D: 6.0
C_{44}	100D×600H	4	Scooping	H/D: 6.0
C_{53}	150D×600H	3	Scooping	H/D: 4.0
C_{64}	150D×600H	4	Scooping	H/D: 4.0
$C_{64/ISC}$	150D×600H	4	Scooping through inverted slump cone (ISC)	Column dimensions and number of sections are known after testing the segregation columns C_{13} to C_{64}.
$C_{64/O}$	150D×600H	4	Scooping through orimet (O)	

*Column diameter (mm); ♣Column height (mm)

150D×450H and 100D×450H columns with 3 sections

100D×600H and 150D×600H columns with 3 sections

100D×600H columns with 4 sections

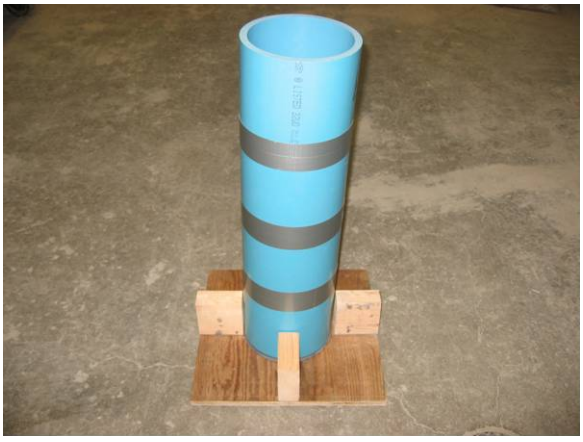

150D×600H columns with 4 sections

Inverted slump cone used for filling

Orimet used for filling

Figure 10.1: Various types of PVC column and filling technique used in the development of segregation column apparatus

10.4.2 Filling Techniques

The segregation columns C_{13} to C_{64} as mentioned in Table 10.1 were filled by scooping. Then the filling technique was changed for the selected column type (C_{64}). Two other filling techniques (scooping through inverted slump cone and scooping through orimet) as mentioned in Table 10.1 were used. The purpose was to evaluate the effect of filling technique on the performance of segregation column apparatus.

10.4.3 Test procedures

The performance of all segregation columns and the effect of filling techniques were investigated using the concrete 'C50R0A2'. The sieve segregation test was also conducted for each concrete batch to examine the static segregation resistance of the concrete. The performance of different segregation columns should be compared for identical segregation resistance of concrete. The sieve segregation test helped to ensure that the segregation resistance remained consistent in all concrete batches.

Test procedure for column segregation:

Different column sizes were used to examine the static segregation resistance of concrete. The top, middle and bottom sections of each segregation column were attached accordingly and sealed using duct tape. An end cap made of PVC was used to close the bottom opening of the column. Then it was placed inside a wooden base support and tightened. Immediately after mixing, the concrete was poured in the column in one layer. For the segregation columns C_{13} to C_{64}, the filling was completed by scooping. No means of consolidation was used during concrete filling. A rest period of 30 minutes was allowed for the columns filled with concrete to maximize the settlement of coarse aggregates. Then, the duct tape was removed without any disturbance and the column sections including the concrete were separated one at a time. A horizontal force was applied at the middle of the section to slide it over a steel separator pan. The concrete from each section was collected and washed on No. 4 (4.75 mm) CSA standard sieve to separate the coarse aggregates. The washing operation was finished in 2 minutes. The coarse aggregates obtained were then surface-dried and weighed separately. Finally, the segregation factor was calculated using two computation

methods based on Equation 10.1 (Method A) and Equation 10.2 (Method B). Duplicate testing was carried out to investigate the performance of each segregation column.

$$Method\ A: SF = \frac{C_B - C_T}{\frac{1}{2}(C_B + C_T)} \times 100\% \qquad \text{(Equation 10.1)}$$

$$Method\ B: SF = \frac{C_B - C_T}{\frac{1}{n}\sum_{i=1}^{i=n} C_i} \times 100\% \qquad \text{(Equation 10.2)}$$

where:

C_T = Surface-dry mass of the coarse aggregates in top section (kg)

C_B = Surface-dry mass of the coarse aggregates in bottom section (kg)

n = Number of the column sections

C_i = Surface-dry mass of the aggregates in 'i'th section (kg)

SF = Segregation factor (%)

The variation in segregation factors obtained from different column sizes was evaluated to determine the proper dimensions and number of sections for the segregation column apparatus. After selecting the desired segregation column apparatus, the technique of concrete filling was changed. In addition to filling by scooping, two other techniques, scooping through inverted slump cone and scooping through orimet, as shown in Figure 10.1 were used and the segregation factor was determined. In filling by scooping through the inverted slump cone, the concrete was taken from the pan by a scoop and placed into the selected column apparatus via the inverted slump cone. A similar placement technique was used in the case of filling by scooping through the orimet. All other experimental steps and the computation procedure for segregation resistance were the same as used for the filling technique by scooping. Both method A and method B were used to calculate the segregation factor of concrete. However, a single concrete batch was used in these two cases. Several operational stages involved in the development of segregation column apparatus are shown in Figure 10.2.

Segregation testing in 100D×600H and 150D×600H columns

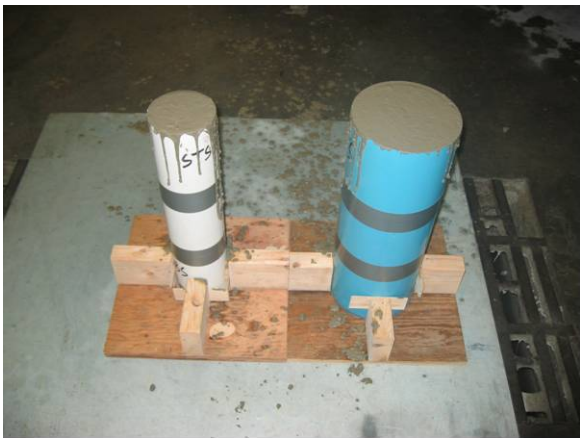

Segregation testing in 100D×450H and 150D×450H columns

Separator pan and segregation testing in 150D×450H column

Coarse aggregates retained after washing the concrete on No. 4 sieve

Figure 10.2: Several operational stages involved in the development of segregation column apparatus

Test procedure for sieve segregation:

A simple approach similar to the test procedure given by Nagataki and Fujiwara (1995) was used to determine the sieve segregation of concrete. The test setup is shown in Figure 10.3. A No. 4 CSA standard sieve (4.75 mm opening) along with a pan was used in this test. The inside diameter of the pan was 305 mm. The diameter of the opening area of the sieve was 290 mm. A 140D×130H mm plexiglass cylindrical container of 2 liter capacity was used for placing the concrete on the sieve.

Apparatus for sieve segregation test

Initial stage of sieve segregation test

Mortar passed through sieve

Coarse aggregates retained on sieve

Figure 10.3: Apparatus and several operational stages of the sieve segregation test

The sieve and pan were weighed. Then the sieve was placed over the pan. The concrete was poured into the cylindrical container in one layer and without any consolidation. Immediately, the concrete was gently emptied onto the sieve without any disturbance and left for 5 minutes rest. A fraction of the mortar passed through the sieve during this time. After the rest period, the sieve and pan assembly including the concrete was weighed. The mass of the concrete sample was determined by subtracting the masses of the sieve and pan. Then the sieve was removed with the leftover concrete. The pan along with the mortar fraction passed was weighed, and the mass of the mortar was determined by subtracting the mass of the pan. Later, the leftover concrete on No. 4 sieve was washed to

obtain the coarse aggregates. The coarse aggregates were surface-dried by absorbent cloths and weighed. The mass of the mortar contained in the concrete sample was determined by subtracting the aggregate mass from the concrete mass. Several operational stages of the sieve segregation test are shown in Figure 10.3. The segregation index was calculated based on Equation 10.3.

$$SI = \frac{M_p}{M_c} \times 100\% \qquad \text{(Equation 10.3)}$$

where:

SI = Segregation index (%)

M_p = Mass of the mortar that passed the sieve (kg)

M_c = Mass of the mortar contained in concrete sample (kg)

10.4.4 Performance of segregation columns

The results of the segregation resistance (segregation factors) obtained from various column sizes are shown in Table 10.2. The results of sieve segregation (segregation indices) for all concrete batches are also shown in Table 10.2. The values of segregation index reveal that the segregation characteristic of the concrete batches was consistent during testing the performance of different columns.

The segregation factors obtained was not reproducible for the columns C_{13}, C_{33} and C_{44}, as can be seen from Table 10.2. These columns were susceptible to the restricted movement of aggregates due to dynamic segregation. The likelihood of dynamic segregation becomes higher with the increased narrowness of column (Daczko 2002). The aggregates can collide with each other due to the limited lateral space leading to a reduced vertical movement. Also, the blocking of concrete movement can occur when a greater number of aggregates interlock within a limited space.

The column C_{23} produced a lower segregation factor than the columns C_{53} and C_{64}, as can be seen from Table 10.2. This is related to the resting height of aggregates (Saak et al. 2001) and the casting height of columns (Daczko 2002, Khayat and Guizani 1997). For a given concrete, the settlement height of the aggregates of certain size should be identical for

all columns with equal shape and diameter if no segregation during placement and no post-placement blocking occur to restrict aggregate movement. When the available vertical space is limited, the downward movement of aggregates can be prohibited before reaching the settlement height. Therefore, the resting height (from the bottom of column) will be greater and more coarse aggregates will be present in the upper section of column. In addition, the casting height for columns C_{53} and C_{64} was higher than that for column C_{23}. An increased casting height increases both bleeding and surface settlement and thus results in a greater degree of column segregation (Khayat and Guizani 1997).

Table 10.2: Sieve and column segregation test results for different columns

Column type		Test serial	Segregation factor, *SF* (%)		Segregation index, *SI* (%)
Designation	Dimensions (mm)		Method A	Method B	
C_{13}	100D×450H	1	2.9	2.9	10.6
		2	12.0	11.8	10.3
C_{23}	150D×450H	1	9.0	9.2	10.6
		2	10.1	10.3	10.9
C_{33}	100D×600H	1	9.7	9.6	10.1
		2	0.9	0.9	11.0
C_{44}	100D×600H	1	11.7	11.6	10.3
		2	-1.5	-1.5	11.0
C_{53}	150D×600H	1	14.4	14.5	10.1
		2	13.8	13.8	9.9
C_{64}	150D×600H	1	15.1	14.9	10.7
		2	14.9	14.7	10.3
$C_{64/ISC}$	150D×600H	1	15.9	16.3	10.0
$C_{64/O}$	150D×600H	1	16.5	16.2	10.7

The columns C_{53} and C_{64} (same size but different number of sections) did not produce any significant difference in segregation factors. Hence, the column C_{64} was selected to simplify the testing operation. Each section of column C_{64} involves a less quantity of concrete. Thus, the sections can be separated easily by a single operator. Also, the concrete quantity was suitable for washing on No. 4 CSA standard sieve having a diameter of 300 mm. The washing operation also took less time.

The columns $C_{64/ISC}$ and $C_{64/O}$ produced slightly higher segregation factor than that of C_{64} as evident from Table 10.2 due to the higher casting height in the presence of orimet and

inverted slump cone. The casting height for the column C_{64} was 600 mm. In the presence of inverted slump cone, the casting height for the column $C_{64/ISC}$ was 900 mm. For the column $C_{64/O}$, the casting height was 1260 mm due to the presence of orimet. The concrete is more prone to segregation when the casting height is greater than 600 mm (ACI 304R-00, 2004). However, no significant variation in segregation factor indicates that the effect of higher casting height was minimized. This is due to the constricted end of the inverted slump cone and orimet as it interrupted the free falling of concrete. Nevertheless, the filling technique of scooping can be chosen for simplicity and ease of testing.

The segregation factors computed by Method A and Method B were similar for all columns as can be seen from Table 10.2. It indicates that the column segregation can be determined by Method A as accurately as Method B. Therefore, Method A can be chosen to calculate the segregation resistance of concrete. It only deals with the top and bottom sections of the column, and thus simplifies the test procedure.

10.4.5 Selection of segregation columns

The column C_{64} filled by scooping was found suitable for measuring the segregation resistance of concretes by Method A after separating the top and bottom sections only with subsequent washing and weighing operations for coarse aggregates. Based on this finding, the segregation column apparatus as shown in Figure 10.4 was constructed. Both the diameter and height of the top and bottom sections are 150 mm. The middle section is 150 mm in diameter and 300 mm in height. The material used for the segregation column was steel. During testing, the middle section can be fastened with the top and bottom sections using the threaded bolts and V-nuts. The entire column can be attached to a base plate. The joints between different sections and between bottom section and base plate are sufficiently sealed to prevent any leakage of fresh concrete.

10.4.6 Determination of performance criteria for column segregation

Three series of tests as shown in Table 10.3 were conducted to determine the performance criteria for column segregation. Both fresh and hardened concretes with different segregation resistances (various segregation indices and segregation factors) were tested.

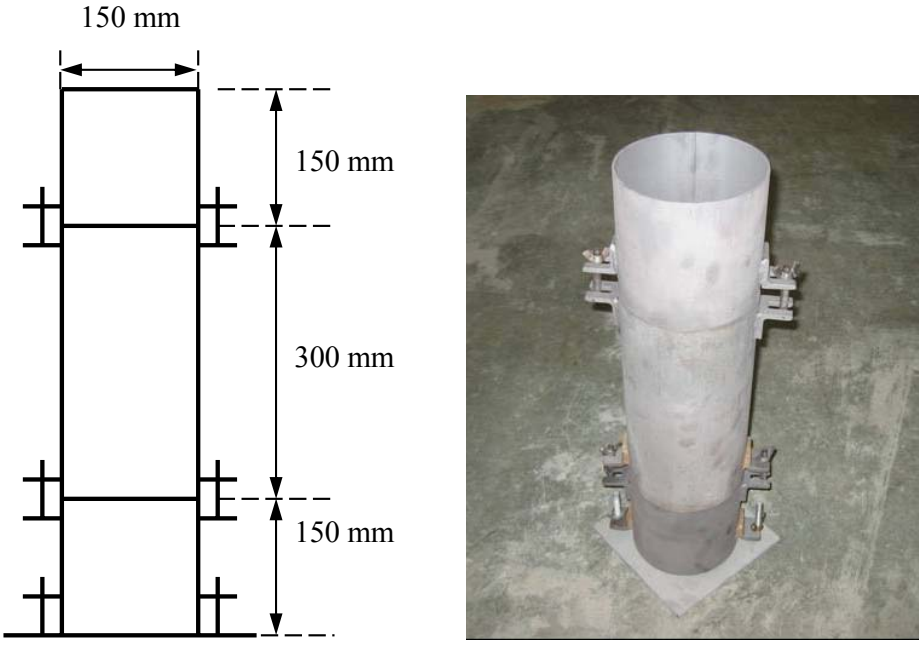

Figure 10.4: Details of the segregation column apparatus

Table 10.3: Test program to determine the performance criteria for the segregation column apparatus

Test series	Concretes tested	Sample/Specimens	Tests conducted
1	C50R0H50, C50R0H75, C50R0H100, C50R0H125	Fresh sample	Slump and slump flow, visual inspection of the concretes in mixer pan and slump flow spread, sieve segregation, and column segregation
2	C50R0H50, C50R0H75, C50R0H100, C50R0H125	Hardened 100D×150H molded cylinders	Compression, ultrasonic pulse velocity, and electrical resistivity
3	C50R0H100, C50R0H125	Hardened 150D×150H cut cylinders	

Test procedures:

In test series 1, the column and sieve segregation tests were conducted on the non-air-entrained concretes C50R0H50, C50R0H75, C50R0H100, and C50R0H125. The primary mixture proportions of these concretes were the same as that of C50R0A2 but the filling

ability (slump and slump flow) was varied using various HRWR dosages (50, 75, 100 and 125% of the saturation dosage). The slump and slump flow were determined to observe the filling ability of concrete. The segregation index was determined by sieve segregation test. In addition, the column apparatus shown in Figure 10.4 was used to determine the segregation factor. The procedures for the sieve and column segregation tests were the same as described in Section 10.4.3.

In case of test series 2, the concretes C50R0H50, C50R0H75, C50R0H100, and C50R0H125 were cast in the column apparatus shown in Figure 10.4 in one layer and without any consolidation. After a rest period of 30 minutes, the portions of concrete were separately collected from the top and bottom sections of the column apparatus and re-mixed by hand using a scoop. Duplicate 100D×150H mm cylinders were cast from each portion of concrete. Hence, four 100D×150H mm cylinders as shown in Figure 10.5 were obtained for each concrete: two from top section and the other two from bottom section. The cylinders molded by using the concrete collected from the top and bottom sections were designated as MT100D×150H and MB100D×150H, respectively. For these specimens, the concrete was poured in two layers and each layer was rodded and tapped in specified manner. The rodding and taping were used since the self-consolidation capacity of concrete was significantly reduced during the rest period of 30 minutes. Immediately after casting, the top faces of the cylinders were covered by the lids and left undisturbed at room temperature. The specimens were de-molded at the age of 24±2 hours and transferred to the fog room for curing. The curing was conducted according to the ASTM standard practice (ASTM C 192/C 192M, 2004) until the day of testing for true electrical resistivity, ultrasonic pulse velocity and compressive strength at the age of 28 days. The tests were conducted in similar manners as discussed in Chapter 9 except for the probe spacing used in resistivity measurement. A probe spacing of 30 mm was used to determine the true electrical resistivity, since the length of concrete cylinders was 150 mm instead of 200 mm.

In test series 3, the concretes C50R0H100 and C50R0H125 were cast in the column apparatus shown in Figure 10.4 in one layer and without any consolidation. Immediately after casting, the top of the column apparatus was covered by a plastic lid and left undisturbed at room temperature. The column specimens were taken out of the apparatus at the age of 24±2 hours and transferred to the fog room for curing in accordance with ASTM C

192/ C 192M (2004). After the completion of curing period, the top and bottom portions of the column specimens were cut and the end faces were ground to get the 150D×150H mm cylinder specimens. Thus, two 150D×150H mm cylinder specimens as shown in Figure 10.5 were obtained from each 150D×600H mm column: one from top and the other from bottom portion of the column, which were designated as CT150D×150H and CB150D×150H, respectively. Duplicate top and bottom specimens were used for each concrete. The hardened cylinders were tested at 28 days for true electrical resistivity, ultrasonic pulse velocity, and compressive strength. The tests were conducted in similar manners as discussed in case of test series 2.

100D×150H mm de-moulded cylinders

150D×150H mm cut cylinders

Figure 10.5: Different types of test specimen used to determine the performance criteria for column segregation of concrete

Performance criteria:

The performance criteria for column segregation were determined based on the results of various tests conducted under series 1 to 3. The results of slump and slump flow, segregation index and segregation factor obtained from test series 1 are given in Table 10.4. The segregation factor and segregation index found for various HRWR dosages were well-correlated, as can be seen in Figure 10.6. This relationship is found based on the segregation characteristics of the concrete with 0.50 W/B ratio and without any RHA (C50R0A2). A similar relationship between segregation index and segregation factor can be observed for any other individual concrete with different slump flows at varying HRWR dosages.

Table 10.4: Segregation test results for performance criteria (series 1)

Concrete	HRWR (%SD)	Slump (mm)	Slump flow (mm)	*SI*	*SF*	Visual observation
C50R0H50	50	175	315	0.1	0	No bleeding
C50R0H75	75	235	450	0.3	0	No bleeding
C50R0H100	100	260	605	10.5	15	Noticeable bleeding in mixer pan
C50R0H125	125	---	690	19.3	24.8	Severe bleeding in mixer pan; aggregate pile and severe bleeding in slump flow spread

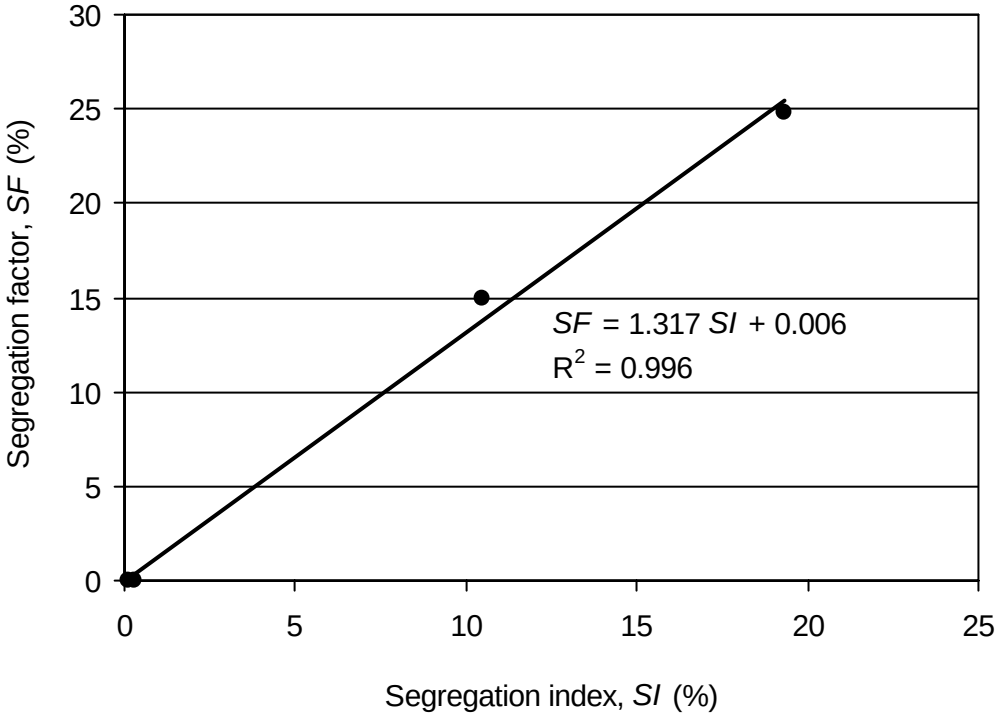

Figure 10.6: Variation of segregation factor with segregation index of concrete

The results of the tests conducted under series 2 and 3 are given in Table 10.5. These are the average results obtained from two duplicate specimens. The degrees of variation in compressive strength, ultrasonic pulse velocity and true electrical resistivity of the cylinder specimens representing the concretes taken from the top and bottom sections of the column apparatus were calculated using Equation 10.4. This equation is based on a similar concept as

used to calculate the segregation factor of concrete (Section 10.4.3). Also, the statistical coefficients of variation for the aforementioned concrete properties were calculated using Equation 10.5. This equation is derived based on the relationship between standard deviation and coefficient of variation.

$$V_{dp} = \frac{\overline{P_b} - \overline{P_t}}{\overline{P}} \times 100\% \qquad \text{(Equation 10.4)}$$

$$V_{cp} = \frac{\sqrt{\left(\overline{P_b} - \overline{P}\right)^2 + \left(\overline{P_t} - \overline{P}\right)^2}}{\overline{P}} \times 100\% \qquad \text{(Equation 10.5)}$$

where:

V_{dp} = Degree of variation in concrete property (strength, pulse velocity, resistivity, etc.)

V_{cp} = Statistical coefficient of variation in concrete property

$\overline{P_b}$ = Average concrete property obtained from two bottom specimens

$\overline{P_t}$ = Average concrete property obtained from two top specimens

$\overline{P} = \frac{1}{2}\left(\overline{P_b} + \overline{P_t}\right)$

The degree of variation and the statistical coefficient of variation for the compressive strength, ultrasonic pulse velocity and true electrical resistivity between top and bottom specimens of the concretes having different segregation indices and segregation factors are shown in Table 10.5. These variations are due to the changes in the internal composition of concrete caused by segregation.

The variation in compressive strength between top and bottom specimens for each concrete was insignificant under series 2, as can be seen from Table 10.5. This is because the distribution of coarse aggregates in concrete specimens was uniform due to re-mixing of the fresh concrete, thus reducing the heterogeneity in the concrete and contributing to produce good interfacial bond between aggregate and mortar. In contrast, the distribution of coarse aggregates was non-uniform in the specimens under series 3, thus increasing the

heterogeneity in the concrete. An increased heterogeneity can considerably decrease the compressive strength of concrete (Mindess et al. 2003). As such, some variations occurred between the compressive strengths of top and bottom specimens of the concretes tested under series 3. Also, the variation in compressive strength increased with greater segregation index and segregation factor. This indicates that the heterogeneity increased with greater segregation.

Table 10.5: Segregation test results for performance criteria (series 2 and series 3)

Concrete	HRWR (%SD)	Test specimens	Compressive strength (MPa)	Ultrasonic pulse velocity (km/s)	True electrical resistivity (kΩ-cm)
Series 2					
C50R0H50 *SI*: 0.1% *SF*: 0%	50	MT100D×150H	52.1	4.918	5.706
		MB100D×150H	52.3	4.911	5.882
			*V_{ds}: 0.4% ♣V_{cs}: 0.3%	*V_{dv}: -0.1% ♣V_{cv}: 0.1%	*V_{dr}: 3.0% ♣V_{cr}: 2.1%
C50R0H75 *SI*: 0.3% *SF*: 0%	75	MT100D×150H	52.7	4.910	5.529
		MB100D×150H	53.2	4.984	5.824
			V_{ds}: 0.9% V_{cs}: 0.6%	V_{dv}: 1.5% V_{cv}: 1.1%	V_{dr}: 5.2% V_{cr}: 3.7%
C50R0H100 *SI*: 10.5% *SF*: 15%	100	MT100D×150H	53.5	4.934	5.103
		MB100D×150H	52.9	5.009	5.952
			V_{ds}: -1.1% V_{cs}: 0.8%	V_{dv}: 1.5% V_{cv}: 1.1%	V_{dr}: 15.4% V_{cr}: 10.9%
C50R0H125 *SI*: 19.3% *SF*: 24.8%	125	MT100D×150H	54.1	4.943	4.412
		MB100D×150H	53.2	5.025	6.000
			V_{ds}: -1.7% V_{cs}: 1.2%	V_{dv}: 1.6% V_{cv}: 1.1%	V_{dr}: 30.5% V_{cr}: 21.6%
Series 3					
C50R0H100 *SI*: 10.5% *SF*: 15%	100	CT150D×150H	36.9	4.951	5.357
		CB150D×150H	39.5	5.034	6.170
			V_{ds}: 6.8% V_{cs}: 4.8%	V_{dv}: 1.7% V_{cv}: 1.2%	V_{dr}: 14.1% V_{cr}: 10.0%
C50R0H125 *SI*: 19.3% *SF*: 24.8%	125	CT150D×150H	28.4	4.967	4.607
		CB150D×150H	31.2	5.119	6.179
			V_{ds}: 9.4% V_{cs}: 6.7%	V_{dv}: 3.0% V_{cv}: 2.1%	V_{dr}: 29.2% V_{cr}: 20.6%

*Degree of variation; ♣Statistical coefficient of variation

The variation in ultrasonic pulse velocity was not significant in both series 2 and 3, as can be seen from Table 10.5. The bottom specimens had more aggregates than the top specimens. The ultrasonic pulse velocity is increased with greater aggregate content since the aggregates generally have a higher elastic modulus than mortar and concrete (Lin et al. 2003). However, the mass density of concrete increased in the bottom specimens due to a greater amount of coarse aggregate and reduced mortar content. This is because the mass density of coarse aggregate is greater than the mass densities of mortar and concrete. An increased mass density decreases the ultrasonic pulse velocity of concrete, since they are inversely related (Neville 1996). For this reason, the effect of higher aggregate content was minimized leading to no significant variation in ultrasonic pulse velocity. In contrast, a considerable variation in true electrical resistivity was observed in series 2 and 3, indicating its good potential for segregation measurement. The top specimens provided significantly lower electrical resistivity than the bottom specimens. This is because more paste or mortar (less coarse aggregate) was present in the top specimens due to segregation, thus producing a greater concentration of pore solution and ions. In particular, the water content was higher since significant bleeding occurred as the coarse aggregates settled down.

The overall statistical coefficient of variation for the in-place compressive strength of concrete in the case of laboratory trial batches is normally not more than 6.7% (Bartlett and MacGregor 1999; ACI 214.4R-03, 2004). This variation consists of within-test and within-member variations. The within-test variation arises due to the improper handling, storing, curing and testing procedures, whereas the within-member variation in compressive strength can occur due to the variations in W/B ratio, air content, and proportions of ingredients such as aggregate, cement, water and admixtures, as caused by segregation. The within-test coefficient of variation is generally 3% (Bartlett and MacGregor 1996). However, the acceptable within-test coefficient of variation (percent one-sigma limit) for 150D×300H mm molded cylinders and 100D×200H mm cored cylinders is ≤ 2.37% (ASTM C39 2004), and ≤ 3.2% (ASTM C 42/C 42M 2004), respectively. In the present study, the maximum within-test coefficient of variation was 2.43% for the cylinder specimens tested under series 2 and 3. Nonetheless, using 3% as the maximum within-test variability, the acceptable limit for the statistical coefficient of variation for the in-place compressive strength due to segregation was determined based on the following equation:

$$V_{css} = \sqrt{V_{cso}^2 - V_{cst}^2} \qquad \text{(Equation 10.6)}$$

where:

V_{cso} = Typical overall coefficient of variation for in-place compressive strength (6.7%)

V_{css} = Acceptable limit for the coefficient of variation for in-place compressive strength

V_{cst} = Maximum within-test coefficient of variation for compressive strength (3%)

The degree of variation (V_{ds}) and the statistical coefficient of variation (V_{cs}) in the compressive strength were strongly correlated, as can be seen from Figure 10.7. This relationship was used to determine the acceptable degree of variation in compressive strength based on the statistical coefficient of variation for the in-place compressive strength due to segregation as obtained from Equation 10.6. The acceptable coefficient of variation for the in-place compressive strength due to segregation was found as $\sqrt{(6.7)^2 - (3)^2} = 6\%$. This provided an acceptable degree of variation in compressive strength of 8.4% from Figure 10.7. It was used to set the criteria for column segregation. The observed degree of variation in compressive strength was plotted versus the segregation factor, as shown in Figure 10.8. The segregation factor corresponding to 8.4% degree of variation in compressive strength was found to be 21% from Figure 10.8.

The degrees of variations in the compressive strength and true electrical resistivity of the concretes tested under series 2 and 3 were also well-correlated, as can be seen from Figure 10.9. Using this relationship, the acceptable variation in true electrical resistivity was determined based on the acceptable variation in compressive strength of 8.4%. The acceptable variation in true electrical resistivity was found as 23.2% from Figure 10.9. It can also be used to fix the criteria for column segregation. The degree of variation in true electrical resistivity was plotted versus the segregation factor of concrete in Figure 10.10. The segregation factor corresponding to 23.2% variation in true electrical resistivity was found as 20.2% from Figure 10.10. Thus the following criteria are proposed to qualify the segregation resistance of SCHPC mixture:

a. SCHPC mixture has a good static segregation resistance if the segregation factor ≤ 20%.
b. SCHPC mixture has a poor static segregation resistance if the segregation factor > 20%.

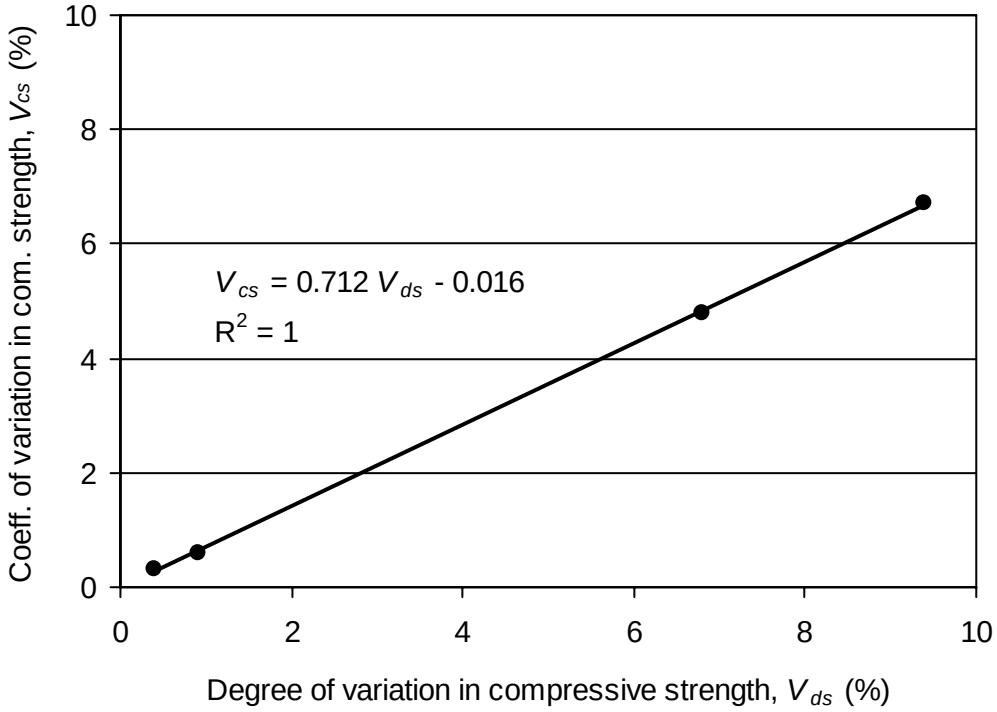

Figure 10.7: Correlation between degree of variation and statistical coefficient of variation in compressive strength

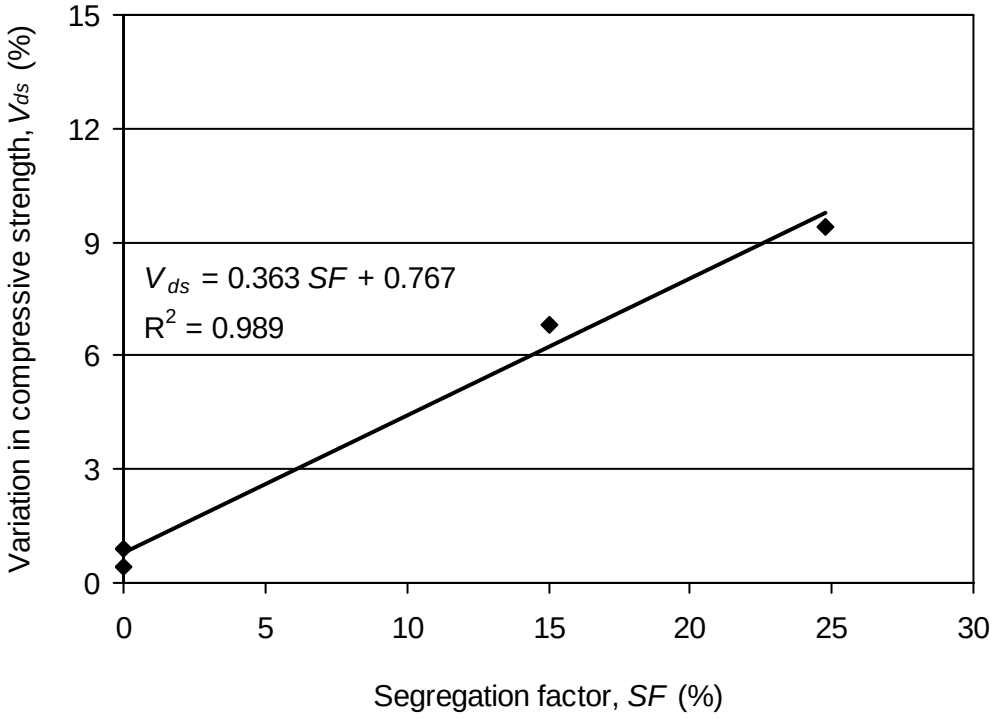

Figure 10.8: Variation of compressive strength with segregation factor of concrete

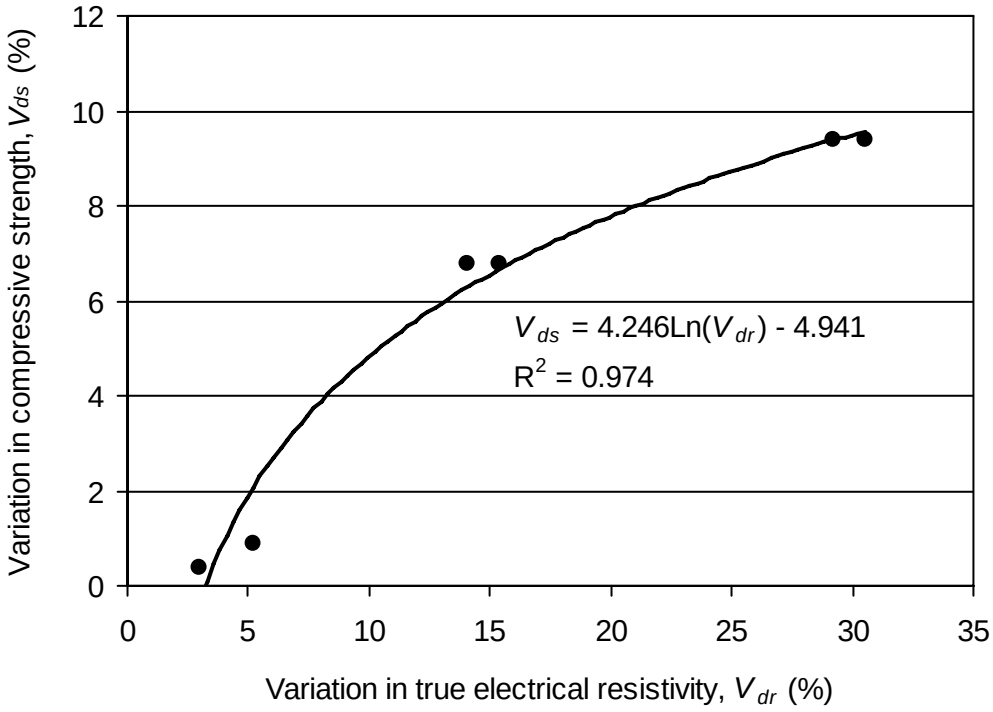

Figure 10.9: Correlation between variations of compressive strength and true electrical resistivity

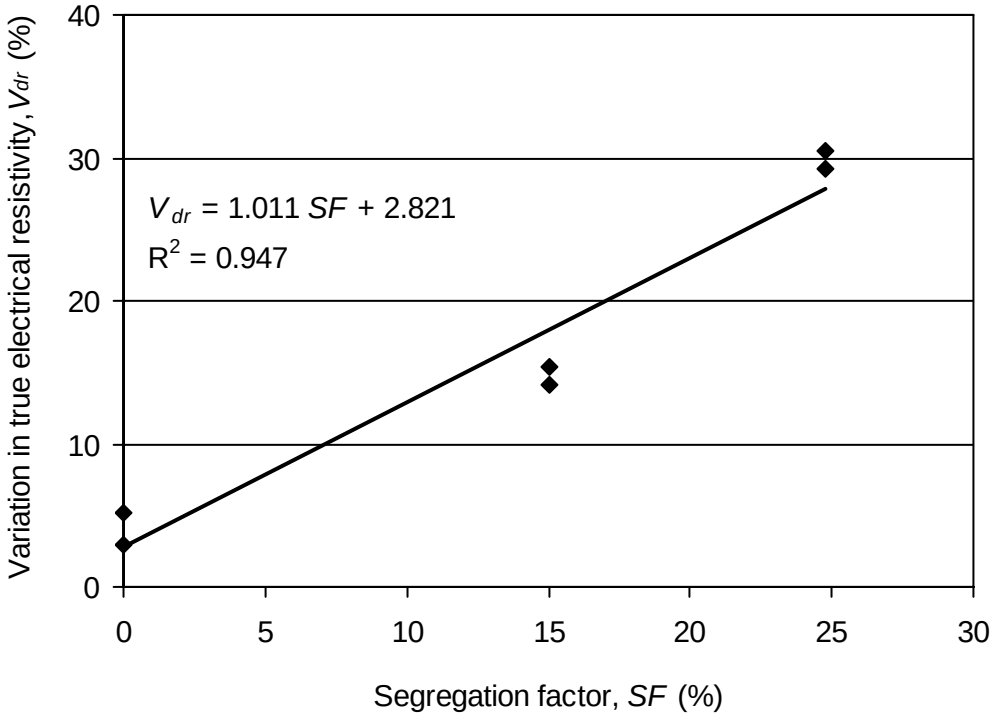

Figure 10.10: Variation of true electrical resistivity with segregation factor of concrete

The criteria for segregation factor obtained above were verified based on the maximum acceptable limit of segregation index. Using Figure 10.6, the segregation index corresponding to the maximum acceptable segregation factor (20%) was found as 15.2%. A segregation index ≤ 10% generally indicates a very good static segregation resistance of SCHPC (Lachemi et al. 2004). However, Perez et al. (2002) reported that the maximum acceptable sieve segregation can be 18%. Thus, the criteria set for the acceptable column segregation are reliable. It is expected that a column segregation ≤ 20% will not have a significant negative impact on the mechanical and transport properties of SCHPC.

10.4.7 Advantages of segregation column apparatus

The segregation column apparatus developed is simple and comfortable to use due to its user-friendly size. It is cost-effective and can be built easily using the available 150D×300H mm cylindrical metal moulds. Also, the quantity of concrete required is less. Due to reduced column size and less concrete quantity, the handling and testing procedures are easier, and thus the entire test can be conducted by a single operator. In addition, the test is faster since the segregation is determined by testing the concretes of top and bottom sections only. The segregation factor is calculated based on the masses of surface-dry coarse aggregates without knowing its saturated or oven-dry masses. The segregation result can be determined within 1 hour from the mixing of concrete. Because of simplicity and faster implementation, the segregation column apparatus developed will be suitable for frequent quality control of SCHPC mixtures at the batching plant, precast concrete factories and job site.

10.5 Testing of Fresh Concretes for Segregation Resistance

The concretes previously tested for fresh and hardened properties (Chapters 8 and 9) were visually inspected for both static and dynamic segregation resistances of concrete. A couple of these concretes were also visually inspected in the presence of VEA. The aggregate settlement in the mixer pan was observed to evaluate the static segregation resistance. The slump flow and orimet and inverted slump cone flow spreads were used to evaluate the static/dynamic segregation resistance. In addition, the concrete flows through orimet and inverted slump cone were assessed to evaluate the dynamic segregation resistance. The details of these tests are given in Chapter 8.

After developing the segregation column apparatus including the test procedure and performance criteria, it was applied to determine the static segregation resistance of SCHPC. A number of concretes were tested to quantitatively determine the static segregation resistance using column apparatus and No. 4 sieve according to the test procedures mentioned in Section 10.4.3. The details of the test program are shown in Table 10.6.

Table 10.6: Test program for segregation resistance of different SCHPCs

Concrete designation	Type of test and observation	Segregation characteristic
C30R0A6, C30R15A6, C30R20A6, C35R0A6, C35R5A6, C35R10A6, C35R15A6, C35R20A6, C35R25A6, C35R30A6, C40R0A6, C40R15A6, C40R20A6, C50R0A6, C50R0A2	Visual inspection of the concrete resting in mixer pan	Static
	Visual inspection of the slump flow and orimet and inverted slump cone flow spreads	Static/dynamic
	Visual inspection during the concrete flow through orimet and inverted slump cone	Dynamic
C35R10A6V, C35R15A6V	Visual inspection of the concrete resting in mixer pan	Static
	Visual inspection of the slump flow spread	Static/dynamic
C30R0A6, C35R0A6, C35R5A6, C35R10A6, C35R15A6, C35R10A6V, C35R15A6V, C40R0A6, C40R15A6, C50R0A2	Sieve segregation	Static
	Column segregation	Static

10.6 Test Results for Segregation Resistance of Concretes

The results of visual inspection for different concretes are given in Table 10.7. In addition, the results of sieve and column segregation tests are presented in Figure 10.11 and 10.12, respectively.

10.6.1 Static segregation resistance

The static segregation resistance of the concretes was evaluated based on the results of visual inspection, and sieve and column segregation tests.

Table 10.7: Results of visual inspection for various SCHPCs

Concrete mixture	Observation on concrete quality in mixer pan and during various flowing ability tests	Segregation resistance	
		Static	Dynamic
C30R0A6, C35R0A6, C50R0A6	Slight bleeding in mixer pan; no bleeding, mortar halo or aggregate pile in slump flow and orimet flow and inverted slump cone flow spreads; no blockage during orimet and inverted slump cone flows; no thick layer of paste on the top of resting concrete in mixer pan	Good	Good
C35R5A6	No bleeding in mixer pan; no bleeding, mortar halo and aggregate pile in slump flow and orimet and inverted slump cone flow spreads; no blockage during inverted slump cone and orimet flows; no thick layer of paste on the top of resting concrete in mixer pan	Good	Good
C35R10A6, C40R15A6, C40R20A6	No bleeding in mixer pan; no bleeding and aggregate pile but minor mortar halo in slump flow and orimet and inverted slump cone flow spreads; no blockage during inverted slump cone and orimet flows; no thick layer of paste on the top of resting concrete in mixer pan	Fair	Fair
C30R15A6, C35R15A6, C35R20A6	Sticky mixture; no bleeding in mixer pan; no bleeding and aggregate pile but significant mortar halo in slump flow and orimet and inverted slump cone flow spreads ; no blockage during orimet and inverted slump cone flows; a thick layer of paste on the top of resting concrete in mixer pan	Low	Good
C30R20A6, C35R25A6, C35R30A6	Highly sticky mixture; no bleeding in mixer pan; no bleeding and aggregate pile but severe mortar halo in slump flow and orimet and inverted slump cone flow spreads; no blockage during orimet and inverted slump cone flows; a very thick layer of paste on the top of resting concrete in mixer pan	Poor	Good
C40R0A6, C50R0A2	Slight bleeding in mixer pan; no bleeding, mortar halo or aggregate pile in slump flow and orimet and inverted slump cone flow spreads; tendency of blockage during orimet flow; no thick layer of paste on the top of resting concrete in mixer pan	Good	Low
C35R10A6V, C35R15A6V	No bleeding in mixer pan; no bleeding, mortar halo or aggregate pile in slump flow spread; no thick layer of paste on the top of resting concrete in mixer pan	Good	Good

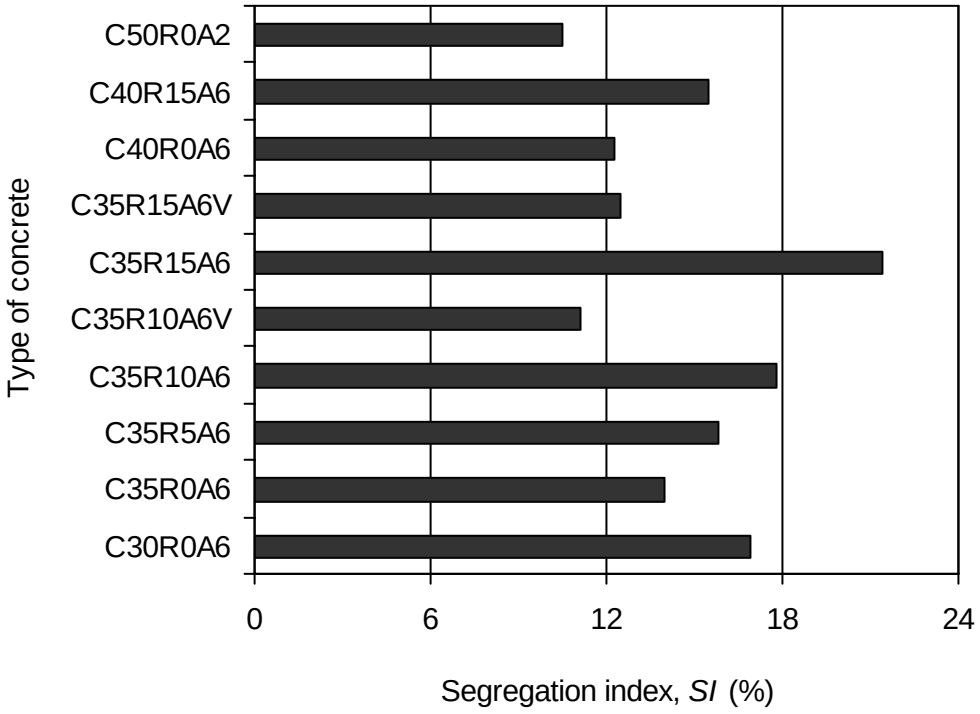

Figure 10.11: Variation of segregation index for different concretes

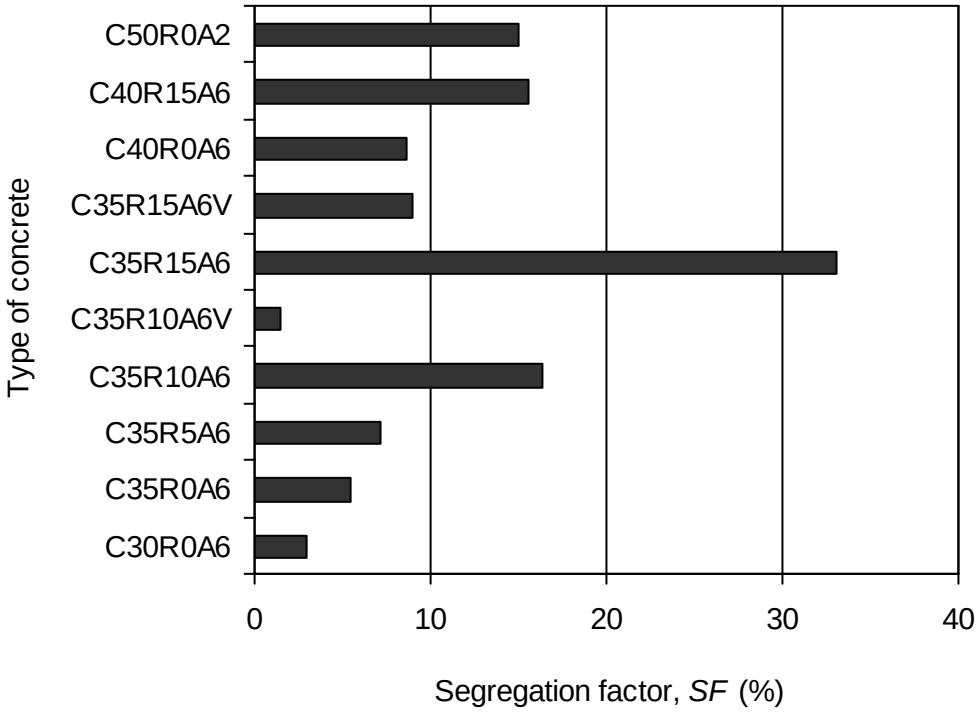

Figure 10.12: Variation of segregation factor for different concretes

Static segregation resistance based on visual observation:

The results from the visual inspection of the quality of concrete in mixer pan, slump flow, and orimet and inverted slump cone flow spreads given in Table 10.7 provided some indication for static segregation resistance. Slight external bleeding was observed in the mixer pan in case of C30R0A6, C35R0A6, C40R0A6, C50R0A2 and C50R0A6 immediately after the completion of mixing. A small amount of bleeding is normal in fresh concrete (FHWA 2006) but a significant amount of bleeding indicates reduced segregation resistance. However, the external bleeding was absent for all RHA concretes with or without any VEA.

A thick layer of binder paste was observed on the top of the resting concrete in mixer pan for C30R15A6, C30R20A6, C35R15A6, C35R20A6, C35R25A6 and C35R30A6 prepared with higher RHA content. It suggests that these concretes were vulnerable to static segregation due to coarse aggregate settlement. In particular, a very thick layer of paste appeared in case of C30R20A6, C35R25A6 and C35R30A6 indicating their susceptibility to severe static segregation. No thick layer of paste emerged in case of C35R15A6V and thus indicated its improved static segregation resistance due to the use of VEA.

No bleeding, mortar halo and aggregate pile appeared in the slump flow and orimet and inverted slump cone flow spreads of C30R0A6, C35R0A6, C35R5A6, C40R0A6, C50R0A2 and C50R0A6, as mentioned in Table 10.7. A minor mortar halo appeared in the flow spreads of C35R10A6, C40R15A6, and C40R20A6 and thus indicated their adequate static segregation resistance. No mortar halo appeared in the slump flow spread in case of C35R10A6V and C35R15A6V. In contrast, significant to severe mortar halo emerged in the flow spreads of C30R15A6, C30R20A6, C35R15A6, C35R20A6, C35R25A6 and C35R30A6, and thus indicated their low to poor static segregation resistance. The slump flows of these concretes, given in Table 10.8, were relatively high and thus indicated their low level of yield stress. In contrast, the plastic viscosity was comparatively high as indicated from the orimet and inverted slump cone flow times given in Table 10.8. However, a concrete with very low yield stress but high viscosity may exhibit static segregation (Cyr and Mouret 2003). This implies that the viscosity is less critical than the yield stress to cause static segregation in concrete, as indicated by severe mortar halo in the flow spread of highly viscous concretes such as C30R20A6 and C35R30A6. The appearances of the flow spreads of several concretes are shown in Figures 10.13a to 10.13c.

Table 10.8: Different mixture parameters, critical mortar yield stress, slump flow, flow time, and air content of various SCHPCs

Concrete type*	D_h	V_m	D_m	V_{ca}	CA/TS	τ_{cmy}	S_f	A_c	Flow time	
									T_o	T_i
C30R0A6	0.88	0.687	2165	0.313	0.395	67.7	710	5.7	6.6	3.8
C30R15A6	1.75	0.693	2125	0.307	0.388	72.7	735	5.3	9.2	5.1
C30R20A6	2.10	0.697	2110	0.303	0.385	74.5	770	5.7	11.5	5.7
C35R0A6	0.70	0.674	2140	0.326	0.409	70.8	690	5.3	5.7	2.9
C35R5A6	0.88	0.677	2130	0.323	0.407	72.1	700	5.5	6.4	3.2
C35R10A6	1.05	0.678	2120	0.322	0.405	73.3	710	5.1	7.2	3.6
C35R10A6V	1.05	0.654	2195	0.328	0.405	64.0	665	3.5	---	---
C35R15A6	1.40	0.680	2110	0.320	0.403	74.5	720	5.1	7.6	3.9
C35R15A6V	1.40	0.659	2175	0.324	0.403	66.5	670	3.8	---	---
C35R20A6	1.75	0.682	2100	0.318	0.401	75.8	710	5.0	8.8	5.1
C35R25A6	2.10	0.686	2080	0.314	0.398	78.3	740	5.6	9.6	5.4
C35R30A6	2.45	0.687	2075	0.313	0.396	78.9	750	5.2	10.4	5.8
C40R0A6	0.60	0.669	2115	0.331	0.420	73.9	665	6.1	4.8	2.3
C40R15A6	1.00	0.671	2090	0.329	0.414	77.0	680	5.2	6.8	2.6
C40R20A6	1.20	0.673	2080	0.327	0.412	78.3	675	5.3	7.1	2.8
C50R0A2	0.50	0.652	2210	0.346	0.439	62.1	600	1.8	2.1	1.2
C50R0A6	0.50	0.654	2095	0.348	0.434	76.4	605	5.2	1.8	1.1

Notation:
A_c: air content (%); CA/TS: coarse aggregate/total solid volume ratio; D_h: dosage of high-range water reducer (% B); D_m: mortar density (kg/m^3); S_f: slump flow (mm); T_i: inverted slump cone flow time (s); T_o: orimet flow time (s); τ_{cmy}: critical mortar yield stress needed to avoid segregation; V_{ca}: coarse aggregate volume (m^3/m^3); V_m: mortar volume (m^3/m^3)

*The numbers after 'C' and 'R' represent W/B ratio and RHA content, respectively

The evaluation of the static segregation resistance of SCHPC by conducting a visual inspection of bleeding, mortar halo and aggregate pile in flow spreads may not be always reliable because these phenomena indicate the lateral stability only (Bonen and Shah 2005). The segregation may occur even none of these phenomena appears in flow spread (EFNARC 2002). For example, the concrete C50R0A2 exhibited no bleeding, mortar halo and aggregate pile in flow spreads but it had relatively high segregation index and factor as obvious from Figures 10.11 and 10.12. However, a concrete segregating in flow spread will definitely segregate after placement. For instance, the concrete C35R15A6 showed significant mortar halo in slump flow, and orimet and inverted slump cone flow spreads. The segregation index and factor of this concrete were also significantly high as evident from Figures 10.11 and 10.12. A similar result was reported by other researchers (Bonen and Shah 2005).

No signs of segregation in slump flow spread (C50R0A2)

No signs of segregation in orimet flow spread (C50R0A2)

Figure 10.13a: Appearances of the slump flow and orimet flow spreads for C50R0A2

No signs of segregation in inverted slump cone flow spread (C50R0A6)

Significant mortar halo in orimet flow spread (C35R15A6)

Figure 10.13b: Appearances of the inverted slump cone flow spread for C50R0A6 and orimet flow spread for C35R15A6

Significant mortar halo in inverted slump cone flow spread (C35R15A6)

Severe mortar halo in slump flow spread (C35R25A6)

Figure 10.13c: Appearances of the inverted slump cone flow spread for C35R15A6 and slump flow spread for C35R25A6

The evaluation of the static segregation resistance based on the visual inspection of the concrete resting in a mixer pan can also be misleading. This is because the absence of significant bleeding or thick layer of paste on the top of resting concrete does not always imply that the SCHPC possesses a good static segregation resistance. For example, no significant bleeding and thick layer of paste were observed for C50R0A2. Yet it provided significant segregation index and factor showing relatively a low static segregation resistance. Also, there was no external bleeding for C35R15A6 but it provided significantly high segregation index and factor indicating very low static segregation resistance. However, a concrete showing significant bleeding and/or a thick layer of paste in mixer pan will definitely segregate after placement.

Segregation index:

The segregation index obtained from the sieve segregation test provided a quantitative measurement for the static segregation resistance of concrete. The segregation indices of various concretes are presented in Figure 10.11. The segregation index varied from 10.5% to 21.4% for different concretes. The concrete with 0.50 W/B ratio and 0% RHA (C50R0A2) produced the lowest segregation index (10.5%). In contrast, the concrete with 0.35 W/B ratio and 15% RHA (C35R15A6) provided the highest segregation index of 21.4%. If a segregation index of 18% is considered as the maximum acceptable limit for adequate segregation resistance, then the concrete C35R15A6 cannot be considered as resistant to segregation.

The segregation index was largely influenced by the horizontal spread or slump flow of concrete as can be seen from Figure 10.14. Similar results were reported in previous research (Rols et al. 1997, Lachemi et al. 2003). The increased slump flow implied that the spread of concrete on the sieve was greater due to lower yield stress. In general, a lower yield stress decreases the segregation resistance of concrete. The higher HRWR dosage and greater mortar volume given in Table 10.7 also indicate that the yield stress was reduced to provide a higher slump flow of concrete. Therefore, more mortar passed the sieve leading to increased segregation index. The segregation indices obtained also imply that the sieve test is inclined to provide the segregation resistance of concrete in horizontal direction. It may not represent

the actual segregation phenomenon of concrete placed in deep sections such as walls and columns. The column segregation test will be a reliable approach in such cases.

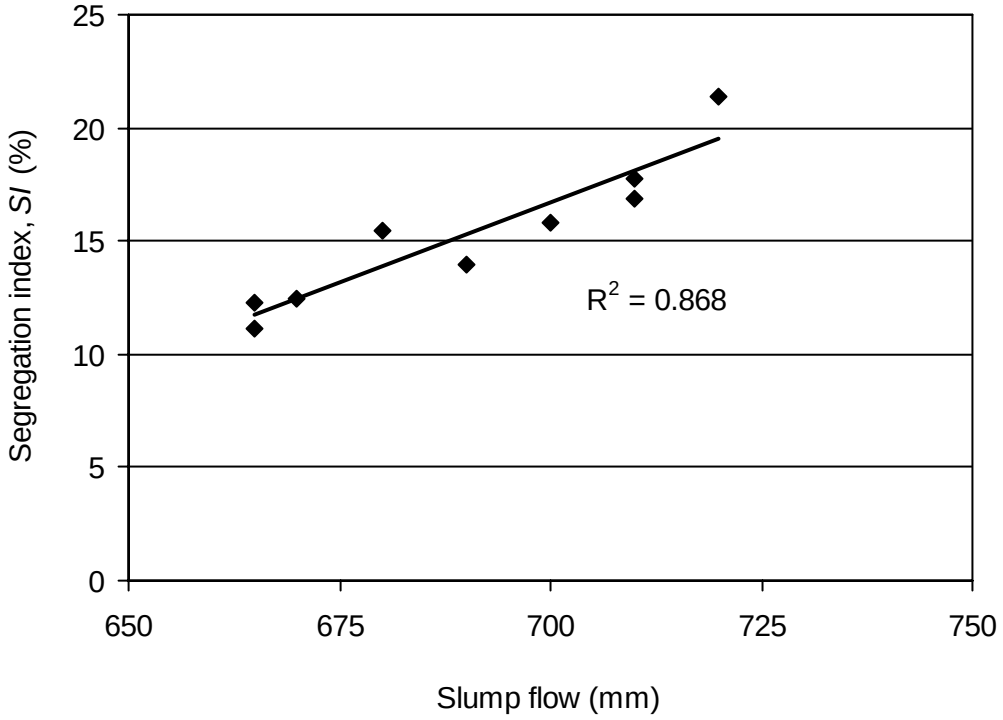

Figure 10.14: Effect of slump flow on the segregation index of SCHPC

Segregation factor:

The column segregation test provided the segregation factor as a quantitative measurement of the static segregation resistance of concrete. The segregation factors obtained from column segregation test did not follow the similar trend of variation as compared to segregation index. It varied in the range of 3% to 33.1%. The lowest segregation factor (3%) was obtained for the concrete with 0.30 W/B ratio and 0% RHA (C30R0A6) where as the highest segregation factor (33.1%) was achieved for the concrete with 0.35 W/B ratio and 15% RHA (C35R15A6). If the maximum acceptable segregation factor is 20%, then the concrete C35R15A6 cannot be considered as resistant to segregation. The overall test results of segregation factor indicate that the coarse aggregate settlement, which is mainly a function of the yield stress, plastic viscosity and density of mortar matrix (Beris et al. 1985, Petrou et al. 2000), varied differently for the concretes tested.

The yield stress and plastic viscosity of the concretes were not determined directly in the present study. However, the slump flow and flow time are strongly correlated with the yield stress and plastic viscosity of concrete, respectively (Níelsson and Wallevik 2003). In addition, the paste or mortar volume affects the yield stress (Wallevik 2006) and viscosity of concrete (Bonen et al. 2007). The slump flow, orimet and inverted slump cone flow times, mortar volume and density, HRWR dosage and RHA content of the concretes tested for column segregation are shown in Table 10.8. The increase in slump flow indicated that the yield stress decreased, and the increase in flow time implied that the plastic viscosity increased although it was not too high to stop the concrete flow. In addition, the increase in matrix (mortar) density suggests that the settlement of coarse aggregate was reduced because it increases the buoyant force acting on aggregates. Indeed, the combined effect of yield stress, plastic viscosity and mortar density determined the extent of segregation factor. The settlement of coarse aggregate occurs when the mortar yield stress is less than the critical value. The critical yield stress of mortar depends on its density. A decrease in matrix density increases the critical yield stress required to avoid segregation (Saak et al. 2001). On the other hand, the plastic viscosity controls the degree of segregation in concrete. A decrease in plastic viscosity increases the settlement rate of coarse aggregate, and thus lessens the segregation resistance of concrete (Bonen and Shah 2005).

10.6.2 Dynamic segregation resistance

The results of visual inspection of the quality of concrete during slump flow, and inverted slump cone flow and orimet flow spreads qualitatively showed the dynamic segregation resistance of concrete. The orimet and inverted slump cone flows also indicated the dynamic segregation resistance of concrete.

Dynamic segregation resistance based on flow spreads:

There was no formation of aggregate pile during slump flow, orimet flow and inverted slump cone flow spreads of the concretes as mentioned in Table 10.7. This is mostly due to low coarse aggregate content and increased mortar volume of concrete as can be seen from Table 10.8. The volume of coarse aggregate was in the range of 30.3% to 34.8%, which is less than the maximum recommended content (35%) for SCHPC (Uomoto and Ozawa 1999).

Consequently, the mortar volume of concrete became higher (> 65%) for this low range of coarse aggregate content. The inter-particle contact between coarse aggregates was decreased at lower aggregate content and increased mortar volume. Therefore, more kinetic energy was available to disperse the coarse aggregates. However, the absence of any signs of dynamic segregation in flow spreads does not mean that the concrete is dynamically stable. This is because the flow spreads can indicate the dynamic segregation of concrete in the lateral direction only.

The flow spread was faster for the concretes with higher W/B ratio and without any RHA. In contrast, the flow spread became slower for the concretes with lower W/B ratio and higher RHA content. In particular, the concrete became sticky in the presence of RHA. The stickiness was increased with increasing RHA content, and the deformation of concrete in flow spread became gradually slower. This observation suggests that the viscosity of concrete was increased with lower W/B ratio and higher RHA content. Indeed, the viscosity played the key role for the dynamic segregation resistance of concrete during horizontal flow by resisting the separation of coarse aggregates.

Dynamic segregation resistance based on vertical concrete flow and flow times:

The vertical flow of concrete was uniform during orimet and inverted slump cone flow tests for the majority of concretes. No tendency of blockage was observed during the orimet and inverted slump cone flows except for C40R0A6 and C50R0A2. This suggests that most of the concretes possessed sufficient dynamic segregation resistance. It is primarily due to the decreased aggregate content and increased plastic viscosity of concrete. The interaction between coarse aggregates leading to blocking of concrete flow is reduced at a lower coarse aggregate content. In addition, a high plastic viscosity results in a high drag force, which decreases the terminal velocity of coarse aggregates, and thus reduces the dynamic segregation in concrete (Saak et al. 2001). The terminal velocity and therefore the dynamic segregation resistance is also a function of matrix density (Saak et al. 2001). However, the concrete flow observed suggests that the effect of plastic viscosity is more predominant than that of matrix density for dynamic segregation resistance.

The orimet and inverted slump cone flow time results for the concretes tested are given in Table 10.8. The concrete flow time became higher with lower W/B ratio and greater

RHA content. The flow time is directly related to the viscosity of concrete (Níelsson and Wallevik 2003). This suggests that that the viscosity was increased for the concretes with lower W/B ratio and higher RHA. Therefore, the unblocked flow time results can provide an indication of dynamic segregation resistance of concrete. Safawi et al. (2003) reported that the degree of segregation is inversely related to the flow time of concrete. The degree of segregation becomes higher when the flow time is lower.

The tendency of blocking was observed for C40R0A6 and C50R0A2 in the first batch but no blocking occurred in repeated batches of both types. The unblocked orimet and inverted slump cone flow times of these two concretes indicate that their viscosity was relatively low. Also, the volume aggregate contents of these two concretes were 33.1% and 34.6% as can be seen from Table 10.8. Thus, the aggregate contents were comparatively high, although below the maximum recommended amount. Due to low viscosity and increased aggregate content, C40R0A6 and C50R0A2 were susceptible to dynamic segregation. Therefore, any variation in coarse aggregate content during placement may trigger the dynamic segregation to occur.

The SCHPC mixture must possess a sufficiently high plastic viscosity to avoid segregation under dynamic condition (Saak et al. 2001). The plastic viscosity helps to keep the coarse aggregates in suspension and thus reduces the dynamic segregation of concrete. However, the plastic viscosity is not a critical factor for the static segregation resistance. The critical matrix (mortar) yield stress and the matrix density play the key roles in static segregation of concrete. Therefore, a dynamically segregation-resistant SCHPC mixture may experience static segregation.

10.6.3 Effect of water-binder ratio

The visual inspection was not effective to exhibit the effect of W/B ratio on the static or dynamic segregation resistance of concretes. This is because the concretes C30R0A6 (W/B: 0.30), C35R0A6 (W/B: 0.35) and C50R0A6 (W/B: 0.50) were equally good on the basis of visual observation, and no signs of segregation were noticed. However, the orimet and inverted slump cone flow time results showed that an increase in W/B ratio decreased the flow time. This suggests that a higher W/B ratio decreases the plastic viscosity, and thus increases the susceptibility of concrete to dynamic segregation. Therefore, the concretes

C40R0A6 (W/B: 0.40) and C50R0A2 (W/B: 0.50) showed a tendency of blockage in orimet and inverted slump cone flow tests, as discussed in Section 10.6.2.

The segregation index was increased with lower W/B ratio as can be seen from Figure 10.15. A similar effect was observed by Bouzoubaâ and Lachemi (2001). This is mainly credited to the increased mortar volume at higher content of cementing material. The slump flow values given in Table 10.8 suggest that the yield stress was reduced due to greater mortar volume and higher HRWR dosage. Therefore, the concrete spread was greater and more mortar passed the sieve resulting in higher segregation index. Although the plastic viscosity of concrete was increased at lower W/B ratio as evident from the higher orimet and inverted slump cone flow time results given in Table 10.8, it did not reduce the segregation index. This is because the viscosity was not sufficiently high enough to significantly reduce the spread of concrete over the sieve. Also, the density of mortar matrix was increased with lower W/B ratio as can be seen from Table 10.8. However, it seems that the effect of increased matrix density on aggregate settlement was absent in sieve segregation test due to the limited sample height and restricted vertical movement of coarse aggregates in concrete. Thus, it was understood that the segregation index was dominated by the flow spread of concrete at reduced yield stress.

The segregation factor was decreased with lower W/B ratio as can be seen from Figure 10.16, which is in contrast with the result of segregation index. A similar effect was noticed by Assaad et al. (2004). This is mainly due to the increased density of mortar matrix at lower W/B ratio. The buoyant force acting on the aggregates was increased when the density of mortar became higher. Also, the lower W/B ratio resulted in higher plastic viscosity, which increased the frictional force acting against the gravity. Consequently, the net downward force was decreased and the settlement of aggregates was reduced. In addition, the coarse aggregate/total solid (CA/TS) volume ratio was decreased at lower W/B ratio as shown in Table 10.8. The segregation resistance of concrete is considerably increased at lower CA/TS volume ratio (Ye et al. 2005).

10.6.4 Effect of rice husk ash

The RHA influenced both static and dynamic segregation resistances of SCHPC. The visual inspection of the flow spreads and resting concrete revealed that the presence of RHA

eliminated external bleeding. However, the increased RHA content caused mortar halo in flow spreads and a thick layer of paste on the top of resting concrete in the mixer pan, and thus indicated less static segregation resistance. The appearance of mortar halo is due to greater differential movement of mortar than coarse aggregates at reduced yield stress. The increased mortar volume and slump flow given in Table 10.8 indicate that the yield stress was reduced with higher RHA content for the HRWR dosages used. But the critical yield stress needed to avoid static segregation (τ_{cmy}) was increased due to the reduced density of mortar matrix as evident from Table 10.8. Therefore, the RHA concretes were more prone to static segregation.

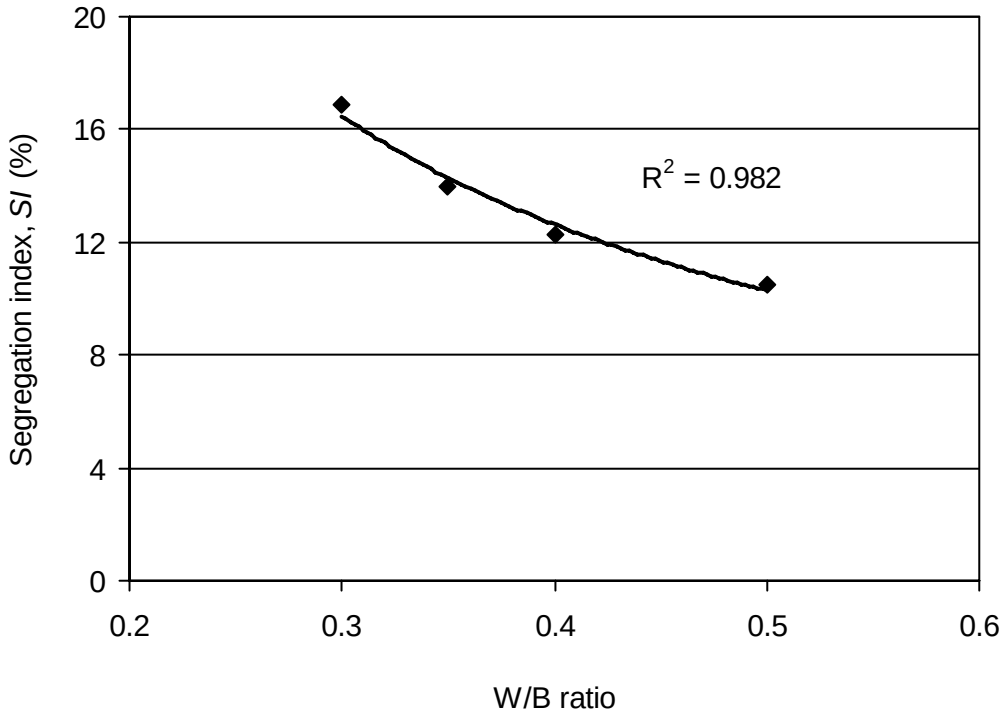

Figure 10.15: Effect of W/B ratio on the segregation index of SCHPC

The visual inspection during orimet and inverted slump cone flows revealed that no dynamic segregation occurred in RHA concretes. The RHA concretes provided slower concrete flow with higher flow time but no tendency of blockage was noticed. This is due to the increased plastic viscosity of concrete. The RHA adsorbed a greater amount of water due to high surface area and thereby reduced the free water content leading to increased plastic

viscosity, as evident from the orimet and inverted slump cone flow time results. The increased plastic viscosity increases the vertical drag force, which decreases the terminal velocity of falling aggregates and thus improves the dynamic segregation resistance of concrete. Although the density of the mortar matrix was reduced, it was not more predominant than the increased vertical drag force to cause dynamic segregation. Thus, it was understood that the increased viscosity played the key role to prevent the separation of coarse aggregates. In addition, the mortar volume was increased and the coarse aggregate content was slightly decreased in the presence of RHA. The increased mortar volume and decreased aggregate content reduced the inter-particle contact between aggregates and thereby eliminated the tendency of dynamic segregation.

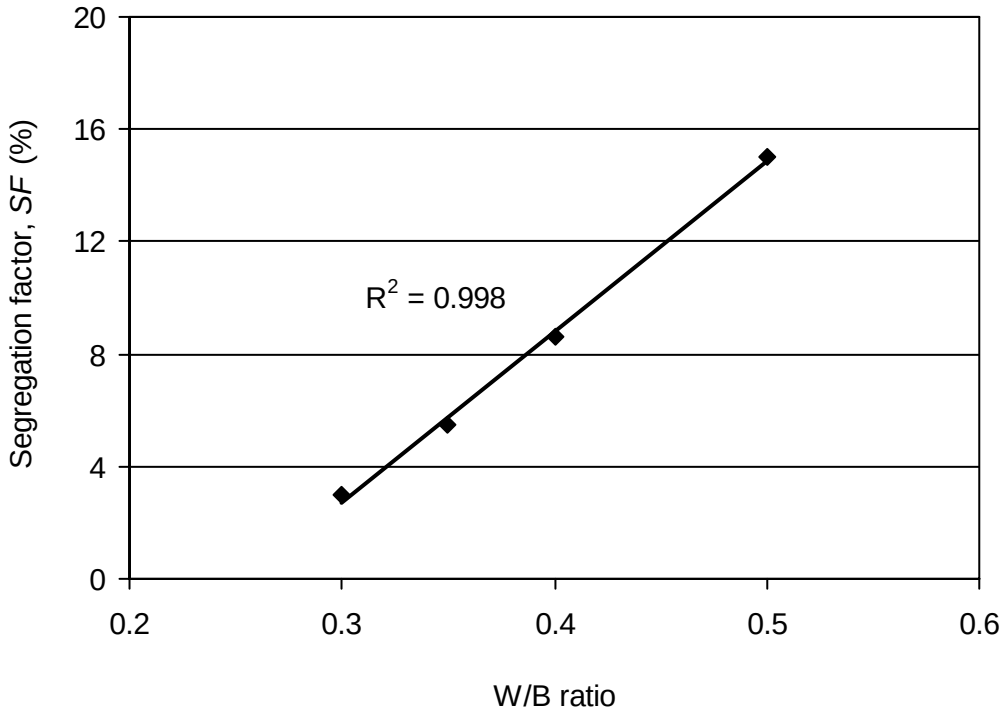

Figure 10.16: Effect of W/B ratio on the segregation factor of SCHPC

The results of sieve and column segregation tests revealed that the concretes with higher RHA content provided lower static segregation resistance. The segregation index was increased with higher RHA content as evident from Figure 10.11. This is because the increase in RHA content increased the mortar volume as can be seen from Table 10.8. The

higher slump flow also indicates that the yield stress was decreased for the HRWR dosages used. Therefore, the concrete spread was higher and that produced greater segregation index for SCHPC.

The RHA significantly affected the segregation factor of concrete, as can be seen from Figure 10.12. It is mostly due to the decreased yield stress and matrix density of concrete. The slump flow was increased with higher RHA content for the HRWR dosages used, suggesting that a low level of yield stress was attained for the RHA concretes. In addition, the volume of mortar matrix increased in the presence of RHA as can be seen from Table 10.8. The increased mortar volume decreases the yield stress of concrete due to enhanced lubrication and greater inter-particle distance between aggregates (Wallevik 2006). Moreover, the increased mortar volume at higher RHA content decreased the density of mortar matrix as evident from Table 10.8. Both yield stress and matrix density affect the static segregation resistance of concrete, as discussed in Section 2.12.1 (Chapter 2). The net downward force acting on the aggregates increases when the matrix density is decreased and the upward restoring or frictional force decreases when the yield stress is decreased. As a result, the settlement of aggregates occurred with a greater equilibrium velocity. Although the increased plastic viscosity induced by the RHA slowed down the settlement rate of falling aggregates, it was not sufficient to significantly reduce the degree of aggregate settlement. This is because the effect of reduced matrix density on the settlement of coarse aggregates can be as high as or even greater than that of plastic viscosity (Bonen and Shah 2005, Saak et al. 2001). A decrease in the matrix density from 2330 to 2190 kg/m^3 (6%) can cause more than a five fold increase in the content of segregated coarse aggregates at the bottom of the column apparatus. In addition, the effect of plastic viscosity becomes less effective when the matrix density is decreased (Bonen and Shah 2005). Indeed, the reduced matrix density and the decreased yield stress together played the key role to cause significant static segregation in SCHPC mixtures containing higher RHA content.

10.6.5 Effect of viscosity-enhancing admixture

The visual observation revealed that the use of VEA improved the segregation resistance of concrete since no signs of segregation appeared in the mixer pan and slump flow spread.

However, this process was unable to quantify the extent of improvement in segregation resistance of the concretes with VEA.

The static segregation resistance of concrete was significantly improved in the presence of VEA. The segregation index of C35R10A6 and C35R15A6 was 17.8% and 21.4%, respectively. When the VEA was used, these two concretes (re-designated as C35R10A6V and C35R15A6V) provided the segregation index of 11.1% and 12.5%, respectively, as can be seen from Figure 10.11. Thus, a significant reduction in segregation index (37 to 42%) was made by the VEA. This is because the spread of the concretes was reduced in the presence of VEA, as evident from the lower slump flow results given in Table 10.8. The viscosity and yield stress of concrete are significantly increased due to the high degree of association and entanglement of VEA polymer chains (Assaad et al. 2004). As a result, the ease of flow was reduced leading to a decrease in concrete spread.

The improvement of segregation resistance by the VEA was more significant from the results of column segregation test. The segregation factor of C35R10A6 and C35R15A6 was 16.4% and 33.1%, respectively. In the presence of VEA, the segregation factor of these two concretes (re-designated as C35R10A6V and C35R15A6V) was reduced to 1.5% and 9.0%, respectively, as can be seen from Figure 10.12. A similar effect of VEA on the segregation resistance of concrete was reported by Khayat and Guizani (1997). In the present study, the reduction in segregation factor was about 73 to 91%. The percent reduction in segregation factor was about twice the percent reduction in segregation index for the concretes tested. The significant reduction in segregation factor is due to the reason that the VEA greatly increases the viscosity and yield stress of mortar matrix (Nagataki and Fujiwara 1995, Khayat 1999). In addition, the use of VEA decreased the air content of concrete for given AEA dosage. In the presence of VEA, the concretes C35R10A6V and C35R15A6V had 3.5% and 3.8% air content, respectively, although the design air content was 6%. The yield stress and plastic viscosity of concrete can be increased with the reduction in air content (Chidiac et al. 2003, Khayat 2000). Also, the volume of mortar matrix was reduced due to the reduced air content and thus its density increased, as can be seen from Table 10.8. These effects were conducive to increase the static segregation resistance of concrete.

The use of VEA improved the segregation resistance of concrete but it caused some reductions in slump flow and air content as mentioned before. The maximum reduction in

slump flow was about 7%. The slump flow of the VEA concretes (C35R10A6V and C35R15A6V) as shown in Table 10.8 still represents a good filling ability of concrete. In addition, the reduction in air content was about 1.3 to 1.6% as compared to the air content obtained in the absence of VEA. The design total air content of 6±1.5% can be achieved by using a slightly increased AEA dosage. This will not have a significant negative effect on achieving adequate static segregation resistance, since the increases in the viscosity and yield stress caused by VEA normally dominate to improve the segregation resistance of concrete.

10.7 Comparison of Sieve and Column Segregation Tests

The factors affecting the static segregation in concrete do not produce similar effects during sieve and column tests. The segregation index given by the sieve test is mainly affected by the yield stress of concrete. But the segregation factor obtained from the column test is affected by the yield stress, plastic viscosity and matrix density of concrete. Therefore, the results of sieve and column tests can be significantly different for a given concrete. A concrete passing the sieve test may or may not pass the column test. This is because the result of the column test also considerably depends on the plastic viscosity and matrix density of concrete. For this reason, the segregation result obtained from the sieve test sometimes can be misleading for the application of SCHPC in vertical members. In such cases, the column test should be carried out to determine the static segregation resistance of concrete. The result obtained from the column apparatus will be more representative for the concrete used in vertical members. In contrast, the sieve test is more appropriate to measure the static segregation resistance of SCHPC to be used in horizontal flat members such as slabs and pavements.

10.8 Suitable Content of Rice Husk Ash

The RHA did not adversely affect the dynamic segregation resistance of concrete due to increased plastic viscosity. In contrast, the RHA decreased the static segregation resistance of concrete as it reduced the density of mortar matrix. The maximum RHA content for the adequate segregation resistance (SI ≤ 18%, SF ≤ 20%) depended on the W/B ratio of concrete. For example, the concrete C40R15A6 (W/B: 0.40) with 15% RHA provided adequate static segregation resistance whereas the concrete C35R15A6 (W/B: 0.35) with

15% RHA provided significantly low static segregation resistance. In addition, the adequate static segregation resistance was obtained for the concretes C35R5A6 and C35R10A6, which were prepared with 5% and 10% RHA, respectively. Based on the results of the present study, 10% RHA content can be considered as the maximum suitable content for segregation-resistant SCHPC without VEA. This amount can be increased if the RHA is used in SCHPC mixture in the presence of a VEA.

10.9 Conclusions

a. The segregation column with 150D×600H mm dimensions and 4 sections was more efficient than any other column to measure the static segregation resistance of concrete. The greater lateral dimension minimized the blocking of aggregate movement and the greater vertical dimension captured the effects of casting and aggregate settlement heights. Also, the column size was user-friendly, and required less quantity of concrete to conduct the test by a single operator.
b. The segregation factor calculated from the top and bottom sections was identical to that calculated from all four sections of the column apparatus. Thus, the consideration of just top and bottom sections simplified the test procedure for column segregation without compromising the accuracy of segregation measurement.
c. The segregation factor was well-correlated with the segregation index and variations in compressive strength and true electrical resistivity of the concrete used for the development of column apparatus.
d. The dynamic segregation was good for most of the concretes due to reduced coarse aggregate content. In addition, the lower W/B ratio and the higher RHA content were conducive to improve the dynamic segregation resistance because the plastic viscosity of concrete was increased.
e. The concretes with 0.40 and 0.50 W/B ratios and without any RHA exhibited less dynamic segregation resistance due to relatively high aggregate content and low viscosity. In contrast, the RHA concretes produced less static segregation resistance due to the decreases in yield stress and matrix density.
f. A concrete showing signs of segregation in flow spreads will definitely segregate after placement but the lack of segregation in flow spreads does not necessarily mean that the

concrete will not segregate after placement. Similarly, the absence of bleeding and/or a thick layer of paste on the top of concrete resting in mixer pan do not imply that the post-placement segregation will not occur. Hence, the visual inspection is often misleading and not reliable.

g. The segregation index obtained from the sieve test increased with lower W/B ratio and higher RHA content due to greater concrete spread at higher mortar volume and HRWR dosage. The increase in segregation index was consistent with the increased slump flow of concrete.
h. The sieve segregation test did not effectively capture the effects of plastic viscosity and matrix density on the segregation resistance of concrete due to limited sample height and restricted coarse aggregate settlement. The column segregation test overcame these deficiencies and thus proved its potential for use as a reliable method to measure the static segregation resistance of SCHPC.
i. The segregation column test should be conducted to measure the static segregation resistance of SCHPC to be cast in vertical members, because the column apparatus can effectively deal with the major factors affecting the segregation in such cases.
j. The concrete with higher flow time and greater matrix density provided lower segregation factor in the absence of RHA despite having an increased slump flow. This indicated that the effect of reduced yield stress was minimized due to higher plastic viscosity and increased matrix density.
k. The segregation factor decreased with lower W/B ratio due to the increases in the viscosity and matrix density of concrete. A W/B ratio in the range of 0.30 to 0.35 was suitable to improve the segregation resistance of SCHPC.
l. The static segregation resistance was reduced in the presence of RHA because it decreased the matrix density of concrete. However, a RHA content in the range of 0% to 10% can be used without any VEA to produce SCHPC with adequate segregation resistance. The RHA content can be increased if used with a VEA.
m. The VEA was very effective to produce segregation-resistant SCHPC incorporating RHA because it increases the yield stress and viscosity of concrete. Thus, the proper combination of HRWR and VEA can be an efficient way of achieving the segregation-free SCHPC.

Chapter 11

Mixture Design of Self-consolidating High Performance Concrete

11.1 General

This chapter describes a mixture design procedure for self-consolidating high performance concrete (SCHPC) and discusses its limitations. The performance requirements, principles of mixture design, materials selection, and requirements for mixture composition are highlighted. In addition, this chapter gives an example of mixture design for a SCHPC.

11.2 Research Significance

The optimization of SCHPC often requires carrying out many trial batches to achieve the desired fresh and hardened properties and durability of concrete. The mixture design method presented herein can be beneficial to obtain an optimum mixture composition of SCHPC with a minimum number of trial batches. The mixture design given is mainly for air-entrained SCHPC including rice husk ash (RHA) as a supplementary cementing material (SCM) at low water-binder (W/B) ratio. However, it is also valid for the SCHPC without any RHA, and can be applied for the non-air-entrained SCHPC. The optimum sand-aggregate (S/A) ratio is used in the design and therefore it requires relatively low binder paste, that is, low binder (cement plus RHA) content. This approach could help the concrete industry to produce SCHPC cost-effectively while satisfying the performance requirements.

11.3 Performance Requirements

The key properties such as filling ability, passing ability, segregation resistance, compressive strength, and durability must be achieved to produce SCHPC. The rheological properties such as yield stress and plastic viscosity should be suitable to obtain the filling ability, passing ability and segregation resistance in desired levels. The porosity and transport properties should be decreased, whereas the electrical resistivity should be increased to improve the durability of SCHPC. In addition, the appropriate air content must be present in SCHPC to obtain good freeze-thaw durability.

11.3.1 Filling ability

The SCHPC must possess good filling ability to achieve self-consolidation capacity. The filling ability is mainly governed by the W/B ratio, amount of cementing materials, and dosage of high-range water reducer (HRWR). The increased amount of cementing material, low W/B ratio and adequate HRWR dosage should be used to obtain an optimum filling ability. While adjusting the W/B ratio and amount of cementing materials, the coarse aggregate content should also be kept below the recommended maximum level (≤ 35% of concrete volume) to maintain a good filling ability.

The slump is not a suitable criterion for SCHPC because of its high flowing ability. Hence, the slump flow is widely used as a performance criterion of filling ability. The range of slump flow is selected based on the type of intended application. Three levels of filling ability can be selected for SCHPC on the basis of slump flow (SCCEPG 2005):

Level 1 filling ability – a slump flow of 550 to 650 mm: It is appropriate for unreinforced or slightly reinforced concrete structures, and for sections with low element shape intricacy, low element length, and high wall thickness.

Level 2 filling ability – a slump flow of 660 to 750 mm: It is most appropriate for moderately reinforced concrete structures; for sections with medium shape intricacy, length and wall thickness, and where concrete flows a medium horizontal distance.

Level 3 filling ability – a slump flow of 760 to 850 mm: It is suitable for elements with highly congested reinforcement, narrow width and complex shape, and typically used for vertical applications with a small maximum size of coarse aggregates and for lateral applications where concrete must flow long horizontal distances.

11.3.2 Passing ability

The SCHPC must possess adequately high passing ability to allow the concrete flow between reinforcing bars. This is mainly governed by the coarse aggregate size and content of concrete. The coarse aggregate content should be below the maximum recommended amount (≤ 35% of concrete volume) to obtain the desired passing ability. The low maximum size of coarse aggregate should also be used to improve the passing ability of SCHPC.

The mortar volume should be sufficiently large to increase the inter-particle spacing between coarse aggregates. The viscosity of the mortar component should also be high to

resist the separation of coarse aggregates. However, it should not be excessively high so that the coarse aggregate cannot pass through the gap between reinforcing bars.

The difference between slump flow and slump cone – J-ring flow can be used as a performance criterion for the passing ability of SCHPC. Two levels of passing ability can be used for SCHPC depending on the type of intended application (ASTM C 1621/C 1621M, 2007; SCCEPG 2005):

Level 1 passing ability - a difference between slump flow and slump cone – J-ring flow of 25 to 50 mm with a minimal noticeable blocking: It is suitable for normal applications with unreinforced or slightly reinforced sections.

Level 2 passing ability – a difference between slump flow and slump cone – J-ring flow of 0 to 25 mm without any visible blocking: It is appropriate for concrete sections with highly congested reinforcement, narrow width, and complex shape.

11.3.3 Segregation resistance

The risk of segregation is usually very high in SCHPC due to high fluidity. The segregation resistance of SCHPC can be improved by decreasing the W/B ratio with increased cementing material or by adding a viscosity-enhancing admixture (VEA). The role of coarse aggregate is also vital to improve the segregation resistance of SCHPC. The segregation resistance is improved when a reduced content and a lower maximum size of coarse aggregate are used.

Both dynamic and static segregations can occur in SCHPC. The requirements for adequate dynamic segregation resistance are more stringent for sections with congested reinforcement or for applications where the concrete is dropped from a greater vertical height and flows a longer horizontal distance (Koehler and Fowler 2006). To achieve a good dynamic segregation resistance, the SCHPC must possess an adequately high plastic viscosity, whereas it must possess a yield stress above the critical value to attain good static segregation resistance. In both cases of segregation, the difference between the densities of coarse aggregate and matrix (paste or mortar) should be as low as possible. The susceptibility to static segregation can be severe if the matrix density of SCHPC is decreased.

The segregation factor obtained from the column apparatus can be used as a criterion for the static segregation resistance of concrete. Two levels of segregation resistance can be proposed for SCHPC as follows:

Level 1 segregation resistance – a segregation factor ranging from 10 to 20%: It is applicable for both horizontal and vertical applications with lower flow distance and lightly reinforced or unreinforced section.

Level 2 segregation resistance – a segregation factor less than 10%: It is preferred for vertical applications with greater flow distance and highly congested reinforcement.

11.3.4 Rheological properties

The rheological properties such as yield stress and plastic viscosity play the vital roles to influence the flowing ability (filling ability and passing ability) and segregation resistance of concrete.

Yield stress:

The yield stress must be low to increase the flowing ability of concrete. In general, the yield stress of SCHPC varies in the range of 0 to 60 Pa (Bonen and Shah 2005). The yield stress requirement depends on the plastic viscosity of concrete. When the plastic viscosity is below 40 Pa.s, the SCHPC should have a yield stress greater than zero. Conversely, the yield stress can be about zero when the plastic viscosity is higher than 70 Pa.s (Wallevik 2003). However, a zero yield stress is detrimental for static segregation resistance. Therefore, an SCHPC mixture should have a yield stress greater than zero. Generally, a yield stress above 10 Pa is considered significant but negligible if it drops below 10 Pa (Wallevik 2003).

The yield stress can be assessed by the slump flow since they are strongly correlated. The slump flow of SCHPC must be higher than 550 mm to achieve a yield stress value below 60 Pa (Níelsson and Wallevik 2003). The flow spread of the mortar component of SCHPC can also be used to represent the slump flow and thus the yield stress of concrete. It was found in the present study that the flow spread of mortar must be higher than 250 mm to obtain a slump flow of concrete greater than 550 mm, which suggests a concrete yield stress below 60 Pa.

Plastic viscosity:

The plastic viscosity of SCHPC should be moderate to maintain good flowing ability and adequately high segregation resistance. A low viscosity is detrimental for both static and

dynamic segregation resistances. Also, a high viscosity reduces the flowing ability of concrete. Generally, the plastic viscosity of SCHPC mixture should be in the range of 20 to 100 Pa.s (Wallevik 2003).

The plastic viscosity can be assessed based on the flow time of concrete because they are generally well-correlated. The orimet and inverted slump cone flow times can provide an indication of the plastic viscosity of concrete. The orimet flow time should be in the range of 2.5 to 9 sec (Grünewald et al. 2004). The corresponding inverted slump cone flow time ranges from 1 to 5 sec, as observed in the present study. The inverted slump cone flow time > 5 sec and the orimet flow time > 9 sec indicate relatively a high viscosity, which should be avoided. Based on the orimet and inverted slump cone flow times of concrete, two levels of viscosity can be defined as follows:

Level 1 viscosity – an inverted slump cone flow time ≤ 2.5 s or an orimet flow time ≤ 5 s: It is expected to provide good flowing ability and self-consolidation capacity with a plastic viscosity ≤ 60 Pa.s (Níelsson and Wallevik 2003). However, the concrete may be susceptible to bleeding and segregation.

Level 2 viscosity – an inverted slump cone flow time > 2.5 s or an orimet flow time > 5 s: It is expected to provide good flowing ability and self-consolidation capacity with a plastic viscosity > 60 Pa.s (Níelsson and Wallevik 2003). This level of viscosity improves the segregation resistance of concrete. However, the inverted slump cone and orimet flow times should not be greater than 5 and 9 s, respectively, to avoid excessively high viscosity.

The flow time of binder paste obtained from the grout flow cone test can also be used to represent the viscosity of corresponding concrete. The flow time of paste is well-correlated with the orimet and inverted slump cone flow times of concrete as observed in the present study. Therefore, the viscosity criteria for the orimet and inverted slump cone flow times can be used to determine the viscosity criterion for the paste flow time. It was obtained in the present study that the flow time of paste should be ≤ 7 sec for level 1 viscosity and > 7 sec for level 2 viscosity. However, it should be ≤ 13 sec to avoid excessively high viscosity.

11.3.5 Compressive strength

The compressive strength of high performance concrete at 28 days must be greater than 40 MPa (Kosmatka et al. 2002), which is also valid for SCHPC. It can be achieved by using low

maximum size of coarse aggregate and reduced W/B ratio, and by incorporating a suitable SCM. Most of the SCMs produce higher strength at later age. For this reason, the 28 days criterion for compressive strength has been modified to 56 days or 91 days in many specifications (ACI 211.4R-93, 2004). However, the 28 days criterion can be used for the RHA concrete. This is because the additional strength gain due to RHA was ≤ 5% at 56 days as compared to the compressive strength at 28 days. The RHA is a highly reactive SCM because of its extremely high specific surface area. Hence, it readily reacts with the $Ca(OH)_2$ liberated from cement hydration to produce additional CSH gel (secondary hydration product), and thus increases the strength from the early age of concrete (Mehta 1992).

The average compressive strength must exceed the specified strength by a sufficient amount so that the probability of getting low strength is small. The average compressive strength of SCHPC can be determined from the specified strength using Equation 11.1 when the proportions are selected based on the laboratory trial batches (ACI 211.4R-93, 2004).

$$f'_{cr} = \frac{f'_c + 9.6}{0.90} \qquad \text{(Equation 11.1)}$$

where:

f'_{cr} = Average compressive strength of concrete (MPa)

f'_c = Specified design compressive strength of concrete (MPa)

11.3.6 Durability

The SCHPC must possess high durability for long service life. The durability is correlated with the porosity, transport properties and electrical resistivity of concrete. A good durability can be achieved by decreasing the porosity and transport properties such as water absorption and water permeability of concrete. In addition, the durability of SCHPC can be enhanced by increasing its electrical resistivity. The total porosity and water absorption should be less than 15% (Hearn et al. 1994, Nokken and Hooton 2002) and 6% (Vanwalleghem et al. 2003), respectively, and the true electrical resistivity must be greater than 5 kΩ-cm (Hearn 1996) to improve the durability of concrete. The ultrasonic pulse velocity and compressive strength can also be used as a predictor of durability because both of these properties are directly

related to concrete quality. An ultrasonic pulse velocity higher than 4575 m/s (Shetty 2001) and a compressive strength greater than 40 MPa (Kosmatka 2002) suggest a low porosity, which contributes to improve the durability of concrete. A low W/B ratio, an optimum S/A ratio, and the presence of a pozzolanic SCM are the key factors to reduce the total porosity and transport properties, and to increase the electrical resistivity, ultrasonic pulse velocity and compressive strength of concrete, thus contributing to enhance concrete durability.

11.3.7 Air content

The air content of SCHPC requiring high freeze-thaw resistance should normally be at least 4.5% (Uomoto and Ozawa 1999). The CSA recommends an air content in the range of 4 to 9% for the aggregate sizes most commonly used in SCHPC (CSA A23.1, 2004). However, an air content of 6% generally corresponds to a spacing factor lower than 230 μm, which is required for good freeze-thaw durability (Lessard et al. 1995). Therefore, an air content of 6±1.5% can be chosen for air-entrained SCHPC.

11.4 Principles of Mixture Design

The optimum S/A ratio improves the physical packing in aggregate skeleton of concrete, and thus reduces the void content. Consequently, less paste is required to obtain a good flowing ability in concrete.

The paste volume must be greater than the void content of aggregate blend to coat and lubricate the aggregates by a layer of excess paste. The excess paste reduces the friction between aggregates and thus enhances the flowing ability of concrete.

The low coarse aggregate content increases the mortar volume as well as the inter-particle distance between aggregates. It reduces the interlocking and bridging of aggregates during concrete flow and thus increases the flowing ability and segregation resistance of concrete.

The increased cementing material at low W/B ratio and adequate HRWR dosage can provide optimum flowing ability and segregation resistance, and thus helps to maintain self-consolidation capacity of concrete.

The optimum flowing ability and segregation resistance can be achieved by adjusting the fluidity and viscosity of concrete through a proper combination of cement and SCM,

limiting the W/B ratio and adding a suitable dosage of HRWR, and optionally adding an adequate dosage of VEA.

The high compressive strength and ultrasonic pulse velocity, low porosity and transport properties, and high electrical resistivity suggesting a good durability are achieved by the compacted aggregates with maximum density and minimum void content at optimum S/A ratio, and by binding them with a paste of low W/B ratio.

11.5 Materials Selection

The constituent materials should satisfy the quality requirements to attain the desired fresh and hardened properties and durability of SCHPC. They should not contain any harmful ingredients in significant quantities that may be detrimental to the properties and durability of concrete.

Coarse aggregate:

The coarse aggregates conforming to ASTM C 33 (2004) can be used to produce SCHPC. The type, shape and size, surface texture, porosity, absorption, gradation, fines content, and reactivity of coarse aggregates should be taken into account to maintain the quality of concrete. Usually, the normal-weight coarse aggregates are used in SCHPC. Round or crushed coarse aggregates or a blend of both can be used. Whatever the type of coarse aggregate chosen, it should be well-graded ($1 \leq$ gradation coefficient ≤ 3) to enhance the flowing ability, segregation resistance and particle packing of concrete. In addition, the low maximum size ($\leq$ 25 mm) should be selected to improve flowing ability, segregation resistance, and strength. The production of SCHPC with good flowing ability and adequately high segregation resistance becomes difficult for the coarse aggregates larger than 25 mm (ASTM C 1611/C 1611M, 2007). The larger size also reduces the strength of concrete. The recommended maximum aggregate size for SCHPC is 9.5-19 mm (EFNARC 2002; ACI Committee 211H, 2006).

Fine aggregate:

The fine aggregates conforming to ASTM C 33 (2004) can be selected for use in SCHPC. The particle shape, surface texture, surface area, void content, absorption, gradation, and

soundness should be considered while selecting the fine aggregate. The crushed and rounded fine aggregates or their blend can be used in SCHPC. The rounded fine aggregate is conducive to the flowing ability whereas the crushed fine aggregate is beneficial to increase the strength of concrete. Nevertheless, the fine aggregate selected for SCHPC should be well-graded to improve the flowing ability and strength of concrete. Fine aggregate with a fineness modulus in the range of 2.5 to 3.2 is preferable to obtain high strength (ACI 211.4R-93, 2004). Well-graded fine aggregate also reduces the void content in aggregate blend and thus improves the physical packing of concrete (Tasi et al. 2006).

Cement:

The cements conforming to ASTM C150 (2004) or ASTM C 1157 (2004) can be used for the production of SCHPC. The proper choice of cement type is dictated by the specific requirements of the desired application.

Rice husk ash:

The non-crystalline amorphous RHA can be used in SCHPC as a pozzolanic SCM. It enhances the grain size distribution and particle packing to improve the cohesiveness of concrete. The RHA increases the viscosity, which is conducive to improve the segregation resistance of concrete. However, it reduces the matrix density, which can decrease the segregation resistance of concrete, particularly at static condition. Also, the RHA increases the paste volume, which enhances the flowing ability of concrete.

In hardened concrete, the RHA can increase the compressive strength by up to 40% or more as observed from the present study. Hence, the use of RHA allows to increase the strength of concrete without further reduction in W/B ratio, or to adopt a higher W/B ratio for the same strength. In addition, the RHA provides significant improvement in concrete properties that govern durability.

The physical and chemical properties of RHA should be suitable to produce SCHPC. The median particle size of RHA must be significantly lower than that of cement for good microfilling ability. The pozzolanic activity index of RHA must be > 85% for good strength gain through pozzolanic reaction. In addition, the specific surface area (surface fineness) must be > 15 m^2/g to achieve a good pozzolanic activity. A higher surface fineness also

decreases bleeding, and increases the cohesiveness of concrete. The silica content of RHA must be ≥ 85% to possess a good pozzolanic activity. Moreover, the igneous loss of RHA should be ≤ 6% to ensure that excessive carbonation did not occur due to the exposure to the atmosphere during prolonged storage.

Mixing water:

The water conforming to ASTM C 94/C 94 M (2004) or CSA A23.1 (2004) can be used to produce SCHPC. In general, the normal tap water is suitable to prepare any concrete. In case of the recycled water recovered from the processes of concrete industry, it must be examined for the acceptance criteria before use in SCHPC to avoid any adverse effect on the quality of concrete.

High-range water reducer:

The use of HRWR is essential for SCHPC to achieve the required flowing ability. The HRWR conforming to ASTM C494/C 494M (2004) or ASTM C 1017/C 1017M (2004) can be used. There are many commercially available HRWRs that can be selected. However, the polycarboxylate-based HRWR is mostly used to produce SCHPC due to its better ability to retain the fluidity of concrete mixture.

Air-entraining admixture:

The AEA conforming to ASTM C 494/C 494M (2004) or ASTM C 260 (2004) can be used to produce the air-entrained SCHPC. The addition of AEA can be accomplished in the same way as in non-self-consolidating concretes.

Viscosity-enhancing admixture:

The use of VEA in SCHPC is not always necessary. However, it can be used to improve the homogeneity and stability of concrete with increased segregation resistance, and to reduce the sensitivity of the mixture due to variations in the proportions and conditions of other constituent materials. In particular, the VEA can be advantageous for the SCHPC containing gap-graded, angular, flat and elongated coarse aggregates and a lower content of cementing material (ACI Committee 211H, 2006).

11.6 Requirements for Mixture Composition

The fine and coarse aggregate contents, S/A ratio, binder content, W/B ratio, water content, paste or mortar volume, and the dosages of chemical admixtures such as HRWR, AEA and VEA play the key roles to form a proper mixture composition of SCHPC.

Coarse aggregate content:

The coarse aggregate content influences the flowing ability, segregation resistance and strength of SCHPC (Nagataki and Fujiwara 1995, Okamura and Ozawa 1995). The coarse aggregate content of SCHPC should be in the range of 28 to 35% of concrete volume (EFNARC 2002, Uomoto and Ozawa 1999). Also, it is suggested that the coarse aggregate content should be about 50% of the dry packed unit weight of aggregate blend (Su et al. 2001). The content of coarse aggregate depends on its maximum size and particle shape as well as on the type of application (ACI Committee 211H, 2006). A higher content can be used if a rounded coarse aggregate of lower maximum size (< 25 mm) is chosen, and when the passing ability is not a concern.

Fine aggregate content:

The fine aggregate content influences the flowing ability of SCHPC (Okamura and Ozawa 1995). Also, the fine aggregate content affects cohesion, and thus the segregation resistance of concrete (Shilstone, Sr. and Shilstone, Jr. 1993). The fine aggregate content should be in the range of 48 to 55% of total aggregates by weight (SCCEPG 2005) or 40 to 50% of mortar volume (EFNARC 2002, Okamura and Ozawa 1995) to produce good flowing ability in SCHPC.

Optimum S/A ratio:

The optimum S/A ratio should be used to decrease the porosity and transport properties, and thus to improve the strength and durability of concrete. However, it should also be conducive to the flowing ability and segregation resistance of SCHPC. The optimum S/A ratio (by weight) usually varies in the range of 0.40 to 0.55 depending on the type and size of fine and coarse aggregates (Domone and Soutsos 1994, Koehler and Fowler 2006, Schrader 1976).

W/B ratio:

The W/B ratio of air-entrained high performance concrete generally ranges from 0.25 to 0.40 (Lessard et al. 1995), which can also be used to produce SCHPC. The weight basis W/B ratio for SCHPC typically ranges from 0.25 to 0.37 (Uomoto and Ozawa 1999, EFNARC 2002). A higher W/B ratio within the above range can be used when a lower maximum size of coarse aggregate and a reactive SCM such as silica fume and RHA are chosen.

Binder content:

The cement alone or with SCM constitutes the binder content of concrete. The recommended minimum binder content to produce durable concrete is 290 kg/m^3 (Su et al. 2001). In high strength and high performance concretes, the binder content more often ranges from 390 to 560 kg/m^3 (ACI 363R-92, 2005; Gutiérrez and Cánovas 1996). The binder content for SCHPC generally varies in the range of 350 to 600 kg/m^3 (EFNARC 2002, SCCEPG 2005, Uomoto and Ozawa 1999).

RHA content:

Rice husk ash has been used in high strength and high performance concretes as a SCM with a content ranging from 5 to 30% of cement by weight (Ismail and Waliuddin 1996, Mahmud et al. 2004, Zhang and Malhotra 1996). However, the high RHA content may reduce the flowing ability of SCHPC due to increased water demand. To maintain adequate flowing ability, a high RHA content requires relatively a high HRWR dosage, which may delay the setting of cement, and thus the early strength gain in concrete can be impeded. In addition, a high RHA content may reduce the segregation resistance by lowering the density of the matrix. A high RHA content can also cause mixing and handling difficulties due to excessive cohesiveness or stickiness. Based on the present study, a RHA content ≤ 15% should be used in SCHPC.

Water content:

The water content of SCHPC generally varies in the range of 150 to 210 kg/m^3 (SCCEPG 2005, Uomoto and Ozawa 1999). However, a water content < 150 kg/m^3 can be used depending on the binder content and effectiveness of HRWR. It was reported that the

minimum water content of high performance concrete can be as low as 120 kg/m^3 (Aïtcin 1995), which is also applicable to SCHPC.

Paste volume:

The paste volume of SCHPC typically ranges from 28 to 40% of total concrete (ACI Committee 211H, 2006; Koehler and Fowler 2006, SCCEPG 2005). A higher paste volume within the above range should be used when a lower maximum size of coarse aggregate is chosen.

The paste volume should be higher than the void content of the aggregate blend plus an excess paste of at least 8% of the concrete volume (Koehler and Fowler 2006). The void content of the optimum aggregate blend can be calculated as follows (ACI 211.4R-93, 2004; Koehler and Fowler 2006):

$$V_{caad} = \left(1 - \frac{BD_{mad}}{\frac{\rho_w}{V_{ta}}\left(V_{fa}\rho_{rfaad} + V_{ca}\rho_{rcaad}\right)} \right) \times 100\% \qquad \text{(Equation 11.2)}$$

where:

V_{caad} = Voids in air-dry basis compacted aggregate blend (%)

BD_{mad} = Maximum bulk density of air-dry aggregate blend (kg/m^3)

V_{ca} = Absolute volume of coarse aggregate (m^3)

V_{fa} = Absolute volume of fine aggregate (m^3)

V_{ta} = Absolute volume of total aggregates (m^3)

ρ_w = Density of water (kg/m^3)

ρ_{rfaad} = Air-dry basis relative density of fine aggregate

ρ_{rcaad} = Air-dry basis relative density of coarse aggregate

After calculating the void content of the optimum aggregate blend and considering 8% excess paste (V_{ep} in m^3/m^3), the minimum paste volume (V_{mp} in m^3/m^3) requirement for SCHPC can be determined as follows:

$$V_{mp} = \left[1 - \left(1 - V_{ep}\right)\left(\frac{100 - V_{caad}}{100}\right)\right] \quad \text{(Equation 11.3)}$$

The paste volume of SCHPC must be ≥ V_{mp} to maintain good flowing ability and adequate segregation resistance.

Mortar volume:

The mortar content of SCHPC is relatively high due to reduced coarse aggregate content. The mortar volume of SCHPC should be in the range of 65 to 72% of concrete volume since the recommended coarse aggregate volume content varies from 28 to 35% (ACI Committee 211H, 2006; Uomoto and Ozawa 1999).

HRWR dosage:

The HRWR dosage greatly depends upon the surface characteristics of cement and SCM such as particle size and specific surface area. The dosage is also affected by the type of HRWR and its compatibility with cement. A very high dosage of HRWR might cause segregation and bleeding in concrete. Therefore, the HRWR dosage should be kept as low as possible. The maximum HRWR dosage for SCHPC can be in the range of 3 to 5% of binder by weight depending on the type of admixture (Kwan 2000).

AEA dosage:

A higher dosage of AEA is generally required for SCHPC to maintain a specified total air content due to the presence of SCM, HRWR and VEA (Khayat 2000, Siebel 1989). However, very high dosage of AEA is not beneficial for the strength and freeze-thaw durability of concrete. In general, the AEA dosage should not exceed 1 to 2% of binder by weight (Nawy 1996).

VEA dosage:

The VEA is recommended to be used in SCHPC when the fresh mixture is too fluid and exhibits an instability (segregation) problem. The dosage of VEA may vary in the range of 0.15 to 0.95% of binder by weight (MBT, 2002).

11.7 Mixture Design Procedure

The mixture design described herein determines the proportions of the constituent materials for a trial mixture of SCHPC. Before finalizing the mixture proportions, the key properties of concrete should be evaluated and the proportions should be adjusted appropriately to satisfy the performance requirements. Various steps of the mixture design are shown in Figure 11.1, and discussed below.

Selection and testing of materials:

Select the constituent materials and examine their suitability to produce SCHPC. Determine the relative density, absorption and moisture content of fine and coarse aggregates; determine the relative density of cement and RHA; and determine the relative density and solid content of HRWR. Select the maximum size of coarse aggregate based on the requirement for the intended use of concrete.

Determining optimum S/A ratio:

Mix the air-dry fine and coarse aggregates using different weight-basis S/A ratios, and determine the bulk density of each compacted aggregate blend according to ASTM C 29/C 29M (2004). Plot the bulk density versus S/A ratio curve. Using this curve, determine the optimum S/A ratio leading to the maximum bulk density (minimum void content) in aggregate blend. The optimum S/A ratio will vary depending on the type, size and gradation of aggregates.

After obtaining the maximum bulk density at optimum S/A ratio, calculate the void content (V_{caad}) of compacted aggregate blend using Equation 11.2 and determine the minimum paste volume required for SCHPC based on Equation 11.3.

Selection of slump flow and estimation of paste volume:

Set the required level of slump flow based on the requirement for the intended use of concrete, as guided in Section 11.3.1. For the chosen slump flow, determine the paste volume using the chart given in Figure 11.2. This chart has been developed based on Equation 8.8 (Chapter 8).

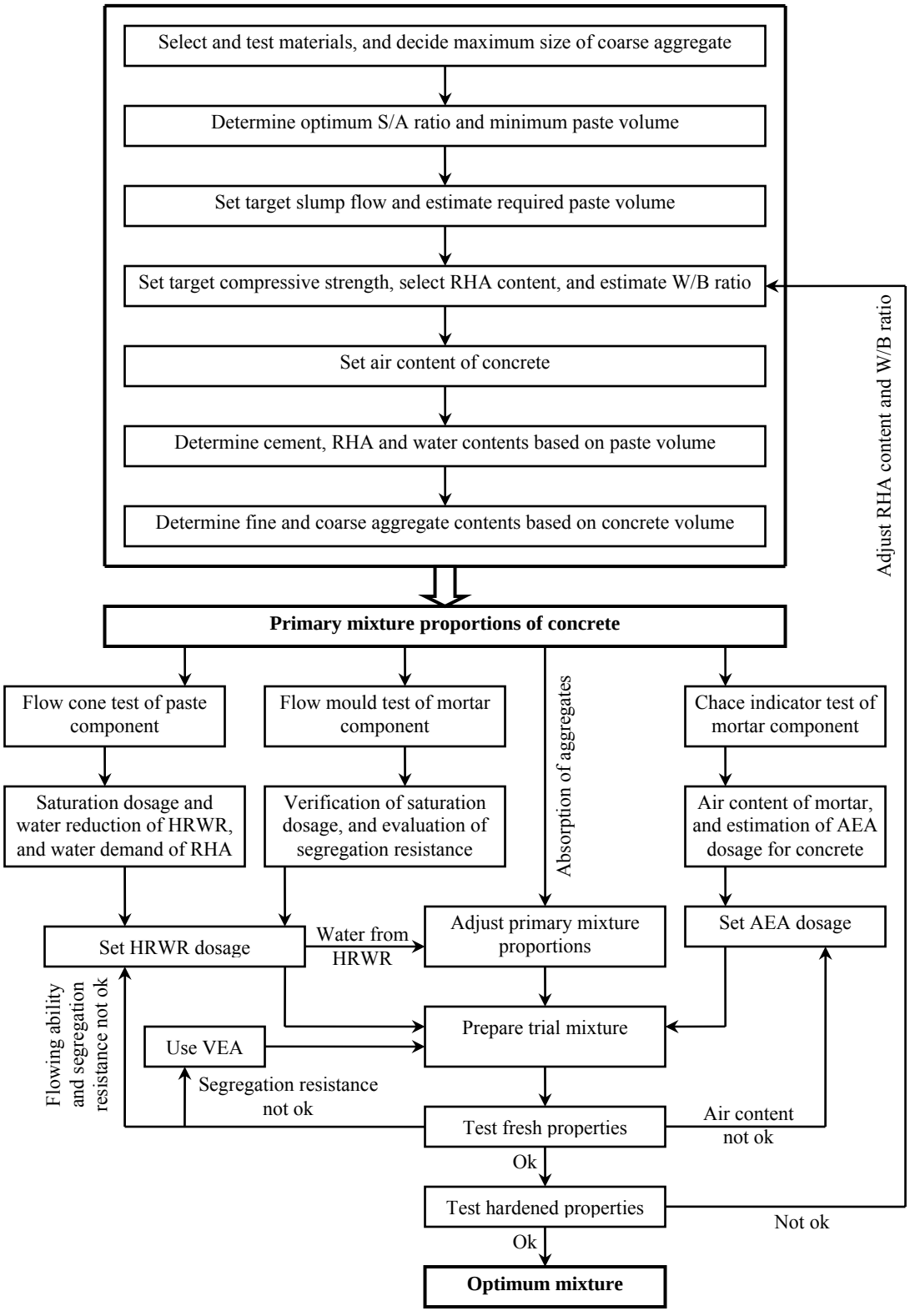

Figure 11.1: Flowchart for mixture design procedure

The chart shown in Figure 11.2 is valid for both air-entrained and non-air-entrained concretes. Since the unit weight (density) of SCHPC mixture may vary in the range of 2200 to 2600 kg/m^3, the values of 2.2 to 2.6 were used for relative density (ρ_r) to produce the chart.

Check whether the paste volume obtained satisfies the minimum paste volume requirement of SCHPC. When the paste volume obtained is less than the minimum paste volume, choose the minimum paste to prepare the trial mixture.

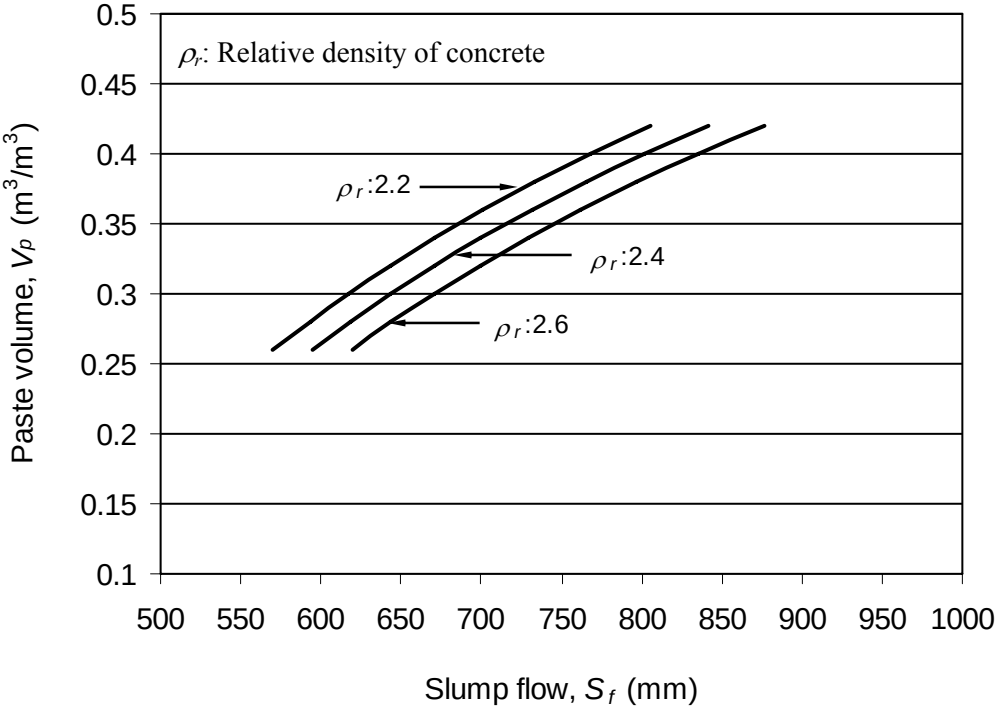

Figure 11.2: Chart for determining paste volume based on slump flow

Selection of strength and RHA content, and estimation of W/B ratio:

Set the specified compressive strength based on the requirement for the intended use of concrete and select the RHA content. Calculate the average compressive strength of concrete using Equation 11.1 before estimating the W/B ratio. It is important to note that the relationship between W/B ratio and compressive strength for conventional concrete may not be valid for SCHPC due to the use of HRWR and optimum S/A ratio. Determine the W/B ratio for the average compressive strength using the chart given in Figure 11.3. This chart has been developed based on Equation 9.10 (Chapter 9).

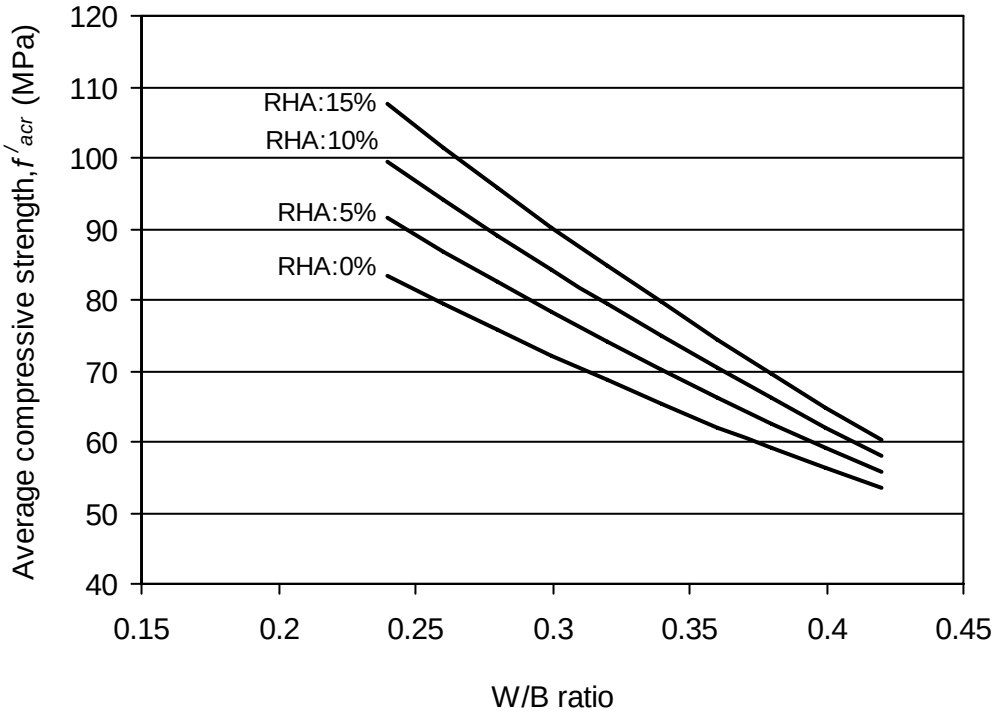

Figure 11.3: Chart for determining W/B ratio based on average compressive strength

The chart shown in Figure 11.3 is valid for the air-entrained SCHPC including 6±1.5% air content. However, it can also be used for non-air-entrained SCHPC by considering the effect of air content on the compressive strength of concrete. It was observed in the present study that 1% increase in air content decreases the compressive strength of concrete by about 4%. Hence, the average compressive strengths of the air-entrained and non-air-entrained SCHPC mixtures can be interrelated using the following equation:

$$f'_{acr} = \frac{100\, f'_{nacr}}{100 + 4\left(A_t - A_p\right)} \qquad \text{(Equation 11.4)}$$

where:

f'_{acr} = Equivalent average compressive strength of air-entrained SCHPC (MPa)

f'_{nacr} = Average compressive strength of non-air-entrained SCHPC (MPa)

A_p = Entrapped air content (%)

A_t = Total design air content (%)

The average compressive strength for the non-air-entrained SCHPC can be determined using Equation 11.1. Then the equivalent average compressive strength of air-entrained concrete can be calculated based on Equation 11.4 when A_t and A_p are known. For this strength, the W/B ratio required can be obtained from Figure 11.3 and used for non-air-entrained SCHPC.

After obtaining the W/B ratio, check whether it fulfills the requirement for SCHPC. The W/B ratio of SCHPC should be ≤ 0.40.

Selection of total air content:

Select a design total air content of 6% for the air-entrained SCHPC. It is suitable for most exposure classes of concrete depicted in CSA A23.1 (2004). Consider 2% design air content (entrapped air content) for the non-air-entrained concrete.

Determining cement, RHA, and water contents:

Based on the known paste volume (V_p), W/B ratio, percent RHA content, and design air content of concrete, the cement, RHA and water contents can be determined using the following equation:

$$\frac{1}{\rho_w}\left[\frac{(1-P_{rha})W_b}{\rho_{rc}}+\frac{P_{rha}W_b}{\rho_{rrha}}+\left(\frac{W}{B}\right)W_b\right]+A_c=V_p \qquad \text{(Equation 11.5)}$$

where:

A_c = Design air content (%)

P_{rha} = RHA content (%B by weight)

ρ_w = Density of water (kg/m^3)

ρ_{rc} = Relative density of cement

ρ_{rrha} = Relative density of RHA

V_p = Paste volume (m^3/m^3)

W/B = Water-binder ratio (by weight)

W_b = Binder (cement plus RHA) weight (kg/m^3)

The binder content is first obtained from Equation 11.5 by solving for W_b. Then the cement, RHA and water contents can be determined based on Equations 11.6 to 11.8, respectively, given below:

$$W_c = (1 - P_{rha})W_b \quad \text{(Equation 11.6)}$$

$$W_{rha} = P_{rha}W_b \quad \text{(Equation 11.7)}$$

$$W_w = \left(\frac{W}{B}\right)W_b \quad \text{(Equation 11.8)}$$

where:

W_c = Weight of cement (kg/m^3)

W_{rha} = Weight of RHA (kg/m^3)

W_w = Weight of water (kg/m^3)

P_{rha} = RHA content (%B by weight)

W/B = Water-binder ratio (by weight)

W_b = Binder (cement plus RHA) weight (kg/m^3)

After obtaining the cement, RHA and water contents, check whether the binder and mixing water quantities fulfill the requirements of SCHPC. The water content should be < 210 kg/m^3 and the binder content must be > 290 kg/m^3.

Calculation of aggregate contents:

When the cement, RHA and water contents, the optimum S/A ratio, and the air content are known, the fine and coarse aggregate contents can be determined based on the following equations:

$$W_{ca} = \left\{1 - \left(\frac{S}{A}\right)_{opt}\right\} \times \{W_{ta}(1 + A_{ca} - M_{ca})\} \quad \text{(Equation 11.9)}$$

$$W_{fa} = \left(\frac{S}{A}\right)_{opt} \times \left\{W_{ta}(1 + A_{fa} - M_{fa})\right\} \quad \text{(Equation 11.10)}$$

$$\frac{1}{\rho_w}\left(\frac{W_c}{\rho_{rc}} + \frac{W_{rha}}{\rho_{rrha}} + \frac{W_{fa}}{\rho_{rfa}} + \frac{W_{ca}}{\rho_{rca}} + W_w\right) + A_c = 1 \quad \text{(Equation 11.11)}$$

where:

W_{ca} = Amount of saturated surface-dry coarse aggregate (kg/m^3)

W_{fa} = Amount of saturated surface-dry fine aggregate or sand (kg/m^3)

W_{ta} = Amount of total aggregate in air-dry condition (kg/m^3)

A_{ca} = Absorption of coarse aggregate (%)

A_{fa} = Absorption of fine aggregate (%)

M_{ca} = Moisture content of coarse aggregate (%)

M_{fa} = Moisture content of fine aggregate (%)

$(S/A)_{opt}$ = Air-dry weight-basis optimum S/A ratio

ρ_{rca} = Saturated surface-dry basis relative density of coarse aggregate

ρ_{rfa} = Saturated surface-dry basis relative density of fine aggregate

The other parameters have been explained before.

At first, the amount of total aggregates is determined by substituting Equations 11.9 and 11.10 in Equation 11.11, and by solving for W_{ta}. Then the coarse and fine aggregate contents are obtained from Equations 11.9 and 11.10, respectively. After obtaining the aggregate contents, check whether the coarse aggregate content and the mortar volume fulfill the requirements for SCHPC. The coarse aggregate content should be ≤ 35% of concrete volume. Consequently, the mortar volume should be ≥ 65% of concrete volume.

Obtaining primary mixture proportions:

The primary mixture proportions are known after obtaining the weight contents of cement, RHA, water, and fine and coarse aggregates. Using these proportions, estimate the unit weight of concrete. Based on the estimated unit weight of concrete, the primary mixture proportions can be further refined by an iteration process.

Determining the dosage of HRWR:

A proper dosage of HRWR for SCHPC can be determined based on its saturation dosage obtained by testing the filling ability of the paste component of concrete using a standard grout flow cone as specified in ASTM C 939 (2004). The saturation dosage is defined as a HRWR dosage beyond which the flow time no longer decreases. The HRWR dosage selected thereby should be below its saturation dosage. This is because the fluidity of concrete does not improve but the risk of segregation or set retardation can increase when the HRWR dosage exceeds the saturation point (Lessard et al. 1995).

The HRWR dosage required greatly depends on its water reduction capacity and the water demand of RHA used. Therefore, consider the water reduction of HRWR and the water demand of RHA while selecting the HRWR dosage. Using the aforementioned flow cone, both of these properties can be determined by testing the filling ability of the paste component of SCHPC with increasing water content but without any HRWR while obtaining similar filing ability given by the selected dosage of HRWR (detailed procedure is described in Chapter 5). In addition, the viscosity of paste should be taken into account while selecting the HRWR dosage. The paste viscosity should not be too low or too high to maintain optimum flowing ability and segregation resistance in concrete. For this, the paste flow time obtained from the flow cone test should be in the range of 5 to 13 sec.

The selected HRWR dosage can be verified by testing the filling ability of the mortar component of SCHPC with a standard flow mould as specified in ASTM C 230/C 230M (2004). There should not be any signs of segregation (bleeding and/or aggregate piling) in the flow spread of mortar to ensure adequate segregation resistance in concrete. In addition, the mortar flow spread should be higher than 250 mm to obtain a good flowing ability in concrete with a slump flow greater than 550 mm.

Determining the dosage of AEA:

A suitable AEA dosage for SCHPC can be estimated by testing the air content of its mortar component using a Chace indicator as specified in AASHTO T 199 (2004). At first, calculate the equivalent mortar air content for the specified concrete air content using Equation 6.1 (Chapter 6). This is approximately 1.5 times the concrete air content. Determine the air content of mortar for various AEA dosages. Plot the air content versus AEA dosage curve.

Using this curve, determine the AEA dosage for the equivalent air content of mortar. Now estimate the AEA dosage for the concrete using Equation 6.2 (Chapter 6). The AEA dosage obtained thereby is applicable for the concrete without any VEA. It needs to be adjusted when a VEA is used in concrete.

Determining the dosage of VEA:

Use a VEA when the stability (segregation resistance) of concrete mixture needs to be improved without changing the primary proportions of concrete. Determine the VEA dosage based on the manufacture's recommended dosage.

Adjusting primary mixture proportions:

The primary proportions of fine and coarse aggregates are obtained in saturated surface-dry condition. If the air-dry fine and coarse aggregates are selected, the aggregate proportions should be corrected considering their absorption and moisture content. Adjust the primary proportions of fine and coarse aggregate using the following equations:

$$W_{caad} = \frac{W_{ca}}{1 + A_{ca} - M_{ca}} \qquad \text{(Equation 11.12)}$$

$$W_{faad} = \frac{W_{fa}}{1 + A_{fa} - M_{fa}} \qquad \text{(Equation 11.13)}$$

where:

W_{caad} = Adjusted air-dry weight of coarse aggregate (kg/m^3)

W_{faad} = Adjusted air-dry weight of fine aggregate (kg/m^3)

A_{ca} = Absorption of coarse aggregate (%)

A_{fa} = Absorption of fine aggregate (%)

M_{ca} = Moisture content of coarse aggregate (%)

M_{fa} = Moisture content of fine aggregate (%)

W_{ca} = Amount of saturated surface-dry coarse aggregate (kg/m^3)

W_{fa} = Amount of saturated surface-dry fine aggregate or sand (kg/m^3)

The proportion of water should also be adjusted based on the absorption of fine and coarse aggregates and the water contribution of HRWR. The adjusted proportion of mixing water can be determined using the following equation:

$$W_{wad} = W_w + \left(W_{ca} - W_{caad} + W_{fa} - W_{faad}\right) - \frac{D_h W_b}{100}\left(1 - \frac{S_h}{100}\right) \quad \text{(Equation 11.14)}$$

where:

W_{wad} = Adjusted weight of mixing water (kg/m^3)

D_h = Dosage of HRWR (%B by weight)

S_h = Solid content of HRWR (% by weight)

W_b = Binder (cement plus RHA) weight (kg/m^3)

W_{ca} = Amount of saturated surface-dry coarse aggregate (kg/m^3)

W_{caad} = Adjusted air-dry weight of coarse aggregate (kg/m^3)

W_{fa} = Amount of saturated surface-dry fine aggregate or sand (kg/m^3)

W_{faad} = Adjusted air-dry weight of fine aggregate (kg/m^3)

W_w = Weight of water (kg/m^3)

Trial mixture and adjustments:

Prepare a trial mixture and determine the key fresh properties such as filling ability, passing ability, segregation resistance and air content. Examine the filling ability, passing ability, and air content based on the test procedures discussed in Chapter 8. Check the segregation resistance using the sieve and column apparatus based on the test procedures discussed in Chapter 10. Increase the HRWR dosage when the filling ability and passing ability are low. Conversely, decrease the HRWR dosage when these two properties are high. When the flowing ability cannot be controlled by adjusting the HRWR dosage (extreme case), adjust the paste volume and RHA content, adjust the aggregate grading, change the maximum size of coarse aggregate or change the type of HRWR. A higher paste volume and a lower RHA content are conducive to obtain the target flowing ability with relatively a low HRWR dosage. Moreover, a greater finer fraction of aggregates and a lower maximum size of coarse aggregate are helpful to achieve a higher flowing ability.

Decrease the HRWR dosage and/or use a VEA when the segregation resistance is not adequate. When the segregation resistance cannot be controlled by the HRWR and VEA (extreme case), decrease the W/B ratio and RHA content, reduce the coarseness of aggregate grading, decrease the maximum size of coarse aggregate or change the type of VEA. Adjust the AEA dosage to obtain the required air content. When the target air content cannot be achieved (extreme case), change the type of AEA.

Cast 100D×200H mm cylinder specimens when the filling ability, passing ability, segregation resistance and air content of concrete are satisfactory. Cure the specimens in accordance with ASTM C 192/C 192M (2004). Determine the compressive strength at 3 and 7 days according to the test procedure mentioned in Chapter 9, and judge the acceptability of hardened concrete. It can be assumed that the other hardened properties will be in the desired levels if the targeted early-age compressive strength is achieved. However, determine the total porosity, electrical resistivity and key transport properties such as water absorption at 28 days based on the test procedures depicted in Chapter 9 to examine whether the expected levels of hardened properties are achieved with an indication of good durability. Increase the RHA content and decrease the W/B ratio if the strength and durability-related properties are not satisfactory. If the expected properties are not achieved with an indication of good durability (extreme case), decrease the maximum size of coarse aggregate.

11.8 Example of Mixture Design

An air-entrained SCHPC is required for the columns in the tenth floor of a high-rise office building. The specified compressive strength is 55 MPa at 28 days. Due to moderately congested reinforcement, a slump flow in the range of 660 to 750 mm, a maximum flow spread reduction of 50 mm in the slump cone – J-ring flow, and a column segregation in the range of 10 to 20% can be considered. In addition, the total porosity and water absorption should be less than 15% and 6%, respectively, and the true electrical resistivity must be greater than 5 kΩ-cm at 28 days to achieve a good service life.

Step 1 – select constituent materials:

An air-dry blend of crushed granite stone and gravel with a maximum size of 19 mm is selected for use as coarse aggregate. The material properties of coarse aggregate are as

follows: saturated surface-dry basis relative density = 2.71, absorption = 1.5%, and moisture content = 0.1%. The coarse aggregate complied with ASTM C 33 (2004) grading requirements. An air-dry natural pit sand meeting ASTM C 33 (2004) requirements is selected to be used as fine aggregate. The material properties of sand are as follows: saturated surface-dry basis relative density = 2.62, absorption = 1%, and moisture content = 0.1%. ASTM Type I (CSA Type GU) cement and non-crystalline amorphous RHA are selected to be used as binders. The cement meets the requirements of ASTM C 150 (2004). The relative densities of cement and RHA are 3.16 and 2.07, respectively. A polycarboxylate-based HRWR is selected to produce the required flowing ability. The relative density and solid content of HRWR are 1.069 and 41%, respectively. A synthetic AEA is selected to produce the required air content. A modified polysaccharide-based VEA is also selected to improve the segregation resistance if needed.

Step 2 – determine optimum S/A ratio and minimum paste volume:

Determine the optimum S/A ratio for the selected air-dry fine and coarse aggregates based on the procedure described in Section 11.7. The optimum S/A ratio found is 0.50. Calculate the void content of optimum aggregate blend using Equation 11.2. The void content found is 20.4%. Now determine the minimum paste volume required using Equation 11.3. The minimum paste volume found is 0.27 m^3/m^3. A brief calculation is shown below:

From Equation 11.2:

$$V_{caad} = \left(1 - \frac{2091}{\frac{997.28}{7.527 \times 10^{-3}} \left(3.827 \times 10^{-3} \times 2.6 + 3.700 \times 10^{-3} \times 2.67 \right)} \right) \times 100\% = 20.4\%$$

From Equation 11.3:

$$V_{mp} = \left[1 - (1 - 0.08) \left(\frac{100 - 20.4}{100} \right) \right] = 0.268 \approx 0.27 \, m^3 / m^3$$

Step 3 – set slump flow and estimate required paste volume:

Set a slump flow of 700. Assuming ρ_r = 2.3, determine the paste volume (V_p) using the chart given in Figure 11.2. The paste volume found is 0.35 m^3/m^3. This is greater than the

minimum paste volume of 0.27 m^3/m^3. Thus, the requirement of minimum paste volume is satisfied.

Step 4 – set compressive strength, select RHA content, and estimate W/B ratio:

Determine the average compressive strength based on the specified compressive strength (55 MPa) using Equation 11.1. The average compressive strength found is 72 MPa. Select a 5% RHA content. Now using the chart given in Figure 11.3, determine the W/B ratio. The W/B ratio found is 0.33. It is < 0.40. Thus, it satisfies the W/B ratio requirement of SCHPC.

Step 5 – select total air content:

Select a total air content of 6%. It satisfies the CSA air content requirement of concrete for most exposure conditions.

Step 6 – determine cement, RHA, and water contents:

Calculate the weight of total binder based on the W/B ratio, percent RHA content in binder, and paste volume using Equation 11.5. The amount of binder found is 441.7 kg/m^3. Thus, the cement content obtained is greater than the recommended minimum cement content of 290 kg/m^3 to improve the durability of concrete. Now calculate the cement, RHA and water contents using Equations 11.6, 11.7, and 11.8, respectively. The amounts of cement, RHA and water found are 419.6, 22.1 and 145.8 kg/m^3, respectively. The water content found is less than the recommended maximum water content of 210 kg/m^3 for SCHPC. A brief calculation is shown below:

From Equation 11.5:

$$\frac{1}{997.28}\left[\frac{(1-0.05)W_b}{3.16}+\frac{0.05W_b}{2.07}+(0.33)W_b\right]+0.06=0.35 \Rightarrow W_b = 441.7\,kg/m^3$$

From Equation 11.6:

$$W_c = (1-0.05)\times 441.7 = 419.6\ kg/m^3$$

From Equation 11.7:

$$W_{rha} = 0.05\times 441.7 = 22.1\ kg/m^3$$

From Equation 11.9:

$$W_w = (0.33) \times 441.7 = 145.8 \ kg/m^3$$

Step 7 – determine fine and coarse aggregate contents:

Calculate the weights of fine and coarse aggregate per unit volume of concrete using Equations 11.9 to 11.11. The fine and coarse aggregate contents found are 861.4 and 865.6 kg/m^3, respectively. The coarse aggregate content is 32% of concrete volume, which is less than 35%. In addition, the fine aggregate content constitutes a mortar volume of 68%, which is greater than 65%. Thus, the requirements of coarse aggregate and mortar volumes for SCHPC are satisfied. A brief calculation is shown below:

From Equation 11.9:

$$W_{ca} = \{1 - (0.50)\} \times \{W_{ta}(1 + 0.015 - 0.001)\} = 0.507 W_{ta} = 0.507 \times 1707.35 = 865.6 kg/m^3$$

From Equation 11.10:

$$W_{fa} = (0.5) \times \{W_{ta}(1 + 0.01 - 0.001)\} = 0.5045 W_{ta} = 0.5045 \times 1707.35 = 861.4 kg/m^3$$

From Equation 11.11:

$$\frac{1}{997.28}\left(\frac{419.6}{3.16} + \frac{22.1}{2.07} + \frac{0.5045 W_{ta}}{2.62} + \frac{0.507 W_{ta}}{2.71} + 145.8\right) + 0.06 = 1 \Rightarrow W_{ta} = 1707.35 kg/m^3$$

Step 8 – decide the dosage of HRWR:

Decide the HRWR dosage based on the procedure described in Section 11.7. At first, determine the saturation dosage of HRWR. Assume it is 1.4% of binder by weight. Then set a HRWR dosage less than the saturation dosage. Start with 70% of saturation dosage, that is, about 1% of binder. Adjust the HRWR dosage if needed.

Step 9 – decide the dosage of AEA:

Decide the AEA dosage based on the procedure depicted in Section 11.7. Start with the estimated AEA dosage. Adjust the AEA dosage if needed.

Step 10 – decide the dosage of VEA:

Decide the VEA dosage based on the manufacturer's recommended dosage if necessary after testing the filling ability, passing ability and segregation resistance of concrete.

Step 11 – adjust primary mixture proportions:

Adjust the proportions of fine and coarse aggregates using Equations 11.12 and 11.13. The adjusted fine aggregate content found is 853.7 kg/m^3. The adjusted coarse aggregate content found is also 853.7 kg/m^3. Now adjust the proportion of mixing water using Equation 11.14. The adjusted water content found is 162.8 kg/m^3.

From Equation 11.12:

$$W_{caad} = \frac{865.6}{1 + 0.015 - 0.001} = 853.7\, kg/m^3$$

From Equation 11.13:

$$W_{faad} = \frac{861.4}{1 + 0.01 - 0.001} = 853.7\, kg/m^3$$

From Equation 11.4:

$$W_{wad} = 145.8 + (865.6 - 853.7 + 861.4 - 853.7) - \frac{1.0 \times 441.7}{100}\left(1 - \frac{41}{100}\right) = 162.8\ kg/m^3$$

Step 12 – prepare trial mixture and decide optimum mixture proportions:

Prepare the trial mixture based on the adjusted primary mixtures, and conduct the tests on the key fresh and hardened concretes as discussed in Section 11.7 to judge the acceptability of the mixture. Decide the final mixture proportions after obtaining the properties and durability in expected levels.

11.9 Limitation of the Design Method

The mixture design given is applicable for normal-weight, air-entrained and non-air-entrained SCHPC with and without RHA. It cannot be applied to the SCHPC incorporating other SCMs, because the design chart for the strength-W/B ratio relationship will be different. However, a similar design procedure can be developed for the SCHPC mixture including other SCMs such as silica fume, fly ash and ground granulated blast-furnace slag.

The proportions given by the design procedure should provide an SCHPC with the desired properties and durability. However, the concrete mixture may not provide the expected performance if the cement and RHA are not suitable, if the gradation of fine aggregate is not good, if the coarse aggregate possesses a poor shape and gradation, if the HRWR is not efficient and compatible with cement, and if the AEA is not efficient and compatible with cement/HRWR.

11.10 Concluding Remarks

a. According to the design method, SCHPC with a slump flow varying from 550 to 850 mm can be produced using a paste volume in the range of 0.24 to 0.42 m^3/m^3.
b. The design method suggests that a paste volume greater than the minimum amount of paste must be used in SCHPC to enhance the flowing ability of concrete.
c. The W/B ratio used in this design method ranges from 0.24 to 0.42 to achieve a compressive strength in the range of 50 to 110 MPa.
d. SCHPC can be produced using this design method with a binder content in the range of 295 to 495 kg/m^3.
e. The RHA content is suggested to use in the range of 0 to 15% in this mixture design to achieve the SCHPC mixtures with the desired level of properties and durability.
f. The optimum S/A ratio used in this design method determines the relative proportions of fine and coarse aggregate contents with minimum void content, and thus maximizes the density of concrete.
g. A coarse aggregate content less than 35% of concrete volume is suggested to use in this design method to enhance the flowing ability and segregation resistance of concrete.
h. In this design method, the HRWR, VEA and AEA, respectively, plays the key role to control the flowing ability, segregation resistance and air content of concrete.
i. SCHPC designed by this method requires relatively low binder content due to less paste requirement at optimum S/A ratio, and thus the design is cost-effective.
j. The mixture design is primarily applicable for air-entrained SCHPC with and without RHA. However, it can be applied for non-air-entrained SCHPC considering the effect of air content on the compressive strength of concrete.

Chapter 12

Summary, Contributions and Recommendations

12.1 General

This chapter provides a summary of the research findings, lists the contributions of the present study, and gives several recommendations for future research.

12.2 Summary

Various self-consolidating high performance concrete (SCHPC) incorporating rice husk ash (RHA) as a supplementary cementing material were produced in the present study. For this, the constituent materials, and the paste and mortar components of the concretes were primarily investigated for key properties. Later, the key fresh properties including segregation resistance and air-void stability, and the major hardened properties of the concretes were determined. The effects of re-mixing, water-binder (W/B) ratio, RHA content, air content, high-range water reducer (HRWR), air-entraining admixture (AEA), and viscosity-enhancing admixture (VEA) were examined. In addition, simple apparatus were developed to measure the filling ability, passing ability and segregation resistance of concrete. Empirical models for the filling ability (slump flow) and compressive strength of SCHPC were also developed. Finally, a design procedure was proposed for the mixture proportion of SCHPC. The main research findings are given below.

Properties of Materials and Aggregate Blends:

a. The properties of constituent materials were suitable to produce SCHPC except for the alkali contents of cement and RHA, which are acceptable for non-reactive aggregates.
b. The maximum bulk density with minimum void content was obtained for the aggregate blend at the weight-basis sand-aggregate (S/A) ratio of 0.50, which is defined as the optimum S/A ratio.
c. The optimum S/A ratio was used in the mixture proportioning of various SCHPCs to improve the hardened properties and durability of concrete through reduced porosity.

Filling Ability of Pastes, Mortars and Concretes:

a. The flow time of SCHPC mixture and its paste component increased with lower W/B ratio and higher RHA content indicating an increased plastic viscosity due to greater volume fraction and surface area of the binder.
b. The higher HRWR dosages decreased the flow time of the pastes and increased the flow spread of the mortars, and thus improved their filling abilities. This is due to the efficient liquefying and dispersing actions of the HRWR resulting in greater fluidity.
c. The mortar filling ability with respect to flow spread increased with lower W/B ratio due to higher paste volume and reduced sand content resulting in lower inter-particle friction. In contrast, the mortar filling ability decreased with higher RHA content due to greater volume fraction and surface area of the binder that increase the viscosity of mortar.
d. The filling ability of mortar with regard to flow spread was influenced by the mixture composition; particularly, the sand content affected the flow spread by affecting the yield stress and plastic viscosity.
e. The filling ability results of the pastes and mortars suggest that a HRWR dosage greater than its saturation dosage can be unsuitable to achieve the required filling ability in concrete due to bleeding and segregation. Thus, the optimum HRWR dosage for concrete can be determined based on the filling ability of paste and mortar so as to facilitate the mixture proportioning of SCHPC.
f. The filling abilities of SCHPC and its paste component were strongly correlated. The orimet and inverted slump cone flow time exhibited very good relationships with the paste flow time with a correlation coefficient of 0.939 and 0.979, respectively. This is because the changes in plastic viscosity due to various W/B ratios and RHA contents followed similar trends in cases of pastes and concretes.
g. The filling abilities of SCHPC and its mortar component were well-correlated with a correlation coefficient of 0.953 in the absence of RHA, since both mortar flow spread and concrete slump flow increased similarly without RHA at lower W/B ratio. In contrast, a poor correlation was observed between the filling abilities of SCHPC and its mortar component in the presence of RHA. This is because the mortar flow spread decreased where as the concrete slump flow increased with higher RHA content.

Air Content of Mortars:

a. The air content of mortar for a given AEA dosage decreased by about 1.5 to 2.5% with the increases in sand and cement contents due to increased yield stress and plastic viscosity, which cause a loss of air-voids.
b. The air content of mortar decreased with lower W/B ratio and higher RHA content due to the increases in binder content, binder surface area and HRWR dosage. The air content of mortar helped to estimate the AEA dosage for the desired air content of concrete, and thus facilitated the mixture proportioning process of SCHPC.

Filling Ability and Passing Ability of Concretes:

a. The filling ability and passing ability criteria were fulfilled for all SCHPCs except for few concretes with a lower W/B ratio and a higher RHA content due to the high viscosity caused by excessive surface area of rice husk ash.
b. The filling ability and passing ability of SCHPC with regard to slump flow, and inverted slump cone and orimet flow spreads with and without J-ring, respectively, increased with lower W/B ratio and higher RHA content due to the increased paste volume of concrete resulting in lower inter-particle friction.
c. The filling ability properties of SCHPC were well correlated with its passing ability properties with a correlation coefficient varying from 0.944 to 1. This is because both filling ability and passing ability properties were influenced similarly by the W/B ratio and RHA content of concrete.
d. The inverted slump cone flow time and spread were well-correlated with the orimet flow time and spread with a correlation coefficient of 0.958 and 0.987, respectively. In addition, the inverted slump cone and orimet flow spreads were strongly correlated in the presence of the J-ring with a correlation coefficient of 0.944. The strong correlations were observed for these properties of SCHPC because they varied similarly with the W/B ratio and RHA content of concrete.
e. The inverted slump cone apparatus with and without a J-ring can be used easily in laboratory and field by a single operator to assess the passing ability and filling ability of concrete based on the performance criteria derived.

Segregation Resistance of Concretes:

a. The visual inspection revealed that the dynamic segregation resistance was good for most of the SCHPC mixtures due to lower W/B ratio, higher RHA content and reduced coarse aggregate content.
b. The static and dynamic segregation resistances of SCHPC mixtures were influenced differently in the presence of RHA. The RHA increased the dynamic segregation resistance of SCHPC by reducing the bleeding and increasing the viscosity of concrete. However, it decreased the static segregation resistance of SCHPC by decreasing the matrix density of concrete.
c. The sieve segregation test provided the static segregation resistance of SCHPC with respect to segregation index, which increased with lower W/B ratio and higher RHA content due to greater concrete spread. However, this test was not effective to capture the effects of viscosity and matrix density on the static segregation resistance of SCHPC.
d. The column segregation test overcame the deficiencies of the sieve segregation test in capturing the effects of plastic viscosity and matrix density, and thus showed its potential for use as a reliable method to measure the static segregation resistance of SCHPC.
e. The segregation factor obtained from the column apparatus was well-correlated with the variation in true electrical resistivity of SCHPC. This is because both varied similarly with the heterogeneity or the variation in internal composition of concrete between top and bottom sections of column apparatus due to coarse aggregate segregation.
f. The column segregation test should be conducted to determine the static segregation resistance of SCHPC to be cast in vertical members, since it can effectively deal with the major factors affecting the segregation in such cases.
g. The segregation factor given by the column apparatus decreased with lower W/B ratio, which increased the viscosity and matrix density of SCHPC. In contrast, the segregation factor increased with higher RHA content, which decreased the matrix density of SCHPC due to increased binder volume.
h. The segregation resistance of SCHPC increased greatly in the presence of VEA, which increases the yield stress and plastic viscosity of concrete. Therefore, the segregation factor of the RHA concretes including VEA was reduced significantly.

Air Content, Air-void Stability and Unit Weight of Concretes:

a. The measured air content of SCHPC was within ±1.0% of the design air content. The demand for the AEA dosage for a given air content increased with lower W/B ratio and higher RHA content due to the increased plastic viscosity of concrete.
b. The estimated and actual AEA dosages for various SCHPCs were well-correlated with a correlation coefficient of 0.983. Hence, the AEA dosage required to achieve a target concrete air content can be determined based on the AEA dosage used for the equivalent mortar air content.
c. The air-void stability in various fresh SCHPC mixtures was excellent. The presence of RHA did not affect the air-void stability at different test stages after re-mixing and the maximum loss of air content over the period of 60 to 90 minutes was less than 1%.
d. The unit weight of SCHPC mixture increased with lower W/B ratio due to greater binder content, but decreased with higher RHA content due to increased paste volume. In addition, a reduction in air content increased the aggregate contents and decreased the total void content, and thus increased the unit weight of SCHPC.

Hardened Properties of Concretes:

a. The hardened properties of SCHPC were improved with lower W/B ratio due to higher binder content, which produced greater hydration products and thus resulted in enhanced paste densification.
b. The higher air content decreased the compressive strength and ultrasonic pulse velocity by due to the increased void content of concrete. The reduction in compressive strength was about 3.8 MPa per 1% increase in air content. In addition, the increased air content decreased the total porosity due to reduced capillary porosity, and thus provided higher electrical resistivity and lower water absorption.
c. The hardened properties of SCHPC were improved in the presence of RHA due to its microfilling and pozzolanic effects.
d. Strong correlations were observed for the hardened properties of SCHPC. The test results for the hardened properties of various SCHPCs also indicated that the concrete durability was improved with lower W/B ratio and higher RHA content.

Optimum RHA content:

a. The filling ability results of the pastes and mortars suggest that a RHA content greater than 15% can be unsuitable for SCHPC due to excessive water demand. In addition, mixing and handling difficulties were experienced for a RHA content higher than 15%.
b. The SCHPC mixtures fulfilled the performance criteria for all fresh properties at a RHA content ≤ 15%, except the static segregation resistance, which was not acceptable for 15% RHA in the absence of VEA. However, all RHA concretes provided the desired hardened properties. The tested properties of the fresh and hardened concretes suggest 15% RHA as the optimum content for SCHPC.

Modeling of Concrete:

a. The filling ability model produced the slump flows close to the measured slump flow values for both air-entrained and non-air-entrained SCHPC mixtures. The computed and measured slump flows were within ±7.6% error.
b. The strength model of SCHPC provided the compressive strengths close to the measured strength values. At least 95% of the measured strength values were accounted for with the derived model of compressive strength.

Mixture Design of Concrete:

a. The proposed mixture design can be used to produce both air-entrained and non-air-entrained SCHPCs with and without RHA providing a slump flow ranging from 550 to 850 mm, and a compressive strength in the range of 50 to 110 MPa.
b. The competency of the proposed mixture design method depends on the HRWR, VEA and AEA, which play key roles to control the flowing ability, segregation resistance and air content of concrete, respectively.

12.3 Contributions

The present study has contributed to the present state of knowledge on SCHPC. The main contributions are:

a. Development of SCHPC utilizing RHA as a supplementary cementing material that is obtained by burning rice husks generated in rice milling industry.

b. Optimization of aggregate blends to obtain maximum bulk density with minimum void content, and thus to reduce the cement content for producing cost-effective SCHPC, while achieving the properties and durability of concrete in desired levels.
c. Evaluation of the filling ability of binder pastes with respect to flow time using a grout flow cone, thus determining the saturation or optimum dosage and water reduction capacity of HRWR, and the water demand of RHA. These steps are useful to select the HRWR dosage and RHA content, and thereby to facilitate the mixture proportioning process of SCHPC.
d. Evaluation of the filling ability of mortars with respect to flow spread using a flow mould, thus verifying the saturation dosage of HRWR obtained from the flow cone test of binder pastes, examining the effectiveness or suitability of the selected HRWR dosage and RHA content, and indicating the segregation resistance of concrete. These steps are helpful for the mixture proportioning process of SCHPC.
e. Assessment of the air content for the mortar component of SCHPC mixture at various AEA dosages using a Chace indicator, and thus estimating the AEA dosage required to achieve the desired air content of concrete. This step is also helpful for the mixture proportioning process of SCHPC.
f. Demonstration of the air-void stability in fresh SCHPC mixture with respect to re-mixing at different plastic stages of concrete.
g. Development of a single-operator inverted slump cone apparatus for measuring the filling ability and passing ability, and for indicating the static/dynamic segregation resistance of SCHPC.
h. Development of a simplified and single-operator segregation column apparatus for measuring the static segregation resistance of SCHPC.
i. Assessment of the degree of segregation in hardened SCHPC using electrical resistivity.
j. Non-destructive assessment for the water absorption, total porosity, electrical resistivity and ultrasonic pulse velocity of SCHPC.
k. Modification of the test procedure for measuring the water absorption and total porosity of SCHPC by vacuum saturation technique.
l. Setting the performance criteria for the inverted slump cone and segregation column apparatus.

m. Development of empirical models for the filling ability and compressive strength of concrete to facilitate the mixture proportioning process of SCHPC with and without RHA.
n. Proposing a mixture design procedure for the air-entrained and non-air-entrained SCHPC with and without RHA.

12.4 Recommendations

There are several aspects that were not investigated in the present study. The following recommendations are given for future research:

a. The effects of RHA on the fresh and hardened properties of SCHPC should be investigated for different types and sizes of coarse aggregate.
b. An experimental investigation should be carried out to examine the efficiency of RHA in refining the microstructure of SCHPC due to microfilling and pozzolanic effects.
c. The effects of various curing conditions on the hardened properties of SCHPC, including drying and autogenous shrinkages, should be examined.
d. The durability performance of SCHPC such as resistances to corrosion, alkali-aggregate reaction, sulfate attack, and freezing and thawing, and the effects of RHA should be investigated.
e. The effects of HRWR on the hardened properties including the electrical resistivity of SCHPC should be investigated with and without various RHA contents.
f. The effects of VEA on the properties and durability of SCHPC with and without various RHA contents should be examined and compared.
g. The performance of inverted slump cone apparatus should be compared with other test devices, particularly V-funnel, which is also widely used to assess the filling ability of SCHPC.
h. The combined effects of RHA and other supplementary cementing materials on the fresh and hardened properties and durability of SCHPC should be investigated.
i. The SCHPC mixtures including RHA should be tested for the rheological parameters such as yield stress and plastic viscosity in addition to the empirical tests for filling ability with respect to flow time and flow spread.

j. The air-void stability in hardened SCHPC with and without RHA should be investigated to ensure the freeze-thaw durability of concrete.
k. The effects of RHA collected from various sources should be investigated with respect to different fresh and hardened properties and durability of SCHPC.
l. A testing device and a test method should be developed to quantitatively measure the dynamic segregation resistance of SCHPC.
m. The effectiveness of the four-point Wenner array probe resistivity meter in identifying the segregation in hardened concrete should be investigated for different SCHPCs including RHA or other supplementary cementing materials.
n. The mixture design procedure developed should be employed to determine the mixture proportions of SCHPC with and without RHA, thus validating its applicability.

References

AASHTO T 199, "Air content of freshly mixed concrete by the Chace indicator", *Standard Specifications for Transportation Materials and Methods of Sampling and Testing*, Part II, American Association of State Highway and Transportation Officials, Washington, D.C., USA, 2004.

ACI 201.2R-01, "Guide to durable concrete", *ACI Manual of Concrete Practice*, Part 1, American Concrete Institute, Farmington Hills, Michigan, USA, 2004, 38pp.

ACI 209R-92, "Prediction of creep, shrinkage, and temperature effects in concrete structures", *ACI Manual of Concrete Practice*, Part 1, American Concrete Institute, Farmington Hills, Michigan, USA, 2004, 47pp.

ACI 211.4R-93, "Guide for selecting proportions for high-strength concrete with portland cement and fly ash", *ACI Manual of Concrete Practice*, Part 1, American Concrete Institute, Farmington Hills, Michigan, USA, 2004, 13pp.

ACI Committee 211H, "Guide for selecting proportions of self-consolidating concrete (SCC)", American Concrete Institute, Farmington Hills, Michigan, USA, 2006.

ACI 212.3R-04, "Chemical admixtures for concretes", *ACI Manual of Concrete Practice*, Part 1, American Concrete Institute, Farmington Hills, Michigan, USA, 2004, 31pp.

ACI 214.4R-03, "Guide for obtaining cores and interpreting compressive strength results", *ACI Manual of Concrete Practice*, Part 1, American Concrete Institute, Farmington Hills, Michigan, USA, 2004, 16pp.

ACI 222R-01, "Protection of metals in concrete against corrosion", *ACI Manual of Concrete Practice*, Part 1, American Concrete Institute, Farmington Hills, Michigan, USA, 2004, 41pp.

ACI 237R-07, "Self-consolidating concrete", *ACI Manual of Concrete Practice*, Part 1, American Concrete Institute, Farmington Hills, Michigan, USA, 2007, 30pp.

ACI 304R-00, "Guide for measuring, mixing, transporting, and placing concrete", *ACI Manual of Concrete Practice*, Part 2, American Concrete Institute, Farmington Hills, Michigan, USA, 2004. 41pp.

ACI 308R-01, "Guide to curing concrete", *ACI Manual of Concrete Practice*, Part 2, American Concrete Institute, Farmington Hills, Michigan, USA, 2001. 31pp.

ACI 363R-92, "State-of-the art report on high-strength concrete", *ACI Manual of Concrete Practice*, Part 5, American Concrete Institute, Farmington Hills, Michigan, USA, 2005. 55pp.

Aïtcin, P.-C., "The use of superplasticizers in high performance concrete", *High Performance Concrete: From Material to Structure*, Y. Malier, ed., E & FN Spon, London, UK, 1994, pp.14-33.

Aïtcin, P.-C., "Developments in the application of high-performance concretes", *Construction and Building Materials,* Vol.9, No.1, 1995, pp.13-17.

Aïtcin, P.-C., "High strength concrete: current trends and applications", *Proceedings of the Fifth International Conference on Concrete Engineering and Technology*, University Malaya, Kuala Lumpur, Malaysia, 1997, pp.37-46.

Aïtcin, P.-C., *High Performance Concrete*, 1st Edition, E & FN Spon, London, UK, 1998. 624pp.

Al-Amoudi, O.S.B., Maslehuddin, M., and Asi, I.M., "Performance and correlation of the properties of fly ash cement concrete", *Cement, Concrete, and Aggregates*, Vol.18, No.2, 1996, pp.71-77.

Ampadu, K.O., and Torii, K., "Chloride ingress and steel corrosion in cement mortars incorporating low-quality fly ashes", *Cement and Concrete Research*, Vol.32, No.6, 2002, pp.893-901.

Assaad, J., Khayat, K.H., and Daczko, J., "Evaluation of static stability of self-consolidating concrete", *ACI Materials Journal*, Vol.101, No.3, 2004, pp.207-215.

ASTM C 29/C 29M, "Standard test method for bulk density ("unit weight") and voids in aggregate", *Annual Book of ASTM Standards*, Vol.04.02, American Society for Testing and Materials, Philadelphia, USA, 2004.

ASTM C 33, "Standard specification for concrete aggregates", *Annual Book of ASTM Standards*, Vol.04.02, American Society for Testing and Materials, Philadelphia, USA, 2004.

ASTM C 39/C 39M, "Standard test method for compressive strength of cylindrical concrete specimens", *Annual Book of ASTM Standards*, Vol.04.02, American Society for Testing and Materials, Philadelphia, USA, 2004.

ASTM C 42/C 42M, "Standard test method for obtaining and testing drilled cores and sawed beams of concrete", *Annual Book of ASTM Standards*, Vol.04.02, American Society for Testing and Materials, Philadelphia, USA, 2004.

ASTM C 94/C 94M, "Standard specification for ready-mixed concrete", *Annual Book of ASTM Standards*, Vol.04.02, American Society for Testing and Materials, Philadelphia, USA, 2004.

ASTM C 114, "Test methods for chemical analysis of hydraulic cement", *Annual Book of ASTM Standards*, Vol.04.01, American Society for Testing and Materials, Philadelphia, USA, 2004.

ASTM C 125, "Standard terminology relating to concrete and concrete aggregates", *Annual Book of ASTM Standards*, Vol.04.02, American Society for Testing and Materials, Philadelphia, USA, 2002.

ASTM C 136, "Standard test method for sieve analysis of fine and coarse aggregates", *Annual Book of ASTM Standards*, Vol.04.02, American Society for Testing and Materials, Philadelphia, USA, 2004.

ASTM C 138/C 138M, "Standard test method for density (unit weight), yield, and air content (gravimetric) of concrete", *Annual Book of ASTM Standards*, Vol.04.02, American Society for Testing and Materials, Philadelphia, USA, 2004.

ASTM C 143/C 143M, "Standard test method for slump of hydraulic-cement concrete", *Annual Book of ASTM Standards*, Vol.04.02, American Society for Testing and Materials, Philadelphia, USA, 2004.

ASTM C 150, "Standard specification for portland cement", *Annual Book of ASTM Standards*, Vol.04.01, American Society for Testing and Materials, Philadelphia, USA, 2004.

ASTM C 192/C 192M, "Standard practice for making and curing concrete test specimens in the laboratory", *Annual Book of ASTM Standards*, Vol.04.02, American Society for Testing and Materials, Philadelphia, USA, 2004.

ASTM C 230/C 230M, "Standard specification for flow table for use in tests of hydraulic cement", *Annual Book of ASTM Standards*, Vol.04.01, American Society for Testing and Materials, Philadelphia, USA, 2004.

ASTM C 231, "Standard test method for air content of freshly mixed concrete by pressure method", *Annual Book of ASTM Standards*, Vol.04.02, American Society for Testing and Materials, Philadelphia, USA, 2004.

ASTM C 260, "Standard specification for air-entraining admixtures for concrete", *Annual Book of ASTM Standards*, Vol.04.02, American Society for Testing and Materials, Philadelphia, USA, 2004.

ASTM C 305, "Standard practice for mechanical mixing of hydraulic cement pastes and mortars of plastic consistency", *Annual Book of ASTM Standards*, Vol.04.01, American Society for Testing and Materials, Philadelphia, USA, 2004.

ASTM C 494/ C494M, "Standard specification for chemical admixtures for concrete", *Annual Book of ASTM Standards*, Vol.04.02, American Society for Testing and Materials, Philadelphia, USA, 2004.

ASTM C 597, "Standard test method for pulse velocity through concrete", *Annual Book of ASTM Standards*, Vol.04.02, American Society for Testing and Materials, Philadelphia, USA, 2004.

ASTM C 618, "Standard specification for coal fly ash and raw or calcined natural pozzolan for use as a mineral admixture in concrete", *Annual Book of ASTM Standards*, Vol.04.02, American Society for Testing and Materials, Philadelphia, USA, 2004.

ASTM C 939, "Standard test method for flow of grout for preplaced-aggregate concrete (flow cone method)", *Annual Book of ASTM Standards*, Vol.04.02, American Society for Testing and Materials, Philadelphia, USA, 2004.

ASTM C 989, "Standard specification for ground granulated blast-furnace slag for use in concrete and mortars", *Annual Book of ASTM Standards*, Vol.04.02, American Society for Testing and Materials, Philadelphia, USA, 2004.

ASTM C 1017/C 1017M, "Standard specification for chemical admixtures for use in producing flowing concrete", *Annual Book of ASTM Standards*, Vol.04.02, American Society for Testing and Materials, Philadelphia, USA, 2004.

ASTM C 1157, "Standard performance specification for hydraulic cement", *Annual Book of ASTM Standards*, Vol.04.01, American Society for Testing and Materials, Philadelphia, USA, 2004.

ASTM C 1240, "Standard specification for use of silica fume as mineral admixture in hydraulic cement concrete, mortar and grout", *Annual Book of ASTM Standards*, Vol.04.02, American Society for Testing and Materials, Philadelphia, USA, 2004.

ASTM C 1610/C 1610M, "Standard test method for static segregation of self-consolidating concrete using column technique", *Annual Book of ASTM Standards*, Vol.04.02, American Society for Testing and Materials, Philadelphia, USA, 2006.

ASTM C 1611/C 1611M, "Standard test method for slump flow of self-consolidating concrete", *Annual Book of ASTM Standards*, Vol.04.02, American Society for Testing and Materials, Philadelphia, USA, 2007.

ASTM C 1621/C 1621M, "Standard test method for passing ability of self-consolidating concrete by J-ring", *Annual Book of ASTM Standards*, Vol.04.02, American Society for Testing and Materials, Philadelphia, USA, 2007.

ASTM D 422, "Standard test method for particle-size analysis of soils", *Annual Book of ASTM Standards*, Vol.04.08, American Society for Testing and Materials, Philadelphia, USA, 2004.

Attiogbe, E.K., See, H.T., and Daczko, J.A., "Engineering properties of self-consolidating concrete", *Proceedings of the First North American Conference on the Design and Use of Self-Consolidating Concrete*, S.P. Shah, J.A. Daczko, and J.N. Lingscheit, eds., Hanley-Wood, LLC, Illinois, USA, 2002, pp.331-336.

Baalbaki, M., and Aïtcin, P.-C., "Cement/superplasticizer/air-entraining agent compatibility", *Proceedings of the Fourth CANMET/ACI International Conference on Superplasticizers and Other Chemical Admixtures in Concrete*, ACI SP-148, V.M. Malhotra, ed., American Concrete Institute, Farmington Hills, Michigan, USA, 1994, pp.47-62.

Baekmark, K., Hansen, H., and Reichert, J., "Stabilized air void system in superplasticized concrete", *Concrete Technology – Past, Present, and Future: Proceedings of V. Mohan Malhotra Symposium*, ACI SP-144, P.K. Mehta, ed., American Concrete Institute, Farmington Hills, Michigan, USA, 1994, pp.177-190.

Banfill, P.F.G., "Rheological methods for assessing the flow properties of mortar and related materials", *Construction and Building Materials*, Vol.8, No.1, 1994, pp.43-50.

Bartlett, F.M., and MacGregor, J.G., "Statistical analysis of the compressive strength of concrete in structures", *ACI Materials Journal*, Vol.93, No.2, 1996, pp.158-168.

Bartlett, F.M., and MacGregor, J.G., "Variation of in-place concrete strength in structures", *ACI Materials Journal*, Vol.96, No.2, 1999, pp.261-271.

Bartos, P.J.M., "Measurement of key properties of fresh self-compacting concrete", *Paper presented in the CEN/STAR PNR Workshop on Measurement, Testing and Standardization: Future Needs in the Field of Construction Materials*, Paris, France, 5-6 June 2000, 6pp.

Bentz, D.P., and Haecker, C.J., "An argument for using coarse cements in high-performance concretes", *Cement and Concrete Research*, Vol.29, No.4, 1999, pp.615-618.

Beris, A.N., Tsamopoulos, J.A., Armstrong, R.C., and Brown, R.A., "Creeping motion of a sphere through a Bingham plastic", *Journal of Fluid Mechanics*, Vol.158, 1985, pp.219-244.

Bigley, C., and Greenwood, P., "Using silica to control bleed and segregation in self-consolidating concrete", *Concrete*, Vol.37, No.2, 2003, pp.43-45.

Bonen, D., and Shah, S.P., "Fresh and hardened properties of self-consolidating concrete", *Progress in Structural Engineering and Materials*, Vol.7, No.1, 2005, pp.14-26.

Bonen, D., Deshpande, Y., Olek, J., Struble, L., Lange, D., and Khayat, K., "Robustness of SCC", *Self-Consolidating Concrete*, D. Lange, ed., The Centre for Advanced Cement-based Materials, Northwestern University, Illinois, USA, 2007, pp.4-22.

Bouzoubaâ, N., and Lachemi, M., "Self-compacting concrete incorporating high volumes of Class F fly ash: preliminary results", *Cement and Concrete Research*, Vol.31, No.3, 2001, pp.413-420.

Brameshuber, W., and Uebachs, S., "Practical experience with the application of self-compacting concrete in Germany", *Proceedings of the Second International Symposium on Self-compacting Concrete*, K. Ozawa and M. Ouchi, eds., COMS Engineering Corporation, Tokyo, Japan, 2001, pp.687-695.

Brandt, A.M., *Cement-based Composites: Materials, Mechanical Properties, and Performance*, E & FN Spon, London, UK, 1995.

Brown, Z.A., and Curry, K.J., "Total sulphur by combustion", *Analytical Methods for Chemical Analysis of Geological and Other Materials*, J.E. Taggart, Jr., ed., U.S. Geological Survey, Denver, Colorado, USA, 2002a, pp.Q1-4.

Brown, Z.A., and Curry, K.J., "Total carbon by combustion", *Analytical Methods for Chemical Analysis of Geological and Other Materials*, J.E. Taggart, Jr., ed., U.S. Geological Survey, Denver, Colorado, USA, 2002b, pp.R1-4.

Bruker, "XRF analysis of chlorine in pressed powder cement samples", *Bruker Analytical X-ray Systems*, Bruker AXS, Inc., Madison, Wisconsin, USA, 2004.

Bui, V.K., Montgomery, D., Hinczak, I., and Turner, K., "Rapid testing method for segregation resistance of self-compacting concrete", *Cement and Concrete Research*, Vol.32, No.9, 2002, pp.1489-1496.

Cameron, I., "Self-compacting concrete: a versatile material", *Concrete*, Vol.37, No.2, 2003, pp.16-18.

CAN/CSA A3001, "Cementitious materials for use in concrete", *Cementitious Materials Compendium*, Canadian Standards Association, Etobicoke, Ontario, Canada, 2003.

Chandra, S., and Björnström, J., "Influence of cement and superplasticizers type and dosage on the fluidity of cement mortars – Part I", *Cement and Concrete Research*, Vol.32, No.10, 2002, pp.1605-1611.

Chang, P.-K., and Peng, Y.-N., "Influence of mixing techniques on properties of high performance concrete", *Cement and Concrete Research*, Vol.31, No. 1, 2001, pp.87-95.

Chidiac, S.E., Maadani, O., Razaqpur, A.G., and Mailvaganam, N.P., "Controlling the quality of fresh concrete – a new approach", *Magazine of Concrete Research*, Vol.52, No.5, 2000, pp.353-363.

Chidiac, S.E., Maadani, O., Razaqpur, A.G., and Mailvaganam, N.P., "Correlation of rheological properties to durability and strength of hardened concrete", *Journal of Materials in Civil Engineering*, Vol.15, No.4, 2003, pp.391-399.

Chini, A.R., Muszynski, L.C., and Hicks, J., *Determination of Acceptance Permeability Characteristics for Performance-related Specifications for Portland Cement Concrete*, Final report submitted to Florida Department of Transportation, BC 354-41, M.E. Rinker, Sr. School of Building Construction, University of Florida, Florida, USA, 2003, 165pp.

Chopin, D., Larrard, F., D., and Cazacliu, B., "Why do HPC and SCC require a longer mixing time?", *Cement and Concrete Research*, Vol.34, No.12, 2004, pp.2237-2243.

Claisse, P., "Transport properties of concrete", *Concrete International*, Vol.27, No.1, 2005, pp.43-48.

Claisse, P.A., Cabrera, J.G., and Hunt, D.N., "Measurement of porosity as a predictor of the durability performance of concrete with and without condensed silica fume", *Advances in Cement Research*, Vol.13, No.4, 2001, pp.165-174.

CNS Farnell, *Operating Manual for PUNDIT plus*, Fulton Group Limited, England, UK, 2000, 31pp.

CNS Farnell, *Operating Instructions for RM MK II Concrete Resistivity Meter*, England, UK, 2004, 22pp.

Collepardi, M., "Assessment of the rheoplasticity of concretes", *Cement and Concrete Research*, 1976, Vol.6, No.3, pp.401-408.

Collepardi, M., "Advances in chemical admixtures for concrete", *Proceedings of an Engineering Foundation Conference on Advances in Cement and Concrete*, M.W. Grutzeck, and S.L. Sarkar, eds., American Society of Civil Engineers, New York, USA, 1994, pp.257-291.

Collepardi, M., and Massidda, L., "The influence of water-reducing admixtures on the cement paste and concrete properties", *Proceedings of a Conference on Hydraulic Cement Pastes: Their Structure and Properties*, Cement and Concrete Association, Slough, UK, 1976, pp.256-267.

Coppola, L., Cerulli, T., and Salvioni, D., "Sustainable development and durability of self-compacting concrete", *Proceedings of the Eighth CANMET/ACI International Conference on Fly Ash, Silica Fume, Slag and Natural Pozzolans in Concrete*, ACI SP-221, V.M. Malhotra, ed., American Concrete Institute, Farmington Hills, Michigan, USA, 2004, pp.29-50.

Coutinho, J.S., "The combined benefits of CPF and RHA in improving the durability of concrete structures", *Cement and Concrete Composites*, Vol.25, No.1, 2003, pp.51-59.

CSA A23.1, *Concrete Materials and Methods of Concrete Construction*, Canadian Standards Association, Etobicoke, Ontario, Canada, 2004.

CSA A23.2, *Methods of Test and Standard Practices for Concrete*, Canadian Standards Association, Etobicoke, Ontario, Canada, 2004.

Cyr, M., and Mouret, M., "Rheological characterization of superplasticized cement pastes containing mineral admixtures: consequences on self-compacting concrete design", *Proceedings of the Seventh CANMET/ACI International Conference on Superplasticizers and other Chemical Admixtures in Concrete*, ACI SP-217, V.M. Malhotra, ed., American Concrete Institute, Michigan, USA, 2003, pp.241-255.

Daczko, J.A., "Stability of self-consolidating concrete, assumed or ensured?", *Proceedings of the First North American Conference on the Design and Use of Self-consolidating Concrete*, S.P. Shah, J.A. Daczko, and J.A. Lingscheit, eds., Hanley-Wood, LLC, Illinois, USA, 2002, pp.223-228.

Das, B.M., *Principles of Foundation Engineering*, Fourth Edition, PWS Publishing, Brooks/Cole Publishing Company, California, USA, 1999. 862pp.

Dehn, F., Holschemacher, K., and Weiβe, D., "Self-compacting concrete (SCC) time development of the materials properties and the bond behaviour", *The Leipzig Annual Civil Engineering Report*, University of Leipzig, Leipzig, Federal Republic of Germany, 2000, pp.115-124.

De Larrard, F., "A mix performance method for high-performance concrete", *High Performance Concrete*, Y. Malier, ed., E & FN Spon, London, UK, 1994, pp.48-62.

Demirboğa, R., Türkmen, İ., and Karakoc, M.B., "Relationship between ultrasonic velocity and compressive strength for high-volume mineral-admixtured concrete", *Cement and Concrete Research*, Vol.34, No.12, 2004, pp.2329-2336.

Dhir, R.K., Hewlett, P.C., and Chan, Y.N., "Near-surface characteristics of concrete: assessment and development of in-situ test methods", *Magazine of Concrete Research*, Vol.39, No.141, 1987, pp.183-195.

Dodson, V.H., *Concrete Admixtures*, First Edition, Van Nostrand Reinhold, Inc., New York, USA, 1990, 211pp.

Domone, P., "Mortar tests for self-consolidating concrete", *Concrete International*, Vol.28, No.4, 2006, pp.39-45.

Domone, P., and Soutsos, M., "An approach to the proportioning of high-strength concrete mixes", *Concrete International*, Vol.16, No.10, 1994, pp.26-31.

Du, L., and Folliard, K.J., "Mechanisms of air entrainment in concrete", *Cement and Concrete Research*, Vol.35, No.8, 2005, pp.1463-1471.

Duval, R., and Kadri, E.H., "Influence of silica fume on the workability and the compressive strength of high-performance concretes", *Cement and Concrete Research*, Vol.28, No.4, 1998, pp.533-547.

EFNARC, *Specifications and Guidelines for Self-Consolidating Concrete*, European Federation of Suppliers of Specialist Construction Chemicals (EFNARC), Surrey, UK, 2002, 32pp.

Erdogdu, S., "Compatibility of superplasticizers with cements different in composition", *Cement and Concrete Research*, Vol.30, No.5, 2000, pp.767-773.

Ferraris, C.F., and De Larrard, F., "Modified slump test to measure rheological parameters of fresh concrete", *Cement, Concrete, and Aggregates*, Vol.20, No.2, 1998, pp.241-247.

Ferraris, C.F., Brower, L., Ozyildirim, C., and Daczko, J., "Workability of self-compacting concrete", *Proceedings of the PCI/FHWA/FIB International Symposium on High Performance Concrete*, L.S. Johal, ed., Precast/Prestressed Concrete Institute, Chicago, USA, 2000, pp.398-407.

FHWA, "Critical properties of concrete", *Integrated Materials and Construction Practices for Concrete Pavement: A State-of-the Practice Manual*, Publication No. HF-07-004, U.S. Department of Transportation and Federal Highway Administration, Washington, USA, 2006, pp.105-170.

Florida Department of Transportation, "Florida method of test for concrete resistivity as an electrical indicator of its permeability", *FM 5-578*, The Florida Department of Transportation, Florida, USA, 2004.

Geiker, M.R., Brandl, M., Thrane, L.N., and Nielsen, L.F., "On the effect of coarse aggregate fraction and shape on the rheological properties of self-compacting concrete", *Cement, Concrete, and Aggregates*, Vol.24, No.1, 2002, pp.3-6.

Gettu, R., Gomes, P.C.C., Agullo, L., and Josa, A., "High-strength self-compacting concrete with fly ash: development and utilization", *Proceedings of Fifth CANMET/ACI International Conference on Recent Advances in Concrete Technology*, ACI SP-200, V.M. Malhotra, ed., American Concrete Institute, Farmington Hills, Michigan, USA, 2001, pp.507-522.

Ghezal, A., and Khayat, K.H., "Optimizing self-consolidating concrete with limestone filler by using statistical factorial design methods", *ACI Materials Journal*, Vol.99, No.3, 2002, pp.264-272.

Gowripalan, N., Cabrera, J.G., Cusens, A.R., and Wainwright, P.J., "Effect of curing on durability", *Durable Concrete*, ACI Compilation 24, American Concrete Institute, Farmington Hills, Michigan, USA, 1992, pp.47-54.

Grünewald, S., Walraven, J.C., Emborg, M., Cärlsward, J., and Hedin, C., "Test methods for filling ability of SCC", *Summary Report of Workpackage 3.1*, Delft University of Technology and Betongindustri, Netherlands, 2004, 6pp.

Gutiérrez, P.A., and Cánovas, M.F., "High-performance concrete: requirements for constituent materials and mix proportioning", *ACI Materials Journal*, Vol.93, No.3, 1996, pp.233-241.

Hansen, M.R., Leming, M.L., Zia, P., and Ahmad, S., "Chloride permeability and AC impedance of high performance concrete", *Proceedings of the Symposium on High Performance Concrete in Severe Environments*, ACI SP-140, P. Zia, ed., American Concrete Institute, Farmington Hills, Michigan, USA, 1993, pp.121-145.

Hassan, K.E., Cabrera, J.G., and Maliehe, R.S., "The effect of mineral admixtures on the properties of high-performance concrete", *Cement and Concrete Composites*, Vol.22, No.4, 2000, pp.267-271.

Hayakawa, M., Matsuoka, Y., and Shindoh, T., "Development and application of super-workable concrete", *Special Concretes: Workability and Mixing, Proceedings of the International RILEM Workshop*, P.J.M. Bartos, ed., E & FN Spon, London, UK, 1994, pp.183-190.

Hearn, N., Hooton, R.D., and Mills, R.H., "Pore structure and permeability", *Significance of Tests and Properties of Concrete and Concrete-Making Materials*, ASTM STP 169C, American Society for Testing and Materials, Philadelphia, USA, 1994, pp. 240-262.

Hearn, N., "On the corrosion of steel reinforcement in concrete", *Proceedings of the 1st Structural Specialty Conference*, Canadian Society for Civil Engineering, Montréal, Quebec, Canada, 1996, pp.763-774.

Hearn, N., Skalny, J., and Bajza, A., "Microstructures and bond in cementitious solids", *Building Research Journals*, Vol.45, No.1, 1997, pp.103-118.

Hossain, K.M.A., "Correlations between porosity, chloride diffusivity and electrical resistivity in volcanic pumice-based blended cement pastes", *Advances in Cement Research*, Vol.17, No.1, 2005, pp.29-37.

Holland, T.C., "High performance concrete", *Concrete Products*, June 1993, pp.19-21.

Hooton, R.D., "Canadian use of ground granulated blast-furnace slag as a supplementary cementing material for enhanced performance of concrete", *Canadian Journal of Civil Engineering*, Vol.27, No.4, 2000, pp.754-760.

Hover, K.C., "Concrete mixture proportioning with water-reducing admixtures to enhance durability: a quantitative model", *Cement and Concrete Composites*, Vol.20, No.2-3, 1998, pp.113-119.

Hu, C., and De Larrard, F., "The rheology of fresh high-performance concrete", *Cement and Concrete Research*, Vol.26, No.2, 1996, pp.283-294.

Hu, C., De Larrard, F., Sedran, T., Boulay, C., Bosc, F., and Deflorenne, F., "Validation of BTRHEOM, the new rheometer for soft to fluid concrete", *Materials and Structures*, Vol.29, No.10, 1996, pp.620-631.

Hu, J., and Wang, K., "Effects of aggregate on flow properties of mortar", *Proceeding of the Mid-Continent Transportation Research Symposium*, Ames, Iowa, Iowa State University, 2005, 8pp.

Hwang, C.L., and Hung, M.F., "Durability consideration of self-consolidating concrete", *Proceedings of the First North American Conference on the Design and Use of Self-Consolidating Concrete*, S.P. Shah, J.A. Daczko, and J.N. Lingscheit, eds., Hanley-Wood, LLC, Illinois, USA, 2002, pp.343-348.

Ismail, M.S., and Waliuddin, A.M., "Effect of rice husk ash on high strength concrete", *Construction and Building Materials*, Vol.10, No.7, 1996, pp.521-526.

ISO 13320-1, *Particle Size Analysis – Laser Diffraction Methods, Part 1: General Principles*, International Organization for Standardization, Geneva, Switzerland, 1999.

Jauberthie, R., Rendell, F., Tamba, S., and Cisse, I., "Origin of the pozzolanic effect of rice husks", *Construction and Building Materials*, Vol.14, No.8, 2000, pp.419-423.

Jana, D., Erlin, B., and Pistilli, M.F., "A closer look at entrained air in concrete", *Concrete International*, Vol.27, No.7, 2005, pp.31-34.

Jin, J., and Domone, P.L., "Relationships between the fresh properties of SCC and its mortar component", *Proceedings of the First North American Conference on the Design and Use of Self-consolidating Concrete*, S.P. Shah, J.A. Daczko, and J.N. Lingscheit, eds., Hanley-Wood, LLC, Illinois, USA, 2002, pp.37-42.

Johnston, C.D., "Deicer salt scaling resistance and chloride permeability", *Concrete International*, Vol.16, No.8, 1994, pp.48-55.

Kaplan, M.F., "Compressive strength and ultrasonic pulse velocity relationships for concrete in columns", *Proceedings of American Concrete Institute*, Vol.54, 1958, pp.675-688.

Kessler, R.J., Powers, R.G., and Paredes, M.A., "Resistivity measurements of water saturated concrete as an indicator of permeability", *Corrosion*, Paper 05261, 2005, 10pp.

Khatri, R.P., and Sirivivatnanon, "Effect of different supplementary cementitious materials on mechanical properties of high performance concrete", *Cement and Concrete Research*, Vol.25, No.1, 1995, pp.209-220.

Khayat, K.H., "Viscosity-enhancing admixtures for cement-based materials – an overview", *Cement and Concrete Composites*, Vol.20, No.2-3, 1998, pp.171-188.

Khayat, K.H., "Workability, testing, and performance of self-consolidating concrete", *ACI Materials Journal*, Vol.96, No.3, 1999, pp.346-353.

Khayat, K.H., "Optimization and performance of air-entrained, self-consolidating concrete", *ACI Materials Journal*, Vol.97, No.5, 2000, pp.526-535.

Khayat, K.H., and Assaad, J., "Air void stability in self-consolidating concrete", *ACI Materials Journal*, Vol.99, No.4, 2002, pp.408-416.

Khayat, K.H., and Guizani, Z., "Use of viscosity-modifying admixtures to enhance stability of fluid concretes", *ACI Materials Journal*, Vol.94, No.4, 1997, pp.332-340.

Kim, H., Park, Y.-D., Noh, J., Song, Y., Han, C., and Kang, S., "Rheological properties of self-compacting high-performance concrete", *Proceedings of the Third CANMET/ACI International Conference*, ACI SP-172, V.M. Malhotra, ed., American Concrete Institute, Michigan, USA, 1997, pp.653-668.

Kim, J.-H., and Robertson, R.E., "Prevention of air void formation in polymer-modified cement mortar by pre-wetting", *Cement and Concrete Research*, Vol.27, No.2, 1997, pp.171-176.

Koehler, E.P., and Fowler, D.W., *ICAR Mixture Proportioning Procedure for Self-consolidating Concrete*, Research Report 108-1, International Center for Aggregates Research, University of Texas at Austin, Texas, USA, 2006, 21pp.

Kosmatka, S.H., Kerkhoff, B., Panareśe, W.C., MacLeod, N.F, and McGrath, R.J., *Design and Control of Concrete Mixtures*, Seventh Edition, Cement Association of Canada, Ottawa, Ontario, Canada, 2002. 356pp.

Kwan, A.K.H., "Use of condensed silica fume for making high strength, self-consolidating concrete", *Canadian Journal of Civil Engineering*, Vol.27, No.4, 2000, pp.620-627.

Lachemi, M., Hossain, K.M.A., Lambros, V., and Bouzoubaâ, N., "Development of cost-effective self-consolidating concrete incorporating fly ash, slag cement, or viscosity-modifying admixtures", *ACI Materials Journal*, Vol.100, No.5, 2003, pp.419-425.

Lachemi, M., Hossain, K.M.A., Lambros, V., Nkinamubanzi, P.-C., and Bouzoubaâ, N., "Self-consolidating concrete incorporating new viscosity modifying admixtures", *Cement and Concrete Research*, Vol.34, No.6, 2004, pp.917-926.

Leslie, J.R., and Cheesman, W.J., "An ultrasonic method of studying deterioration and cracking in concrete structures", *Journal of the American Concrete Institute*, Vol.21, No.1, 1949, pp.17-36.

Lessard, M., and Aïtcin, P.-C., "Testing high performance concrete", *High Performance Concrete: From Material to Structure*, Y. Malier, ed., E & FN Spon, London, UK, 1994, pp.196-213.

Lessard, M., Baalbaki, M., and Aïtcin, P.-C., "Mix design for air-entrained high performance concrete", *Proceedings of the International Conference on Concrete under Severe Conditions: Environment and Loading*, Vol.2, K. Sakai, N. Banthia, and O.E. Gjørv, eds., E & FN Spon, London, UK, 1995, pp.1025-1034.

Lin, Y., Lai, C.-P., and Yen, T., "Prediction of ultrasonic pulse velocity (UPV) in concrete", *ACI Materials Journal*, Vol.100, No.1, 2003, pp.21-28.

Litvan, G.G., "Pore structure and frost susceptibility of building materials", *Proceedings of the RILEM/IUPAC International Symposium on Pore Structure and Properties of Materials*, Prague, Czech Republic, September 18-21, 1973, 14pp.

Maeda, N., Wada, I., Kawakami, M., Ueda, T., and Pushpalal, G.K.D., "Chloride diffusivity of concrete incorporating rice husk ash", *Proceedings of the Fifth CANMET/ACI International Conferences on Recent Advances in Concrete Technology*, ACI SP-200, V.M. Malhotra, ed., American Concrete Institute, Farmington Hills, Michigan, USA, 2001, pp.291-308.

Mahmud, H.B., Majuar, E., Zain, M.F.M., and Hamid, N.B.A.A., "Mechanical properties and durability of high strength concrete containing rice husk ash", *Proceedings of the Eighth CANMET/ACI International Conference on Fly Ash, Silica Fume, Slag and Natural Pozzolans in Concrete*, ACI SP-221, V.M. Malhotra, ed., American Concrete Institute, Farmington Hills, Michigan, USA, 2004, pp.751-765.

Mailvaganam, N.P., *Concrete Admixtures Handbook*, Noyes Publication, New Jersey, USA, 1994, pp.1000-1006.

Malhotra, V.M., "Fly ash, slag, silica fume, and rice-husk ash in concrete: a review", *Concrete International*, Vol.15, No.4, 1993, pp.23-28.

Mather, B., "Curing of concrete", *Proceedings of Lewis H. Tuthill International Symposium on Concrete and Concrete Construction*, ACI SP-104, G.T. Halvorsen, ed., American Concrete Institute, Farmington Hills, Michigan, USA, 1987, pp.145-159.

MBT, "Rheomac VMA 362", *Information Sheet*, Master Builders, Inc., Brampton, Ontario, Canada, 2002.

McCarter, W.J., Ezirim, H., and Emerson, M., "Absorption of water and chloride into concrete", *Magazine of Concrete Research*, Vol.44, No.158, 1992, pp.31-37.

Mehta, P.K., "Rice husk ash – a unique supplementary cementing material", *Proceedings of the CANMET/ACI International Symposium on Advances in Concrete Technology*, V.M. Malhotra, ed., Athens, Greece, 1992, pp.407-430.

Mehta, P.K., "Mineral Admixtures for Concrete – an Overview of Recent Developments", *Advances in Cement and Concrete: Proceedings of an Engineering Foundation Conference*, M.W. Grutzeck, and S.L. Sarkar, eds., American Society of Civil Engineers, New York, USA, 1994, pp. 243-256.

Mehta, P.K., *Method for Producing a Blended Cementitious Composition*, United States Patent, No. US 6451104 B2, 2002, 13pp.

Mehta, P.K., and Aïtcin, P.-C., "Microstructural basis for selection of materials and mix proportions for high strength concrete", *Second International Symposium on High Strength Concrete*, ACI SP-121, W.T. Hester, ed., American Concrete Institute, Farmington Hills, Michigan, USA, 1990, pp.265-282.

Mehta, P.K., and Folliard, K.J., "Rice husk ash – a unique supplementary cementing material: durability aspects", *Proceedings of the Second CANMET/ACI International Symposium on Advances in Concrete Technology*, ACI SP-154, V.M. Malhotra, ed., American Concrete Institute, Farmington Hills, Michigan, USA, 1995, pp.531-541.

Mehta, P.K., and Monteiro, P.J.M., *Concrete: Microstructure, Properties, and Materials*; Second Edition, McGraw-Hill Companies, Inc., New York, USA, 1993. 548pp.

Mindess, S., Young, J.F., and Darwin, D., *Concrete*, Second Edition, Prentice Hall, New Jersey, USA, 2003, 644pp.

Monroe, C.F., *Personal Communication*. Manager of Technical Services, Degussa Master Builders Ltd, Brampton, Ontario, Canada, 2004.

Moranville-Regourd, M., "Microstructure of high performance concrete', *High Performance Concrete*, Y. Malier, ed., E & FN Spon, London, UK, 1994, pp.3-13.

Morris, W., Moreno, E.I., and Sagüés, A.A., "Practical evaluation of resistivity of concrete in test cylinders using a Wenner array probe", *Cement and Concrete Research*, Vol.26, No.12, 1996, pp.1779-1787.

Murata, J., "Flow and deformation of fresh concrete", *Materials and Structures*, Vol.17, No.98, 1984, pp.117-129.

Murata, J., and Kikukawa, H., "Viscosity equation of fresh concrete", *ACI Materials Journal*, Vol.89, No.3, 1992, pp.230-237.

Nagai, T, Kojima, T., and Miura, T., "Application of high-strength/superworkable concrete to thin-wall prestressed concrete products", *Magazine of Concrete research*, Vol.51, No.3, 1999, pp.153-162.

Nagataki, S., "Mineral admixtures in concrete: state of the art and trends", *Proceedings of V. Mohan Malhotra Symposium on Concrete Technology: Past, Present, and Future*, SP-144, P.K. Mehta, ed., American Concrete Institute, Farmington Hills, Michigan, USA, 1994, pp.447-482.

Nagataki, S., and Fujiwara, H., "Self-compacting property of highly flowable concrete", *Proceedings of the Second CANMET/ACI International Symposium on Advances in Concrete Technology,* SP-154, V.M. Malhotra, ed., American Concrete Institute, Farmington Hills, Michigan, USA, 1995, pp.301-314.

Naik, T.R., and Malhotra, V.M., "The ultrasonic pulse velocity method", *CRC Handbook on Nondestructive Testing of Concrete*, V.M. Malhotra, and N.J. Carino, eds., CRC Press, Florida, USA, 1991.

Nawy, E.G., *Fundamentals of High Strength High Performance Concrete*, Longman Group Limited, London, UK, 1996. 340pp.

Nehdi, M., El-Chabib, H., and El-Naggar, H., "Cost-effective SCC for deep foundations", *Concrete International*, Vol.25, No.3, 2003a, pp.95-103.

Nehdi, M., Duquette, J., and El-Damatty, A., "Performance of rice husk ash produced using a new technology as a mineral admixture in concrete", *Cement and Concrete Research*, Vol.33, No.8, 2003b, pp.1203-1210.

Nehdi, M., Mindess, S., and Aïtcin, P.-C., "Rheology of high-performance concrete: effect of ultrafine particles", *Cement and Concrete Research*, Vol.28, No.5, 1998, pp.687-697.

Nehdi, M., Pardhan, M., Koshowski, S., "Durability of self-consolidating concrete incorporating high-volume replacement composite cements", *Cement and Concrete Research*, Vol.34, No.11, 2004, 2103-2112.

Neville, A.M. *Properties of Concrete*, Fourth and Final Edition, John Wiley & Sons, Inc., New York, USA, 1996, 844pp.

Neville, A.M., and Brooks, J.J., *Concrete Technology*, Addison-Wesley Longman, Inc., Essex, England, UK, 1999, 438pp.

Níelsson, I., and Wallevik, Ó.H., "Rheological evaluation of some empirical test methods-preliminary results", *Proceedings of the Third International Symposium on Self-compacting Concrete*, O. Wallevik, and I. Nielsson, eds., RILEM Publications, Bagneux, France, 2003, pp.59-68.

Noguchi, T., Oh, S.G., and Tomosawa, F., "Rheological approach to passing ability between reinforcing bars of self-compacting concrete", *Proceedings of the First International RILEM Symposium on Self-compacting Concrete*, Â. Skarendahl, and Ö. Petersson, ed., RILEM Publications, Bagneux, France, 1999, 12pp.

Nokken, M.R., and Hooton, R.D., "Dependence of rate of absorption on degree of saturation of concrete", *Cement, Concrete, and Aggregates*, Vol.24, No.1, 2002, pp.20-24.

Okamura, H., and Ouchi, M., "Self-compacting concrete", *Journal of Advanced Concrete Technology*, Vol.1, No.1, 2003, pp.5-15.

Okamura, H., and Ozawa, K., "Self-compactable high-performance concrete in Japan", *Proceedings of the International Workshop on High-Performance Concrete"*, ACI SP-159, P. Zia, ed., American Concrete Institute, Farmington Hills, Michigan, USA, 1994, pp.31-44.

Okamura, H., and Ozawa, K., "Mix design for self-compacting concrete", *Concrete Library of JSCE*, No.25, 1995, pp.107-120.

Okamura, H., Ozawa, K., and Ouchi, M., "Self-compacting concrete", *Structural Concrete*, Vol.1, No.1, 2000, pp.3-17.

Ouchi, M., Nakamura, S., Osterberg, T., Hallberg, S.-E., and Lwin, M., "Applications of self-compacting concrete in Japan, Europe and the United States", *Proceedings of the 3rd PCI/FHWA International Symposium on High Performance Concrete*, US Department of Transportation and Federal Highway Transportation (FHWA), Orlando, Florida, USA, 2003, 20pp.

Owens, P.L., "Water and Its Role in Concrete – Part 1 and Part 2", *Durable Concrete*, ACI Compilation 24, American Concrete Institute, Farmington Hills, Michigan, USA, 1992, pp.18-38.

Ozyildirim, C., and Lane, D.S., "Evaluation of self-consolidating concrete", *Final Report*, VTRC 03-R13, Virginia Transportation Research Council, Virginia, USA, 2003, 15pp.

Palacios, M., and Puertas, F., "Effect of superplasticizer and shrinkage-reducing admixtures on alkali-activated slag pastes and mortars", *Cement and Concrete Research*, Vol.35, No.7, 2005, pp.1358-1367.

Parrott, L.J., "Variations of water absorption rate and porosity with depth from an exposed concrete surface: effects of exposure conditions and cement type", *Cement and Concrete Research*, Vol.22, No.6, 1992, pp.1077-1088.

Perez, N., Romero, H., Hermida, G., and Cuellar, G., "Self-compacting concrete, on the search and finding of an optimized design", S.P. Shah, J.A. Daczko, and J.N. Lingscheit, eds., *Proceedings of the First North American Conference on the Design and Use of Self-consolidating Concrete*, Hanley-Wood, LLC, Illinois, USA, 2002, pp.101-107.

Perraton, D., Aïtcin, P.-C., and Carles-Gbergues, A., "Permeability, as seen by the researcher", *High Performance Concrete: From Material to Structure*, Y. Malier, ed., E & FN Spon, London, UK, 1994, pp.186-195.

Persson, B., "A comparison between mechanical properties of self-compacting concrete and the corresponding properties of normal concrete", *Cement and Concrete Research*, Vol.31, No.2, 2001, pp.193-198.

Petrou, M.F., Harries, K.A., Gadala-Maria, F., and Kolli, V.G., "A unique experimental method for monitoring aggregate settlement in concrete", *Cement and Concrete Research*, Vol.30, No.5, 2000, pp.809-816.

Pigeon, M., Plante, P., and Plante, M., "Air-void stability, part I: influence of silica fume and other parameters", *ACI Materials Journal*, Vol.86, No.5, 1989, pp.482-490.

Pigeon, M., "Frost resistance, a critical look", *Concrete Technology – Past, Present, and Future: Proceedings of V. Mohan Malhotra Symposium*, ACI SP-144, P.K. Mehta, ed., American Concrete Institute, Farmington Hills, Michigan, USA, 1994, pp.141-158.

Price, B., "BP invests heavily in lightweight concrete for North Sea", *Concrete*, Vol.28, No.10, 1994, pp.9-13.

Regional Municipality of Waterloo, *Tap Water Quality,* Data collected through personal communication with P. Clarke, Water Quality Specialist, Region of Waterloo, Ontario, Canada, 2003.

Rixom, R., and Mailvaganam, N., *Chemical Admixtures for Concrete*, Third Edition, E & FN Spon, London, UK, 1999, 437pp.

Rols, S., Ambroise, J., and Pera, J., "Development of an admixture for self-levelling concrete", *Proceedings of the Fifth CANMET/ACI International Conferences on Superplasticizers and Other Chemical Admixtures*, ACI SP 173, V.M. Malhotra, ed., American Concrete Institute, Farmington Hills, Michigan, USA, 1997, pp.493-510.

Roper, H., "Mineral admixtures in cements for general use and special purposes", *Proceedings of the Engineering Foundation Conference on Advances in Cement and Concrete*, M.W. Grutzeck, and S.L. Sarkar, eds., American Society of Civil Engineers, New York, USA, 1994, pp.236-242.

Roy, D.M., "High-performance concrete: superior microstructure for long-term durability", *Proceedings of the International Workshop on High-Performance Concrete*, ACI SP-159, P. Zia, ed., American Concrete Institute, Farmington Hills, Michigan, USA, 1994, pp.393-408.

Russell, H.G., "ACI defines high-performance concrete", *Concrete International*, Vol.21, No.2, 1999, pp.56-57.

Saak, A.W., Jennings, H.M., and Shah, S.P., "New methodology for designing self-compacting concrete", *ACI Materials Journal,* Vol.98, No.6, 2001, pp.363-371.

Saak, A.W., Jennings, H.M., and Shah, S.P., "A generalized approach for the determination of yield stress by slump and slump flow", *Cement and Concrete Research*, Vol.34, No.3, 2004, pp.363-371.

Safawi, M.I., Iwaki, I., and Miura, T., "The segregation tendency in the vibration of high fluidity concrete", *Cement and Concrete Research*, Vol.34, No.2, 2004, pp.219-226.

Saucier, F., Pigeon, M., and Plante, M., "Air-void stability, part III: field tests of superplasticized concretes", *ACI Materials Journal*, Vol.87, No.1, 1990, pp.3-11.

SCCEPG, *The European Guidelines for Self-compacting Concrete: Specification, Production and Use*, Self-compacting Concrete European Project Group, The European Federation of Concrete Admixtures Associations, West Midlands, UK, 2005, 63pp.

Schemmel, J.J., Arora, V., and Williams, J., "Split addition of a HRWR and its effect on high-performance concrete", *Proceedings of the Fourth CANMET/ACI International Conference on Superplasticizers and Other Chemical Admixtures in Concrete*, ACI SP-148, V.M. Malhotra, ed., American Concrete Institute, Farmington Hills, Michigan, USA, 1994, pp.301-316.

Schrader, E.K., and Munch, A.V., "Deck slab repaired by fibrous concrete overlay", *Journal of the Construction Division: Proceedings of the American Society of Civil Engineers*, Vol.102, No.C01, 1976, pp.179-196.

Schutter, G.D., Audenaert, K., Boel, V., Vandewalle, L., Dupont, D., Heirman, G., Vantomme, J., and D'hemricourt, J., "Transport properties in self-compacting concrete and relation with durability: overview of a Belgian research project", *Self-Compacting Concrete: Proceedings of the Third International RILEM Symposium*, RILEM Proceedings 33, O. Wallevik, and I. Nielsson, eds., RILEM Publications, Bagneux, France, 2003, pp.799-807.

Schwartzentruber, L.D., Roy, R.L., and Cordin J., "Rheological behaviour of fresh cement pastes formulated from a self-compacting concrete (SCC)", *Cement and Concrete Research*, Vol.36, No.7, 2006, pp.1203-1213.

Selvaraj, R., Muralidharan, S., and Srinivasan, S., "The influence of silica fume on the factors affecting the corrosion of reinforcement in concrete – a review", *Structural Concrete*, Vol.4, No.1, 2003, pp.19-23.

Seto, K., Yanai, S., Ohno, T., and Yasunaga, M., "Application of high strength and self-compacting concrete for continuous diaphragm walls", *Proceedings of the First International Conference on High Strength Concrete*, A. Azizinamini, D. Darwin, and C. French, eds., American Society of Civil Engineers, Virginia, 1997, pp.622-635.

Shah, S.P., Daczko, J.A., and Lingscheit, J.N., eds., *Proceedings of the First North American Conference on the Design and Use of Self-Consolidating Concrete*, Hanley-Wood, LLC, Illinois, USA, 2002, 426pp.

Shetty, M.S., *Concrete Technology: Theory and Practice*, S. Chand and Company Ltd., New Delhi, India, 2001, 637pp.

Shilstone, Sr., J.M., "Concrete mixture optimization", *Concrete International*, Vol.12, No.6, 1990, pp.33-39.

Shilstone, Sr., J.M., and Shilstone, Jr., J.M., "High performance concrete mixtures for durability", *Proceedings of the Symposium on High Performance Concrete in Severe Environments*, ACI SP-140, P. Zia, ed., American Concrete Institute, Farmington Hills, Michigan, USA, 1993, pp.281-306.

Shilstone, Sr., J.M., and Shilstone, Jr., J.M., "Performance-based concrete mixtures and specifications for today", *Concrete International*, Vol.24, No.2, 2002, pp.80-83.

Shindoh, T., and Matsuoka, Y., "Development of combination-type self-compacting concrete and evaluation test methods", *Journal of Advanced Concrete Technology*, Vol.1, No.1, 2003, pp.26-36.

Siebel, E., "Air-void characteristics and freezing and thawing resistance of superplasticized air-entrained concrete with high workability", *Proceeding of the Third International Conference on Superplasticizers and Other Chemical Admixtures in Concrete*, ACI SP-119, V.M. Malhotra, ed., American Concrete Institute, Farmington Hills, Michigan, USA, 1989, pp.297-319.

Sonebi, M., "Medium strength self-compacting concrete containing fly ash: modelling using factorial experimental plans", *Cement and Concrete Research*, Vol.34, No.7, 2004a, pp.1199-1208.

Sonebi, M., "Applications of statistical models in proportioning medium-strength self-consolidating concrete", *ACI Materials Journal*, Vol.101, No.5, 2004b, pp.339-346

Struble, L., Szecsy, R., Lei, W.-G., and Sun, G.K., "Rheology of cement paste and concrete", *Cement, Concrete and Aggregates*, Vol.20, No.2, 1998, pp.269-277.

Struble, L., and Hawkins, P., "Hydraulic cements – physical properties", *Tests and Properties of Concrete*, ASTM STP 169C, American Society for Testing and Materials, Philadelphia, 1994, pp.449-461.

Struble, L., and Sun, G.-K., "Viscosity of portland cement paste as a function of concentration", *Advanced Cement Based Materials*, Vol.2, No.2, 1995, pp.62-69.

Su, N., Hsu, K.-C., and Chai, H.-W., "A simple mix design method for self-compacting concrete", *Cement and Concrete Research*, Vol.31, No.12, 2001, pp.1799-1807.

Su, J.K., Cho, S.W., Yang, C.C., and Huang, R., "Effect of sand ratio on the elastic modulus of self-compacting concrete", *Journal of Marine Science*, Vol.10, No.1, 2002, pp.8-13.

Sugita, S., Yu, Q., Shoya, M., Tsukinaga, Y., and Isojima, Y., "The resistance of rice husk ash concrete to carbonation, acid attack and chloride ion penetration", *Proceedings of the Third CANMET/ACI International Conference on High Performance Concrete: Design and Materials and Recent Advances in Concrete Technology*, ACI SP-172, V.M. Malhotra, ed., American Concrete Institute, Farmington Hills, Michigan, USA, 1997, pp.29-43.

Taggart, Jr., J.E., and Siems, D.F., "Major element analysis by wavelength dispersive X-ray fluorescence spectrometry", *Analytical Methods for Chemical Analysis of Geological and Other Materials*, J.E. Taggart, Jr., ed., U.S. Geological Survey, Denver, Colorado, USA, 2002, pp.T1-9.

Tanigawa, Y., and Mori, H., "Analytical study on deformation of fresh concrete", *Journal of Engineering Mechanics*, Vol.115, No.3, 1989, pp.493-508.

Tanigawa, Y., Mori, H., Kurokawa, Y., and Komura, R., "Rheological study on slumping behaviour of fresh Concrete", *Transactions of the Japan Concrete Institute*, Vol.14, 1992, pp.1-8.

Tasi, C.T., Li, S., and Hwang, C.L., "The effect of aggregate gradation on engineering properties of high performance concrete", *Journal of ASTM International*, Vol.3, No.3, 2006, pp.1-12.

Taylor, M.R., Lydon, F.D., and Barr, B.I.G., "Mix proportions for high strength concrete", *Construction and Building Materials*, Vol.10, No.6, 1996, pp.445-450.

Tomas, D.G., "Transport characteristics of suspensions: III. Laminar flow properties of flocculated suspensions", *Journal of American Institute for Chemical Engineers*, Vol.7, No.3, 1961, pp.431-437.

Tumidajski, P.J., "Relationship between resistivity, diffusivity and microstructural descriptors for mortars with silica fume", *Cement and Concrete Research*, Vol.35, No.7, 2005, pp.1262-1268.

Uomoto, T., and Ozawa, K., "Recommendation for self-compacting concrete", *JSCE Concrete Engineering Series 31*, Japan Society of Civil Engineers, Tokyo, Japan, 1999, 77pp.

Vanwalleghem, H., Blontrock, H., and Taerwe, L., "Spalling tests on self-compacting concrete", *Proceedings of the Third International Symposium on Self-compacting Concrete*, O. Wallevik, and I. Nielsson, eds., RILEM Publications, Bagneux, France, 2003, pp.855-862.

Vegas, P. "Rice production and marketing", Sage V Foods, LLC, Los Angeles, California, USA, 2004.

Videla, C., and Gaedicke, C., "Modeling portland blast-furnace slag cement high-performance concrete", *ACI Materials Journal*, Vol.101, No.5, 2004, pp.365-375.

Vom Berg, W., "Influence of specific surface and concentration of solids upon the flow behaviour of cement pastes", *Magazine of Concrete Research*, Vol.31, No.109, 1979, pp.211-216.

Wallevik, J.E., "Relationship between the Bingham parameters and slump", *Cement and Concrete Research*, Vol.36, No.7, 2006, pp.1214-1221.

Wallevik, Ó.H., "Rheology – a scientific approach to develop self-compacting concrete", *Proceedings of the Third International Symposium on Self-compacting Concrete*, O. Wallevik, and I. Nielsson, eds., RILEM Publications, Bagneux, France, 2003, pp.23-31.

Wallevik, O., and Nielsson, I., eds., *Self-Compacting Concrete: Proceedings of the Third International RILEM Symposium*, RILEM Proceedings 33, RILEM Publications, Bagneux, France, 2003, 1028pp.

Watson, N., "Self-compacting concrete: the future of precast cladding", *Concrete*, Vol.37, No.2, 2003, pp.40-41.

Westerholm, M., *Rheology of the Mortar Phase of Concrete with Crushed Aggregate*, Licentiate Thesis, Division of Mineral Processing, Department of Chemical Engineering and Geosciences, Luleå University of Technology, Sweden, 2006, 94pp.

Whiting, D.A., and Nagi, M.A., *Manual on Control of Air Content in Concrete*, Portland Cement Association, Skokie, Illinois, USA, 1998, 48pp.

Xie, Y., Liu, B., Yin, J., and Zhou, S., "Optimum mix parameters of high-strength self-compacting concrete with ultrapulverized fly ash", *Cement and Concrete Research*, Vol.32, No.3, 2002, pp.477-48.

Ye, Y., Bonen, D., and Shah, S.P., "Fresh properties and segregation resistance of self-compacting concrete", *Proceedings of the Second North American Conference and the Fourth International RILEM Symposium on Self-consolidating Concrete*, Centre for Advanced Cement-based Materials, Northwestern University, Illinois, USA, 2005, pp.621-627.

Yen, T., Tang, C.-W., Chang, C.-S., and Chen, K.-H., "Flow behaviour of high strength high-performance concrete", *Cement and Concrete Composites*, Vol.21, No.5-6, 1999, pp.413-424.

Yu, Q., Sawayama, K., Sugita, S., Shoya, M., and Isojima, Y., "The reaction between rice husk ash and $Ca(OH)_2$ solution and the nature of its product", *Cement and Concrete Research*, Vol.29, No.1, 1999, pp.37-43.

Zain, M.F.M., Safiuddin, M., and Yusof, K.M., "A study on the physical properties of freshly mixed high performance concrete", *Cement and Concrete Research*, Vol.29, No.9, 1999, pp.1427-1432.

Zain, M.F.M., Safiuddin, M., and Yusof, K.M., "Influence of different curing conditions on the strength and durability of high performance concrete", *Proceedings of the Fourth ACI International Conference on Repair, Rehabilitation and Maintenance of Concrete Structures, and Innovations in Design and Construction*, ACI SP-193, V.M. Malhotra, ed., American Concrete Institute, Farmington Hills, Michigan, USA, 2000, pp.275-292.

Zhang, M.-H., and Malhotra, V.M., "High-performance concrete incorporating rice husk ash as a supplementary cementing material", *ACI Materials Journal*, Vol.93, No.6, 1996, pp.629-636.

Zhang, M.H., Lastra, R., and Malhotra, V.M., "Rice-husk ash paste and concrete: some aspects of hydration and the microstructure of the interfacial zone between the aggregate and paste", *Cement and Concrete Research*, Vol.26, No.6, 1996, pp.963-977.

Zhu, W., and Bartos, P.J.M., "Permeation properties of self-compacting concrete", *Cement and Concrete Research*, Vol.33, No.6, 2003, pp.921-926.